IMPROVEMENT OF GEOTECHNICAL PROPERTIES OF CLAYEY SOIL BY MIXING PLASTIC WASTES

Thesis submitted by

P. V. RAGHU

DOCTOR OF PHILOSOPHY (ENGINEERING)

DEPARTMENT OF CIVIL ENGINEERING
Faculty Council of Engineering & Technology
Jadavpur University
Kolkata-700032, India

2018

INDEX No. 36/12/Engineering

1. Title of the Thesis:

IMPROVEMENT OF GEOTECHNICAL PROPERTIES OF CLAYEY SOIL BY MIXING PLASTIC WASTE.

2. Name, Designation and Institution of the Supervisor

(1) Professor (Dr) S. P. MUKHERJEE,
Professor,
Department of Civil Engineering,
Jadavpur University,
Kolkata – 700 032, India.

(2) Professor SANKAR CHARKRABARTI
Former Professor,
Department of Civil Engineering,
Jadavpur University,
Kolkata – 700 032, INDIA.

3. List of Publication Journal papers:

(1) Raghu, P.V., Sengupta, P.K., Mukherjee, S.P. and Chakrabarti Sankar (2013) Improvement of Bearing capacity of clayey soil PET bottle strips, International Journal of innovative Research in Science, Engineering and Technology. 2(9).

(2) Raghu, P.V., Mukherjee, S.P. and Chakrabarti Sankar (2014) Upgradation of Geotechnical Parameter by waste plastic Admixture in Soil, Journal of Environmental Research and Development. 8(3A):759-765.

(3) Raghu, P.V., Mukherjee, S.P. and Chakrabarti S. (2015) Improvement of shear strength of clayey soil using randomly distributed PET bottle strips, Journal of Environmental Research and Development. 10(1):65-72.

4. List of Patents: Nil.

5. List of Presentations in National/Inter National/ Conferences/Workshops:
NIl.

CERTIFICATE FROM THE SUPERVISORS

This is to certify that the Thesis entitled "IMPROVEMENT OF GEOTECHNICAL PROPERTIES OF CLAYEY SOIL BY MIXING PLASTIC WASTES" submitted by Sri. P.V. RAGHU, who got his name registered on 6th August, 2012 for the award of Ph. D. (Engineering) degree of Jadavpur University, is absolutely based upon his own work under the joint supervision of (Prof.) Dr. S. P. MUKHERJEE and Prof. (Former) SANKAR CHAKRABARTI and that neither his Thesis nor any part of the Thesis has been submitted for any degree / diploma are only other academic award anywhere before.

PROF.(Dr.) S.P. MUKHERJEE PROF(FORMER) SANKAR CHAKRABARTI

(Signature of Supervisors & date with Official seal)

ACKNOWLEDGEMENTS

I express my sincere gratitude and respect to my supervisors, Dr. S.P. Mukherjee, Professor and former Professor Sankar Chakrabarti, Department of Civil Engineering for the excellent support and guidance throughout the research work. This research would not have been possible without their support and guidance. I am extremely thankful to both supervisors with their readiness for academic discussions and general help which were of immense value to me.

I am extremely appreciative for the research experience at the Jadavpur University, which would not have been possible without the support of Professors, Dr. Arup Guha Neyogi, Head of Civil Engineering Department, Professor S. N. Mukherjee, Professor R. B. Sahu, Dr. G.N. Bhandari, Dr. P. Aitch, Dr. S.K. Biswas and Dr. Narayana Roy, Faculty members of Soil Mechanics and Foundation Engineering Division. I am also thankful to Soil Mechanics Laboratory supporting staff Sri. Robin Pal, Sri. Apurba Banerjee, Ranjit Kushari and others for their support and cooperation during my experimental work in the laboratory, I am thankful to Mr. Rana Acharya, Mr. Pratim Sengupta, P.G. Students and Ms. Smita Tung, Ms. Poulami Ghosh and Mr. Atriya Chowdhary, Research Scholars of this University for their timely help and cooperation.

I take this opportunity to express my deep gratitude and thanks for Commissioner and Joint Director, Department of Technical Education, Government of Telangana, Hyderabad for permitting me to do the Ph.D., under Q.I.P(Poly) Scheme. I am extremely thankful to my colleagues of the Department.

On the personal front, I shall be very much thankful to my loving parents Sri. P. Venkat Swamy and Smt. Satyamma, wife Smt. Bhargavi, children Smt. Sruthi and Chi. Prudhvi and my son-in-law Sri. B. Gowtham, my in laws Sri. T. Narasimham and Smt. Nirmala for their endurance in supporting me throughout my research work.

I express my sincere gratitude, respect and love to my spiritual Guruji Brahmasri Gurajada Bhavani Shankar Sharmagaru and spiritual club members Sri Sri Ram, Sri Bikshapathi, Sri. Brahmaiah, Sri Swami Ramji and Late Sartyanarayana Murthy.

Finally, I thank the ALMIGHY for driving me to realize my dream of completing this research work.

P. V. RAGHU

CONTENTS

LIST OF FIGURES

LIST OF TABLES

Symbols and Notations

ASTM - American Society for Testing and Material
C - Cohesion of soil
CBR - California Bearing Ratio
C_u - Uniformity Coefficient
CP - Confining Pressure
DD - Dry Density
e - Void Ratio
E - Modulus of Elasticity
FC - Fiber Content
HDPE - High Density Polyethylene
IS - Indian Standard
LDPE - Low Density Polyethylene
MC - Moisture Content
MDD - Maximum Dry Density
NCL - Normal Compression Line
OMC - Optimum Moisture Content
PET - Polyethylene Terephthalate
PVC - Polyvinyl Chloride
q_u - Unconfined Compressive Strength
RDFS - Randomly Distributed fiber in soil
S - Shear Strength
SC - Strip Content
Sr - Shear Strength of reinforced soil
UU - Unconsolidated Undrained
ϕ - Angle of internal friction or friction angle
AR - Aspect Ratio
AR1 - Aspect Ratio of 1
AR2 - Aspect Ratio of 2
AR3 - Aspect Ratio of 3
q - Ultimate Bearing Capacity
B - Footing Width
Pr -Percentage of Reinforcement
q -Ultimate Bearing Capacity
B -Footing Width
Sp -Settlement
ν - Poisson's Ratio
E -Young's Modulus
ψ -Dilatancy Angle

ABSTRACT

In these days geotechnical engineers often encounter weak subsoil, down to an appreciable depth, in respect of low to medium foundation load in and around a main city in India. This happens due to rapid urbanisation, which leads to exhaust the lands for construction. Thus there arises the need for use of reclaimed lands covering filled up areas developed for construction purposes. This necessitates ground improvement since the earlier low lying areas, which have been developed, were either marshy lands or agricultural ones. This is because shallow foundation with ground improvement may be cost effective in comparison to deep foundation.

Recycling plastic waste for the purposes of construction is one of the major challenges in the world at present. PET (polyethylene terephthalate) strips obtained from drinking water bottle wastes may be used as an admixture of soil to improve its strength characteristics, and the mix may be used for filling of reclaimed land for ground improvement.

With this in view, the present research work has been carried out with one type of locally collected clayey soil and two types of amended soil (clayey soil with 10% sand and 20% sand separately). These soils have been reinforced with randomly mixed PET bottle strips of different values of aspect ratio (length/width) of 1, 2 and 3 with constant width of 5 mm. For each aspect ratio the strips were mixed with 0.5%, 1%, 1.5% and 2% by weight of soil. Improvement of shear strength parameters and consolidation characteristics of the soil with admixture of PET bottle strips have been studied in the laboratory. The characterization of soil reinforced with PET bottle strips have been done by conducting routine laboratory tests like Atterberg's limits, grain size distribution, standard Proctor test, unconfined compressive strength test and UU triaxial test. This study has shown that the optimum percentage of PET bottle strip reinforcement is 1% in case of soil compacted with energy corresponding to standard Proctor compaction. Therefore, compressibility characteristics of three types of soil mixed with 1% of PET bottle strips have been obtained in the laboratory. In order to study the effect of improvement of bearing capacity of footings placed on soil reinforced with PET bottle strips, small scale model footing tests have been carried out with square footings of 5 cm and 10 cm sizes. The tests have been done with the original clayey soil and two types of amended soils in the laboratory, with and without PET bottle strips. In case of tests with PET bottle strip reinforcements, 1% PET bottle strips for different aspect

ratios have been used since earlier tests suggested that this is the optimum percentage of reinforcement. To supplement the experimental results, numerical analyses have been also done by PLAXIS 3D software to compare the bearing capacities obtained from experimental and numerical studies. Subsequently statistical modelling has been done to obtain an expression for bearing capacity of footings resting on the reinforced soil in terms of maximum dry density, optimum moisture content, shear strength parameters, aspect ratio and percentage of PET bottle strip reinforcements. The present study focuses on increase of shear strength, decrease of compressibility of the reinforced soil. This has resulted in increase of bearing capacity of footings with addition of PET bottle strips. The bearing capacity of footings placed on such amended soil was found to increase on an average by 95% (for locally collected soil) and 56% (in case of amended soils) for 5 cm and 10 cm footings.

Chapter 1

INTRODUCTION

1.0 General

Ground improvement is becoming necessary day by day with rapid growth of urbanisation because reclaimed lands are sometimes found to be very weak for construction of structures with low to medium foundation pressure. In those cases, shallow foundations may be preferred since deep foundation may not be cost effective. Hence the need of ground improvement arises for those cases.

Despite the ban in some Indian states, the use of plastic products, such as polythene bags, bottles, containers, and packaging strips, is increasing by leaps and bounds. As a result, open waste dumps are continuously filling up with this valuable resource. In many areas waste plastic is collected for recycling and reuses. The bottled water is fastest growing beverage industry in the world. Recycling plastic wastes formed due to use of water bottles has become one of the challenges worldwide. Plastic bottle recycling has not kept pace with the increase in virgin resin polyethylene terephthalate (PET) sales and the reuse becomes necessary for maintaining ecological balance. The best way to handle the increasing pressure of waste plastic on open dumps is to utilize it for ground improvement particularly for reclaimed land, after shredding with desired values of the aspect ratio (length to width ratio) and strip content. Moreover an environmental concern is also included by utilization of waste plastic materials and they can be made useful for improving the soil characteristics and to solve problems related to the disposal of waste plastic material.

The techniques employed to improve the properties of soil in respect of strength and other relevant characteristics of soil can be put into the following categories.

A. Soil stabilization by binding agent: It is the process of improving the engineering properties of soil by mixing some binding agent thus binding the soil particles like lime and cement.

B. Soil stabilization with reinforcement in the form of continuous planer members/sheets: Soils are strong in compression but weak in tension. This weak property of soil is improved by introducing reinforcing elements in the direction of tensile stress. Reinforcement material generally consists of galvanized or stainless steel strips, bars, grids, or fabrics of specified material, or wood polymer and plastic

etc. the reinforcement is placed or layered at specific direction and position, more or less the same way as steel in concrete.

C. Soil stabilization with randomly mixed fibres/discrete members called ply soil: Soil stabilization with randomly mixed fibres/discrete members called ply soil: Randomly distributed fibres in soil (RDFS) are among the latest technique in which fibres of desired type and quantity are added in the soil, mixed and laid. The composite material is called 'ply soil'. Thus the method of preparation of RDFS is similar to conventional stabilization techniques.

In this context many investigations have been carried out by many investigators.

Naeini and Sadjadi (2008), Gosavi et al. (2004), Consoli et al. (2005), Dutta and Venkatapparao (2007), Babu and Chouksey (2010) studied improvement of soil with inclusion of fibre reinforcements. They found some remarkable improvement of soil with increase of strength parameters leading to an increase in residual strength, ductility and energy absorption capacity. Further, **Chandrasekhar et al. (1998), Basudhar et al. (2007), Sharma et al. (2009), Madhavilatha and Somwanshi (2009), Al-Saidi (2009), Kumar and Kaur (2012)** also found on the basis of experimental and numerical studies that use of reinforcements result in increase in bearing capacity of footing placed on reinforced soil compared to that for unreinforced soil.

A detailed literature review has been presented in Chapter 2.

1.1 The Present Study

Based on the literature review presented in chapter 2, the following objective and scope have been chosen for the present study.

1.1.1 Objectives

The objectives of the present study are as follows:

1. To study the engineering properties of soil reinforced with PET bottle strips including its undrained shear strength parameters.
2. To find the optimum proportion of PET bottle strips in respect of improvement of soil.
3. To study compressibility characteristics and improvement of bearing capacity of footings placed on reinforced soil for optimum content of PET bottle strips.

1.1.2 Scope

The scope of the work is outlined as follows:

A. Collection of locally available clay from Jadavpur area, preparation of amended soil samples of different types with different percentages (10% and 20%) of sands.

B. Collection of PET bottles and preparation of PET bottle strips in proper form.

C. Conducting the Laboratory tests for determining the following properties of original and two amended soils both with and without PET bottle strips. PET bottle strips have been mixed with different proportions and at different values of aspect ratio (ratio of height to width of each fibre) of 1, 2 and 3. For each aspect ratio the strips were mixed with 0.5%, 1%, 1.5% and 2% by weight of soil. The following properties of original and amended were found.

   i) Liquid limit, plastic limit, plasticity index.

   ii) Optimum moisture content, maximum dry density and undrained shear strength parameters of reinforced and unreinforced soils.

D. Conducting the laboratory tests for determining the properties of the PET bottle strips like (a) width, (b) thickness, (c) tensile strength and (d) density.

E. Based on the study of material properties an attempt has been made to observe the optimum percentage of fibre, at which the optimum values of various parameters such as MDD (Maximum dry density), OMC (optimum moisture content), UCS (unconfined compressive strength), E (Modulus of Elasticity), Shear Strength Parameters (c and ϕ) occur for different aspect ratios in case of reinforced soils.

F. Further compressibility characteristics of unreinforced and reinforced soils with optimum percentage of PET bottle strips have been found.

G. Model footing tests have been carried out on both unreinforced and reinforced soil for the optimum percentage of reinforcement. Reinforcement with aspect ratio of 1, 2 and 3 has been adopted to prepare foundation beds with reinforced soil. Different sizes of model (square footings of 5 cm and 10 cm sizes) have been used to obtain the effect of width of foundation in case of reinforced soil.

H. Numerical analyses have also been done by PLAXIS 3D software to compare the results with experimental ones.

I. Multiple linear regressions have been carried out to obtain an empirical relationship for ultimate bearing capacity of footings in terms of different parameters of soil and fibre (PET bottle strips).

1.2 Organization of the Thesis

The thesis has been organized with **seven** different chapters as follows:

An **Introduction** to the current research work has been presented in **Chapter 1.** This chapter also deals with objective and scope of the study.

Chapter 2 presents a detailed **Literature Review** related to both experimental and theoretical studies separately on the relevant field of research.

Chapter 3 deals with **Materials and Their Properties,** which deals with different materials used for the study, i.e., locally available clayey soil, sand and PET bottle strips. This chapter depicts the test procedures adopted for determination of appropriate material properties of clay, sand and PET bottle strips. This chapter concludes with presentation of results along with a discussion on the results.

Chapter 4 describes equipment and procedure of **Model Footing Tests** and presentation of their results.

Chapter 5 presents methodology of **Numerical Analysis** and presentation of numerical results.

Chapter 6 incorporates a detailed **Discussion on Results of Experimental and Numerical Studies** on model footing tests.

Chapter 7 brings out the **Summary, Conclusions and Suggestions for Further Research**.

An **Abstract** of the dissertation has been presented at the beginning of this dissertation.

Chapter 2

LITERATURE REVIEW

2.0 General

Reinforced soil has been the interest of many researchers throughout last few decades. Many studies are being carried out in this respect till date. Investigation on reinforced soil can be classified into experimental and theoretical Studies. Review of some important experimental and numerical studies on reinforced soil is arranged separately in chronological order in the following sections.

2.1 Experimental Studies

In this section the past works available on experimental works on reinforced soil have been discussed in chronological order.

Waldron (1977) carried out direct shear test using a large direct shear device to study the effect of plant roots on the soil shearing resistance. He carried out the test with four varieties of plant roots and using a soil mixture of silt, clay and sand. He proposed a simple force equilibrium model to describe the load deformation characteristics of soils reinforced with plant roots. He used the original Mohr-Coulomb's equation of shear strength ($s = c + \sigma \tan\phi$) in a modified form, for root reinforced soil as $s_r = c + \sigma \tan\phi + \Delta S$, s_r being the shear strength of root reinforced soil and ΔS being increase in shear strength on account of root reinforcement; c and ϕ had indicated the shear strength parameters of the soil.

Gown et al. (1978) classified reinforcement into two major categories, ideally inextensible and ideally extensible inclusions. Metal strips, rods, nails used in reinforcement soil fall under the category of ideally inextensible inclusion, while natural or synthetic fibres used in ply are extensible inclusion. Mats of geotextiles or geogrid nets used in reinforced soil are relatively much less extensible in comparison to fibres used in ply soil. As compared with very stiff elements of reinforced soil, current developments make use of more extensible and less stiff reinforcements in the form of discrete inclusions (ply soil). In addition to this ply soil also appears to be economic.

Gray and Ohashi (1983) conducted a series of direct shear tests on dry sand reinforced with synthetic (PVC), natural (reed), and metallic (copper wire) fibres to evaluate the effect of parameters such as fibre orientation, fibre content, fibre area ratio, fibre stiffness on contribution to shear strength. Based on the experimental results, the authors concluded that

(i) shear strength increased was directly proportional to the fibre area ratio, fibre content and fibre stiffness. (ii) shear strength increased were maximum for fibre orientations of 60^{o} with respect to the shear surface. (iii) fibre reinforcements behaved as "ideally extensible" inclusions. They did not rupture during shear. Their main role was to limit the amount of post peak reduction in shear resistance in dense sand. (iv) shear strength envelopes for fibre reinforced sand clearly showed the existence of a threshold confining stress below which the fibres did tend to slip or pull out. Envelopes were parallel to each other for confining stresses above this threshold stress. According to the authors, the behaviour, in turn, indicated that the fibres did not affect the angle of internal friction of soil above this stress. A typical illustration of threshold confining stress was obtained as shown in Fig. 2.1 (after Gray and Ohashi, 1983). A theoretical model based on limit equilibrium of forces was used to examine the influence of fibre modulus, diameter, initial orientation and elongation during shear; skin friction between fibre and sand; angle of internal friction and relative density of the sand.

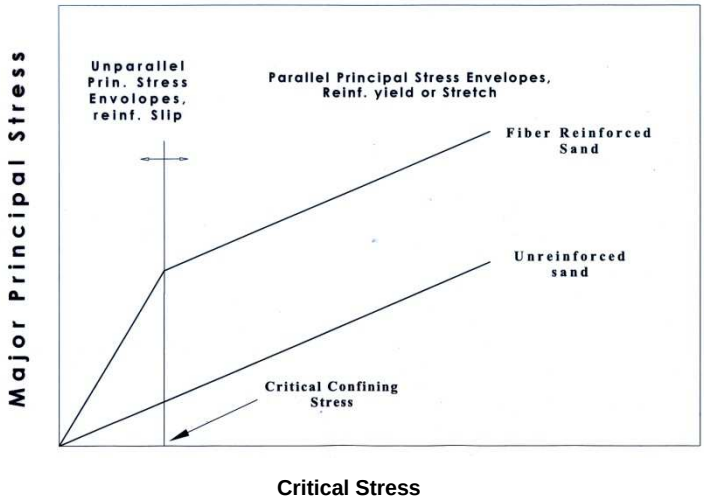

Fig. 2.1: Effect of fibre inclusion on failure envelope of sand
(after Gray and Ohashi, 1983)

Fibre reinforcement in this study consisted of a long elastic fibre extending an equal length over either side of a potential shear plane of sand.

Gray and Al-Refeai (1986) conducted a series triaxial compression tests on dry sand reinforced with continuous, oriented fabric layers and also with randomly distributed discrete fibres. Test results showed that both types of reinforcement systems increased strength and modified the stress-deformation behavior of sand in a significant manner. The following main

conclusions emerged from the study. (i) continuous, oriented fabric inclusions markedly increased the ultimate strength, increased the axial strain at failure, and in most cases limited reductions in post-peak loss of strength as shown in Fig.2.2. (ii) Discrete, randomly distributed fibres increased both the ultimate strength and the stiffness of reinforced sand. (iii) At the same aspect ratio, confining stress and weight fraction, rougher (not stiffer) fibres tended to be more effective in increasing strength.

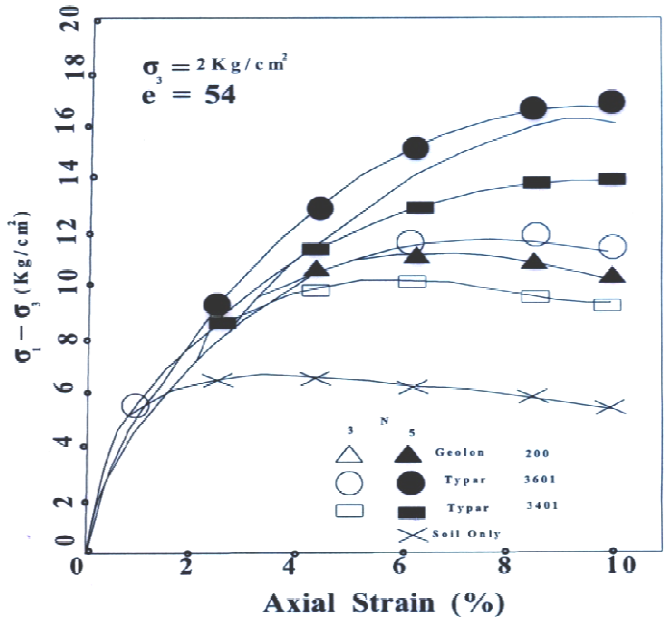

Fig. 2.2: Deviator stress vs. axial strain Curves
(after Gray and Al-Refeai, 1986)

Setty and Rao (1987) carried out triaxial tests, CBR tests and tensile strength tests on silty sand, reinforced with randomly distributed polypropylene fibres. The test results indicated that the soils showed significant increase in cohesion intercept (5.7 times) and a slight decrease in angle of internal friction (i.e., overall effect was to increase shear strength), with an increase in fibre content up to 3% (by weight). Adding fibres up to 2% increase in dry strength, but afterwards there was a decrease in dry strength.

Gray and Maher (1990) carried out triaxial compression tests on sand reinforced with discrete, randomly distributed fibres and observed the influence of various fibre properties on soil behavior. They found that a better gradation i.e. increase in coefficient of uniformity (C_u), lower sphericity and smaller average grain size (D_{50}) of sand resulted in higher fibre contribution to strength. In addition to the experimental program they proposed a force equilibrium model based on statistical analysis for randomly

distributed discrete fibre reinforced sand. The orientation of the fibres on the average was expected to be perpendicular to the plane of shear failure in triaxial compression test. The failure plane was observed to be the same as given by Mohr-Coulomb failure criteria i.e., oriented at an angle of $(45^o + \phi/2)$ with horizontal.

Lindh and Eriksson (1991) conducted field experiments to study the suitability of fibres for road construction. They constructed test stretches of 20 m and 40 m road by incorporating plastic fibres in sand and compared the performance with unreinforced stretch of road. The effect of plastic fibres on the stability of the sand was observed to be effective. This was confirmed after about two years use by traffic, when the test stretches were reported to have performed well, with no rutting of the road surface.

Fatani et al. (1991) conducted direct shear tests and pull-out tests, at modified Proctor density of 2.08 t/m^3 and corresponding moisture content of 8.9%, $\phi = 37^o$ and $\delta = 23^o$, ϕ and δ being angle of internal friction and angle of wall friction respectively. Results of direct shear tests revealed that residual strength of composite was 200% to 300% higher than that of unreinforced soil. Best orientation of fibre was found to be oriented at 60^o to shear plane. Pull-out tests revealed that well graded sand gave highest anchorage capacity indicated by friction angle δ.

Maher and Ho (1994) carried out unconfined compressive strength, splitting-tension, three point-bending and hydraulic-conductivity tests on kaolinite soil reinforced with polypropylene fibres at different water contents and evaluated the mechanical properties of the composite soil. The experiment was conducted in a universal testing machine with digital data acquisition system for performing unconfined compression test, split tension and flexural (using beam and third point loading) tests and flexible wall parameter set up for measurement of the hydraulic conductivity of fibre- clay composite. They observed that inclusion of randomly distributed fibres significantly increased the peak compressive strength, ductility, splitting tensile strength, and flexural toughness of kaolinite clay as shown in Fig. 2.3. The fibre inclusion increased the hydraulic conductivity of the composite and increase was more pronounced at higher fibre contents.

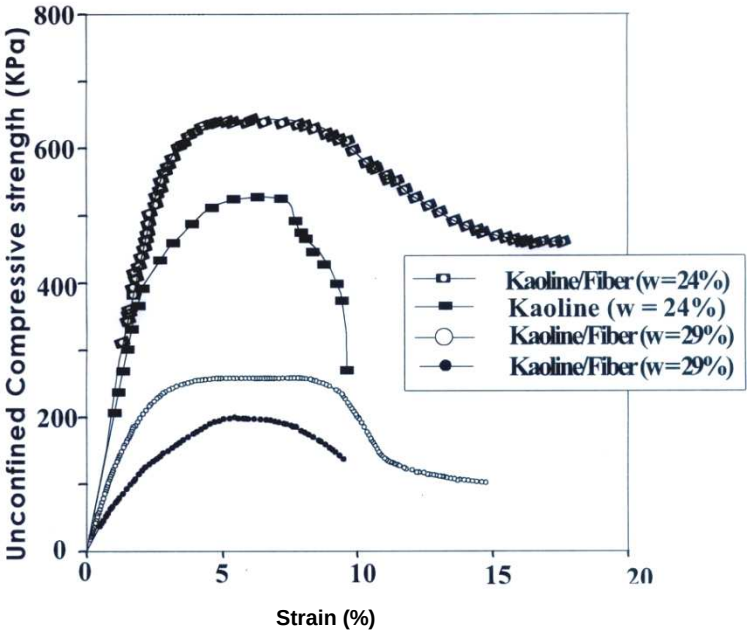

Fig. 2.3: Unconfined compressive strength vs. Strain
(after Maher and Ho, 1994)

Michalowaski and Zaho (1996) found an energy based homogenization technique, which was used to evolve a design criterion. The failure condition consisted of two parts; first the tensile failure of fibre and second the slip of fibre. The transfer from one part to another was smooth. Theoretical and experimental results were in good agreement.

Wasti and Butun (1996) carried out laboratory model tests on a strip footing 50 mm (width) × 250 mm (length) supported by sand reinforced by randomly distributed polypropylene fibre. Reinforced sand sample was 1.2 m × 0.51 m × 0.75 m (depth) size. Results indicated that reinforcement of sand caused an increase in the ultimate bearing capacity values and the settlement at the ultimate load in general. The big mesh size was found to be superior to the other inclusion considering the increase in ultimate bearing capacity values.

Mandal and Manjunath (1995) used geo-grid and bamboo sticks as vertical reinforcement elements and studied their effect on the soil bearing capacity. Geo grid and bamboo sticks were installed along each side of a strip footing to increase the bearing capacity of a sand subgrade. At a distance of 0.5B from the centre of the footing of width B, the load displacement behaviour of the footing was modified significantly and the occurrence of general shear failure was eliminated. It could be recommended that two rows of reinforcing elements, one on each side, be driven vertically, with sufficient length, at a distance of 0.5B from the centre of footing would be most effective. At the same inclination angle, outwardly

inclined reinforcement was found to be more effective than inwardly inclined reinforcement. However, vertical reinforcement was found to be more effective than both outwardly and inwardly inclined reinforcements.

Ranjan et al. (1994) conducted a series of triaxial compression tests on sand, reinforced with discrete randomly distributed fibres, both synthetic (plastic) and natural (coir, bhabar). The influence of fibre characteristics (i.e., fibre content, aspect ratio, and surface friction), soil characteristics and confining stress on shear strength of reinforced soil were analyzed. They observed that (i) the principal stress envelopes for fibre-reinforced soils were curvilinear having transition at confining stress, called critical confining stress (σ_{crit}) below which the fibres tended to slip or pullout. An increase in fibre aspect ratio, l/d, resulted in a lower value of the critical confining stress. (ii) the inclusion of fibres caused an increase in peak shear strength and reduction in the loss of post-peak stress. Thus residual strength was higher as compared to unreinforced soil. Shear strength increased approximately linearly with increasing amounts of fibres up to 2% (approximately) by weight, beyond which the gain in strength was smaller. They presented a mathematical model based on regression analysis of test results. Since the failure envelopes of fibre-reinforced soils were curvilinear with a transition at certain confining stress, termed as critical confining stress (σ_{crit}), two mathematical equations were developed. They were as follows:

For $\sigma_3 < \sigma_{crit}$,

$$\log(\sigma_{1f}) = 1.09 + 0.4 \log(fc) + 0.28 \log(l/d) + 0.27 \log(f^*) + 1.1 \log(f) + 0.68 \log(\sigma_3) \quad ..(2.1)$$

(σ_{1f}) being shear strength of fibre-reinforced soil, fc being fibre content, l/d is aspect ratio, $f = (c/\sigma_n + \tan\phi)$, σ_3 being minor principal stress or cell pressure, $f^* = (c_a/\sigma_n + \tan\phi)$ being skin friction coefficient, c_a and σ_n is represented adhesion intercept and vertical stress respectively and ϕ meant the angle of skin friction.

For $\sigma_3 > \sigma_{crit}$, a similar expression was developed for calculating shear strength of fibre reinforced soil , which is given,

$$\sigma_{1f} = 8.78\,(wf)^{0.35}\,(l/d)^{0.26}\,(f^*)^{0.06}\,(f)^{0.84}\,(\sigma 3)^{0.73} \quad \ldots\ldots (2.2)$$

wf being the fibre content and other symbols being as defined earlier.

Coefficients of determination, R^2 for the above two equations were found to be 0.91 and 0.93 respectively.

Nataraj and Mainis (1997) conducted compaction, unconfined compression, direct shear, CBR test. Compaction characteristics of the fibre reinforced soils were similar to that of the unreinforced soils. They observed that addition of fibres to clay and sand specimens resulted in substantial increase in the measure value of the peak friction angle and cohesion. The increase in compression strength was obtained as a function of fibre content and moisture content. The CBR values also increased significantly with the addition of fibres. Finally, the test results indicated that optimum fibre content was 0.3% of the dry unit weight of the soil specimen.

Ranjan et al. (1999) took a moist sample of clay to make a central hole, which was filled with a moist mixture of sand and fibre. Fibres inclusion improved both strength and stiffness of cohesionless soil. In triaxial tests on unreinforced soil showed peak of normal stress at 10% - 20% of axial strain, but reinforced soil did not show any peak, so 15% - 20% of strain was taken as failure. Figure 2.4 shows deviator stress vs. axial strain curves as obtained by the authors. In principal stress envelope, at the critical confining pressure, fibre tended to slip/pull out. Critical confining pressure decreased with increase of aspect ratio. Critical confining pressure remained unaffected by fibre content. Shear strength increased linearly with increasing the amount of fibre up to 2%, afterwards gain was smaller. Residual strength of reinforced soil was higher than of unreinforced soil.

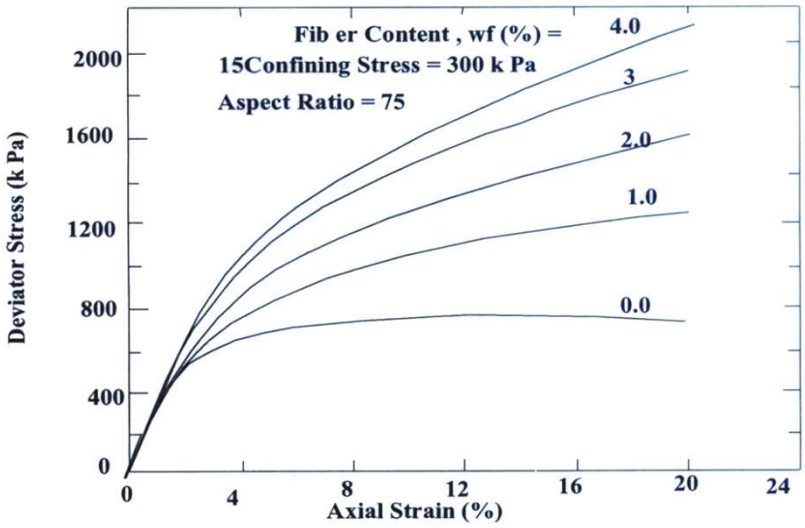

Fig. 2.4: Deviator stress vs. axial strain curves

(after Ranjan et al., 1999)

Alawaji (2000) carried out several model load tests to investigate the potential benefits of geogrid-reinforced sand over collapsible soil to control wetting-induced collapse settlement.

Tests were carried out using 100 mm diameter circular plate and tensor SS2 geogrid. The width and the depth of the geogrid were varied to determine their effects on the collapsible settlement, deformation modulus and bearing capacity ratios. The results showed that there was significant difference in the structural combination of the tested geogrid which ranged from 99% reduction in settlement to 2000% increase in elastic modulus and 320% increase in bearing capacity. It was found that the efficiency of the sand-geogrid system increased with the increasing geogrid reinforcement at model scale.

Dash et al. (2001) performed some laboratory-model tests on strip footing supported by a sand bed reinforced with geocell mattress and presented the results. Based on the model test results, the depth of placement and the dimensions of the geocell layer for mobilising maximum bearing capacity improvement were determined. While performing the test, some parameters, such as pattern of geocell formation, pocket size, height and width of the geocell mattress, the depth to the top of geocell mattress, tensile stiffness of the geogrids used and the relative density of the sand were varied. From the tests results it was concluded that pressure-settlement behaviour of the strip footing on geocell reinforced sand was approximately linear even up to a settlement of about 50% of the footing width and a load as high as 8 times the ultimate capacity of the reinforced one and very good improvement in the footing performance could be obtained even with geocell mattress of width equal to the width of the footing. Besides the author concluded that the optimum width of the geocell layer was around 4 times the footing width and the optimum aspect ratio of geocell pockets for supporting strip footings was found to be around 1.67.

Yamamoto and Otani (2002) carried out a series of model load tests on both unreinforced soil and reinforced foundations. A rigid-plastic finite element analysis considering the effect of geometrical non linearity had been conducted to quantitatively investigate both the increase of calculated bearing capacity and the progress in deformation localization corresponding to the settlement of a loading plate. The analysis was done considering the soil and the reinforcing element as composite material. According to their results the deformation properties of reinforced foundations were totally different from those of unreinforced foundation.

Consoli et al. (2002) carried out unconfined compression and drained triaxial tests on uncemented and cemented sands, reinforced with plastic fibre (polyethylene terephthalate) and observed as follows:

(i) Fibre inclusion improved both the peak strength and ultimate strength for uncemented and cemented sands.

(ii) Fibre length improved the unconfined compressive strength to a large extent as shown in Fig. 2.5. Uncemented sand showed a proportionally greater increase. For cemented sand longer the fibre, higher was its efficiency in increasing the ultimate strength. (iii) Addition of fibres increased the peak friction angle; for uncemented sands it increased from 37^o to 43^o and for cemented sands from 43^o to 49^o.

Fibre inclusion reduced the brittle behavior of cemented sands.

Boushehrian et al. (2003) performed some laboratory model tests and numerical analysis to investigate the bearing capacity of circular and ring footings on reinforced sand. Both experimental and numerical studies indicated that when a single layer of reinforcement was used there was an optimum reinforcement embedment depth for which the bearing capacity increased. The authors also recommended an optimum vertical spacing of the reinforcement layers for multi-layer reinforced sand. The bearing capacity was also found to increase with increasing number of reinforcement layers. The bearing capacity of those model footings were affected by the distance of separation between the first layer of reinforcement and base of the footing and the vertical spacing between the reinforcement layers for a given soil.

Kumar and Tabor (2003) performed unconfined compression tests on soil specimens prepared at degrees of compaction of 93%, 96% and 99% at the maximum dry unit weight determined using the standard Proctor test. Samples compacted at 93% showed higher increase in the peak and residual strength compared to the samples compacted to higher densities. For samples compacted at 93% of maximum dry density obtained from standard Proctor test with 0.3% fibres, the residual strength was found to increase approximately 20 times the residual strength of unreinforced sample, compared to approximately 4 times strength increase in case of the peak strength.

Gosavi et al. (2004) conducted standard Proctor test, direct shear test and soaked CBR test in the laboratory. Value of OMC increased and MDD decreased up to fiber content $f_c = 2\%$. The trends were reversed on further increase in fibre content. Value of cohesion (c) increased and angle of internal friction of soil (ϕ) decreased with f_c up to 2%. With further increase of f_c, c decreased and ϕ increased. CBR increased by 42% to 55% for $f_c = 1\%$. With increases in f_c, CBR values decreased. Safe bearing capacity increased by 33.58% and 29.67% due to addition of 2% woven fabrics and fibre glass with aspect ratio 50 and 500 respectively.

Consoli et al. (2005) took unreinforced sands and sands reinforced with randomly distributed polypropylene fibres (0.5% by weight, 24 mm in length and 0.023 mm thick), subjected to high pressure isotropic compression tests to investigate the effect of fibre addition on the triaxial stress-strain response of the composite material, including the effects of confining stress and fibre characteristics. Two important observations were as follows:

1. Insertion of fibres into sand changed its behaviour significantly. Two distinct and parallel normal compression lines (NCL) for the fibre reinforced and non-reinforced sands were observed. Both loose and dense fibre-reinforced sand specimens were found to tend towards a unique NCL when plotted in specific volume space, and
2. When the fibres were exhumed from the sample, it was found that they had both extended and broken. When the sample underwent isotropic compression, the fibres suffered large plastic tensile deformation and some of them reached breaking point. The isotropic compression caused relative movement among particles and consequently produced tensile stress in the fibres located among them.

Casagrande et al. (2006) studied the effect of fibre reinforcement in highly plastic clay with high initial water content and void ratio and at very large shear displacements, using the ring shear apparatus. Their salient observations were as follows:

1. The fibre-reinforced specimens showed peak strengths significantly higher than the non-reinforced specimens at all confining pressures and exhibited greater post peak strain softening.
2. Although the fibre insertion increased the peak strength, the effect was not as large as observed for some other soils. Probably number of fibres per unit volume would be lower. Another reason might be a lower shearing resistance between the fibre surface and the surrounding soil.
3. Ring shear tests on fibre reinforced and non-reinforced silty sand ($e = 0.55$) and fine sand ($e = 0.65$), e representing the void ratio, yielded an increase of peak strength of 115% and 165% respectively at a normal stress of 100 kPa. The improvement of bentonite was about 25% at the same normal stress.
4. The fibres had little effect on residual shear strength mobilized at large displacements, where bentonite was very low. The increased strength due to insertion of fibres was found to deteriorate at large shear displacements.

5. Peak strength improved slightly with increased fibre length because longer fibre allowed greater stresses to be developed in the fibre due to greater anchoring effect of the increased frictional resistance between the fibre and surrounding soil.

Dutta and Venkatappa Rao *(*2007) presented regression models for predicting the behaviour of sand mixed with waste plastics and the following conclusions were drawn.

1. The energy absorption capacity of sand mixed with HDPE/LDPE waste plastic strips increased with an increase in aspect ratio (AR), strip content (SC) and confining pressure (CP).
2. The deviator stress of sand mixed with HDPE/LDPE waste plastic strips increased with increase in AR, SC and CP.
3. The initial stiffness of sand mixed with LDPE waste plastic strip increased with an increase in SC and CP.
4. The cohesion increased with an increase in AR and SC in the mixture.
5. Friction angle increased with an increase in AR and SC.

Figures 2.5 and 2.6 show the effect of AR, HDPE SC, and CP on energy absorption capacity and the effect of AR, LDPE SC, and CP on energy absorption capacity respectively, as was obtained by the authors.

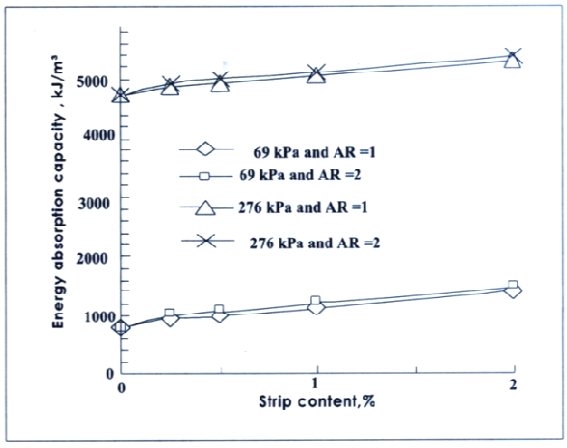

Fig. 2.5: Effect of AR, HDPE SC, and CP on energy absorption capacity

(after Dutta and Rao, 2007)

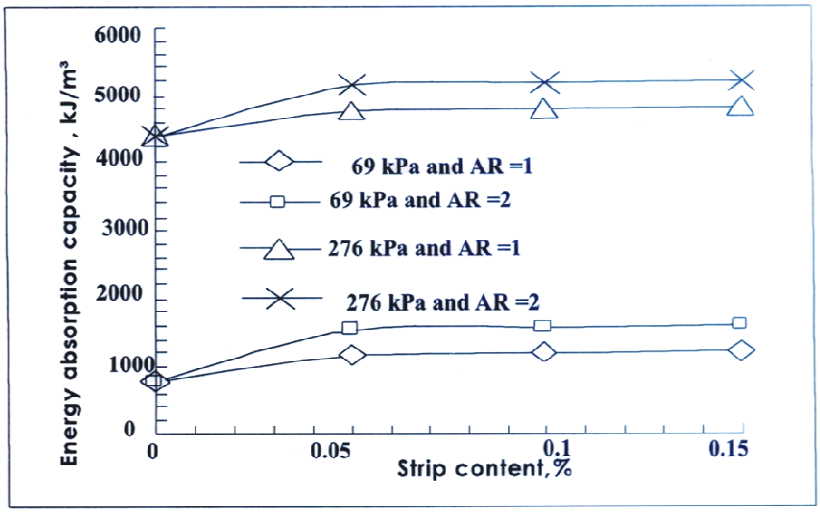

Fig. 2.6: Effect of AR, LDPE SC, and CP on energy absorption capacity

(after Dutta and Rao, 2007)

Naeini and Sadjadi (2008), used the waste polymer materials which had been chosen as the reinforcement material and it was randomly included in to the clayey soils with different plasticity indices at five different percentages of fibre contents (0%, 1%, 2%, 3%, 4%) by weight of original soil. Effects of Random Fibre Inclusion on consolidation, hydraulic conductivity, swelling, shrinkage limit and desiccation cracking of clays on the strength and compressibility characteristics of the reinforced soil had been studied and appreciable improvement of their characteristics was noted. A detailed review of past works carried out by several researchers has been presented in the next chapter.

Chandra et al. (2008) conducted the static triaxial tests on unreinforced and reinforced soils as well as on other pavement layers at a confining pressure of 40 kPa. These stress-strain data were used as input parameters for evaluating the vertical compressive strain at the top of subgrade soils using elastoplastic finite-element analysis. They observed as follows:

1. CBR values of soils A (clay), B (silt) and C (silty sand) were found to be 1.16, 1.95 and 6.20 respectively, which increased to 4.33%, 6.42% and 18.03% respectively, due to fibre reinforcement.

2. The static modulus of soils A, B and C, uniaxial compressive strength tests were found to be 3.824 MPa, 4.836 MPa and 5.572 MPa, respectively. These increased to 7.16 MPa, 9.056 MPa and 9.712MPa respectively, at optimum fibre content. If the pavement section was kept the same for unreinforced and reinforced sub grade soil A, B, and C, the

pavement resting on reinforced subgrade soils A, B, and C yielded CBR values of 3.35, 2.28, and 1.94 respectively.

3. For a constant thickness of base and DBM the thickness of sub-base reduced by 38.52%, 26.23% and 16.67% respectively, for reinforced soils A, B and C. The pavement resting on reinforced subgrade soils was beneficial in reducing the construction materials.

Sharma et al. (2009) developed an analytical solution to estimate the ultimate bearing capacity of geogrid reinforced soil foundations (RSF) for both sandy and silty clay soils. The author proposed failure mechanism for reinforced soil foundations based on the results of their experimental study on model footing tests. Stability analyses were conducted on the proposed failure mechanisms to include the effect of reinforcement tension on the bearing capacity of RSFs. Bearing capacity formulas that incorporate the contribution of reinforcements to the increase in bearing capacity were then developed for RSF of sand and silty clay soils. Since the mobilisation of tensile force in the reinforcement layers were needed to quantify the increase in the bearing capacity, a reasonable estimation of the tensile force along with the reinforcement was also proposed. The results of the laboratory model tests conducted on reinforced sand and silty clay foundations were compared with some analytical solution and the predicted values using the proposed models. The proposed analytical solutions were also verified by the results of large scale model tests.

Madhavilatha and Somwanshi (2009) conducted laboratory model tests using square model footings on geo synthetic reinforced sand. Bearing capacity of footings on geosynthetic reinforced sand was evaluated and the effect of various reinforcement parameters like the type and the tensile strength of geosynthetic material, amount of reinforcement, layout and configuration of geosynthetic layers below the footing on the bearing capacity improvement of the footing were studied through systematic model studies. They made some conclusions about the behaviour of square footing resting on sand reinforced with multiple layers of geosynthetics on the basis of results obtained from the experimental and numerical studies. Effective depth of the zone of reinforcement below a square footing was found to be twice the width of footing. Within the effective reinforcement zone, the optimum spacing of reinforced layers is about 0.4 times the width of the footing. Apart from the tensile strength of reinforcement, its layout and configuration played vital roles in increasing bearing capacity. Aperture size and flexibility of geosynthetic material were found to be important parameters for the design.

Phani Kumar et al. (2008) presented the data obtained from a series of laboratory plate load tests. The authors used geogrid-reinforced sand beds and improvement in load settlement response was studied. It was found that it resulted in improved load settlement response. The vertical compressive loads required to be applied for a deformation of 0.5 mm for fine sand, medium sand and coarse sand reinforced by single geogrid were, respectively 83 N, 44 N and 47 N, while in the case of unreinforced sand beds they were equal to 63 N, 38 N and 47 N. Increasing no of geogrid layer improved the behaviour further.

Vinod et al. (2009) performed some laboratory model tests to investigate the effect of braided coir rope reinforcement on load settlement behaviour of square model footing founded on loose sand. Based on the findings of the study, they concluded that: provision of braided coir rope reinforcement layer(s) improved the load carrying capacity of the model footing substantially at all levels of normalised settlement. The optimum location of the reinforcement was at about 0.4B below the base of the model footing of width B. Strength improvement ratio increased appreciably with increase in length of braided coir rope up to length ratio of 3. Strength improvement ratio increased almost proportionately with decrease in the vertical spacing of reinforcement. Provision of single and multiple layers of reinforcement could result in strength improvement ratio as high as about 3.4 and 6.6 respectively.

Al-Saidi (2009) presented the results of laboratory models test on the behaviour of a model footing resting on loose sand reinforced by geogrids under inclined load. Several parameters were studied in order to find the general behaviour of improvement in the soil by using the geogrid. These parameters include depth of reinforcement layer, vertical spacing of reinforcement layers and the angle of inclination of load. The results showed that the optimum ratio of reinforcement for the first layer is 0.5. The increase of such ratio between vertical spacing layer and footing width above 1 has no effect on soil improvement.

Choudhary et al. (2010) carried out a series of CBR tests on randomly reinforced soil by varying percentage of HDPE with different length and proportion. The following conclusions were drawn from their study.

1. Addition of HDPE strips to local sands increased the CBR value.
2. The maximum improvement in CBR was obtained when the strip content was 4% and for aspect ratio of 3.

3. The reinforcement benefit increased with an increase in waste plastic strip content and length.

The maximum CBR value of a reinforced system was approximately 3 times that of an unreinforced system as shown in Fig. 2.7.

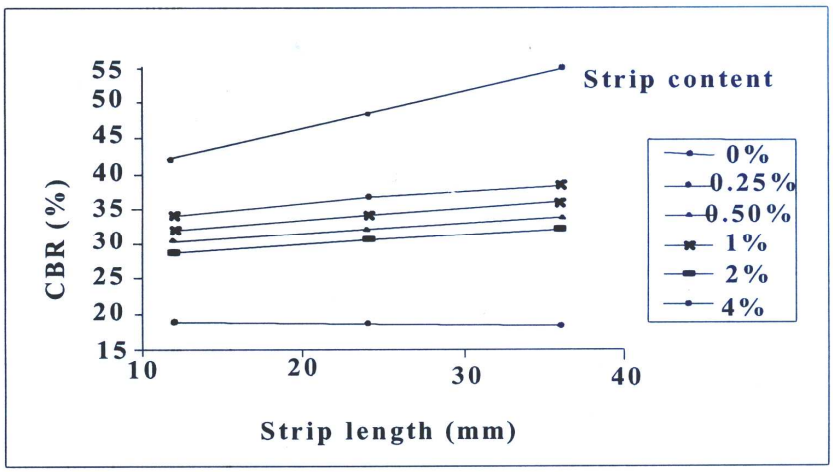

Fig. 2.7: CBR vs. strip length (after Choudhary et al., 2010)

Babu and Chouksey (2010) carried out experiments on stress-strain response of plastic waste mixed soil. Based on test results, they observed that the strength of soil is improved and compressibility reduced significantly with addition of a small percentage of plastic waste to the soil and there by bearing capacity improvement and settlement reduction in the design of shallow foundation.

Mohamed (2010) carried out small scale laboratory experimental programme systematically in a 500 mm × 500 mm × 200 mm tank to investigate the effect of width and depth of soft pocket on the ultimate bearing capacity of unreinforced loose and dense sand beds. The main conclusions from the experimental investigation were: The existence of soft pockets had a major impact in reducing the capacity of the soil to resist surface loads. With the increase in the width of soft pockets the bearing capacity reduced dramatically. It was found that for a soft pocket of similar footing width placed at a depth equal to footing width B, the bearing capacity reduced by 55% in loose sand and 70% in dense sand. Soft Pockets within the depth of 1.5B below the footing interfere with the failure zone underneath the foundation and result in significant loss to the carrying capacity. Failure of the reinforcing layers in loose sand beds was largely due to low frictional resistance between reinforcing layers and surrounding soil.

Maheshwari et al. (2012) investigated the influence of randomly distributed fibres on highly compressible clayey soil, series of laboratory model footing tests were conducted. The

dosages of polyester fibres having 12 mm in size were taken as 0.25%, 0.50% and 1.00%. The results of load settlement curve of different sizes of square footing on unreinforced soil and soil reinforced with various amount and depths of fibre reinforced soil were recorded. The results indicate that reinforcement of highly compressible clayey soil with randomly distributed fibres caused an increase in the ultimate bearing capacity and decrease in settlement at the ultimate load.

Rao et al. (2012) found from their experiments that fiber reinforced soil may be considered as a function of fibre weight fraction, aspect ratio and surface friction, soil characteristics (i.e. angle of internal friction) and its density and confining stress on shear strength of reinforced soils.

Kumar and Kaur (2012) investigated the potential benefits of fibre reinforced soil foundations over unreinforced sands subjected to inclined loads using total of 93 small scale model footing load tests. The effects of soil reinforcement (percentage of fibres), thickness of reinforced layer, soil density and load inclination on some prominent parameters such as ultimate bearing capacity, vertical settlement and horizontal deformation were investigated in this study. Test results indicated that the use of fibre reinforced sand made considerable improvement in ultimate bearing capacity, vertical settlement and horizontal deformation of foundation. A statistical model using multiple linear regression analysis based on the experimental data for predicting the settlement (Sp) of square footing on reinforced sand at any load applied was done where the dependent variable was predicted settlement (Sp).

Ahmadi and Bonab (2012) did experimental and analytical investigations of small-scale physical model tests. For this purpose, a set of tests were conducted with and without reinforcement on the top of the backfill. The specimens were different in terms of parameters like the number of geotextile layers, the vertical distance between layers and the strip footing distance from the wall. Soil failure in the bearing capacity step and the backfill shear zones was analysed using particle image velocimetry methods. Bearing capacity of the strip footings was studied using analytical procedures. The results indicated that a reinforcing top zone of the flexible retaining structures might be more appropriate than unreinforced case. The ultimate bearing capacity and wall deflection could be significantly improved by increasing the number of reinforcement layers. When three layers of reinforcement were used, there was an optimum vertical spacing of the layers at which the bearing capacity was the greatest. The study showed that the analytical solution and the results from the experimental models were in good agreement.

The **Colorado Division of Highways (2013)** suggested use of flexible reinforced soil retaining structures to meet architectural and environmental constraints in the design of I-70 at sites underlain by compressible soils in Glenwood Canyon. Four wall systems were constructed: Reinforced earth, Retained earth, Wire wall and Geotextile reinforced walls. The geotextile reinforced-soil retaining wall tests were described, and design, construction, and instrumentation details were provided. The test wall was 300 ft long and approximately 15 ft high. The wall incorporated four nonwoven geotextiles (each in two weights) in 10 test segments. Instrumentation was provided to monitor settlements and surface and internal deformation of the reinforced soil. The test wall had a gunnite facing. The wall was designed by conventional methods. However, some segments were assigned lower-than-usual factors of safety to provide a more critical test. Since construction, the wall had settled from 6 to more than 18 in due to foundation consolidation. Test wall performance, however, had been satisfactory, and none of the segments had exhibited distress. Wall design and performance relative to laboratory geotextile strength and creep test results were analysed, and it was concluded that safe, economical geotextile walls could be designed by existing methods.

Chandra Shekar Arya et al. (2013) carried out an experimental study to investigate the dry density and CBR behaviour of waste plastic (PET) content on stabilized red mud, fly ash and red mud fly ash mix. PET bottle of size less than 20 mm and bigger than 4.75 mm was taken and mixed in different proportions of 0.5, 1, 2, 3 and 4% by dry weight of red mud, fly ash, and red mud fly ash mix. From the test results it was found that with inclusion of plastic (1) The dry density of red mud, fly ash, red mud fly ash mix increases at 2% plastic content. And there after with the inclusion of plastic there is no increase in dry density. (2) The dry density of red mud, fly ash, red mud fly ash mix at 2% plastic content was found to increase from 1.53 g/cc, 1.21 g/cc, 1.38 g/cc to 1.62 g/cc, 1.27 g/cc, 1.44 g/cc. (3) The unsoaked and soaked CBR values increased with the varying plastic content and found to be optimum at 2% plastic content. (4) The unsoaked CBR values of unreinforced red mud, fly ash and red mud fly ash mix is found to be 2.92%, 8.03% and 7.6%. The unsoaked CBR values of reinforced red mud, fly ash and red mud fly ash is found to be 9.72%, 11.84% and 10.66% at 2% plastic content.

Haider Mohammed Mekkiya (2013) carried out experimental study on new soil improvement method with a minimum cost by using polymer fiber materials having a length of 3 cm in both directions and 2.5 mm in thickness, distributed in uniform medium dense sandy soil at different depths (b, 1.5b and 2b) below the footings. Three square footings have been used (5 cm, 7.5 cm and 10 cm) to carry the above investigation by using lever arm

loading system design for such purposes. These fibers were distributed from depth of (0.1b) below the footing base down to the investigated depth. It was found that the initial vertical settlement of footing was highly affected in the early stage of loading due to complex soil-fiber mixture (SFM) below the footing. The failure load value for proposed model in any case of loading increased compared with the un-reinforced soil by increasing the depth of improving below the footing. The bearing capacity ratio (BCR) for soil-fiber mixture has been increased by ratio of (1.4 to 2.5), (1.7 to 4.9) and (1.8 to 8) for footings (5 cm, 7.5 cm and 10 cm) respectively. The yield load-settlement for soil-fiber mixture system started at settlement of about 1.1% b while the yield load in un-reinforced soil started at smaller percentage which reflects the benefits of using such fiber material for improving soil behaviour. It is concluded that, the bearing capacity ratio increased from unreinforced to reinforced condition which reflect the benefit of using such polymer fiber material underneath footing as minimum cost solution for increasing the bearing capacity and reduces soil settlement.

Mahali and Sinha (2015) carried out a series of California bearing ratio (CBR) tests on reinforced stone dust. Three different sizes of PET strips were used in this study. The effect of strips content (0.25% to 2%) and length on the CBR value of reinforced stone dust were investigated. It was investigated that maximum CBR value of reinforced system is approximately 2.79 times that of unreinforced system.

Kala (2017) experimentally investigated the utilization of waste plastic as geotechnical material to solve both geotechnical and environmental problem. It was observed that there is considerable increase in bearing capacity value with the inclusion of plastic waste addition of 4% PET bottle plastic waste can improve the shear strength of the soil sample up to 39.9 kN/m^2.

2.2 Theoretical Studies

Review of some important theoretical studies on reinforced soil is arranged in chronological order as follows:

Chandrasekhar et al. (1998) carried out a plane strain elastic interaction analysis of a strip footing resting on a reinforced bed by utilizing a combined analytical and finite element method (FEM). After obtaining the stiffness matrix for the reinforced soil bed, the reinforced zone has been idealised as an equivalent orthotropic infinite strip (composite approach) and a multi layered system (discrete approach). In the analysis the interface between the strip

footing and the reinforced half plane had been assumed as (i) frictionless and (ii) fully bonded. The load-deformation behaviour of the reinforced soil obtained using above modelling had been compared with some available analytical and model tests results. The importance of performing the combined interaction analysis, taking into account of the deformational characteristic of the soil and the flexural behaviour of the foundation, had been brought out. The force distribution along the reinforcement was computed using Boussinesq's stress distribution theory. It was shown that the composite approach was simple to use and required minimum computational effort compared with the other methods, without sacrificing the accuracy of predictions. The analysis presented by the authors was based on elastic theory.

Belal and George (2000) carried out finite element analysis of reinforced soil retaining walls subjected to seismic loading. The meshing of the model consisted of 744 elements and 930 nodes. The elements were discretized into 4 noded quadrilateral elements. The retaining wall was designed as pseudo-static design procedure. Soil model was considered as Drucker Pager model. The properties of the soil were taken as Young's modulus E = 82680 kPa, Poisson's ratio = 0.3, cohesion c = 0, unit weight = 1628 kg/m^3, angle of internal friction $\phi = 37.5^o$ and angle of soil dilation $\psi = 10^o$.

Kellezi and Stromann (2003) analyzed spud can penetration for multi-layered critical soil conditions. Mohr-Coulomb elasto-plastic constitutive soil model was formulated for sand and clay layers considering the available soil parameters. Based on the same parameters extended Drucker Prager (DP) parameters for sand and von Mises parameters for clay were derived and used in the final FEM calculations. Two axisymmetric parts were created for soil and spud can and assembled them together in the initial phase. Spud can was taken as weightless material. 'Contact pair' modelled the non-linear soil-spud can interaction during penetration. The bottom spud can area was modeled as 'Master Surfaces' and the sea bottom area were modeled as 'Slave Surface'. A friction coefficient with its value of 0.6 is used for the tangential behavior between the spud can contact surface and soil, based on the parameters of the soil layer in contact. An elastic slip of 0.005 m was predefined for the study.

Basudhar et al. (2007) analyzed the behavior of a geotextile-reinforced sand-bed using the finite element method with a strip loading. The proposed method was calibrated and validated by comparing the results for some standard problems. Parametric studies examined the effect of reinforcement depth, the ratio of the modulus of elasticity of the geotextile and the soil, the variation of soil modulus with depth and soil layer properties on the settlement of the

footings. Based on the parametric study they concluded that the ratio of modulus of elasticity of soil (E_s) and the geotextile (E_g) played a role to detect the slip between soil and geotextile occurring along the contact surface, the reduction in settlement ratio at a modular ratio of 200 is about 12%, for a single layer of geotextile reinforcement the optimal placement depth is 0.6b, b being the strip width, the shear force in the geotextile increased up to a distance of 0.5 times of b from center and then decreased.

Madhavilatha et al. (2009) incorporated the numerical simulation of the behavior of Geo-cell reinforced sand foundation. The study was done with finite element analysis. The analyses were performed using displacement control method. Vertical deformation was applied in small increments of 0.025 mm per load step. Laboratory model testing was simulated numerically using the finite element code GEOFEM. Eight noded quadrilateral meshing was selected for finite element analysis by ABAQUS. The meshing consisted of 378 nodes and 1213 nodal points. As boundary condition or support condition roller support was taken at the two side faces of the model and hinge support was selected as the bottom boundary of the model.

Jie Gu (2011) carried out the numerical modeling of reinforced soil foundation by finite element modeling software. In geometrical modeling length to width ratio was considered as 10 hence taken as plain strain problem. He analyzed the model as 2-D plain strain model. Dimension of the domain was 7.5B×7.5B (B = foundation width) with 16500 elements. Soil was discretized using 8 noded iso-parametric elements as geogrid was modeled with surface element following Coulomb friction law. Uniform vertical downward displacement was applied. Horizontal displacements at the interface between footing and the soil were restrained to zero assuming perfect roughness to the interface and symmetry of the footing. The vertical displacement was applied in 1000 increments. In initial condition geostatic stress was applied. Gravity load due to the soil was applied in the first step of analysis. In Material modeling three types of material modeling were created; soil model, geogrid model and soil-geogrid interaction model. Soil model was taken as extended Drucker Pager model with isotropic elasto-plastic continuum. Interaction between two deformable bodies or a deformable body and a rigid body was considered in the model.

2.3 Motivation of the Present Research

It is observed from the literature review that **Gosavi et al. (2004), Consoli et al. (2005), Dutta and Venkatapparao *(*2007) and Babu and Chouksey (2010)** studied improvement of soil occurs with fibre inclusion. The overall engineering behaviour of soils improves with increase of strength indicated by peak friction angle and cohesion intercept leading to an increase in residual strength, ductility and energy absorption capacity.

Further **Chandrasekhar et al. (1998), Basudhar et al. (2007), Sharma et al. (2009), Madhavilatha and Somwanshi (2009), Al-Saidi (2009), Kumar and Kaur (2012)** also found that use of reinforcements results in increase in bearing capacity of footing placed on reinforced soil compared to that for unreinforced soil.

Thus it appears that there is scope of study on behaviour of clay mixed with randomly distributed plastic fibre obtained from waste PET bottles lies in recycling of plastic waste to reduce environmental hazard. Mixing of waste plastic strips with soil may therefore be done to increase the strength and stability of soil. In this context the present investigation has been carried out to study the behaviour of clayey soil mixed with waste PET bottle strips. This apart there remains a further scope of finding out the bearing capacity of footings with the soil improved with PET bottle strips. With this in view the present study has been carried out, with the objectives and scope of work outlined in Chapter 1, to examine the improvement of soil with PET bottle strips and also its effect on bearing capacity of footings.

Chapter 3

MATERIALS

3.0 General

In order to study the effect of ground improvement with use of PET bottle strips three types of soil have been used in the present study. To produce two more types of soil in addition to the primarily collected clayey soil itself the soil has been mixed with 10% and 20% sand. Different mixes have been obtained for those three types of soil by mixing them with different percent of PET bottle strips having different aspect ratios. Thus three types of materials, namely, soil, sand and PET bottle strips have been used in this study. They have been depicted in details in respect of their characterization and properties in the following sections.

3.1 Primary Clayey Soil

The clayey soil has been collected from some location at Jadavpur near Jadavpur University, Kolkata, West Bengal, India.

3.1.1 Sand

In this study, all experimental works have been undertaken with one type of locally collected sand. The sand is medium grained uniform quarry sand having sub-angular particles of weathered quartzite.

3.1.2 Soil Types Used

For the current investigation collected clayey soil and two types of amended soil (with sand) have been used in this present study. The three types of soil namely S1, S2 and S3 have been identified as follows:

1) Clayey soil (S1).
2) Soil with 90% clayey soil and 10% sand by weight of dry soil (S2).
3) Soil with 80% clayey soil and 20% sand by weight of dry soil (S3).

3.1.3 PET Bottle Strips as Reinforcement

For the present study, plastic strips have been obtained from PET bottles, procured for this purpose. Strips of required sizes of 5 mm × 5 mm, 5 mm × 10 mm and 5 mm × 15 mm with aspect ratios of 1, 2 and 3 have been prepared by cutting the PET bottles. These strips have been used as reinforcement. The content of PET bottle strips has been varied with 0.5%,

1.0%, 1.5% and 2.0% to study the effect of the variation of content with different proportion of the soil-reinforcement mixes. Typical waste PET bottle strips are shown in Fig. 3.1.

Fig. 3.1: PET bottle strips

3.2 Soil-reinforcement Mixes

The three types of soil namely S1, S2 and S3 as mentioned above have been mixed with reinforcements with three aspect ratios (1, 2 and 3). The combinations of all these mixes have been indicated in Table 3.1.

Table 3.1: Soil Reinforcement Mixes

Sl. No.	Soil Type	Aspect Ratio	% of Mix
1	S1	Nil	0
2	S1	1	0.5
3	S1		1
4	S1		1.5
5	S1		2
6	S1	2	0.5
7	S1		1
8	S1		1.5
9	S1		2
10	S1	3	0.5
11	S1		1
12	S1		1.5
13	S1		2
14	S2	Nil	0
15	S2	1	0.5
16	S2		1
17	S2		1.5
18	S2		2
19	S2	2	0.5
20	S2		1
21	S2		1.5
22	S2		2
23	S2	3	0.5
24	S2		1
25	S2		1.5
26	S2		2
27	S3	Nil	0
28	S3	1	0.5
29	S3		1
30	S3		1.5
31	S3		2
32	S3	2	0.5
33	S3		1
34	S3		1.5
35	S3		2
36	S3	3	0.5
37	S3		1
38	S3		1.5
39	S3		2

3.3 Material Properties

In order to determine different properties of original clayey soil, two types of soils amended with sand without PET bottle strips and also properties of different soil-reinforced mixes, various laboratory tests have been conducted. Each test has been performed thrice and the average value has been taken.

3.3.1 Test Program

In this section various tests conducted for determination of properties of three different types of soil, PET bottle strips and soil-PET bottle strip mixes have been described as mentioned in the test programs for different soil types- original and amended soils and PET bottle strip mixes have been presented in Tables 3.2, Table 3.3 and Table 3.4 respectively. The program tests of different types of materials have been presented in the following sections.

Soil-PET bottle strips mixes have been prepared with 3 types of soil (S1, S2 and S3) and PET bottle strips with 3 aspect ratios (1, 2 and 3) and for each aspect ratio 4 strip contexts (0.5%, 1.0%, 1.5% and 2.0%) have been taken. In this way total number of tests on each type mix becomes 36. The test program is furnished in Table 3.2 and 3.3 for soil and sand respectively.

Table 3.2: Test Program for soils (S1, S2 andS3)

Test	No. of tests	Remarks
Hydrometer Test		
Liquid Limit	3	
Plastic Limit	3	1 no. test for each
Standard Proctor Test: Maximum Dry Density and		type of soil
Optimum Moisture Content	3	S1, S2 and S3 for
Unconfined Compressive Strength	3	each test
Unconsolidated Undrained Triaxial Test	3	
Consolidation Test	3	

Table 3.3: Test Program for Sand

Test	No. of test
a. Sieve analysis test	1

Tests on plastic strips have been carried out for identification of characteristics of PET bottle strips has been presented in Table 3.4**.**

Table 3.4: Test Program for PET Bottle Strips

Property	No. of test
Average width	1
Average thickness	1
Average tensile strength	1
Density	1
Water absorption	1

The test program for soil-PET bottle strip mixes has been presented in Table 3.5.

Table 3.5: Test Program for Soil-PET Bottle Strip Mixes

Test	No. of tests	Remarks
Standard Proctor test: Maximum dry density (kN/m^3) and Optimum moisture content (%)	36	For each mix 1 no. test of each type
Unconfined compressive strength	36	
Unconsolidated undrained test	36	
Consolidation Test	36	

3.4 Test Procedures

Procedures of tests for determining engineering properties of different types of soil, PET bottle strips and soil-PET bottle strip mixes have been described in this section.

The three types of soil namely Clayey soil (S1), Soil with 90% clayey soil and 10% sand by weight of dry soil (S2) and Soil with 80% clayey soil and 20% sand by weight of dry soil (S3) without PET bottle strips has been tested. In this relevance procedure of Atterberg's limit, grain size distribution, standard Proctor compaction test, unconfined compressive strength test, and triaxial test (UU) have been described in this section. For locally available sand, particle size analysis by sieving method and for determination of tensile strength,

density and water absorption of PET bottle strips a brief procedure has been depicted in this section. In case of soil samples mixed with plastic strip of aspect ratios of 1, 2 and 3 procedures of standard Proctor test, unconfined compressive strength test and triaxial tests have been followed appropriately. Consolidation test was carried out on soil-PET bottle strip mixes have been performed after obtaining optimum percentage of plastic strip content to observe the change in compressibility behaviour of soil due to addition of strips of PET bottles.

3.4.1 Tests on Soil Samples

In order to determine the properties of clayey soil and sand amended clayey soils with PET bottle strips an attempt has been made to carry out various relevant tests for determination of their different properties. The procedures of these tests are described in the following sections.

3.4.1.1 Atterberg's Limit

Casagrande liquid limit device is used to determine the Liquid limit and plastic limit of the soil as per IS-2720 (Part 5).

The liquid limit of fine-grained soil is the water content at which soil behaves practically like a liquid but has small shear strength. Its flow closes the groove in just 25 blows in Casagrande liquid limit device and the corresponding water content is considered as liquid limit.

The plastic limit of fine-grained soil is the water content of the soil below which it ceases to be plastic. It begins to crumble when rolled into threads of 3 mm diameter and the corresponding water content is taken as the plastic limit.

3.4.1.2 Grain Size Distribution

Grain size distribution of the soil is to be determined by standard hydrometer method using a hydrometer confirming to IS-2720 (Part 4). This method is applicable, if less than appreciable percent of the material passes 75 micron IS sieve. A 100 ml soil suspension is prepared in a measuring cylinder with 50 g of dry soil and 5 g deflocculating agent (Sodium hexameta phosphate). The hydrometer reading is taken at 0 min, un1/4 min, ½ min, 1 min, 2 min, 4 min, 8 min, 15 min, 30 min, 60 min and 24 hour from the start of the test. The hydrometer reading is then corrected for meniscus correction, dispensing agent correction and temperature correction. Immersion correction is considered from 2 min, with the help of calibration curve of the hydrometer to find the depth of centre of hydrometer. The particle

size settling at the level of centre of hydrometer and the corresponding percent finer has been determined. The grain size distribution curve has then been plotted.

3.4.1.3 Standard Proctor Test

This Indian Standard code IS-2720 (Part 7) lays down the method for the determination of the relation between the water content and the dry density of soils using light compaction. In this test a 2.6 kg rammer falling through a height of 310 mm is used. The soil is uniformly mixed with requisite quantity of water. Then it is subjected to light compaction in proctor method. The soil is compacted in three layers applying 25 blows of hammer on each layer. The actual water content and dry density is then determined. The maximum dry densities and optimum moisture content of the unreinforced and reinforced soils are determined by standard proctor compaction. About 3 kg of dry soil passing through 20 mm IS sieve is taken. For compaction of soil-fibre mix, the required amount of fibre has been mixed with the dry soil before adding water. The test has been repeated for different water contents to find the optimum moisture content and maximum dry density.

3.4.1.4 Unconfined Compressive Strength Test

This Indian Standard code, IS-2720 (Part 10) describes the method for determining the unconfined compressive strength of clayey soil, undisturbed, remoulded or compacted, using controlled rate of strain. It is the load per unit area at which an unconfined cylindrical specimen of soil will fail in the axial compression test. Unconfined compression tests are carried out on cylindrical specimens of 38 mm diameter and 76 mm height. These specimens have been prepared at maximum dry unit weight and optimum moisture content state, with standard compaction. Initially all of the soil and half of the water and fibres are mixed, after which the proportions of water and fibre are gradually increased up to optimal water content and the required fibre percentage. The mix has been compacted in Proctor mould with desired water content and density. Then specimens have been extracted from the mould for carrying out unconfined compressive strength test. Stress-strain curves have been drawn and ultimate compressive strength has been determined for reinforced and unreinforced soil. Typically failed samples after the test are shown in Fig. 3.2.

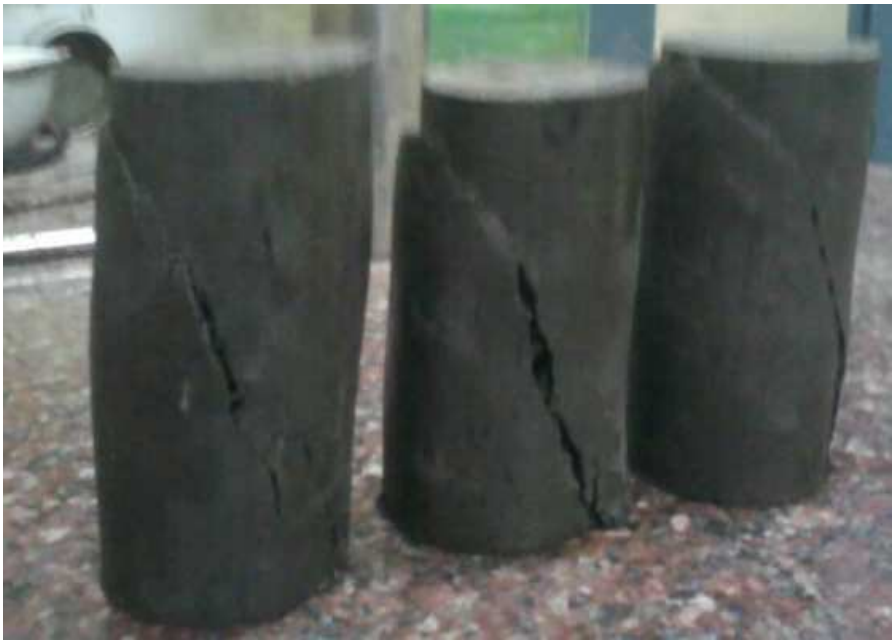

Fig. 3.2: Samples after failure

3.4.1.5 Triaxial Test (UU)

IS-2720 (Part 11) describes the test for the determination of the shear strength parameters of a specimen of saturated cohesive soil in the triaxial compression apparatus under conditions in which the cell pressure is maintained constant and there is no change in the total water content of the specimen. Unconsolidated undrained triaxial tests have been conducted on unreinforced and reinforced soil samples at the fibre contents and the aspect ratios. This test is limited to specimens in the form of right cylinders of nominal diameter 38 mm and of height 76 mm, twice the nominal diameter. The cylindrical specimens are prepared in a way similar to that explained earlier in unconfined compression tests. The tests have been conducted at three different confining pressures of 50 kPa, 100 kPa and 150 kPa. The stress-strain behaviour has been studied for both reinforced and unreinforced soils. Typically failed samples at the maximum axial stress at different confining pressures are shown in Fig. 3.3.

Fig. 3.3: Samples after failure at different confining pressures

3.4.1.6 Consolidation Test

This test was performed as per IS 2720 (Part 15) to determine the coefficient of volume change that a laterally confined soil specimen undergoes when subjected to different vertical pressures. From the measured data, the e vs. log p curve has been plotted. These data are useful in determining the coefficient of volume change and the pre-consolidation pressure of the soil. In addition, the data obtained have been used to determine the coefficient of consolidation of the soil. The soil sample has been kept inside oedometer ring, with a porous stone and filling paper at the top and another porous stone and filter paper at the bottom. The load on the sample was applied through a lever arm, and the compression of the specimen was measured by a micrometer dial gauge. The load intensity has been doubled every 24 hours. The specimen has been kept saturated with water throughout the test. Consolidation tests have been run in floating ring type oedometer under standard load increment ratio starting from 0.25 kg/cm^2 and going up to 8 kg/ cm^2 as is generally done.

3.4.2 Tests on Sand

The test procedure of grain size analysis of locally available sand has been described in this section.

3.4.2.1 Grain Size Analysis

The grain size analysis for sand was performed in accordance IS 2720 (Part 4) with recommended sieve sizes. An oven dried sample of soil retaining on 75 μm sieve was tested

with sieve sizes of IS 4.75 mm, 2 mm, 1 mm, 600 μm, 425 μm, 212 μm, 150 μm and 75 μm. Sieving was performed by arranging those sieves one over the other in order of mesh opening with largest aperture sieve on top and smallest one at the bottom. A pan is kept at the bottom and a cover is fixed at the top. The sand sample is put in the top sieve and the whole assembly was fitted on a sieve shaking machine. The assembly was shaken for 10 minutes. The portion of soil sample retained on each sieve was weighed to determine cumulative percentage retained and corresponding percentage finer in order to draw grain size distribution curve.

3.4.3 Test on PET Bottle Strips

In order to determine the properties of PET bottle strips different relevant tests for determination of its tensile strength, density and water absorption have been carried out.

3.4.3.1 Average Thickness

Thickness of PET bottle strips was measured by micrometer with least count of Vernier scale of 0.01 mm. In order to find the average thickness ten samples were tested. The variation ranged between $\pm$ 0.02 mm.

3.4.3.2 Tensile Strength

ASTM D638 describes the test method covers the determination of the tensile properties of plastics in the form of standard dumbbell-shaped test specimens when tested under defined conditions of pre-treatment, temperature, humidity, and testing machine speed. This test method can be used for testing materials of any thickness up to 14 mm. Tensile strength of PET bottle strip has been obtained by testing according to the method given in ASTM D638.

3.4.3.3 Density

ASTM D792 describes the method of determination of the specific gravity (relative density) and density of solid plastics in forms such as sheets, rods, tubes or moulded items. The density of PET bottle strip has been obtained following the method given in ASTM D792.

3.4.3.4 Water Absorption

In this test the plastic strips were immersed into the water for 24 hours for examining the water absorption capacity of the PET bottle strips. In this way, the water absorption of PET bottle strips was determined with respect to its dry weight.

3.5 Presentation of Results of Material Testing

In this section an attempt has been made to present the test results of soil, PET bottle strips and soil-PET bottle strip mixes to summarize the material properties based on the results of the tests conducted as per the test programs described earlier.

3.5.1 Test Results on Sand

In this section the results of tests on sand have been presented to find properties of clean sand used to prepare two types of amended soils. Grain size distribution curve of clean sand has been presented in Fig. 3.4. The characterization and strength properties of clean sand have been presented in Table 3.6.

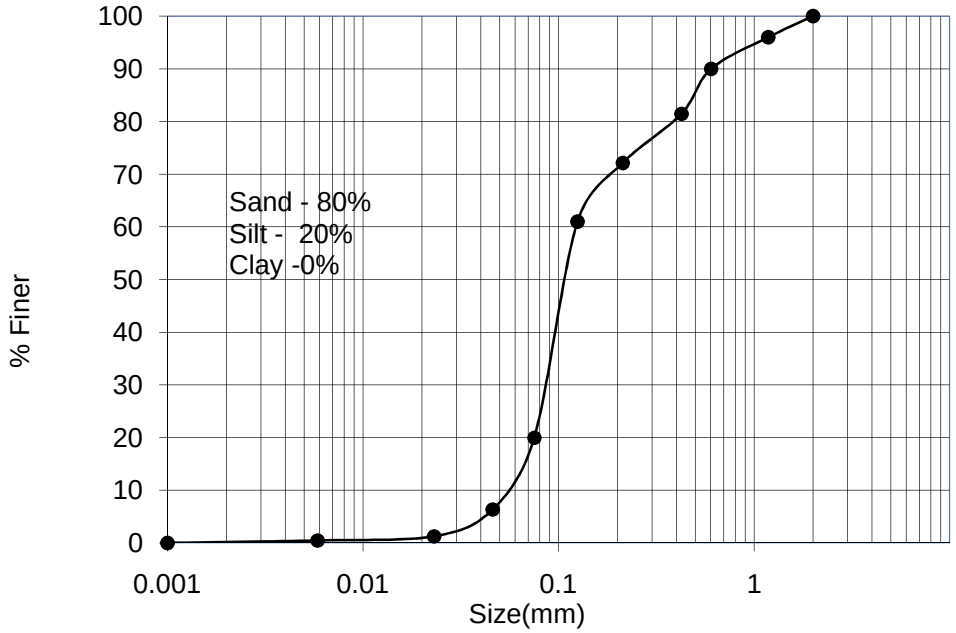

Fig. 3.4: Grain size distribution curve of sand

Table 3.6: Properties of Sand

Test	Grain Size Distribution
Grain size	Sand 80%
	Silt 20%

3.5.2 Test Results on PET Bottle Strips

In this section the results of tests on PET bottle strips have been presented in Table 3.6. These properties are useful to understand the composite properties of soil-PET bottle strip mixes.

Table 3.7: Properties of PET bottle strips

Sl. no.	Test	Test Results
1	Average thickness	0.5 mm
2	Average tensile strength	184.8 kg/cm^2
3	Density	1.38 gm/cm^3
4	Water absorption	nil

3.5.3 Test Results on Soil Type (S1)

In this section the results of tests on Soil Type S1 have been presented to find various properties of this soil type. Grain size distribution curve of clayey soil has been presented in Fig. 3.5. Standard Proctor Compaction curves for clayey soil have been shown in Fig. 3.6. Figures 3.7 and 3.8 present axial stress-strain curves obtained from UU triaxial tests and Mohr circles respectively to obtain strength parameters.

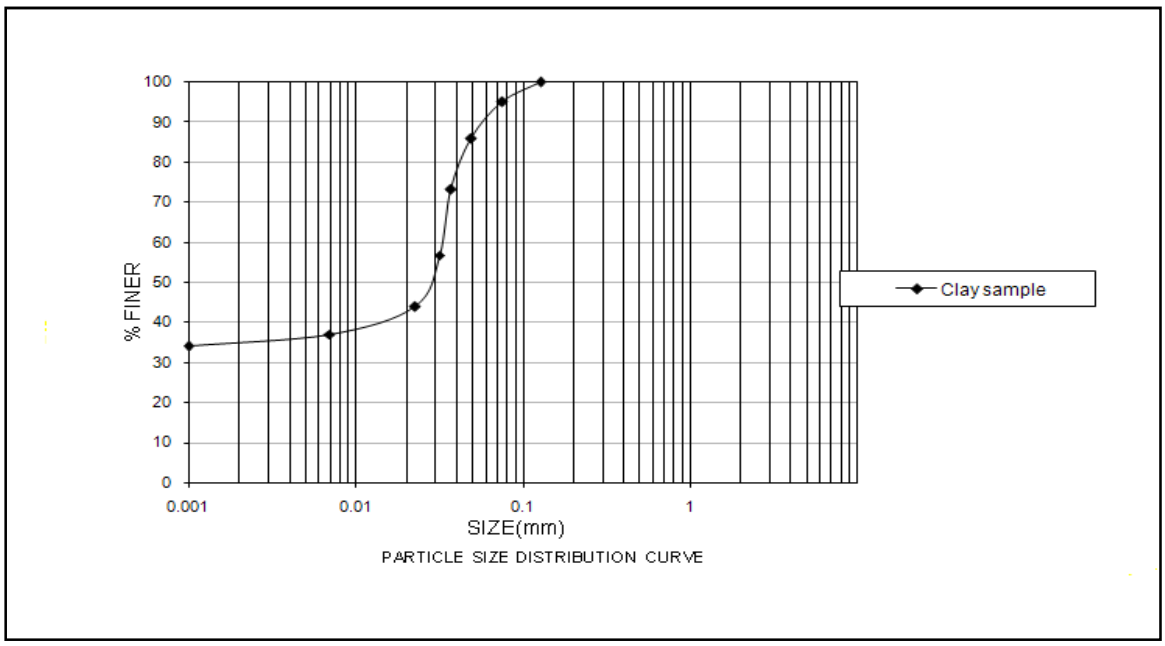

Fig. 3.5: Grain size distribution curve of the clayey S1 type soil

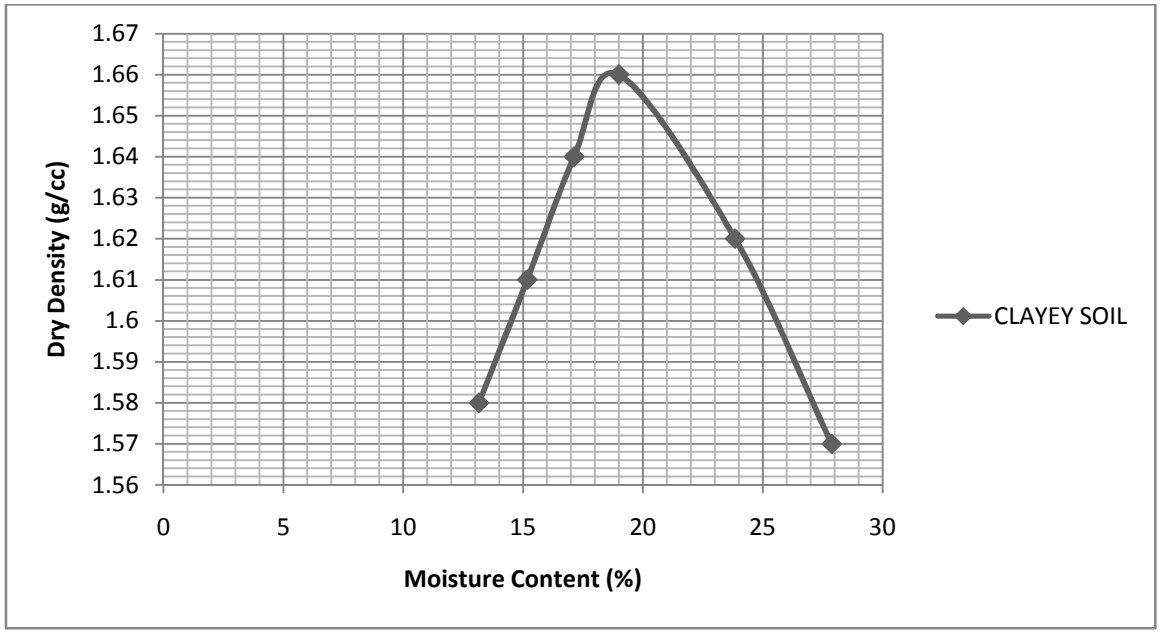

Fig. 3.6: Standard Proctor Compaction Curve

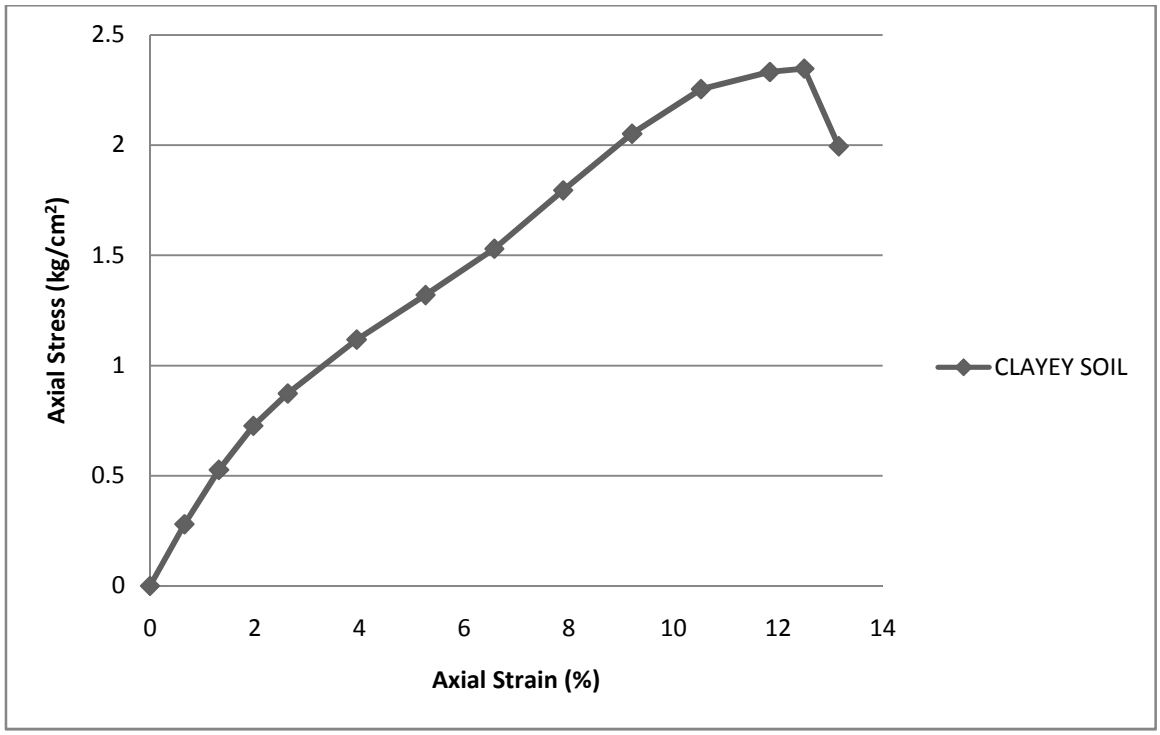

Fig. 3.7: Axial Stress vs. Axial Strain Curve

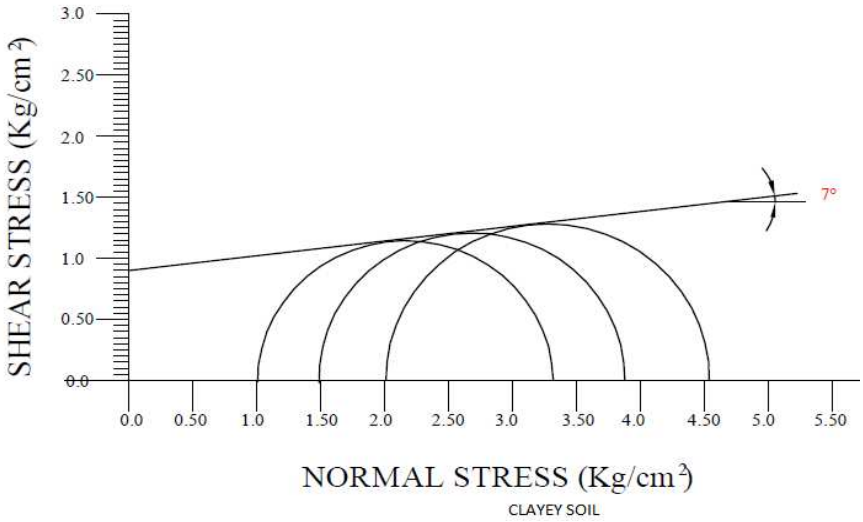

Fig. 3.8: Mohr circle- Shear stress vs. Normal stress

3.5.4 Test Results of Soil Type (S2)

This section presents the results of tests on Soil Type S2 to obtain various properties of this soil type. Grain size distribution curve of clayey soil has been presented in Fig. 3.9. Standard Proctor Compaction curves for clayey soil have been shown in Fig. 3.10. Figures 3.11 and 3.12 present axial stress-strain curves obtained from UU triaxial tests and Mohr circles respectively to obtain strength parameters.

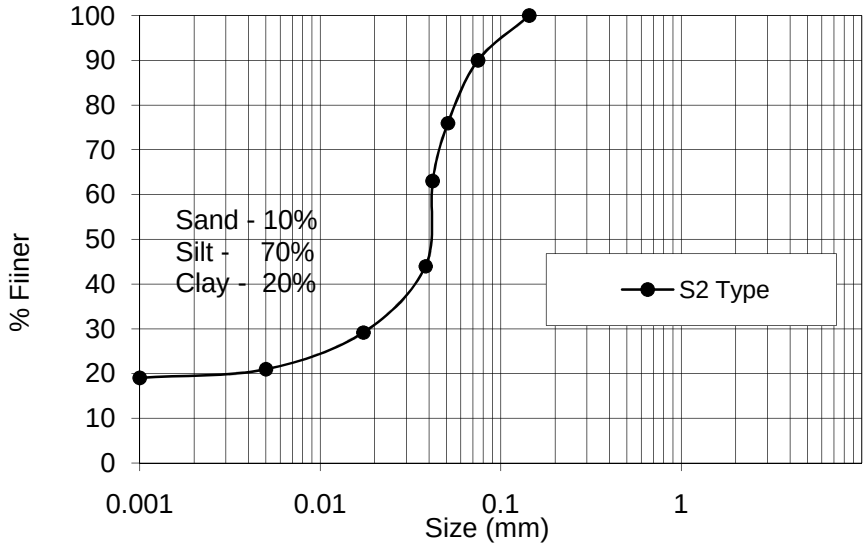

Fig. 3.9: Grain size distribution curve of the S2 Type soil

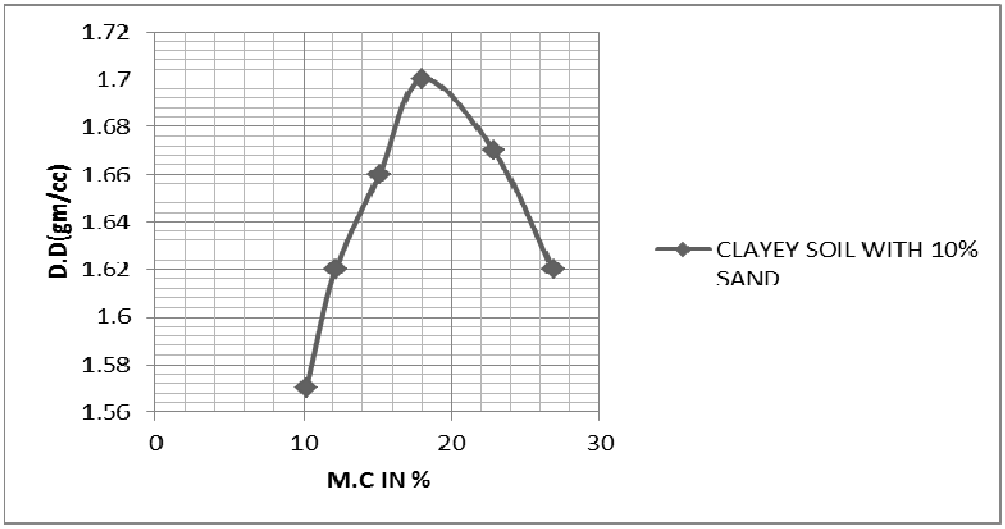

Fig. 3.10: Standard Proctor Compaction Curve

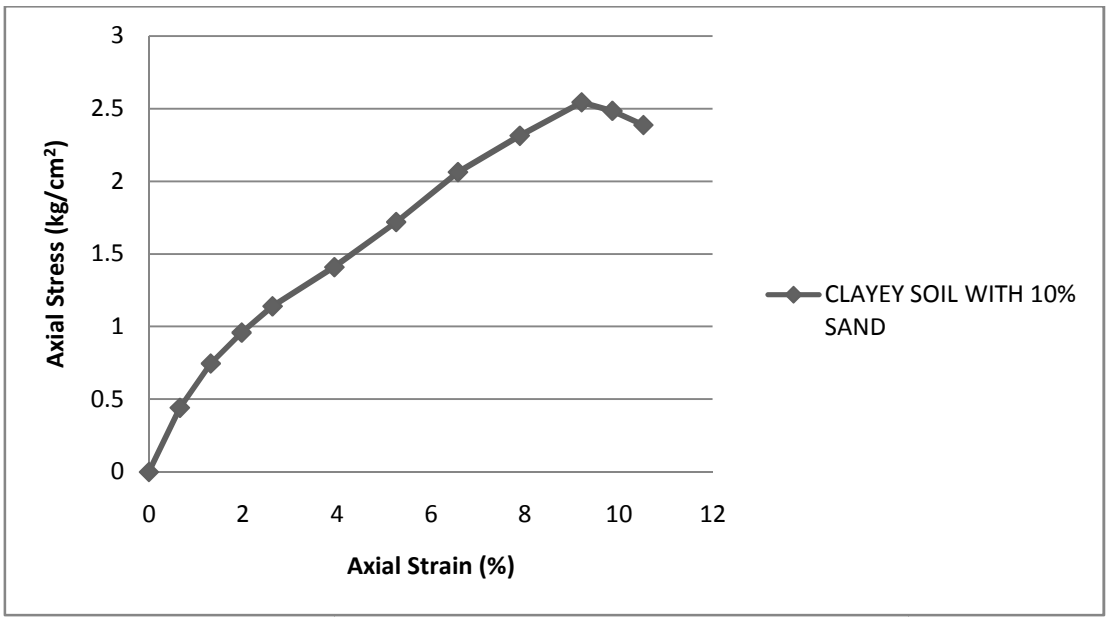

Fig. 3.11: Axial stress vs. axial strain curve

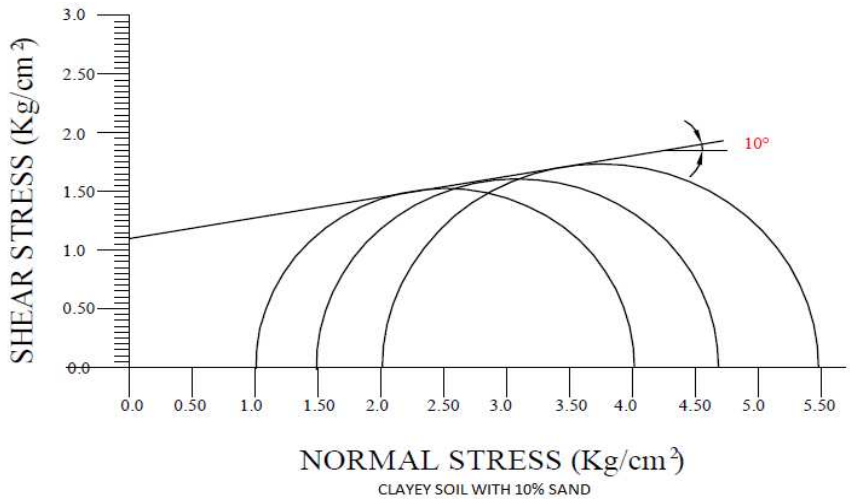

Fig. 3.12: Mohr circle- Shear stress vs. Normal stress

3.5.5 Test Results of Soil Type (S3)

In this section the results of tests on Soil Type S3 have been presented to find various properties of this soil type. Grain size distribution curve of clayey soil has been presented in Fig. 3.13. Standard Proctor Compaction curves for clayey soil have been shown in Fig. 3.14. Figures 3.15 and 3.16 present axial stress-strain curves obtained from UU triaxial tests and Mohr circles respectively to obtain strength parameters.

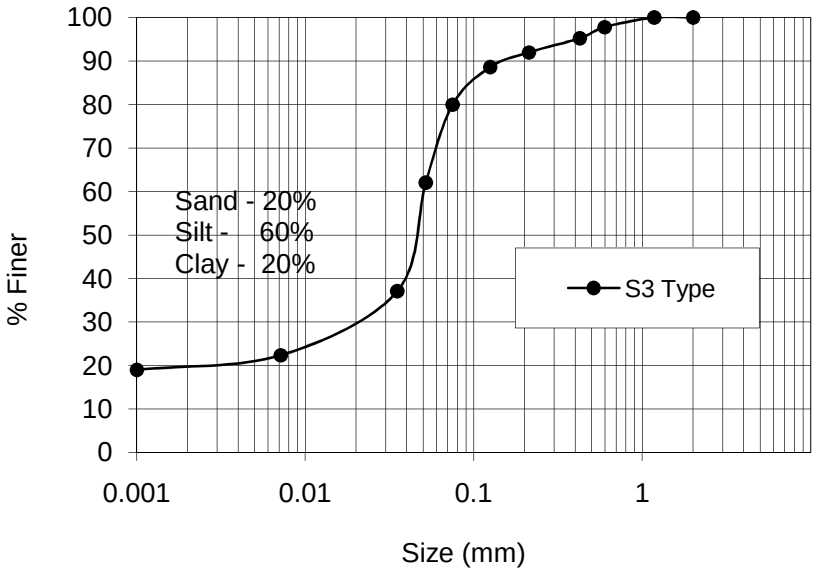

Fig. 3.13: Grain size distribution curve of the S3 Type soil

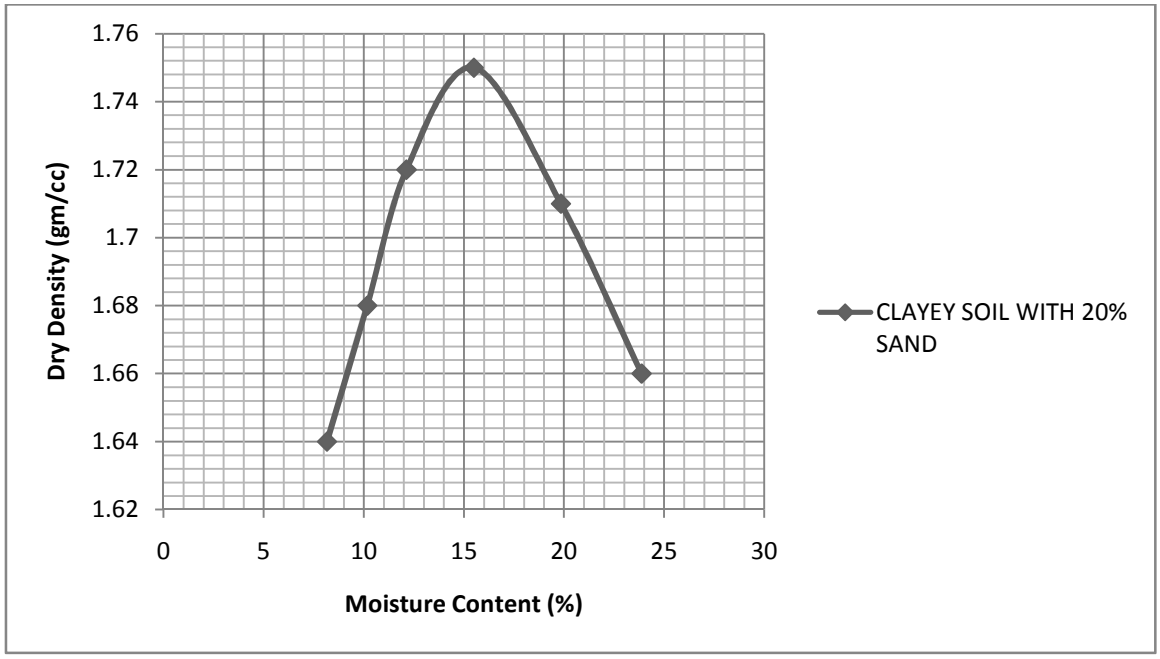

Fig. 3.14: Standard Proctor Compaction Curve

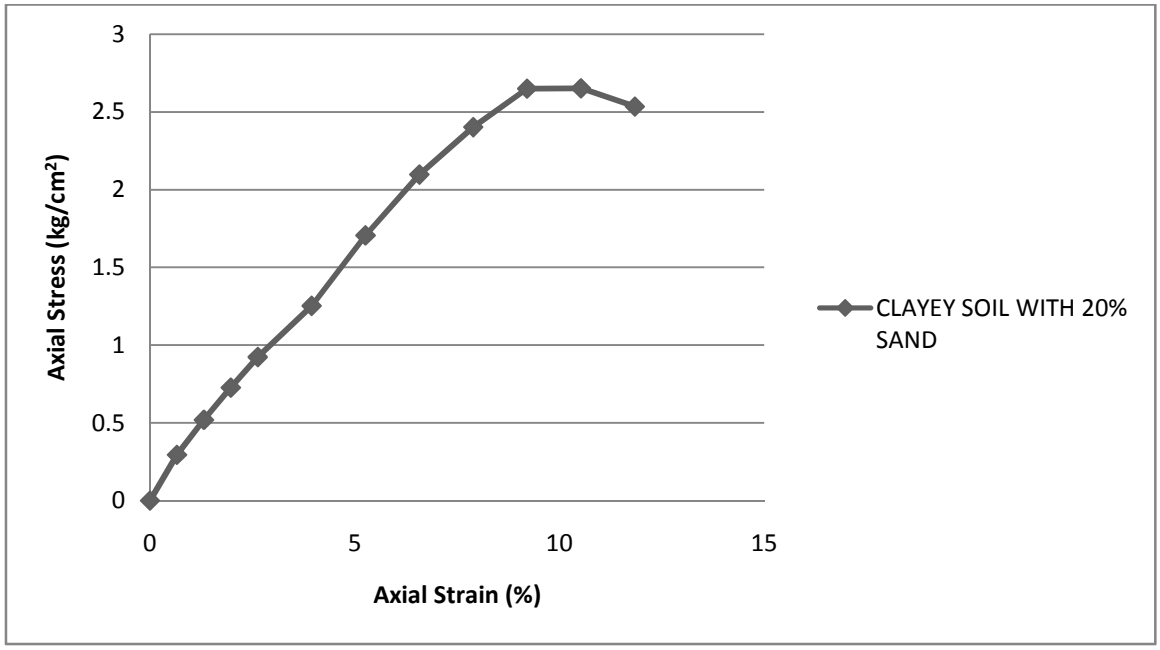

Fig. 3.15: Axial stress vs. axial strain

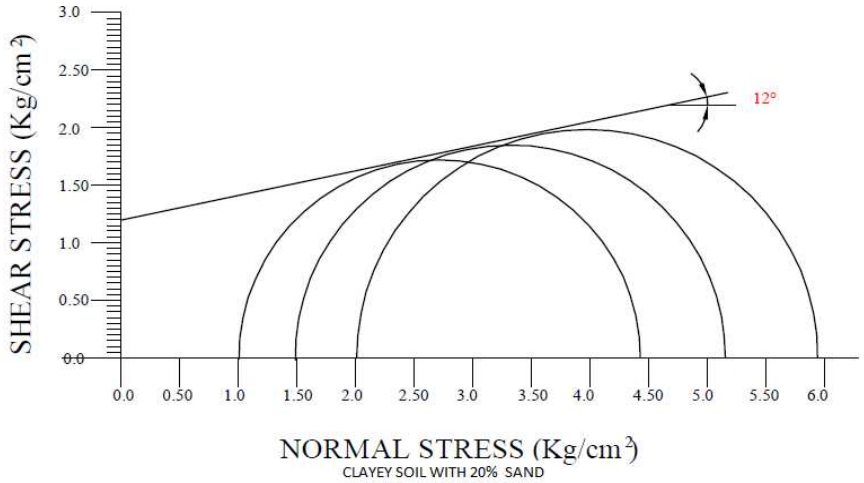

Fig. 3.16: Mohr circle- Shear stress vs. Normal stress

Based on all these figures an attempt has been made to obtain the properties of soil of different types. The characterization and strength properties of different types of soil have been presented in Table 3.7.

Table 3.7: Properties of Soil

Test	Property	Soil Type		
		S1	S2	S3
Grain size	Clay (%)	34	29	25
	Silt (%)	59	56	51
	Sand (%)	7	15	24
Atterberg's Limit	Liquid Limit (%)	54	48	42
	Plastic Limit (%)	22.64	23	24
	Plasticity Index (%)	31.36	25	18
Standard Proctor Compaction	Max. Dry Density (g/cm^3)	1.65	1.72	1.8
	Optimum Moisture Content (%)	19	18	15.4
UU Triaxial	Cohesion (kg/cm^2), c	0.9	1.1	1.2
	Angle of Internal Friction (ϕ)	7^o	10^o	12^o
	Modulus of Elasticity (kg/cm^2), E	13	15	18

3.6 Results of Tests on Soil-PET Bottle Strip Mix

The results of the tests conducted on soil-PET bottle strip mixes have been presented in this section. Based on the tests carried out according to the test program presented earlier in Table 3.5, the obtained results have been furnished in graphical forms in the following sections.

3.6.1 Mix S1+AR1

In this section the results of tests on different types of soil have been presented to find various properties of these soil types. Standard Proctor Compaction curves, axial stress-strain curves as obtained from UU triaxial tests and Mohr circles of stress for determination of shear strength parameters for the mix for strip content of 0.5%, 1.0%, 1.5% and 2.0% have been shown in Figs. 3.17 to 3.19, 3.20 to 3.22, 3.23 to 3.25 and 3.26 to 3.28 respectively.

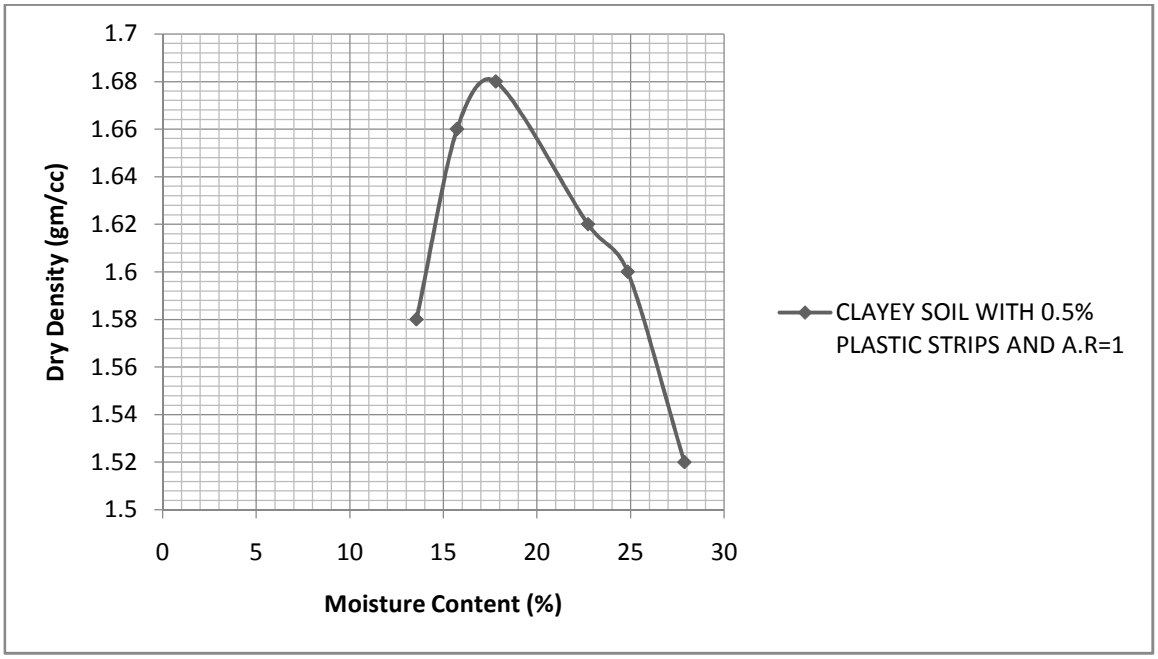

Fig. 3.17: Standard Proctor Compaction Curve

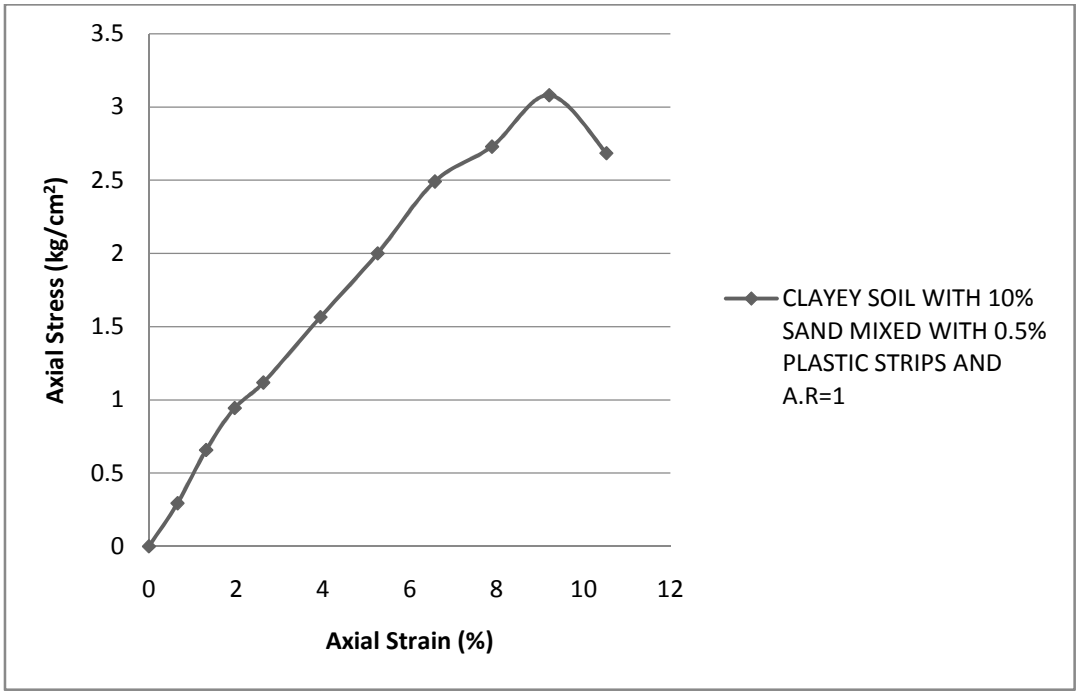

Fig. 3.18: Axial stress vs. Axial strain

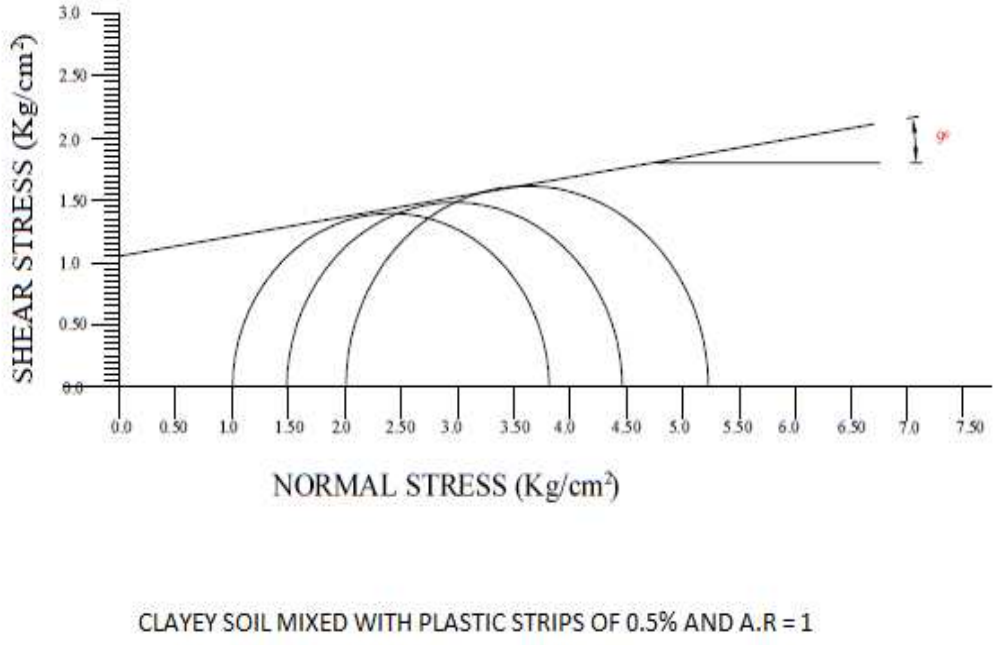

Fig. 3.19: Mohr Circle - Shear stress vs. Normal stress

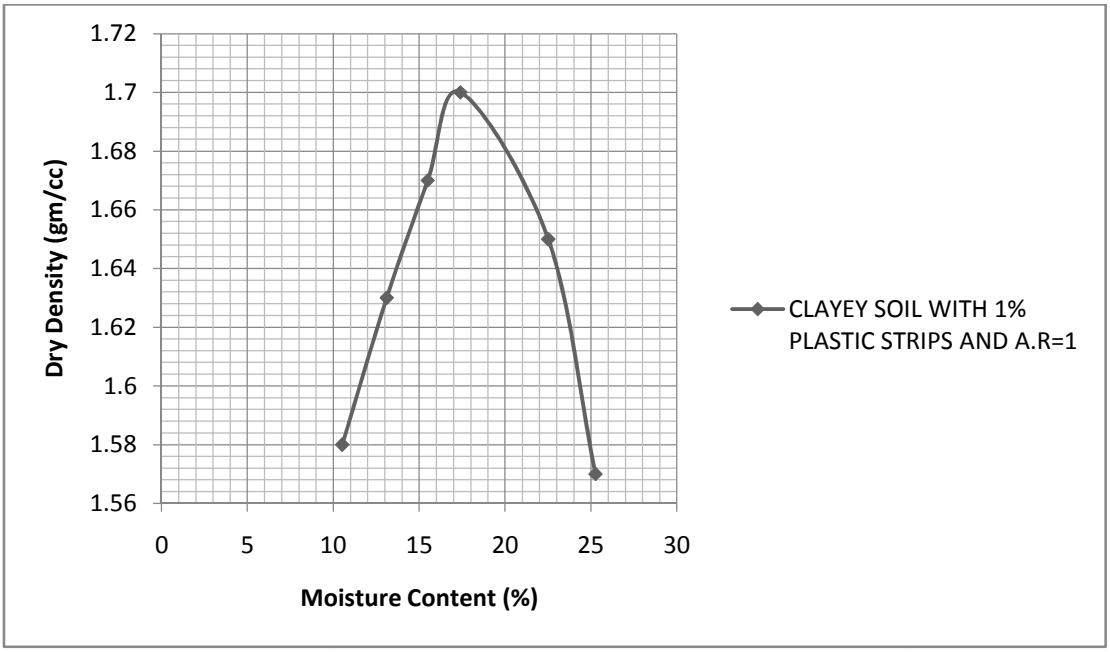

Fig. 3.20: Standard Proctor Compaction Curve

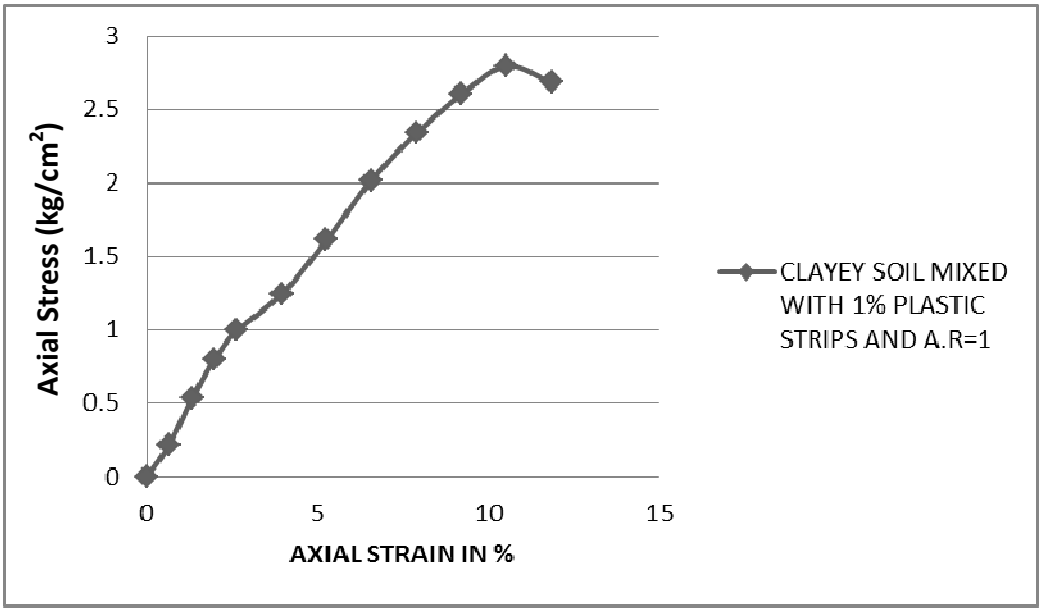

Fig. 3.21: Axial stress vs. Axial strain

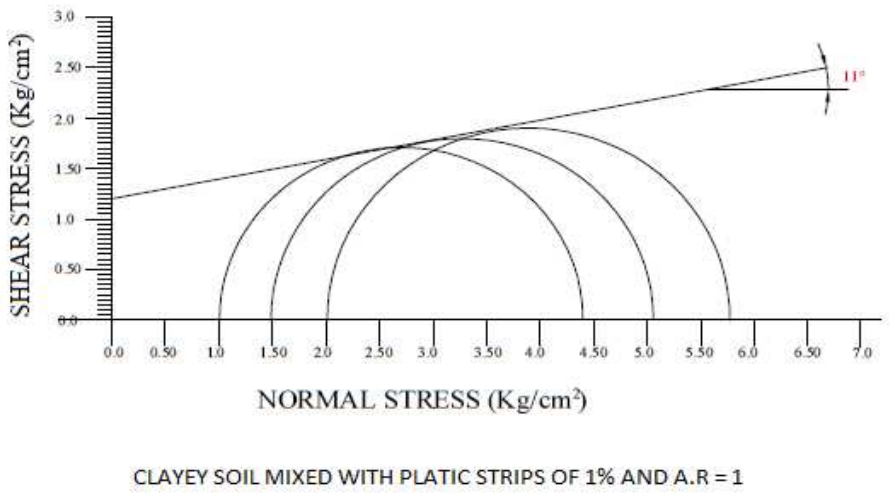

Fig. 3.22: Mohr Circle - Shear stress vs. Normal stress

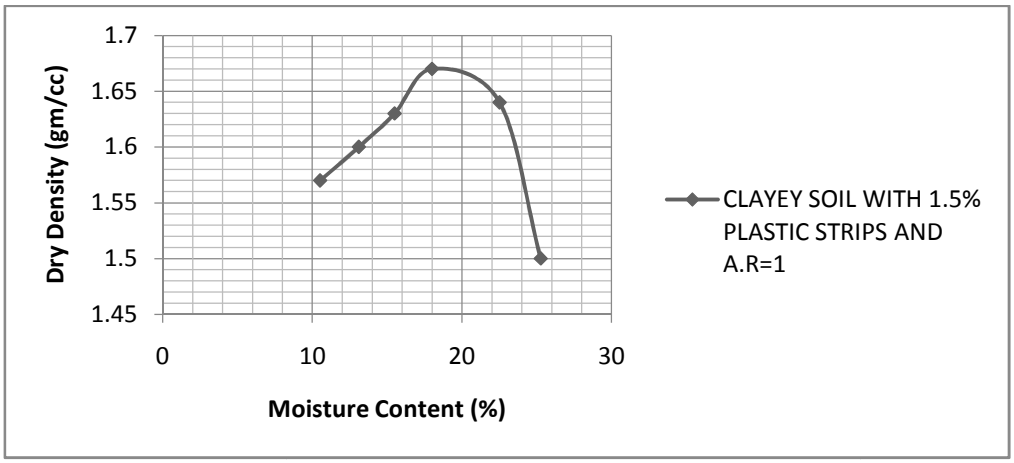

Fig. 3.23: Standard Proctor Compaction Curve

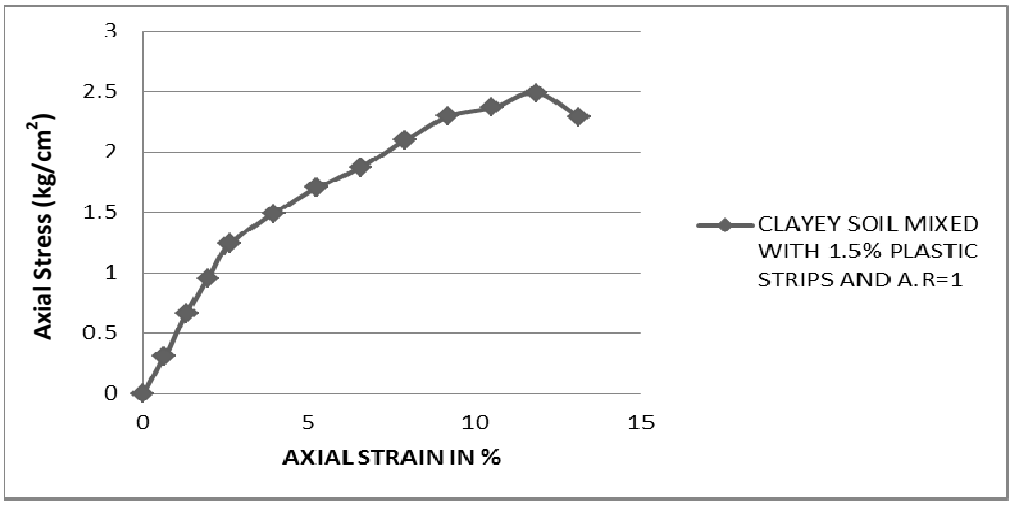

Fig. 3.24: Axial stress vs. Axial strain

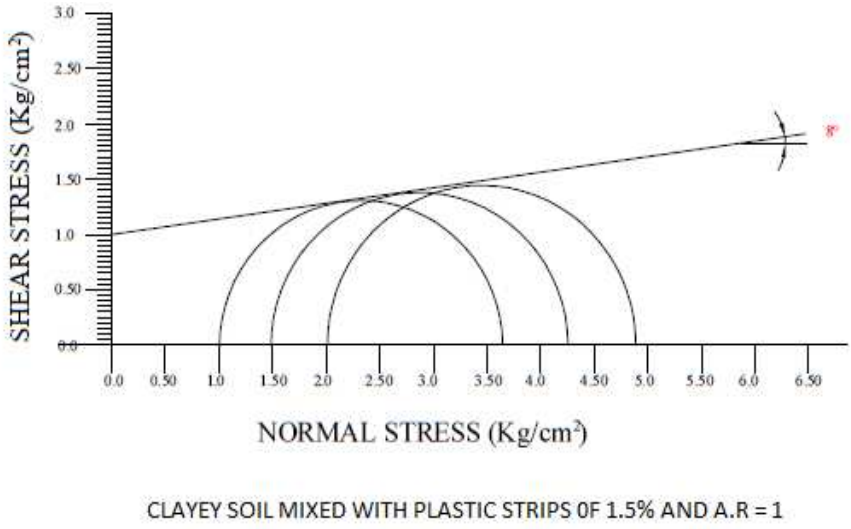

Fig. 3.25: Mohr Circle - Shear stress vs. Normal stress

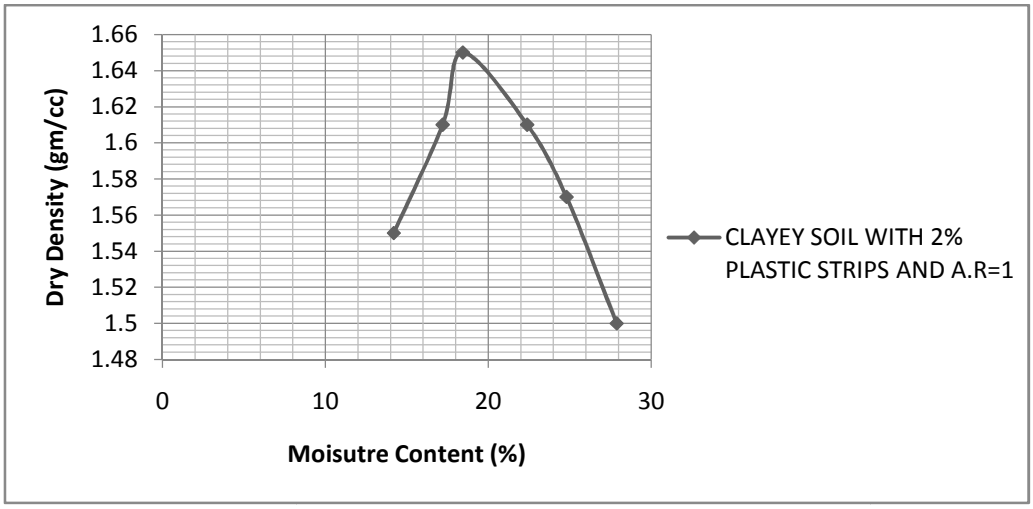

Fig. 3.26: Standard Proctor Compaction Curve

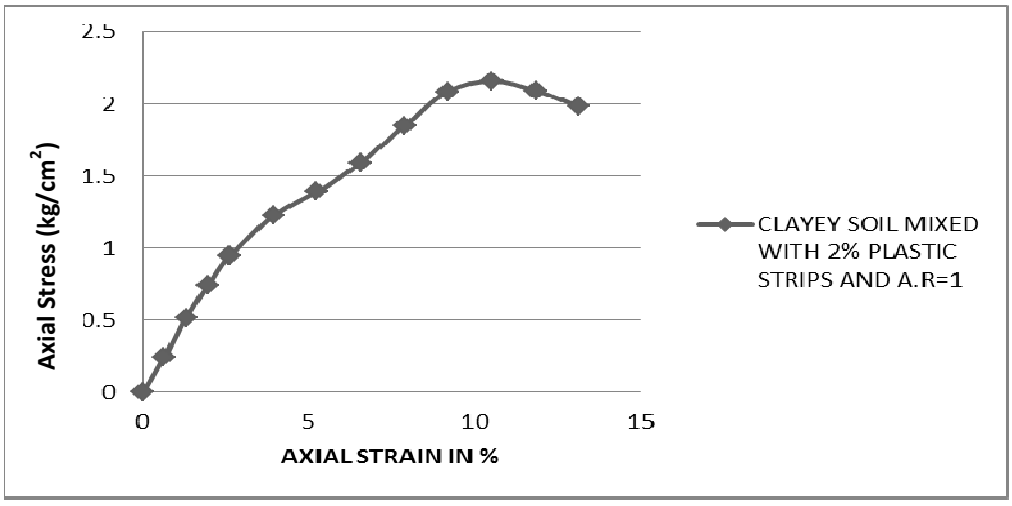

Fig. 3.27: Axial stress vs. Axial strain

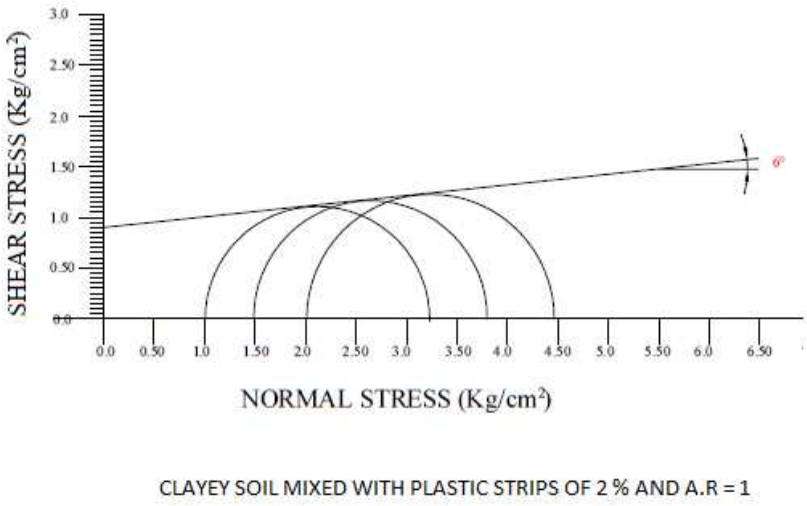

Fig. 3.28: Mohr Circle - Shear stress vs. Normal stress

3.6.2 Test Result of S1+AR2

In this section the results of tests on different types of soil have been presented to find various properties of these soil types. Standard Proctor Compaction curves, axial stress-strain curves as obtained from UU triaxial tests and Mohr circles of stress for determining shear strength parameters for the mix for strip content of 0.5%, 1.0%, 1.5% and 2.0% have been shown in Figs. 3.29 to 3.31, 3.32 to 3.34, 3.35 to 3.37 and 3.38 to 3.40 respectively.

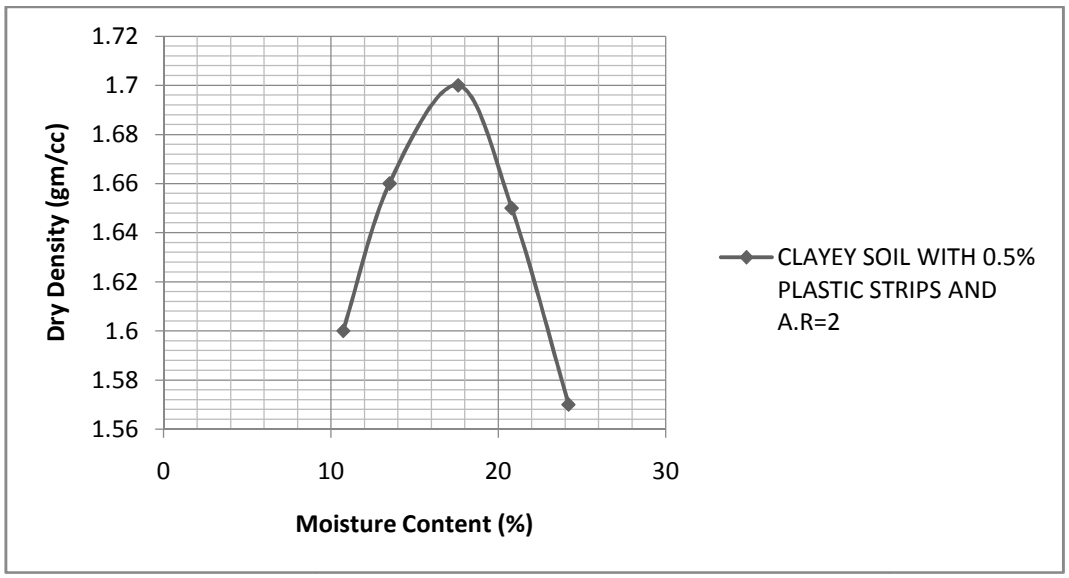

Fig. 3.29: Standard Proctor Compaction Curve

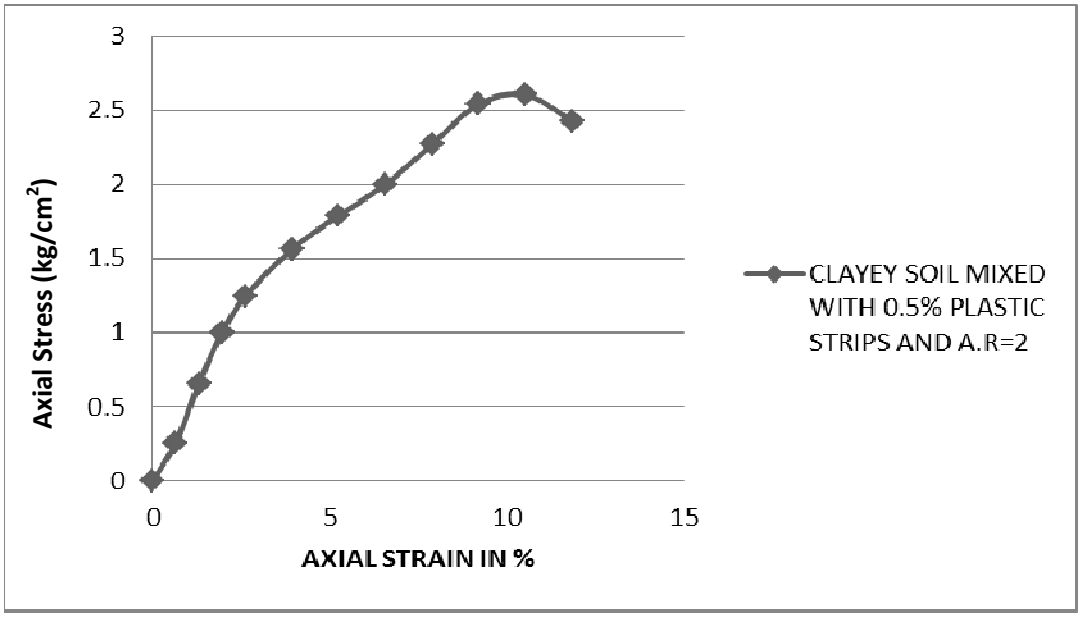

Fig. 3.30: Axial stress vs. Axial strain

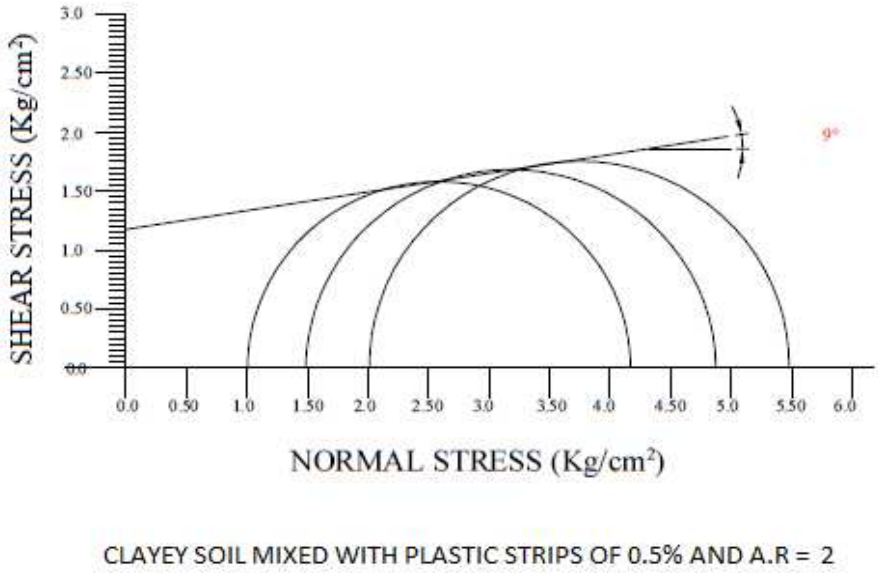

Fig. 3.31: Mohr Circle - Shear stress vs. Normal stress

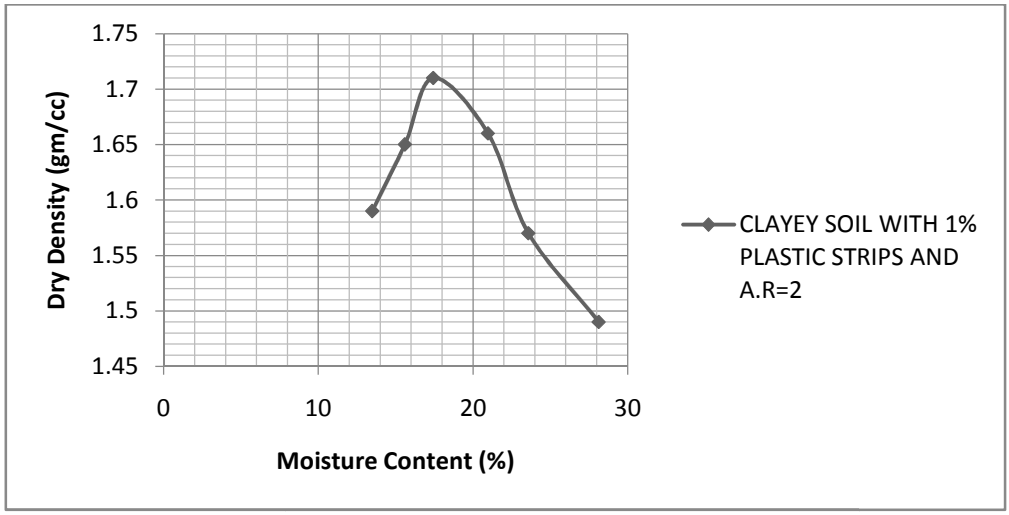

Fig. 3.32: Standard Proctor Compaction Curve

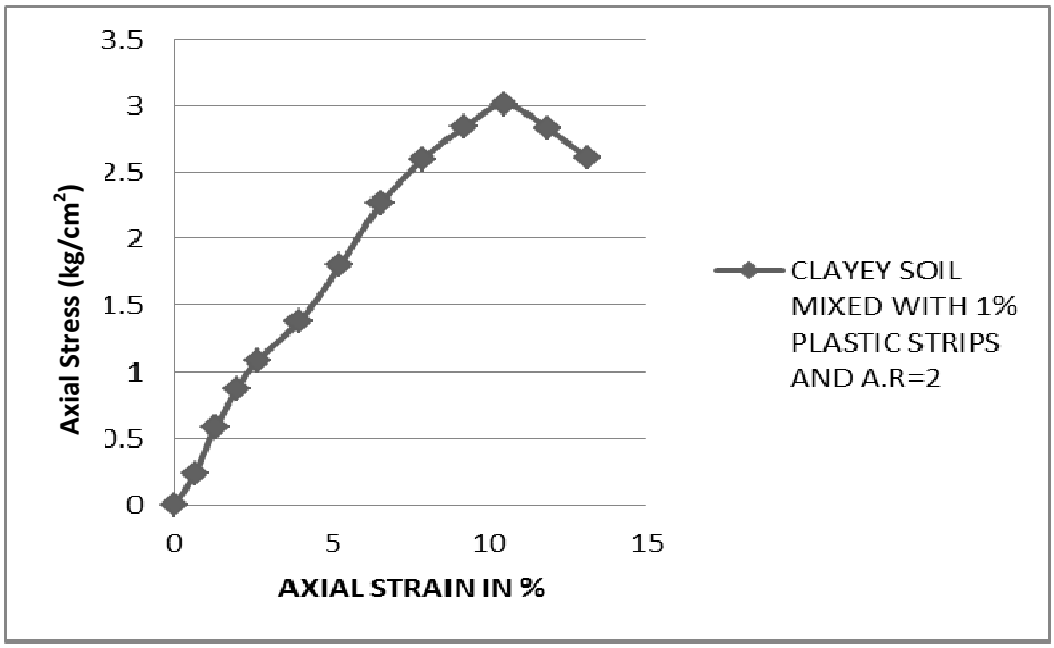

Fig. 3.33: Axial stress vs. Axial strain

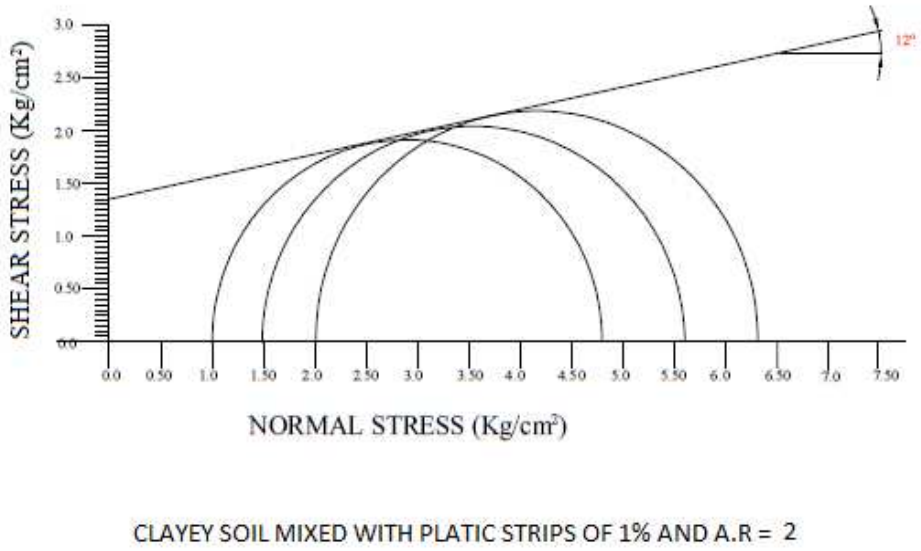

Fig. 3.34: Mohr Circle - Shear stress vs. Normal stress

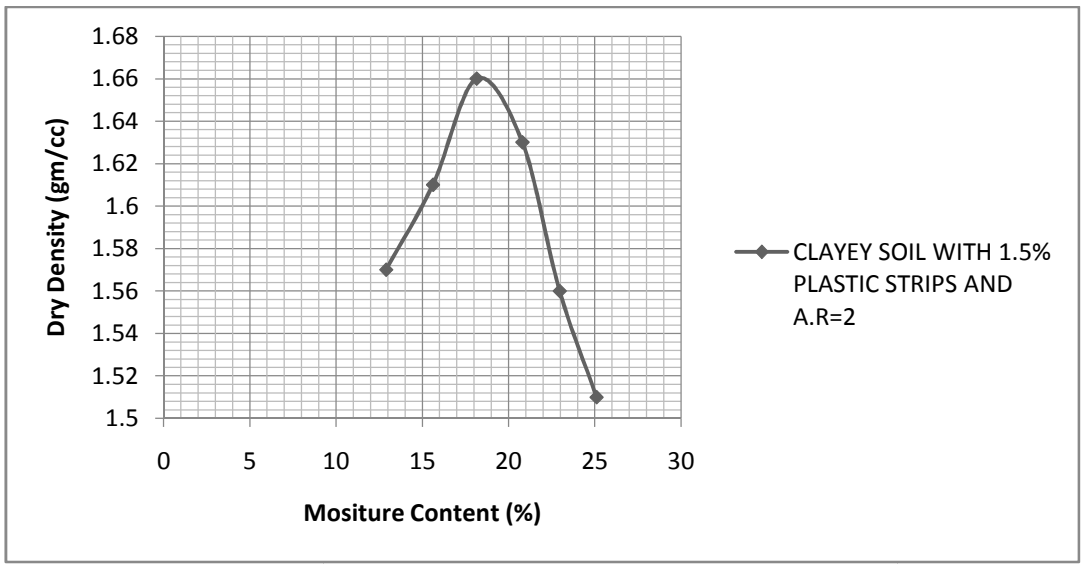

Fig. 3.35: Standard Proctor Compaction Curve

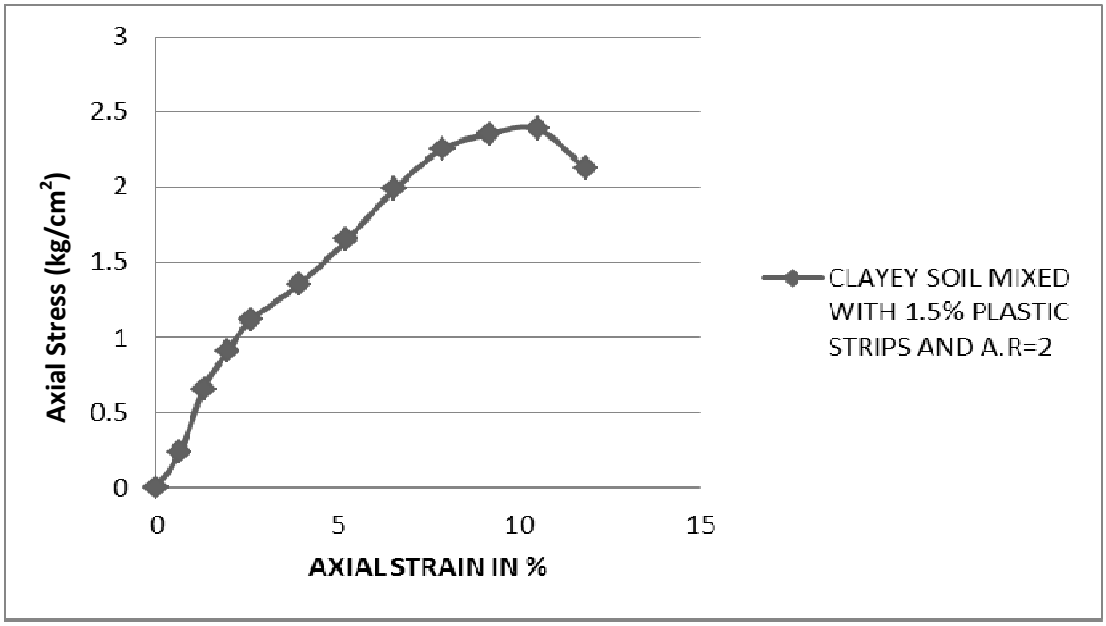

Fig. 3.36: Axial stress vs. Axial strain

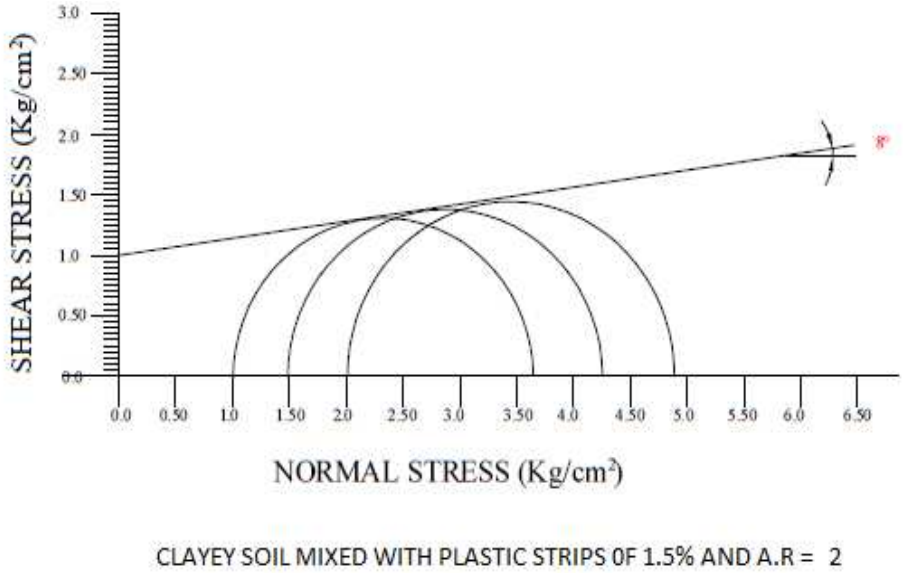

Fig. 3.37: Mohr Circle - Shear stress vs. Normal stress

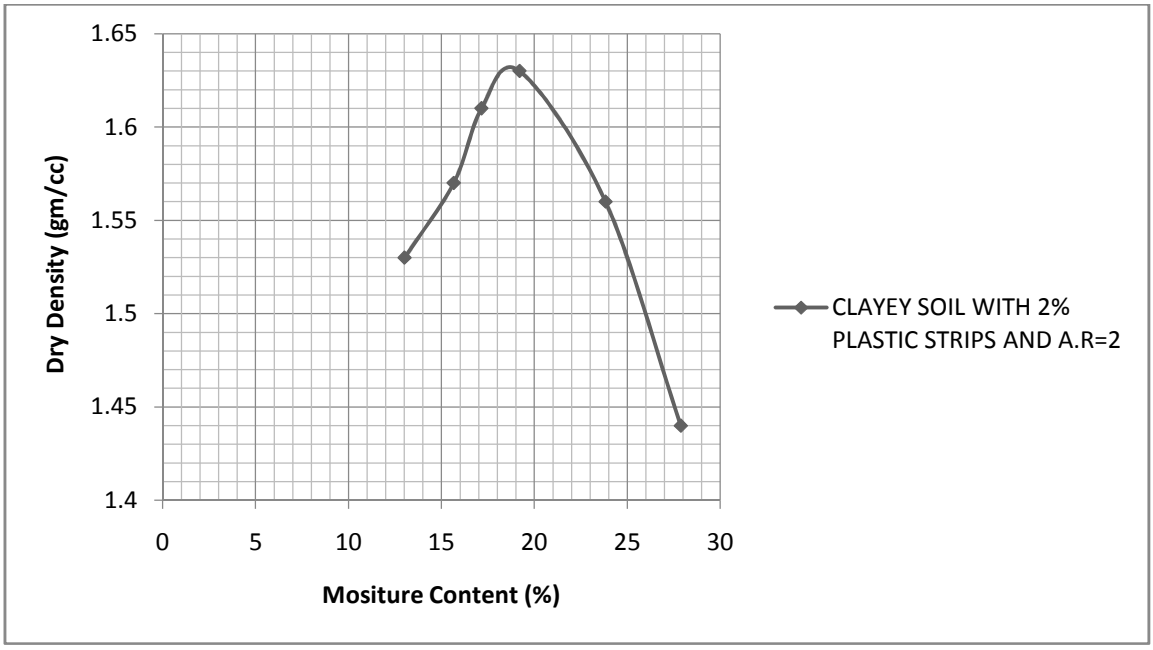

Fig. 3.38: Standard Proctor Compaction Curve

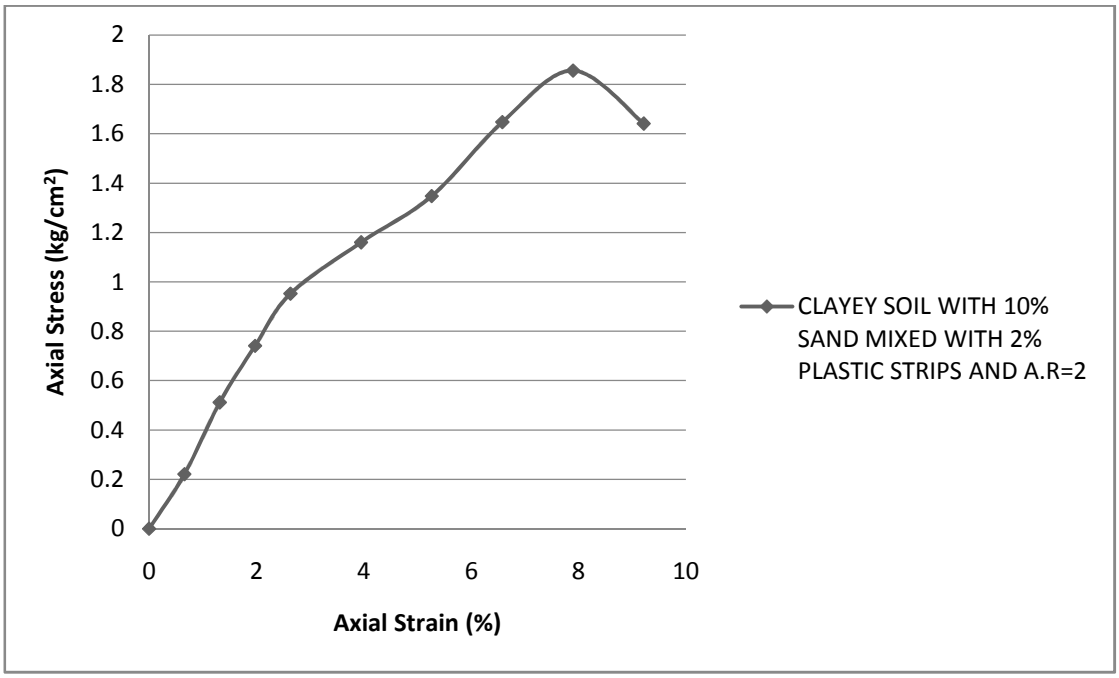

Fig. 3.39: Axial stress vs. Axial strain

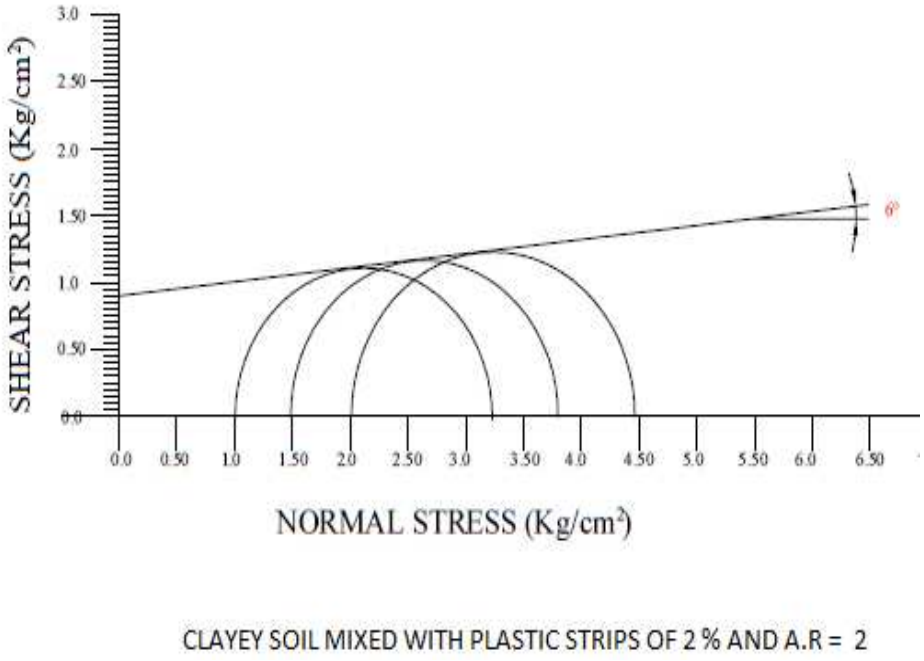

Fig. 3.40: Mohr Circle - Shear stress vs. Normal stress

3.6.3 Test Result of S1+AR3

In this section the results of tests on different types of soil have been presented to find various properties of these soil types. Standard Proctor Compaction curves, axial stress-strain curves as obtained from UU triaxial tests and Mohr circles of stress for determining shear strength parameters for the mix for strip content of 0.5%, 1.0%, 1.5% and 2.0% have been shown in Figs. 3.41 to 3.43, 3.44 to 3.46, 3.47 to 3.49 and 3.50 to 3.52 respectively.

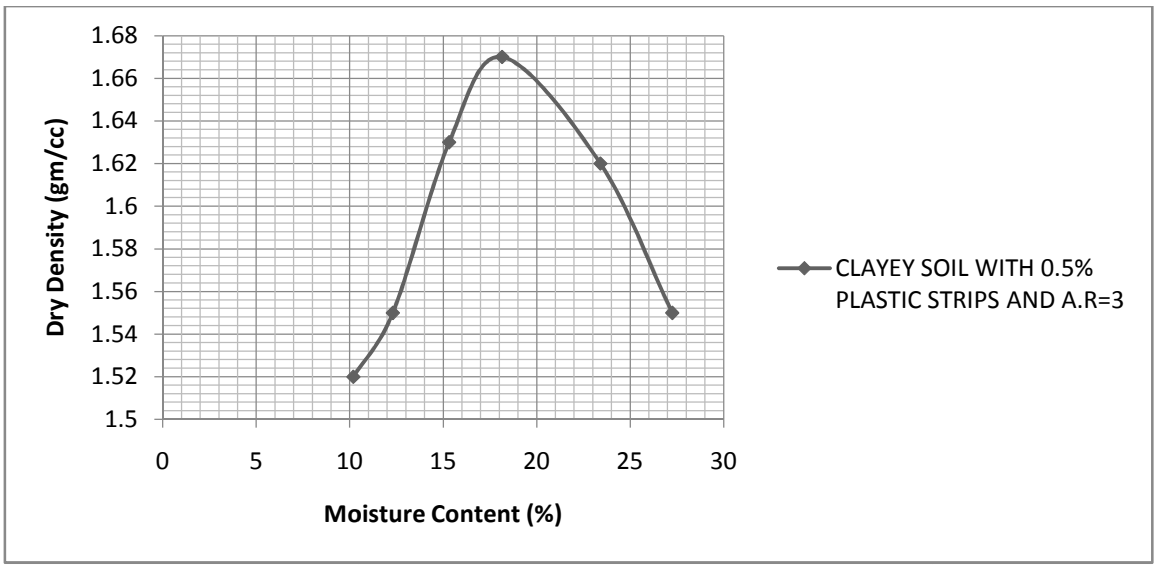

Fig. 3.41: Standard Proctor Compaction Curve

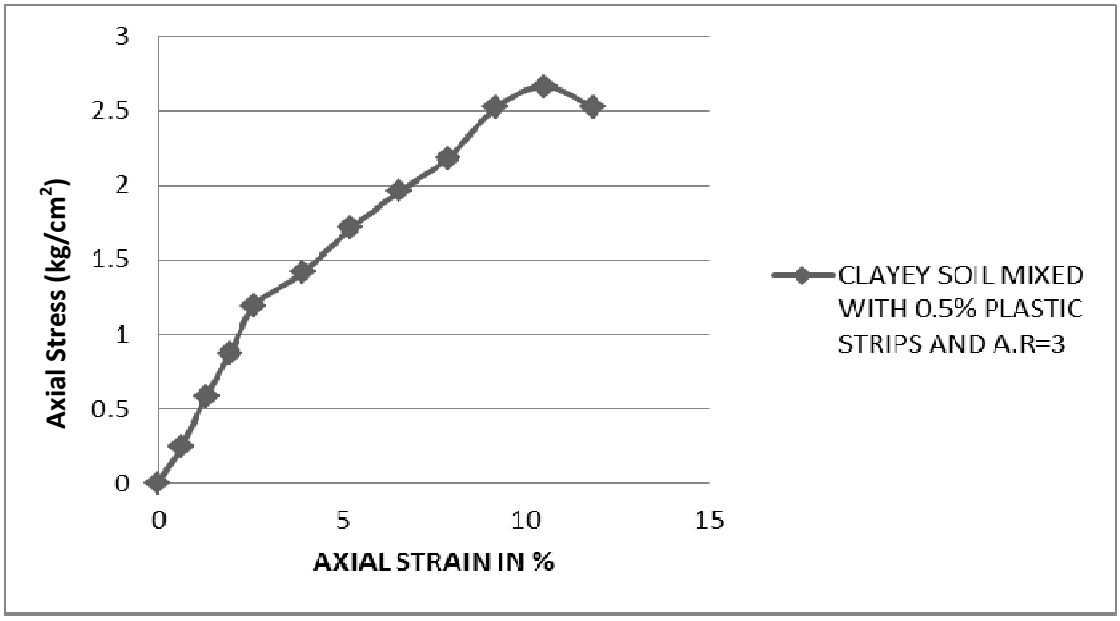

Fig. 3.42: Axial stress vs. Axial strain

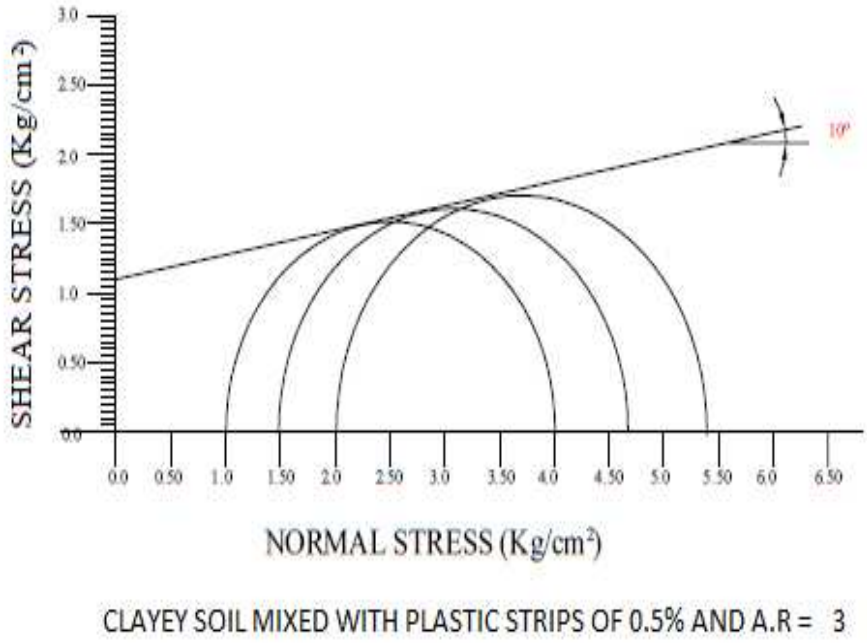

Fig. 3.43: Mohr Circle - Shear stress vs. Normal stress

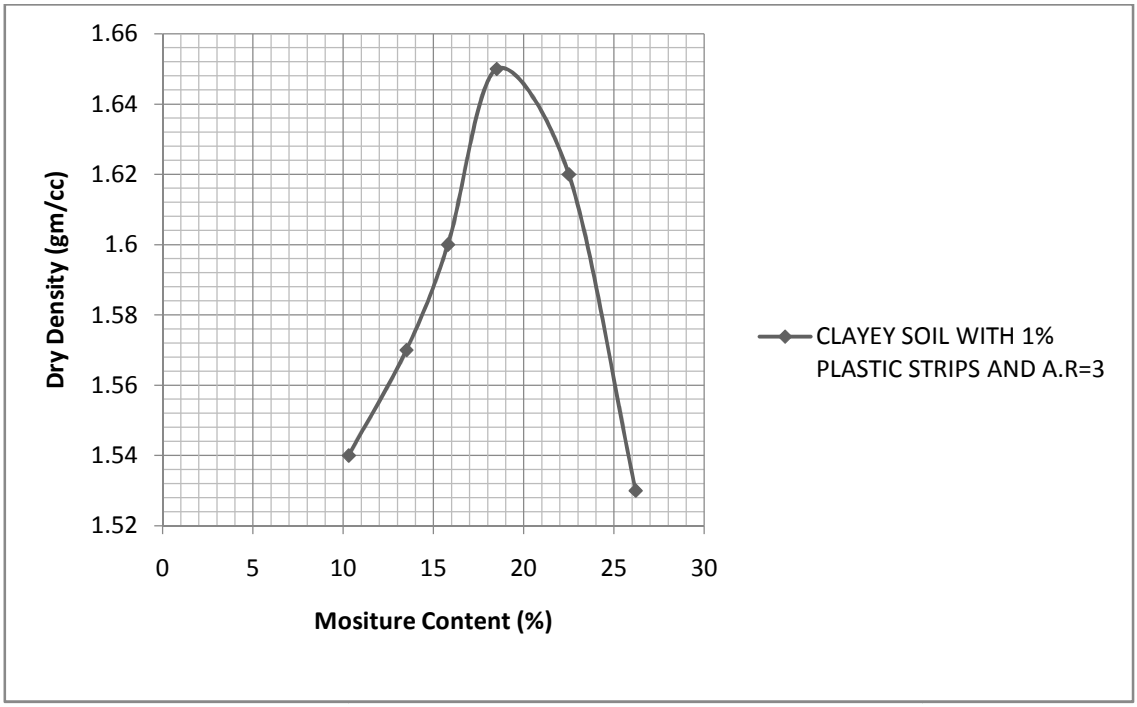

Fig. 3.44: Standard Proctor Compaction Curve

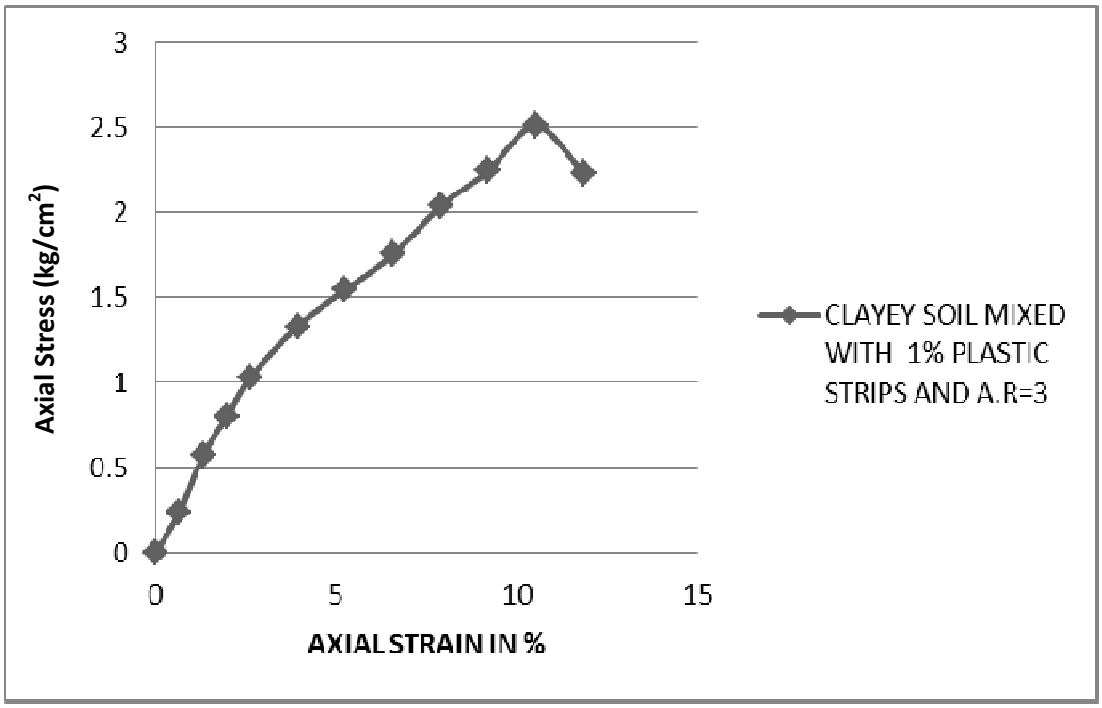

Fig. 3.45: Axial stress vs. Axial strain

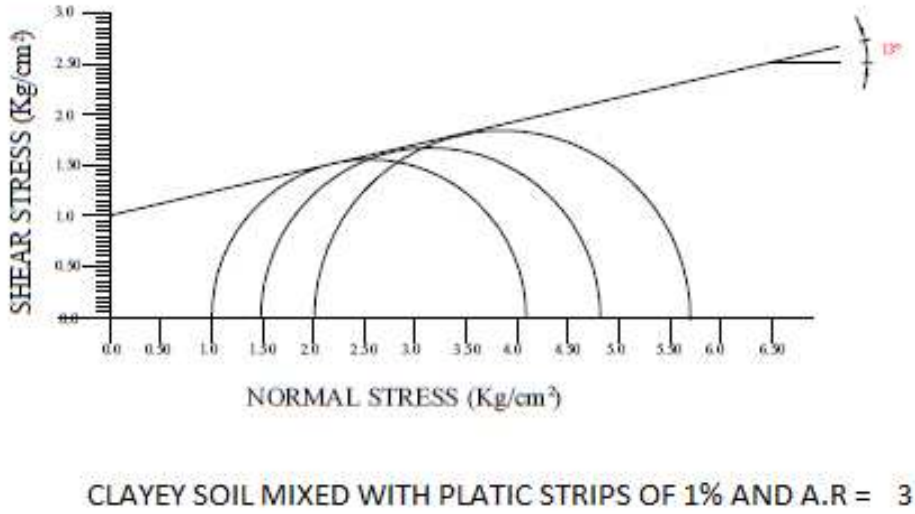

Fig. 3.46: Mohr Circle - Shear stress vs. Normal stress

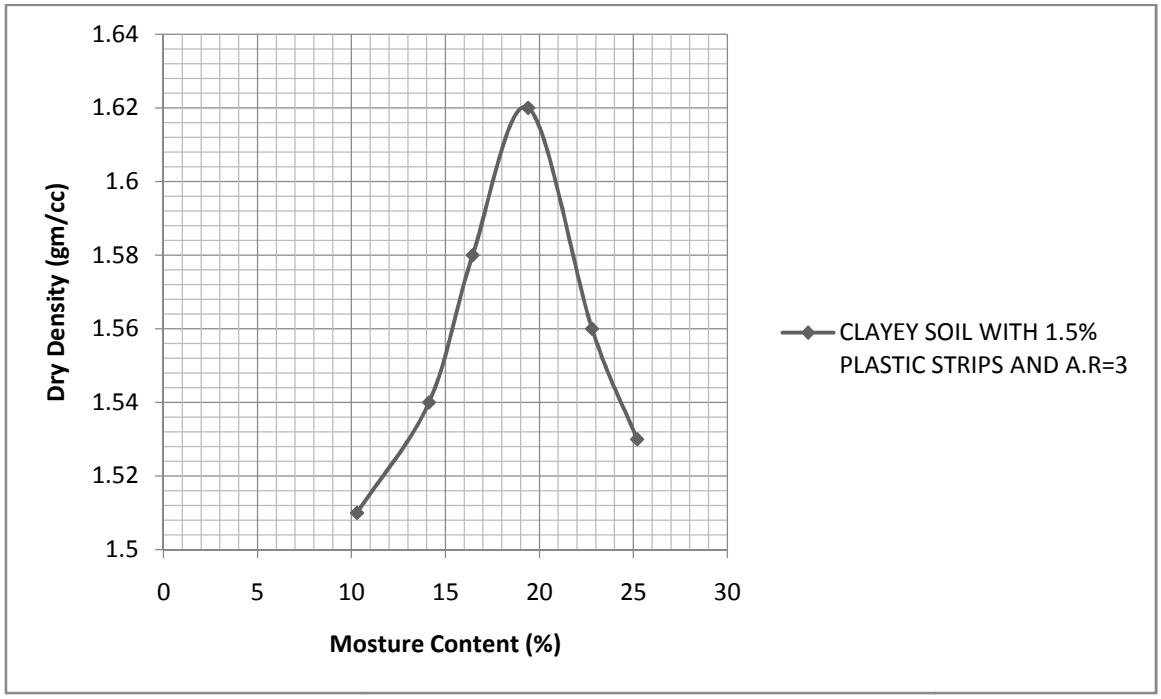

Fig. 3.47: Standard Proctor Compaction Curve

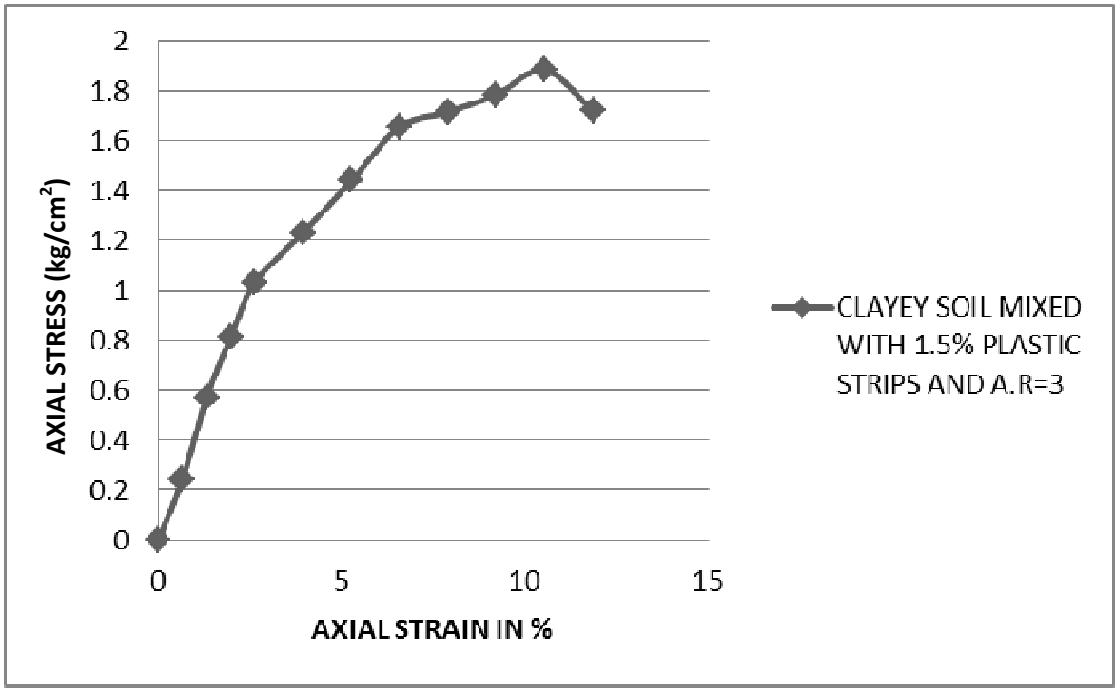

Fig. 3.48: Axial stress vs. Axial strain

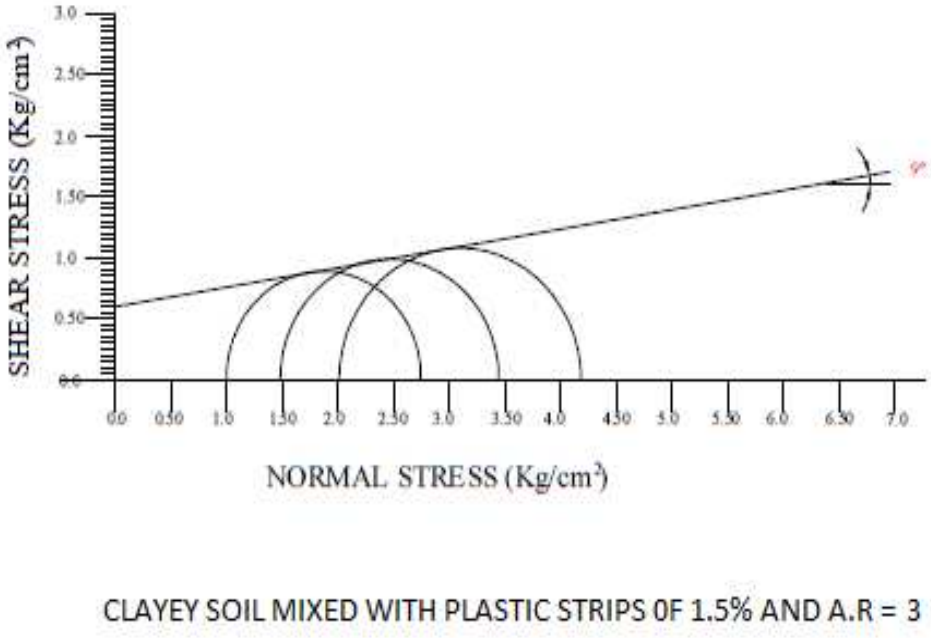

Fig. 3.49: Mohr Circle - Shear stress vs. Normal stress

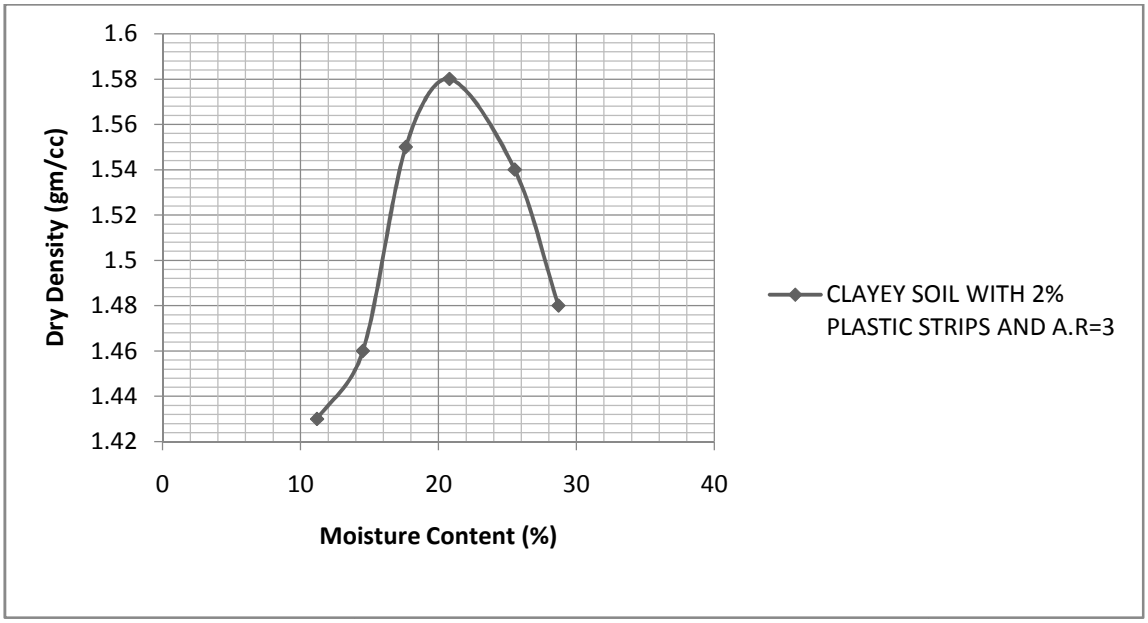

Fig. 3.50: Standard Proctor Compaction Curve

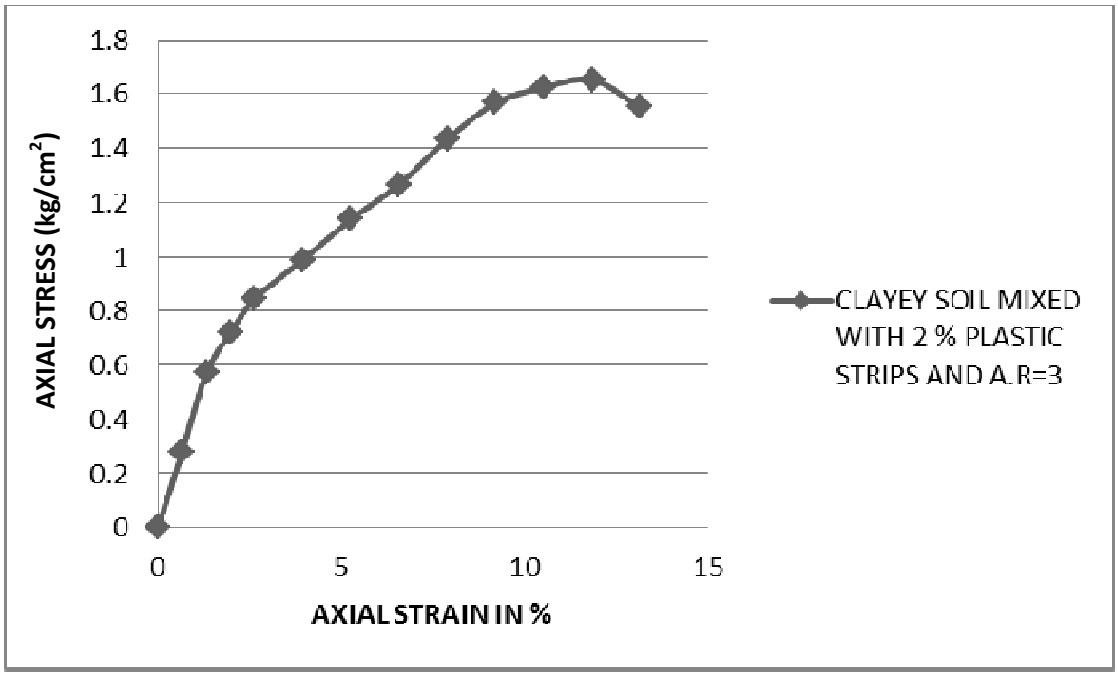

Fig. 3.51: Axial stress vs. Axial strain

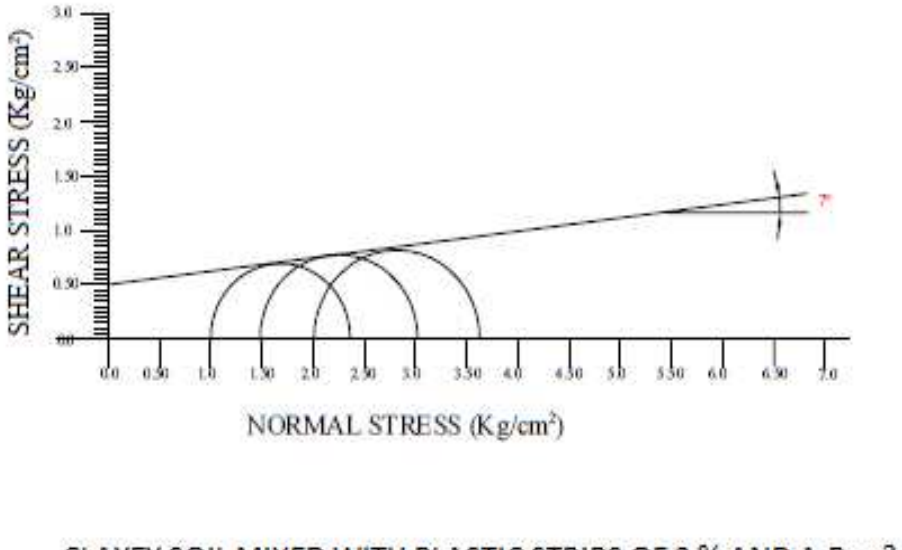

Fig. 3.52: Mohr Circle - Shear stress vs. Normal stress

3.6.7 Test Result of S2+AR1

In this section the results of tests on different types of soil have been presented to find various properties of these soil types. Standard Proctor compaction curves, axial stress-strain curves as obtained from UU triaxial tests and Mohr circles of stress for determining shear strength parameters for the mix for strip content of 0.5%, 1.0%, 1.5% and 2.0% have been shown in Figs. 3.53 to 3.55, 3.56 to 3.58, 3.59 to 3.61 and 3.62 to 3.64 respectively.

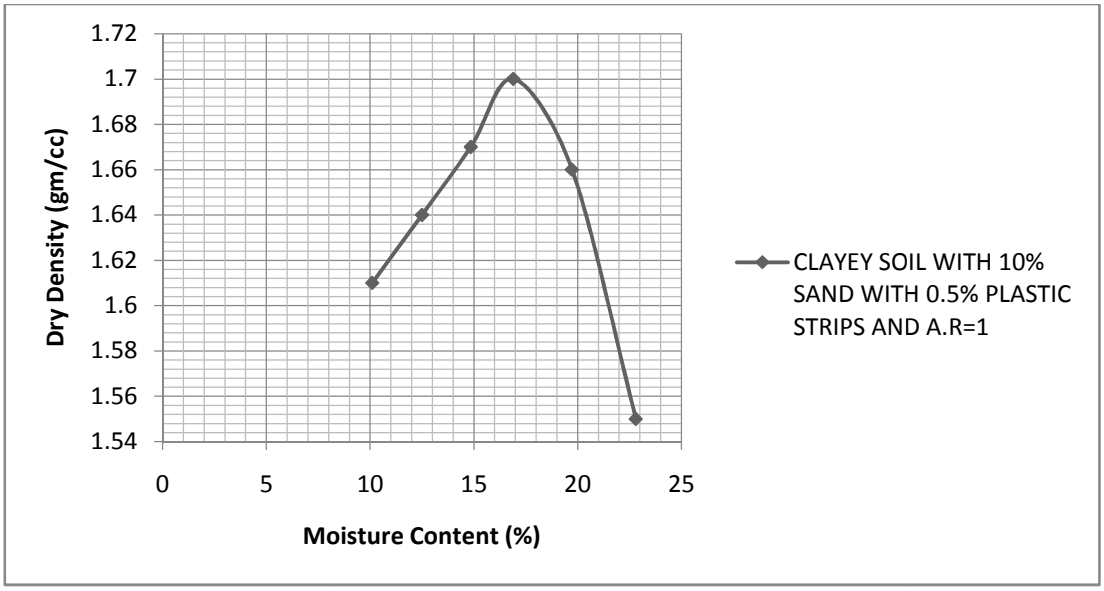

Fig. 3.53: Standard Proctor Compaction Curve

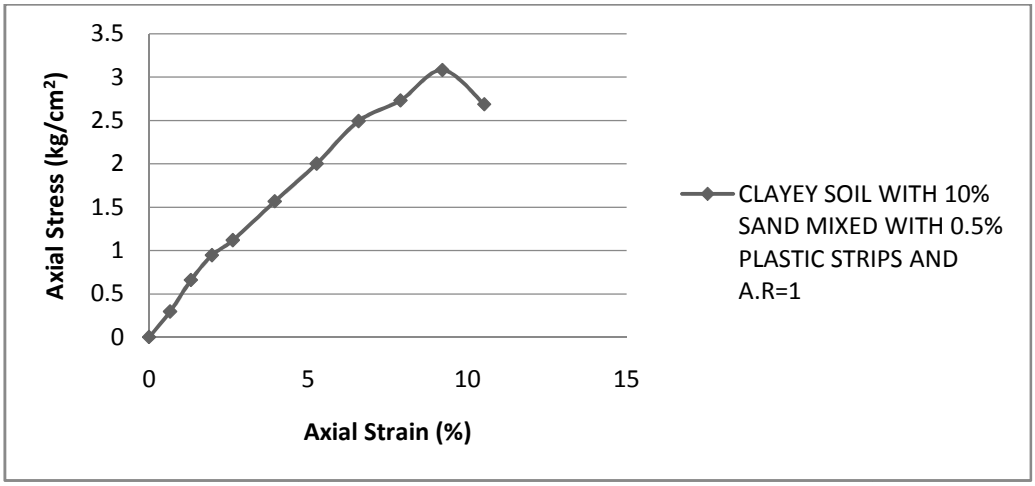

Fig. 3.54: Axial stress vs. Axial strain

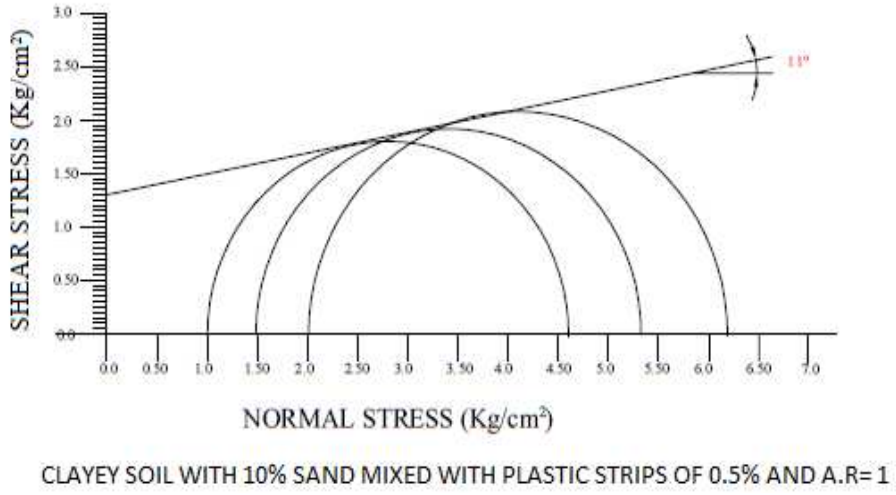

Fig. 3.55: Mohr Circle - Shear stress vs. Normal stress

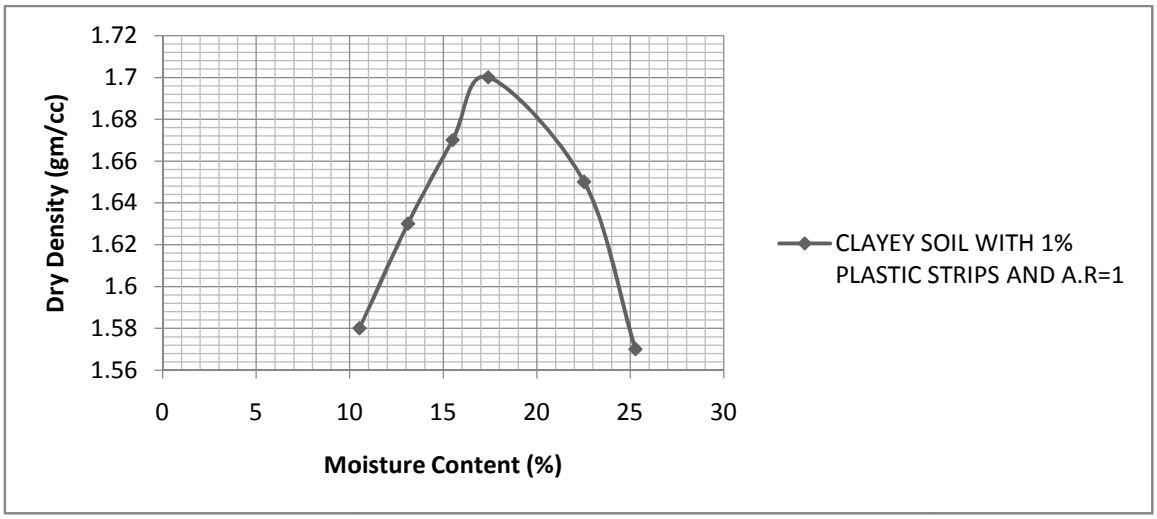

Fig. 3.56: Standard Proctor Compaction Curve

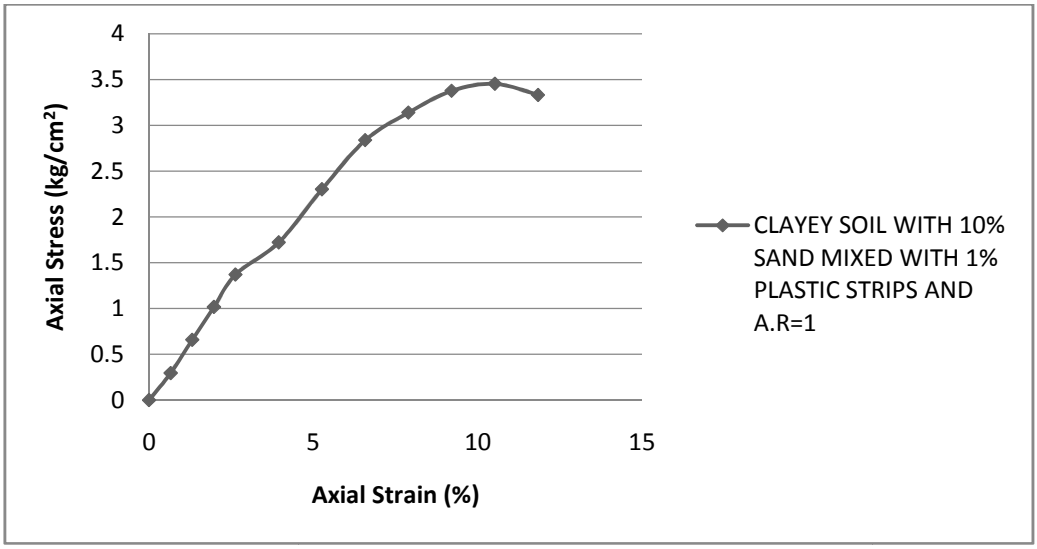

Fig. 3.57: Axial stress vs. Axial strain

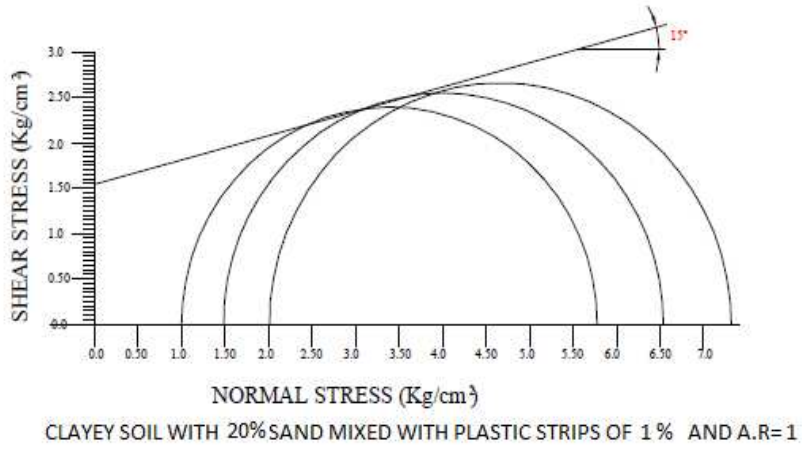

Fig. 3.58: Mohr Circle - Shear stress vs. Normal stress

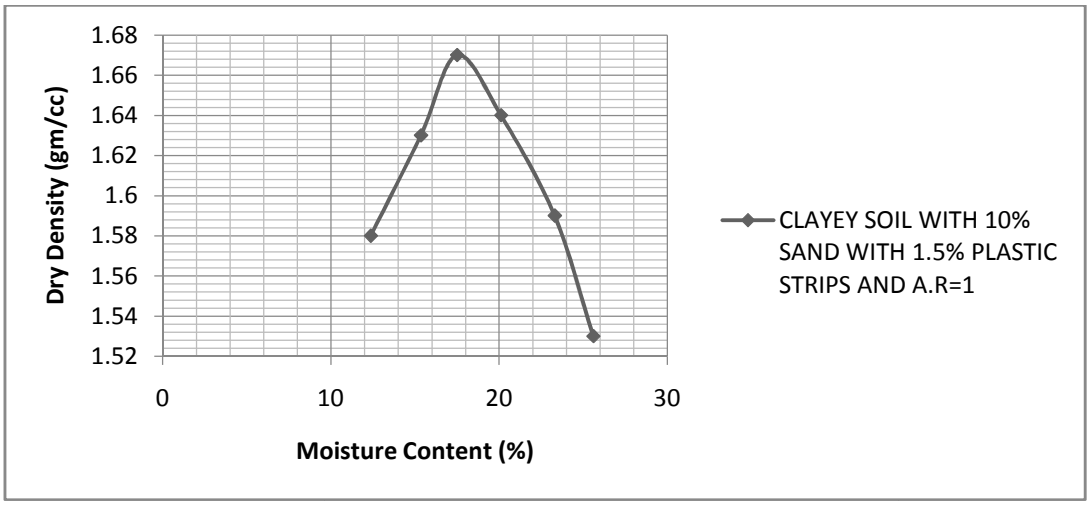

Fig. 3.59: Standard Proctor Compaction Curve

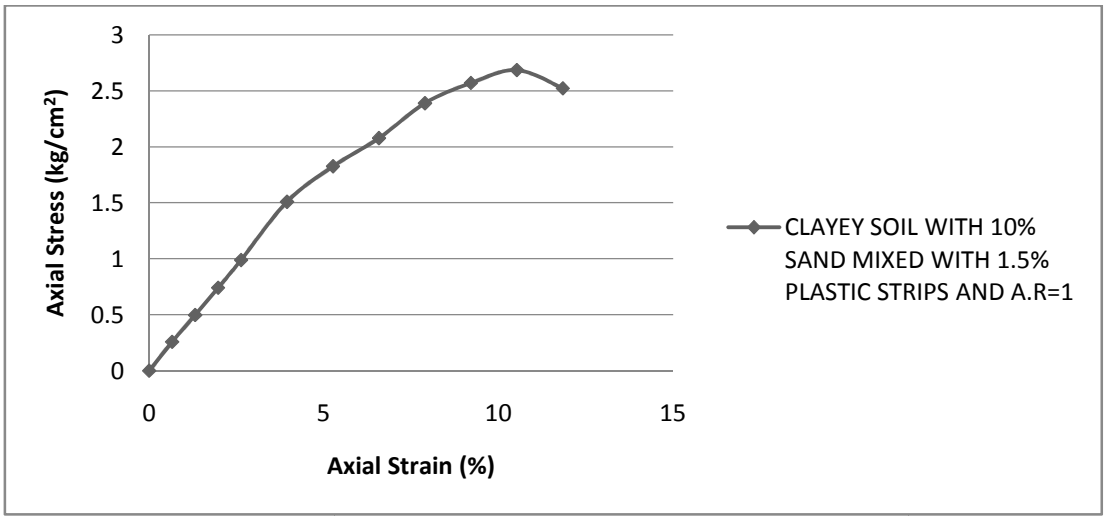

Fig. 3.60: Axial stress vs. Axial strain

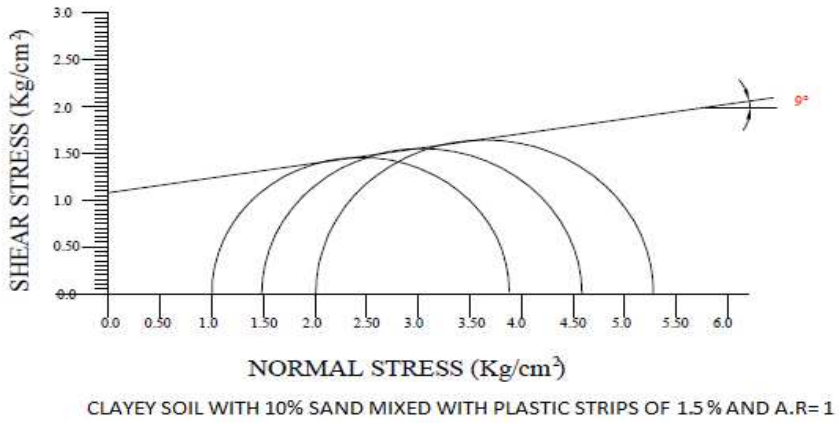

Fig. 3.61: Mohr Circle - Shear stress vs. Normal stress

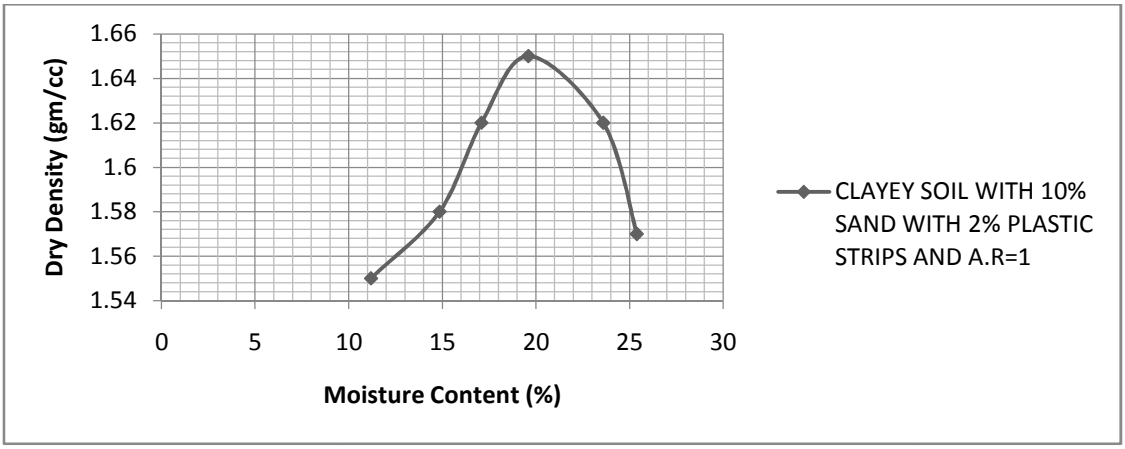

Fig. 3.62: Standard Proctor Compaction Curve

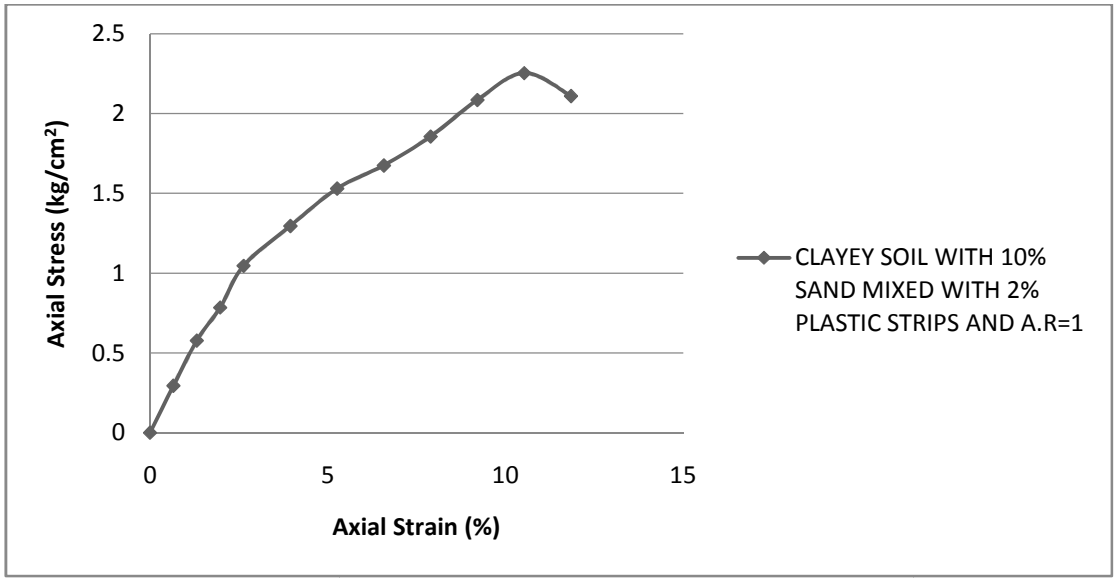

Fig. 3.63: Axial stress vs. Axial strain

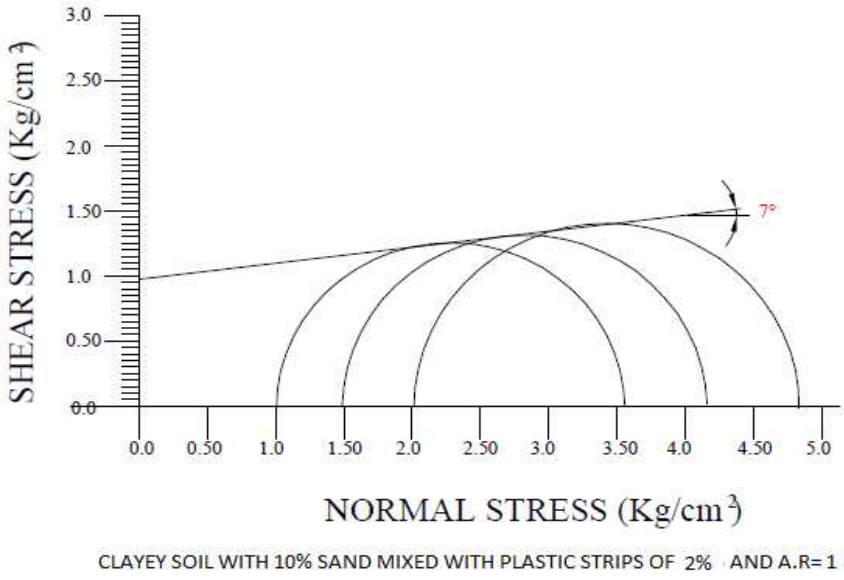

Fig. 3.64: Mohr Circle - Shear stress vs. Normal stress

3.6.8 Test Result of S2+AR2

In this section the results of tests on different types of soil have been presented to find various properties of these soil types. Standard Proctor Compaction curves, axial stress-strain curves as obtained from UU triaxial tests and Mohr circles of stress for determining shear strength

parameters for the mix for strip content of 0.5%, 1.0%, 1.5% and 2.0% have been shown in Figs. 3.65 to 3.67, 3.68 t 3.70, 3.71 to 3.73 and 3.74 to 3.76 respectively.

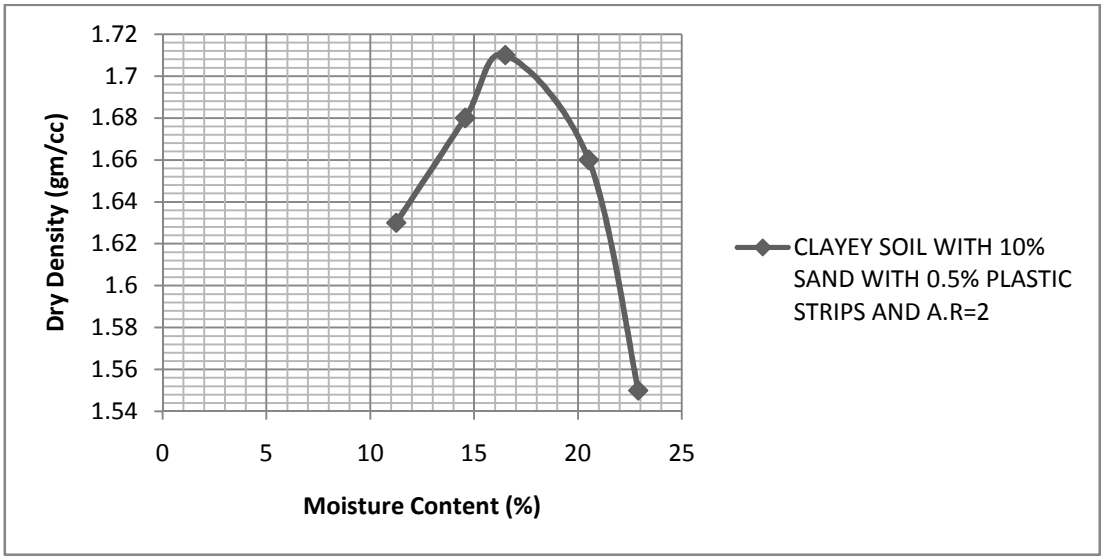

Fig. 3.65: Standard Proctor Compaction Curve

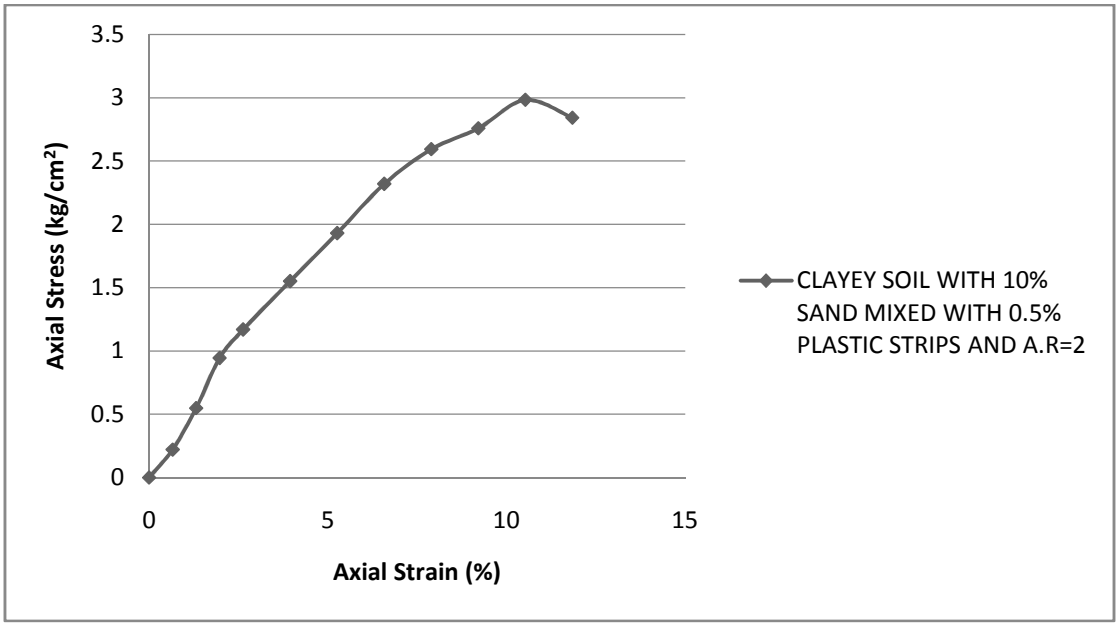

Fig. 3.66: Axial stress vs. Axial strain

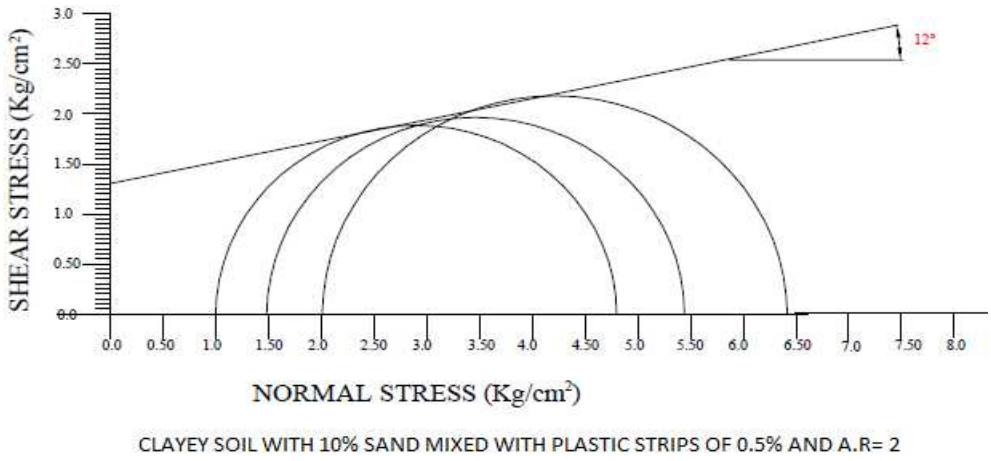

Fig. 3.67: Mohr Circle - Shear stress vs. Normal stress

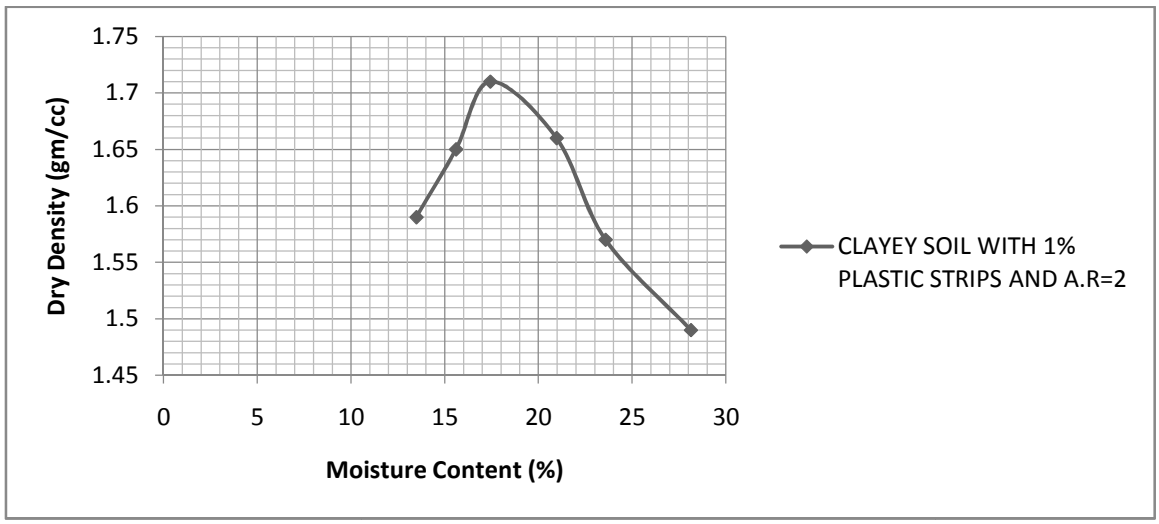

Fig. 3.68: Standard Proctor Compaction Curve

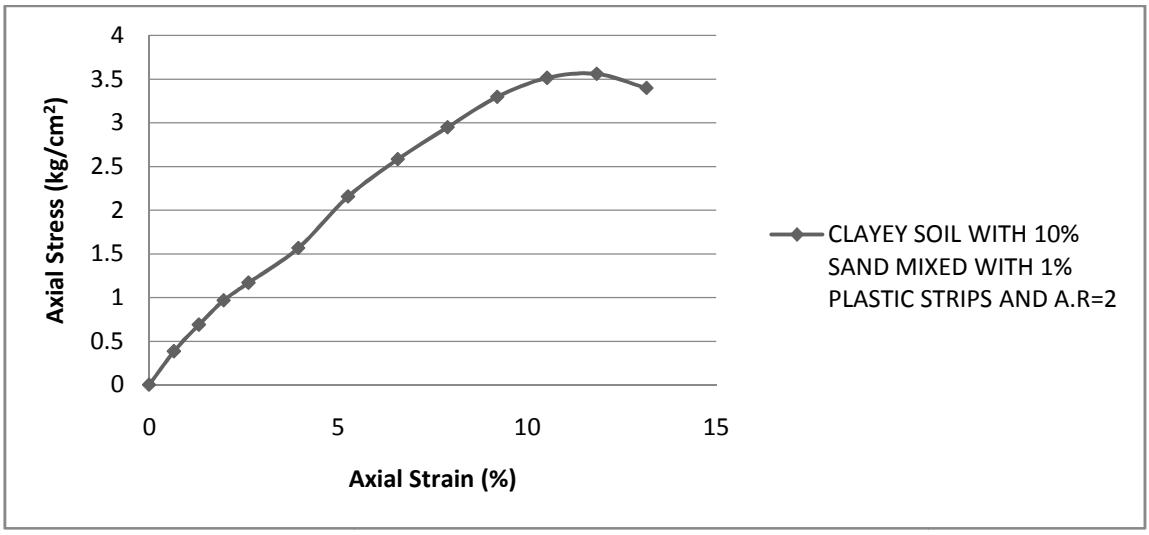

Fig. 3.69: Axial stress vs. Axial strain

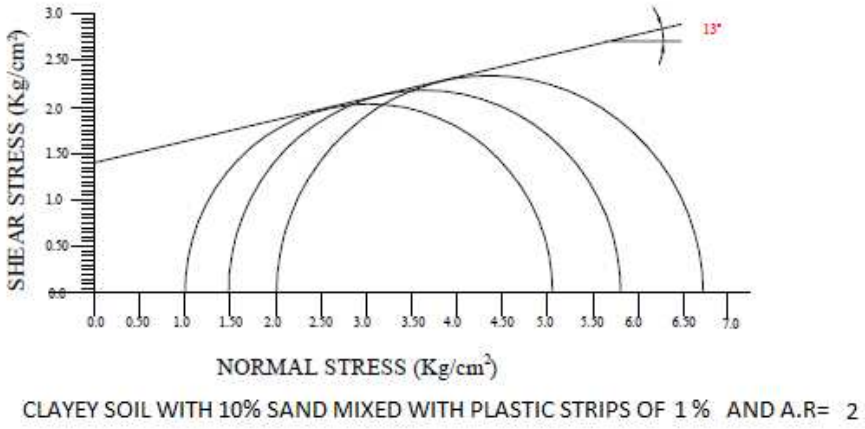

Fig. 3.70: Mohr Circle - Shear stress vs. Normal stress

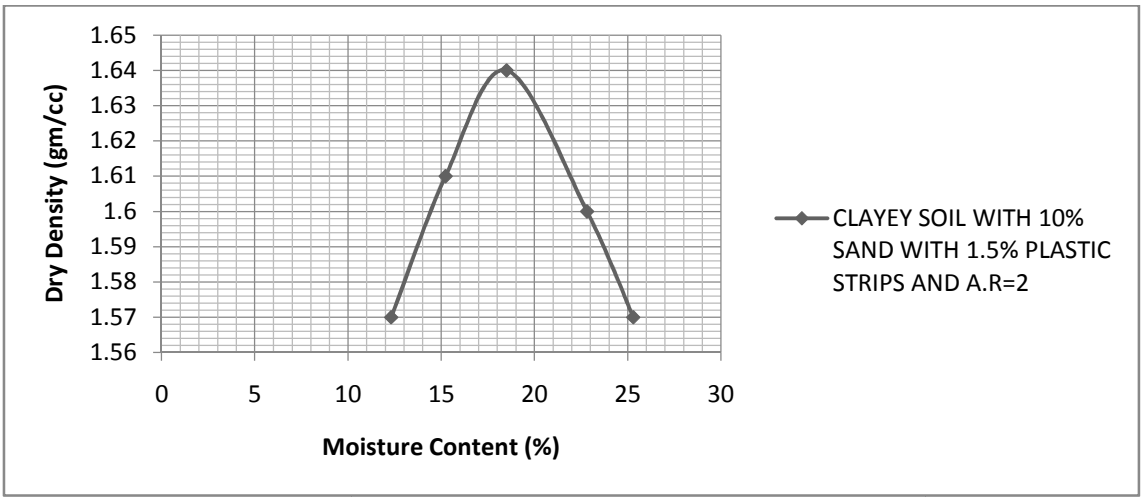

Fig. 3.71: Standard Proctor Compaction Curve

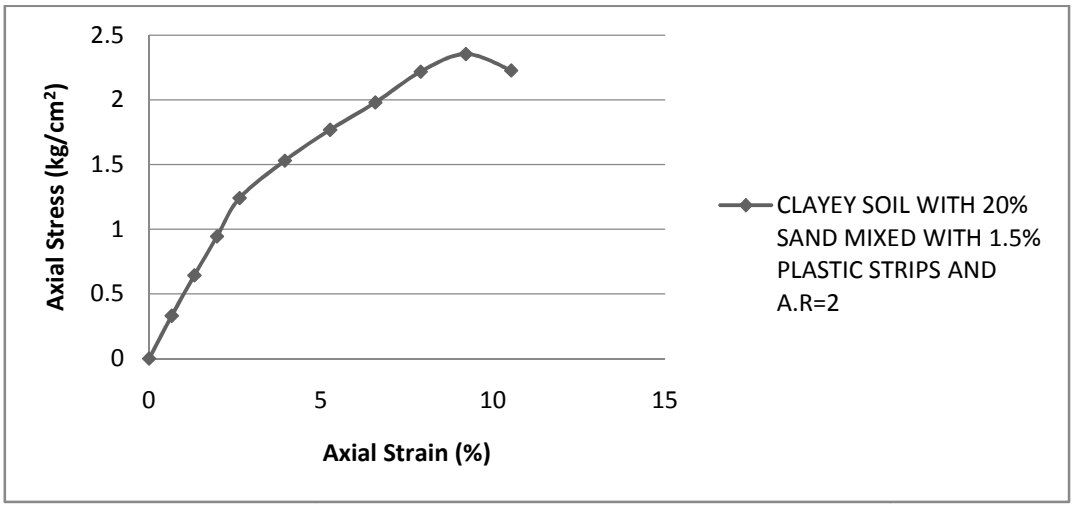

Fig. 3.72: Axial stress vs. Axial strain

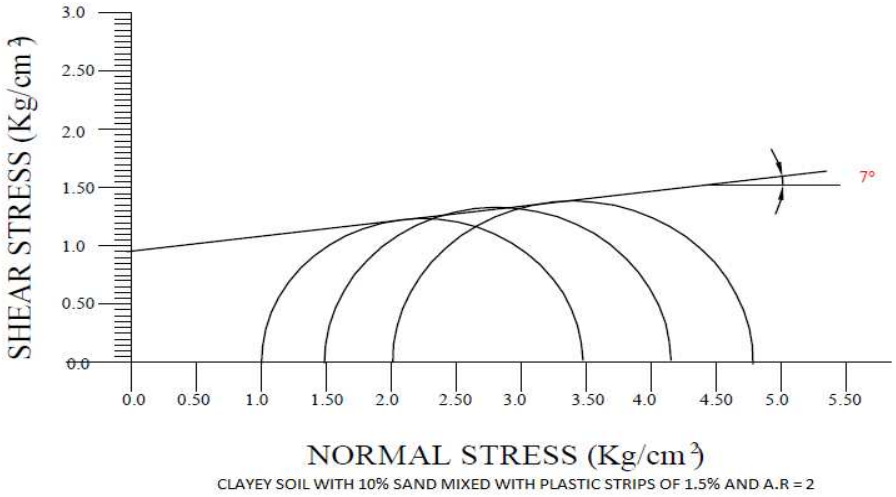

Fig. 3.73: Mohr Circle - Shear stress vs. Normal stress

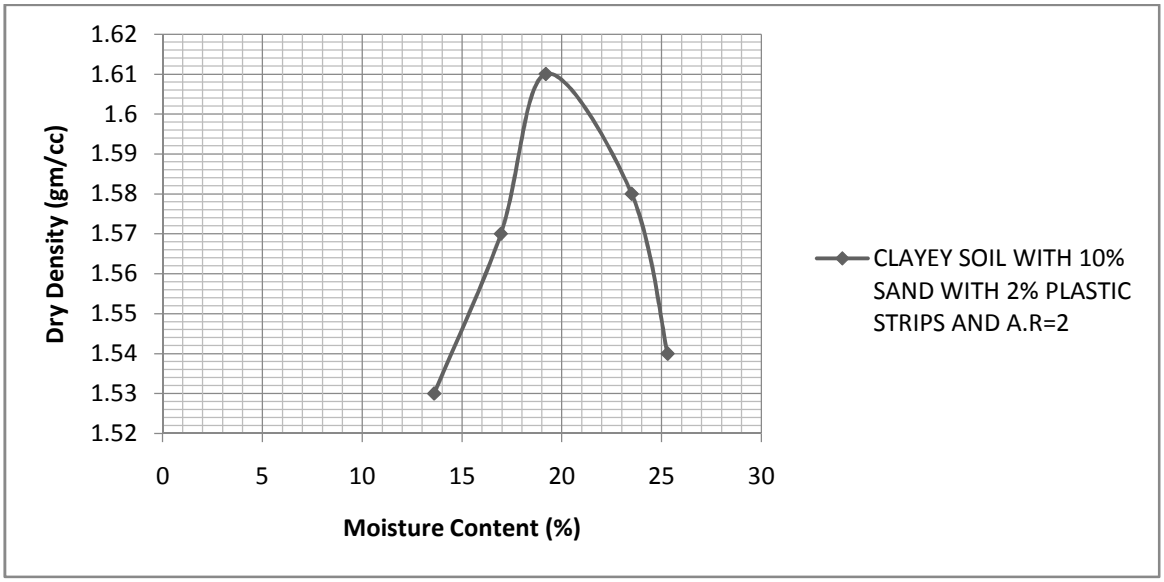

Fig. 3.74: Standard Proctor Compaction Curve

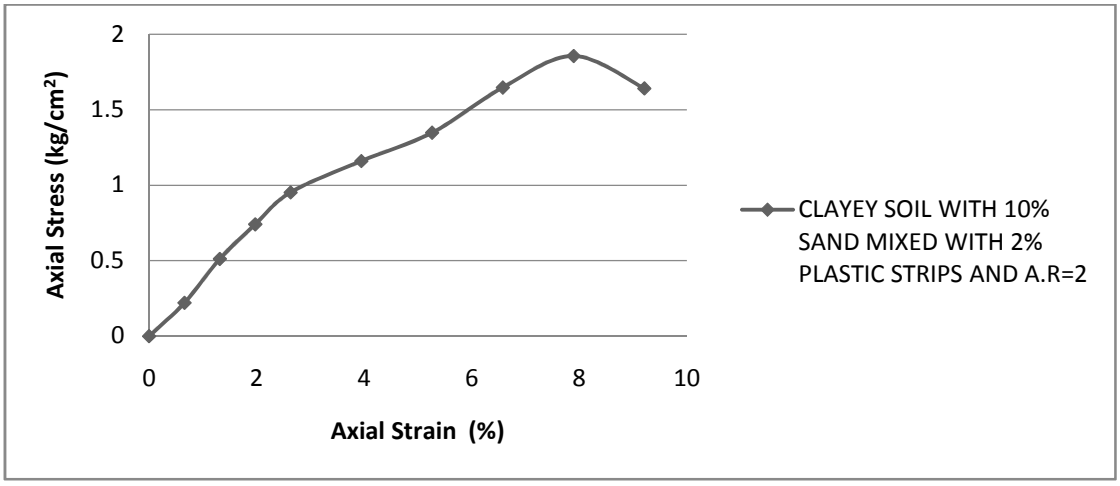

Fig. 3.75: Axial stress vs. Axial strain

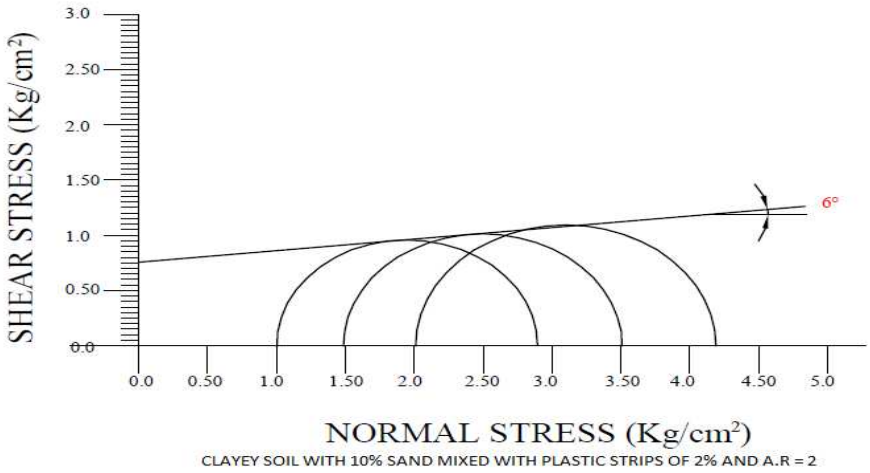

Fig. 3.76: Mohr Circle - Shear stress vs. Normal stress

3.6.9 Test Result of S2+AR3

In this section the results of tests on different types of soil have been presented to find various properties of these soil types. Standard Proctor Compaction curves, axial stress-strain curves as obtained from UU triaxial tests and Mohr circles of stress for determining shear strength parameters for the mix for strip content of 0.5%, 1.0%, 1.5% and 2.0% have been shown in Figs. 3.77 to 3.79, 3.80 to 3.82, 3.83 to 3.85 and 3.86 to 3.88 respectively.

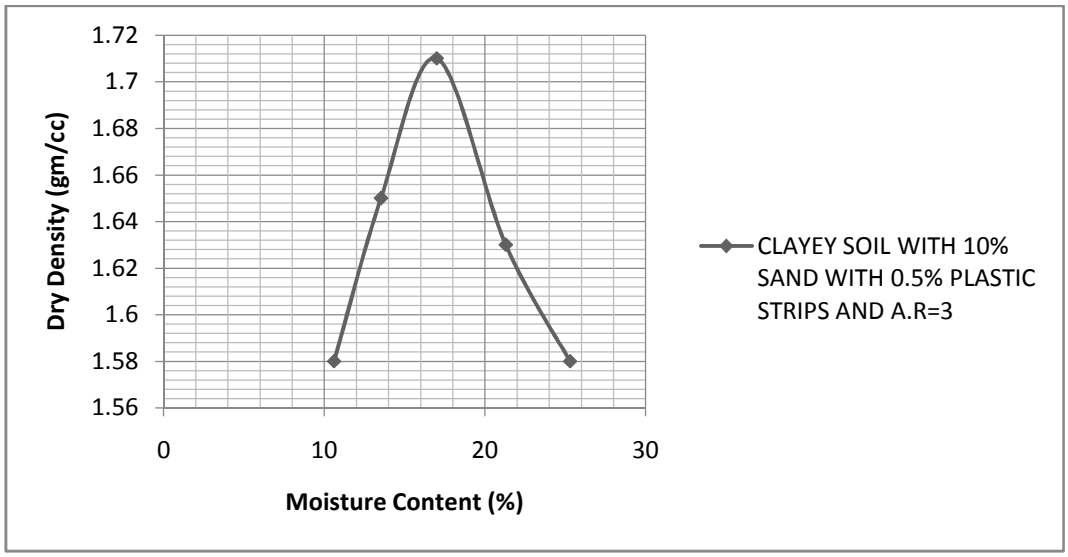

Fig. 3.77: Standard Proctor Compaction Curve

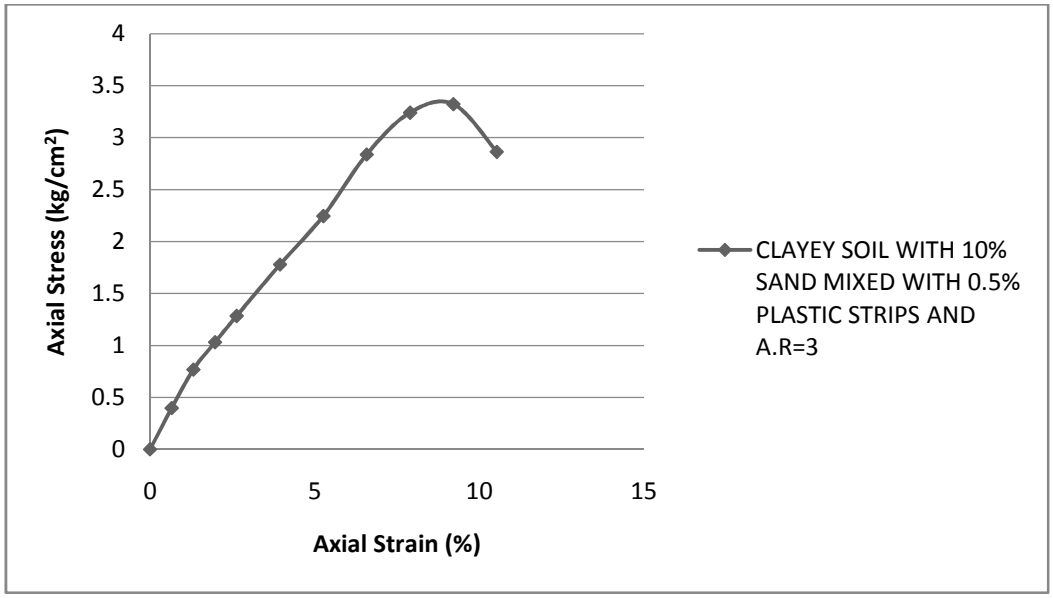

Fig. 3.78: Axial stress vs. Axial strain

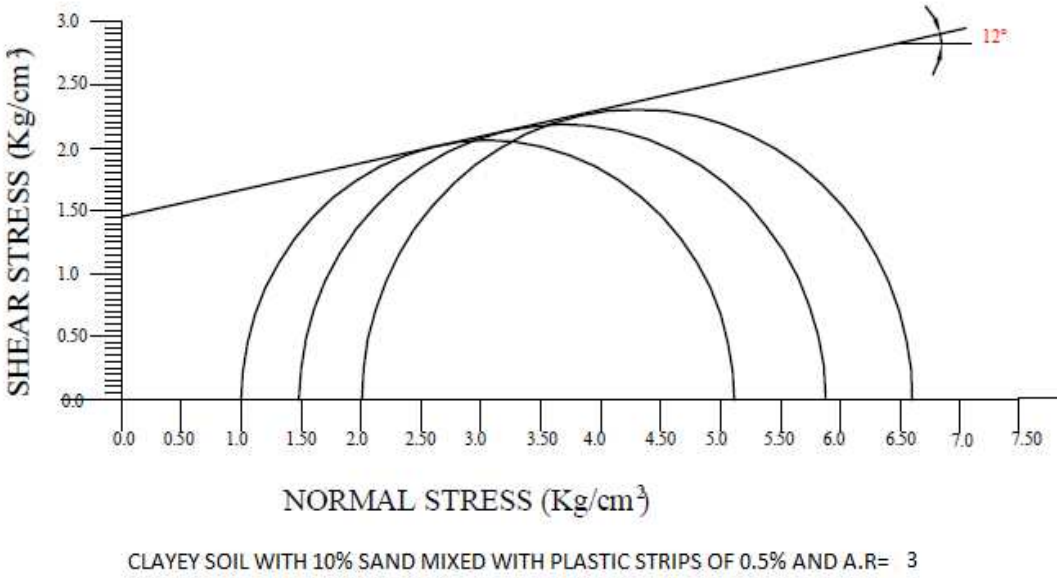

Fig. 3.79: Mohr Circle - Shear stress vs. Normal stress

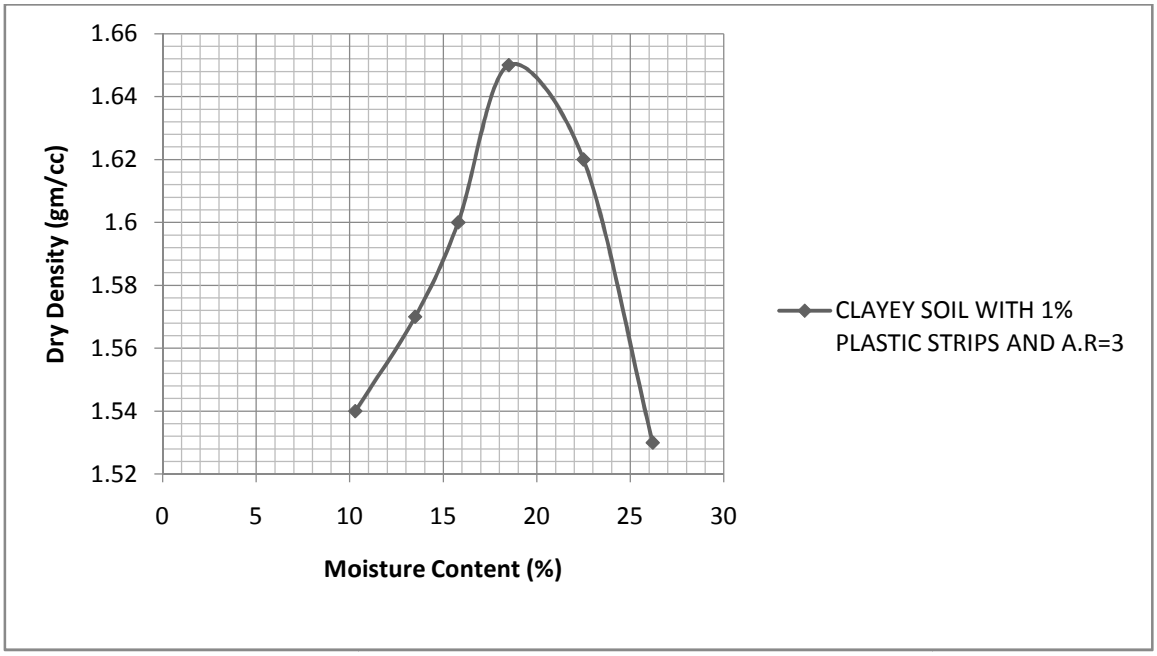

Fig. 3.80: Standard Proctor Compaction Curve

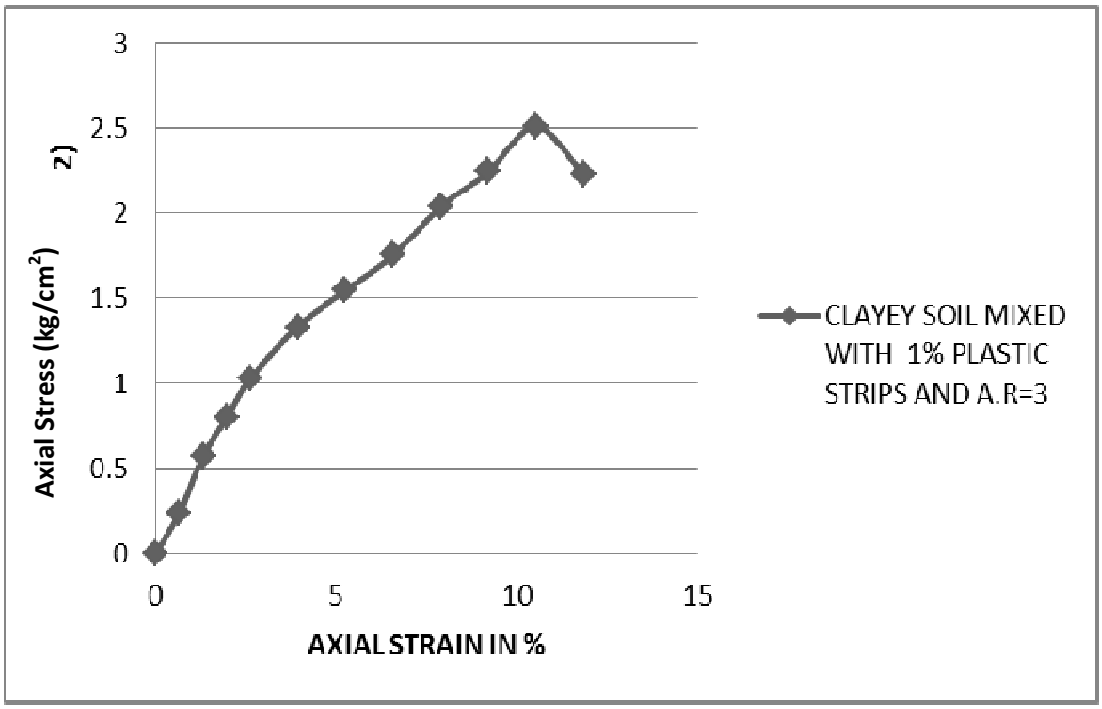

Fig. 3.81: Axial stress vs. Axial strain

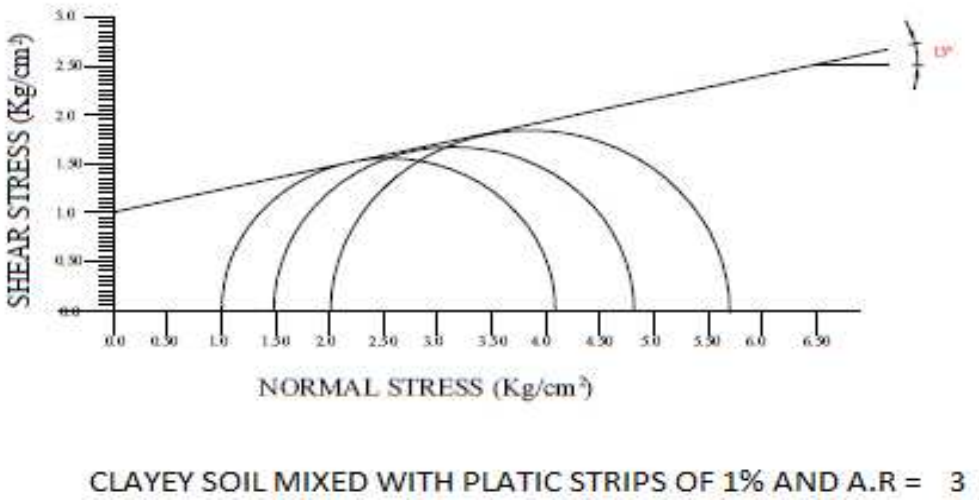

Fig. 3.82: Mohr Circle - Shear stress vs. Normal stress

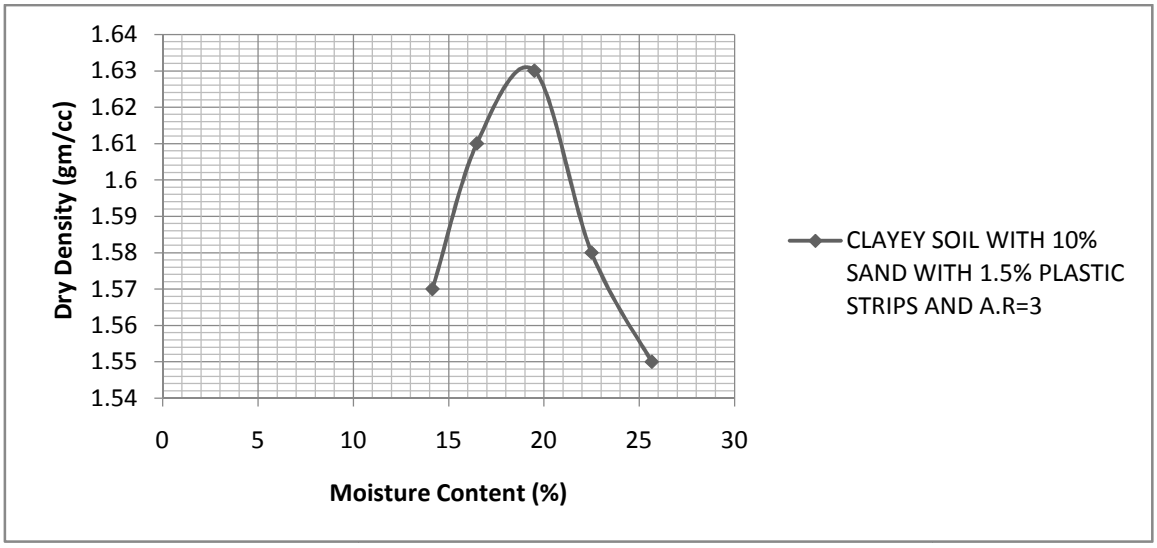

Fig. 3.83: Standard Proctor Compaction Curve

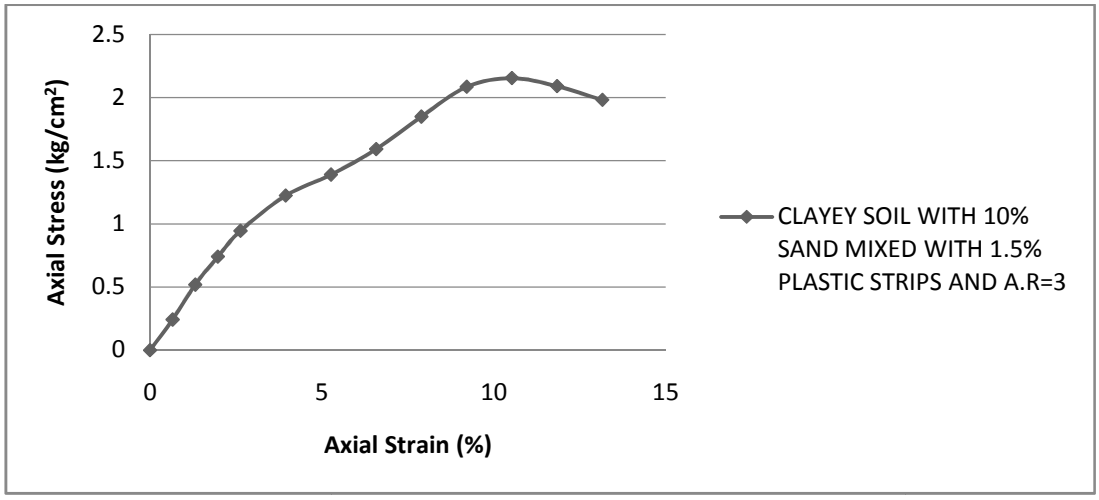

Fig. 3.84: Axial stress vs. Axial strain

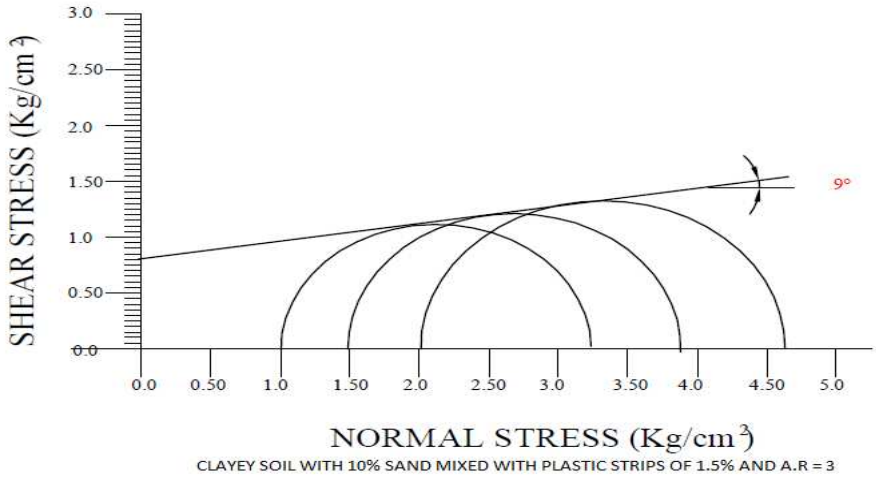

Fig. 3.85: Mohr Circle - Shear stress vs. Normal stress

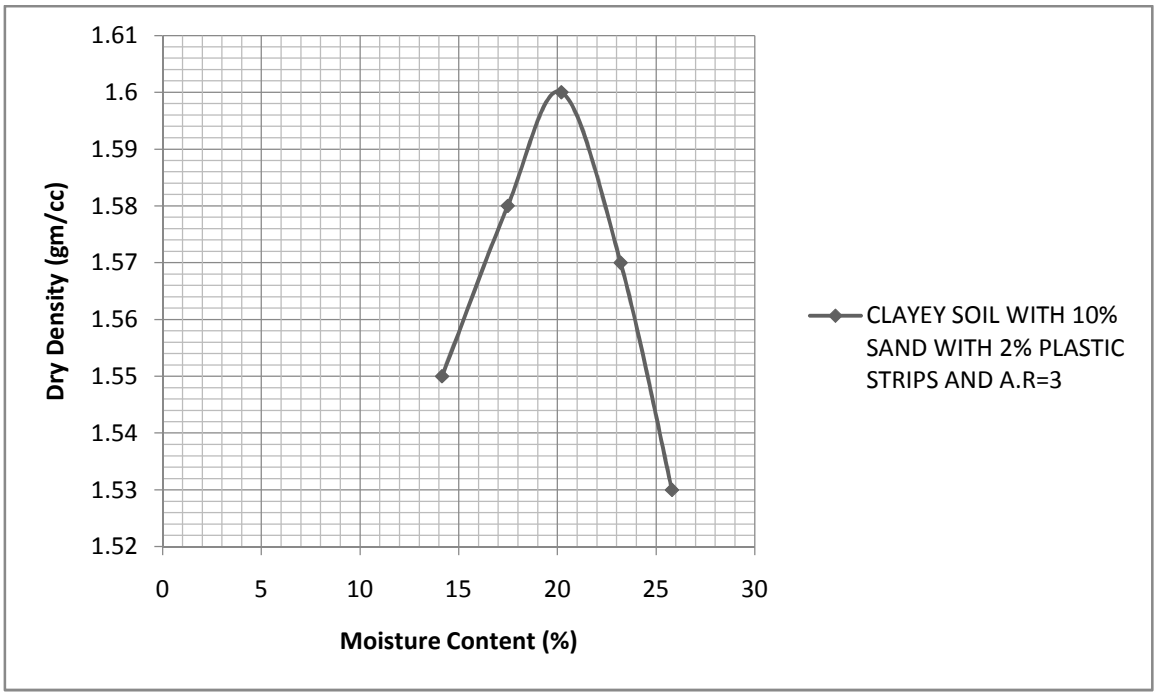

Fig. 3.86: Standard Proctor Compaction Curve

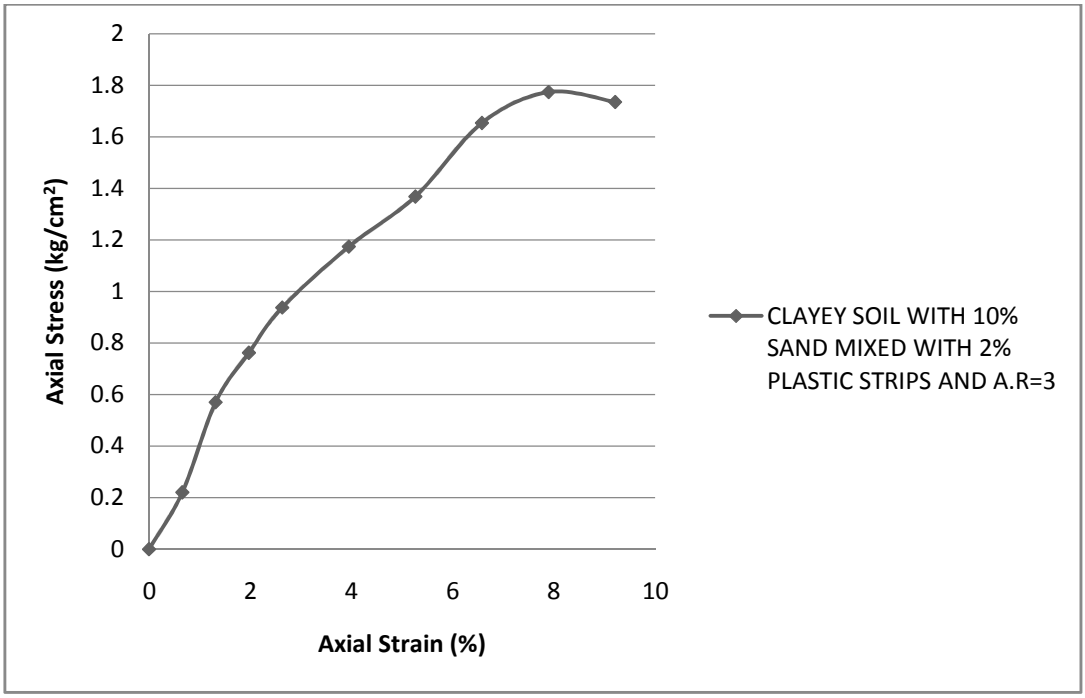

Fig. 3.87: Axial stress vs. Axial strain

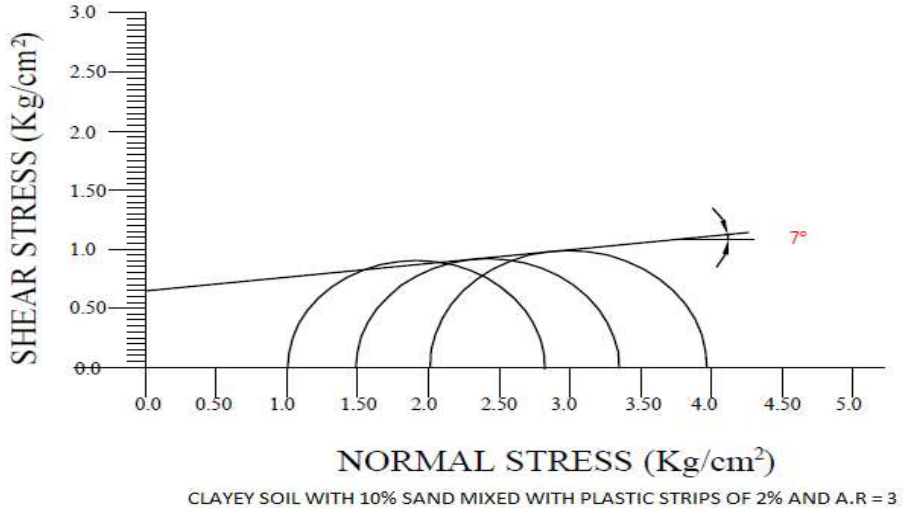

Fig. 3.88: Mohr Circle - Shear stress vs. Normal stress

3.6.10 Test Result of S3+AR1

In this section the results of tests on different types of soil have been presented to find various properties of these soil types. Standard Proctor Compaction curves, axial stress-strain curves as obtained from UU triaxial tests and Mohr circles of stress for determining shear strength

parameters for the mix for strip content of 0.5%, 1.0%, 1.5% and 2.0% have been shown in Figs. 3.89 to 3.91, 3.92 to 3.94, 3.95 to 3.97 and 3.98 to 3.100 respectively.

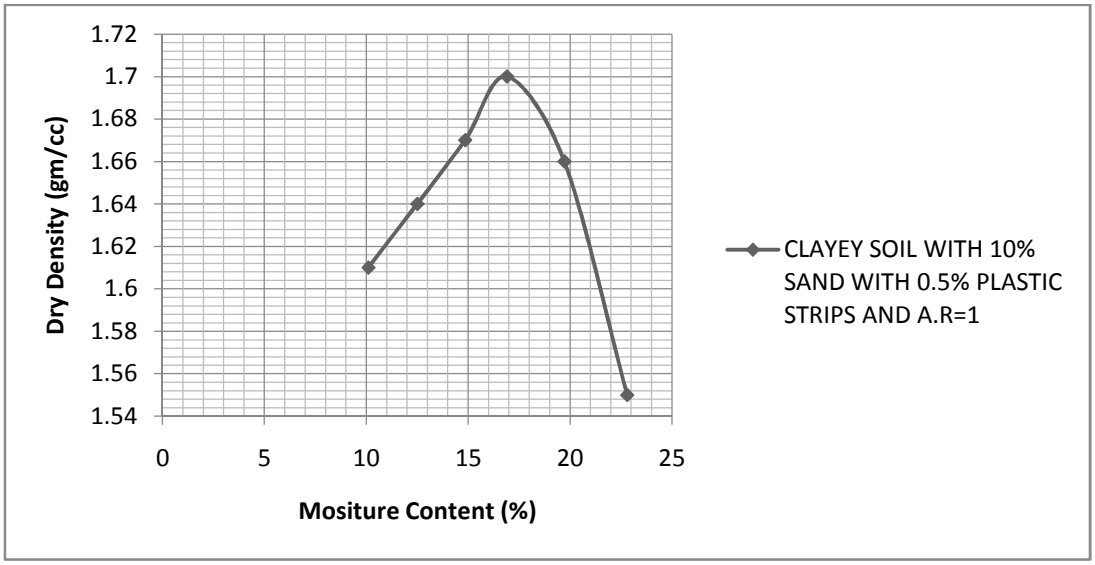

Fig. 3.89: Standard Proctor Compaction Curve

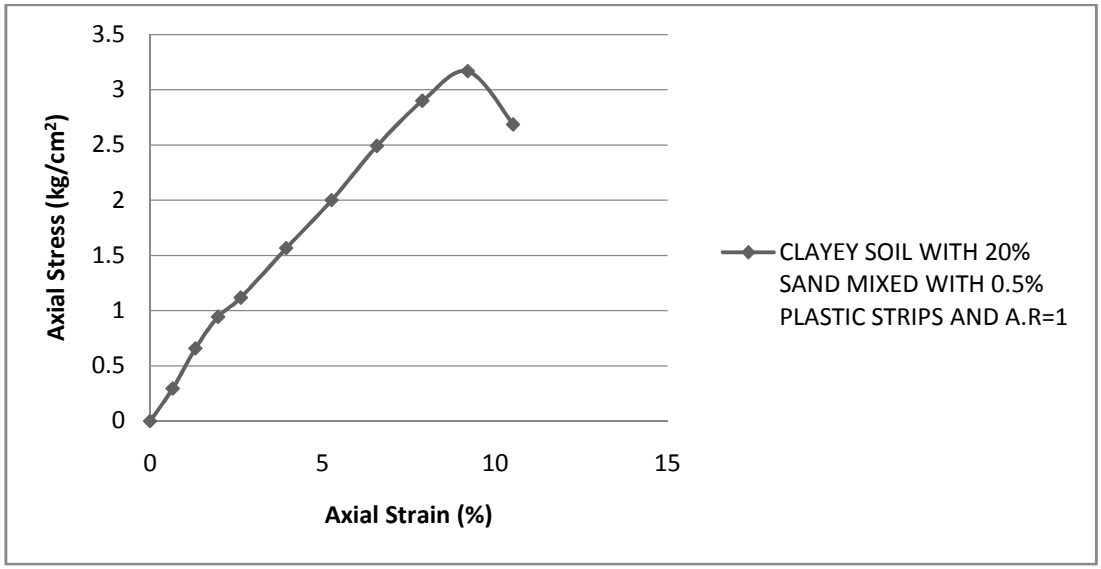

Fig. 3.90: Axial stress vs. Axial strain

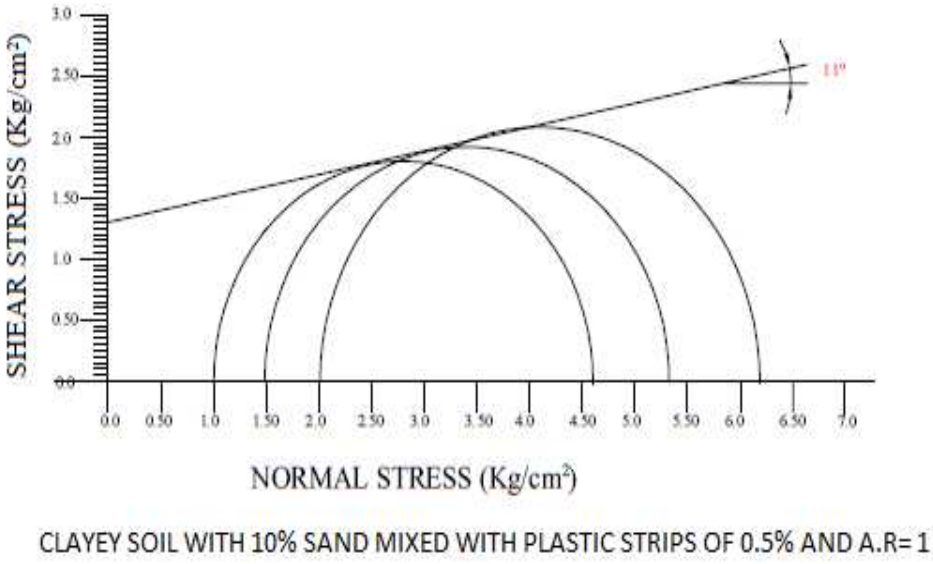

Fig. 3.91: Mohr Circle - Shear stress vs. Normal stress

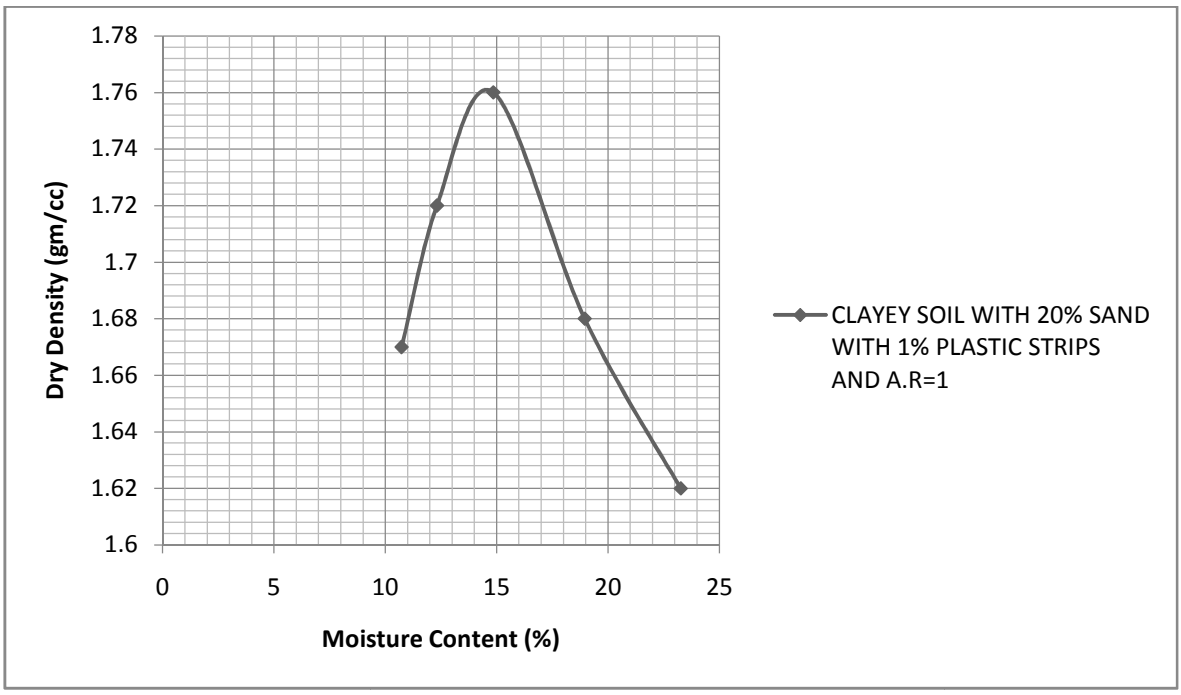

Fig. 3.92: Standard Proctor Compaction Curve

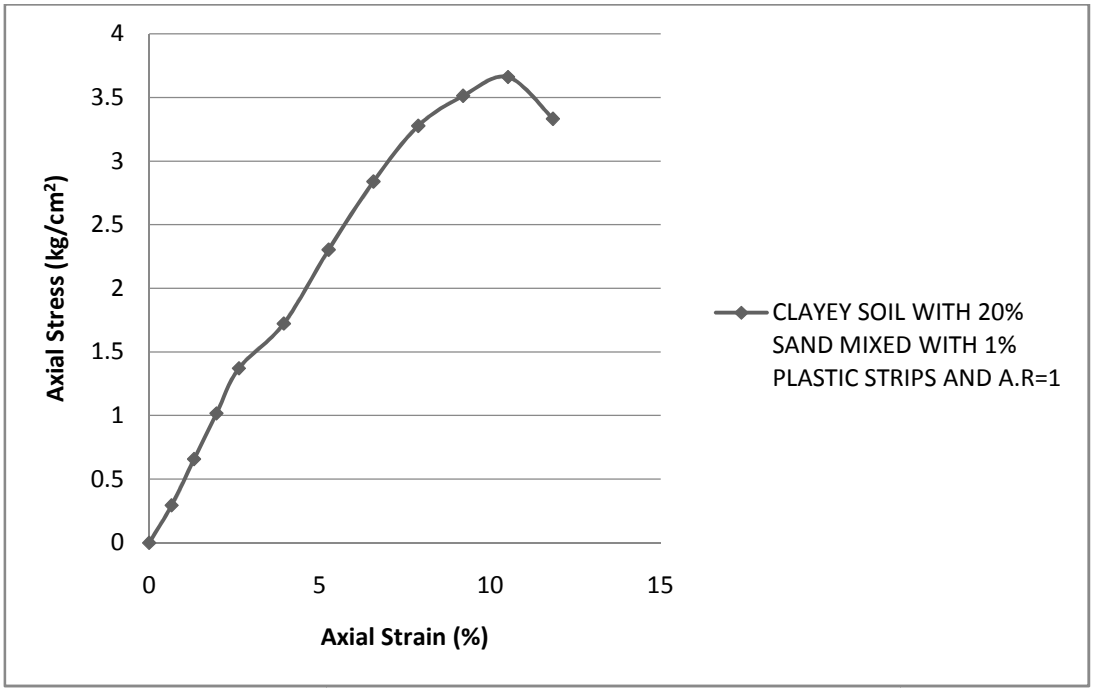

Fig. 3.93: Axial stress vs. Axial strain

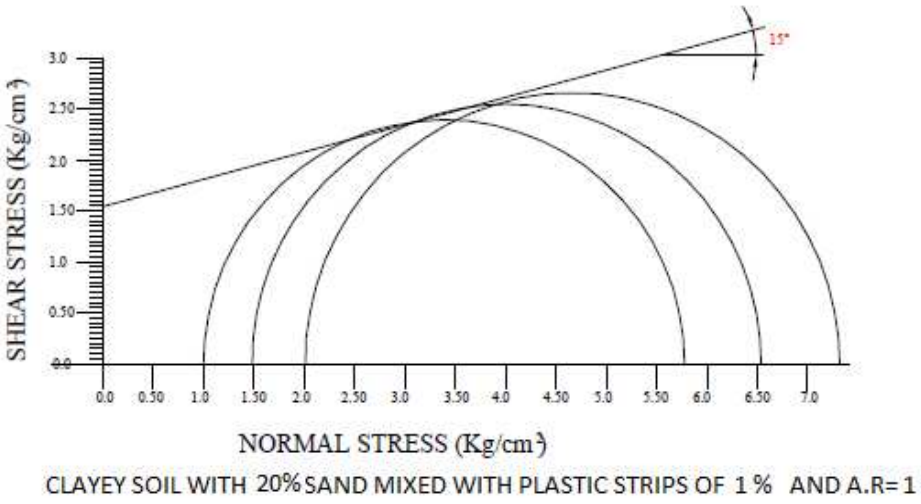

Fig. 3.94: Mohr Circle - Shear stress vs. Normal stress

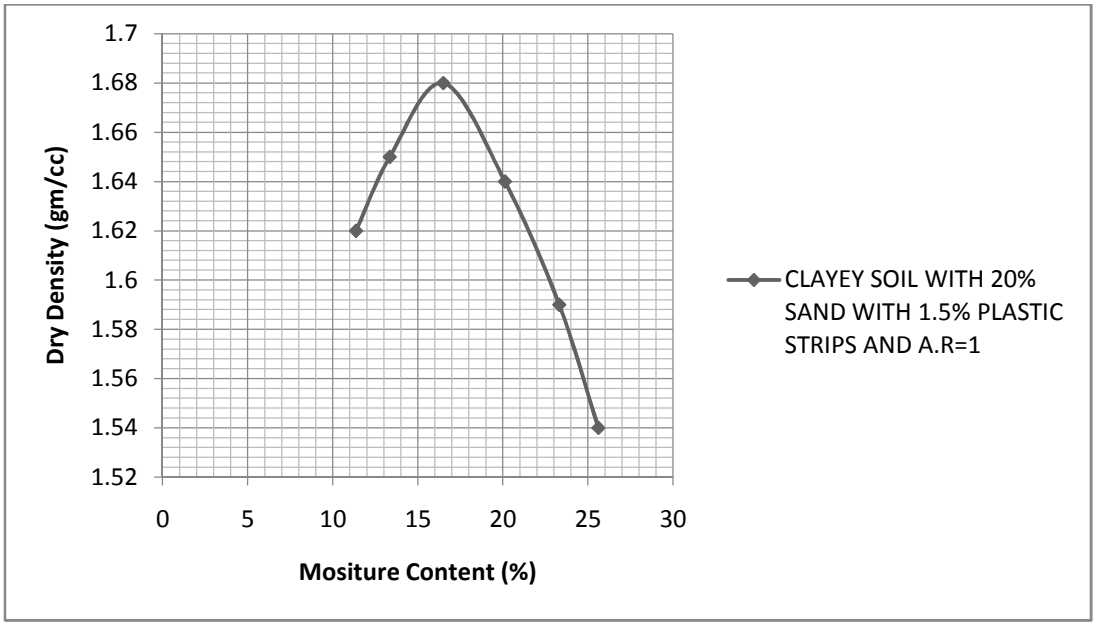

Fig. 3.95: Standard Proctor Compaction Curve

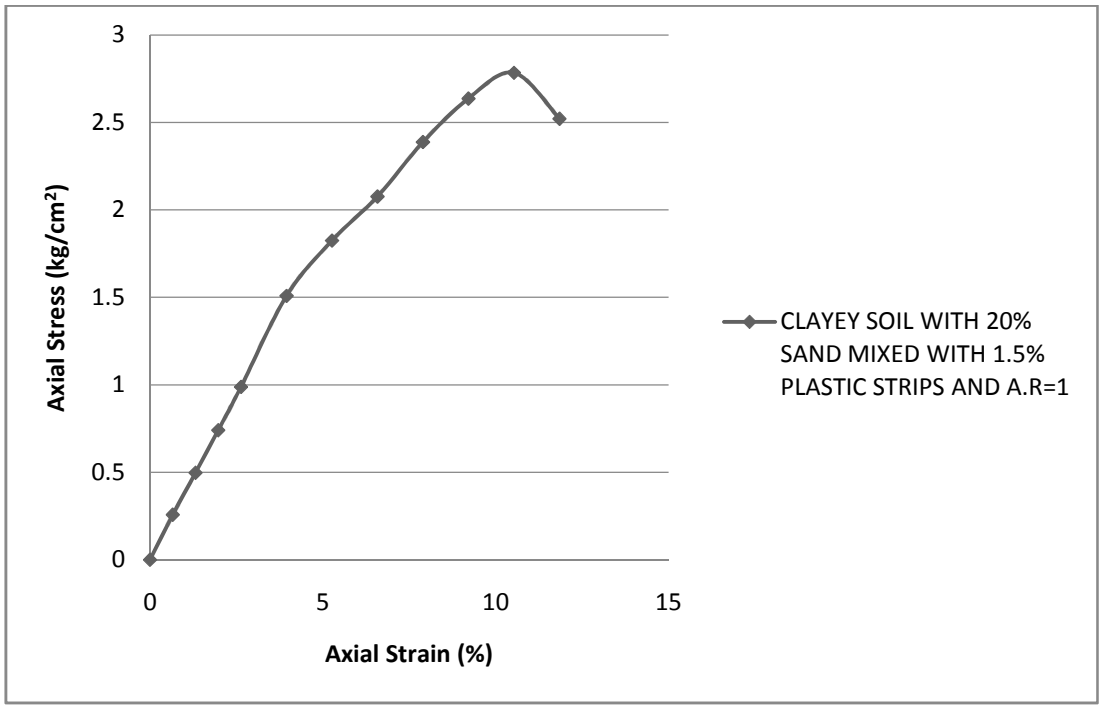

Fig. 3.96: Axial stress vs. Axial strain

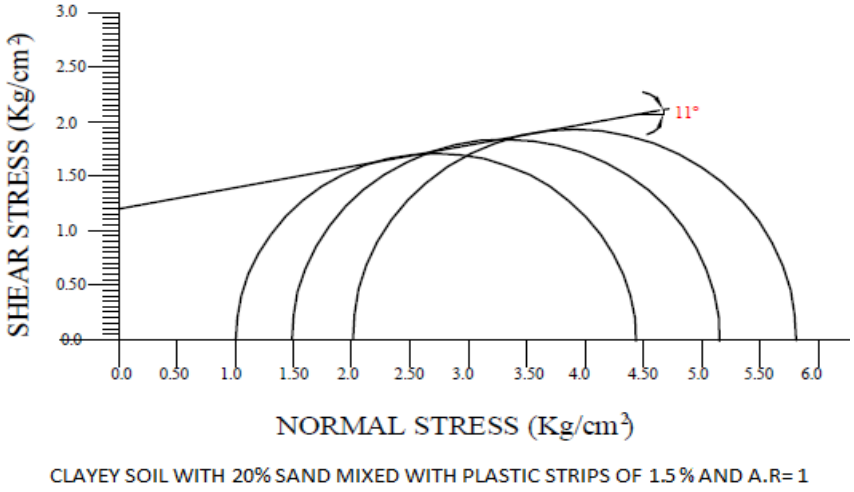

Fig. 3. 97: Mohr Circle - Shear stress vs. Normal stress

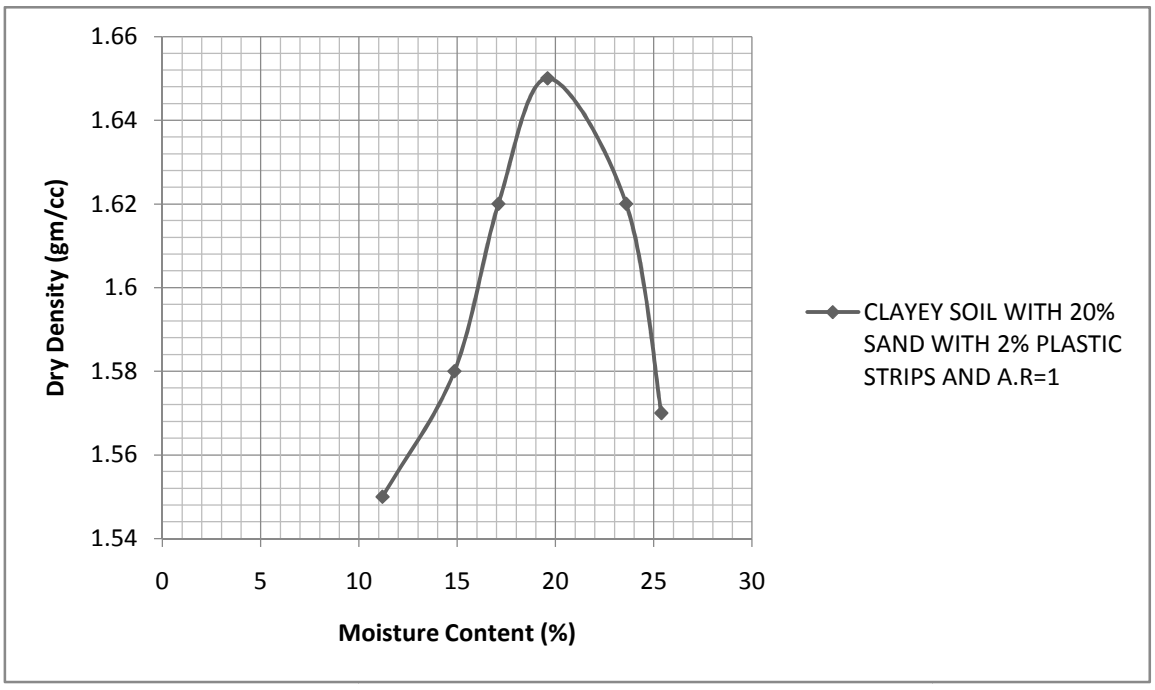

Fig. 3.98: Standard Proctor Compaction Curve

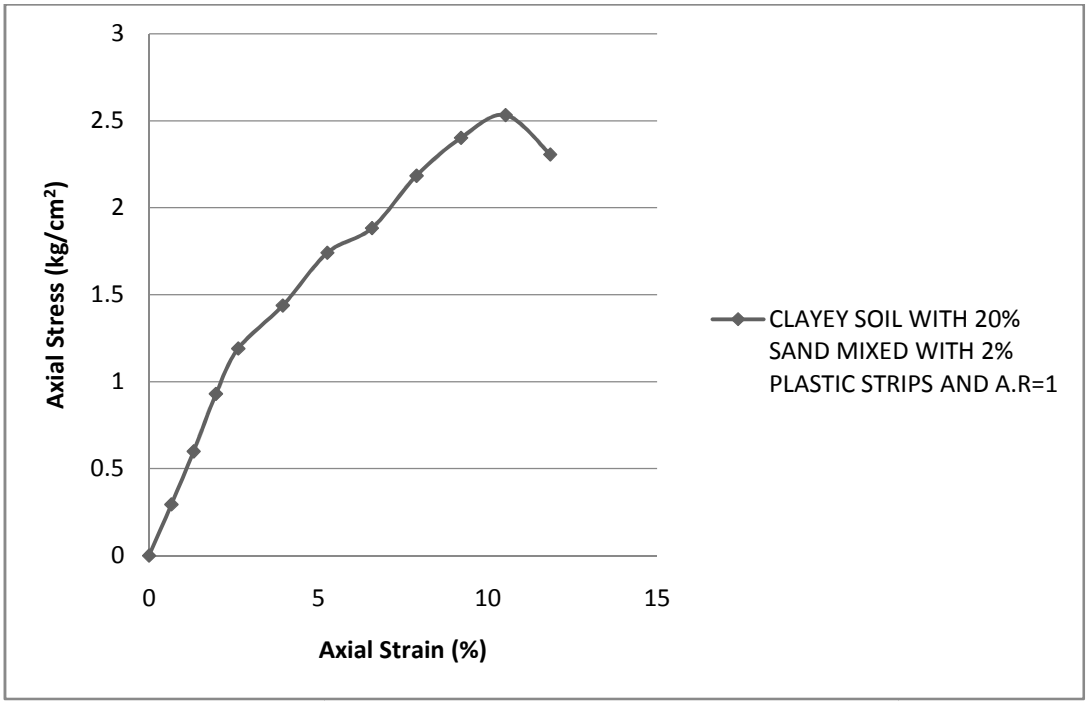

Fig. 3.99: Axial stress vs. Axial strain

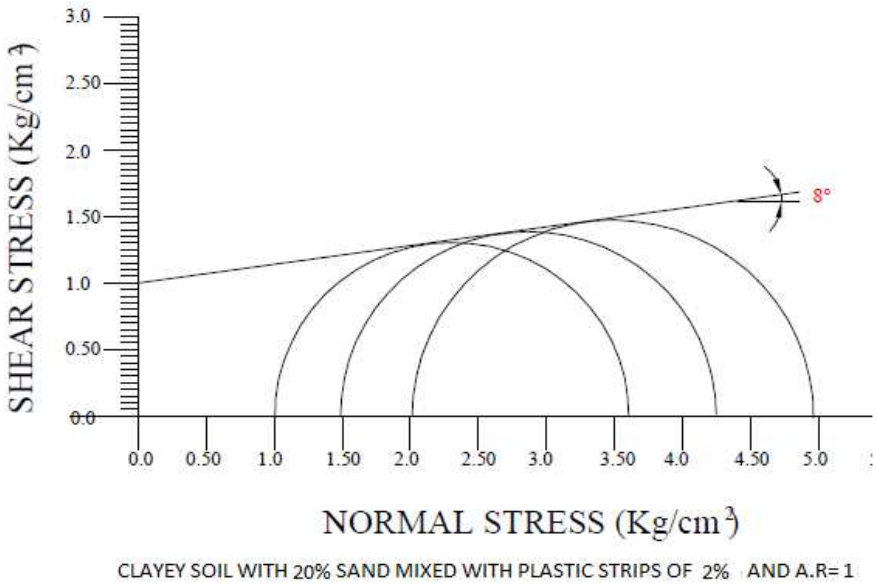

Fig. 3.100: Mohr Circle - Shear stress vs. Normal stress

3.6.11 Test Result of S3+AR2

In this section the results of tests on different types of soil have been presented to find various properties of these soil types. Standard Proctor Compaction curves, axial stress-strain curves as obtained from UU triaxial tests and Mohr circles of stress for determining shear strength parameters for the mix for strip content of 0.5%, 1.0%, 1.5% and 2.0% have been shown in Figs. 3.101 to 3.103, 3.104 to 3.106, 3.107 to 3.109 and 3.110 to 3.112 respectively.

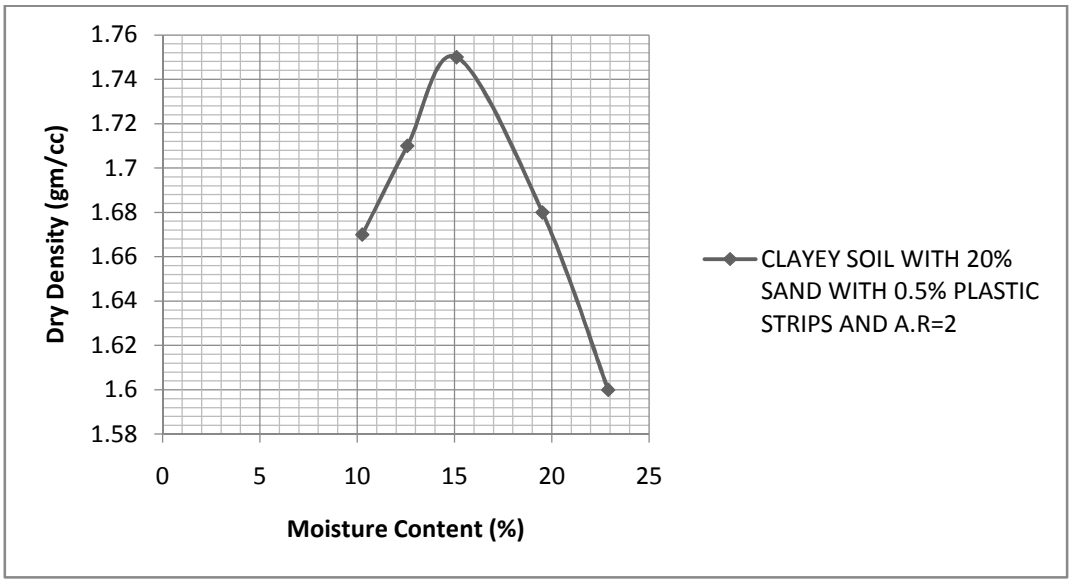

Fig. 3.101: Standard Proctor Compaction Curve

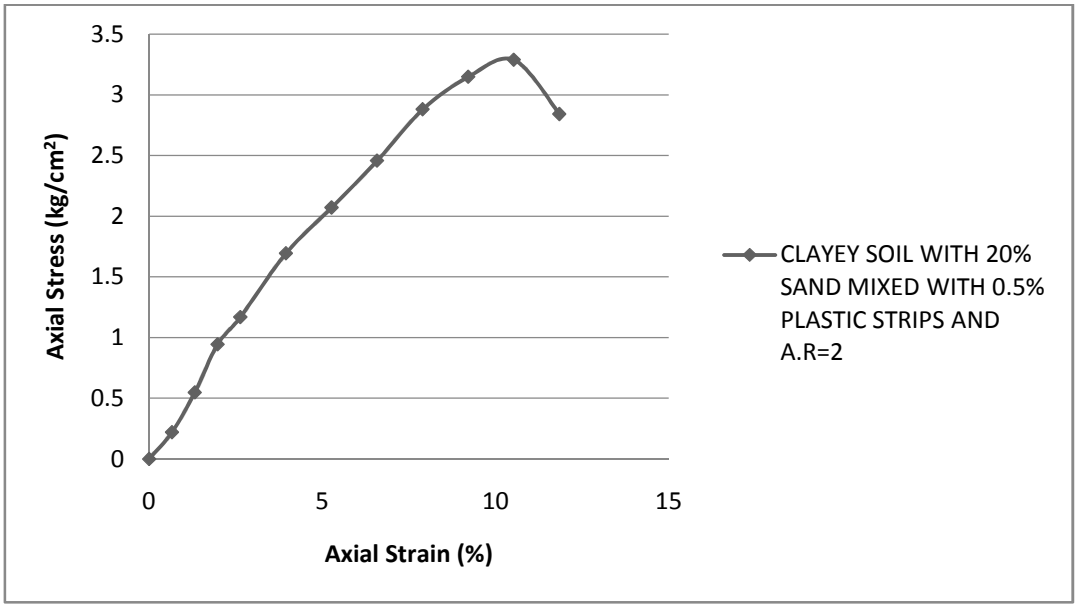

Fig. 3.102: Axial stress vs. Axial strain

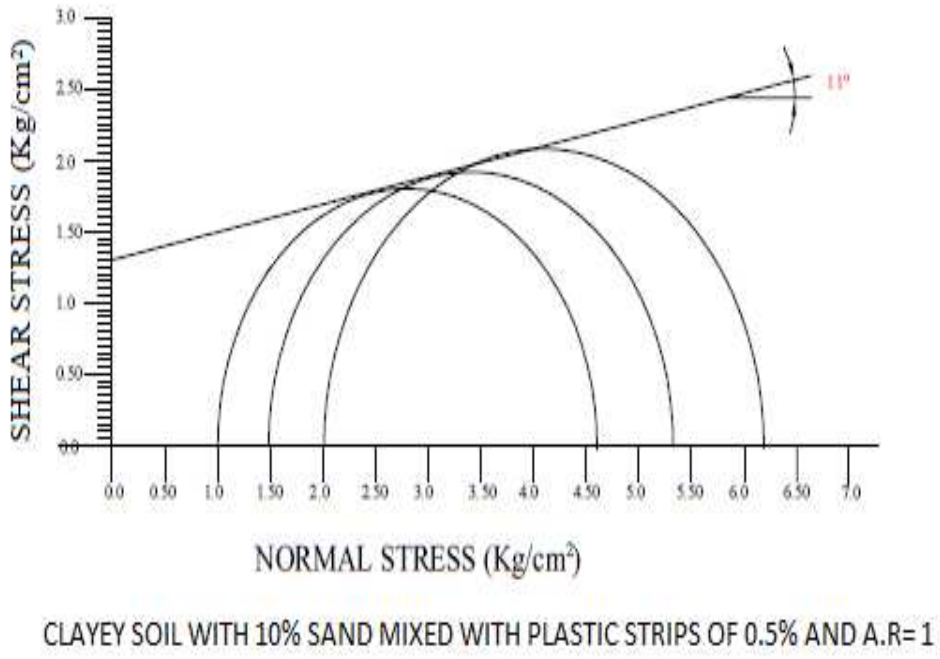

Fig. 3.103: Mohr Circle - Shear stress vs. Normal stress

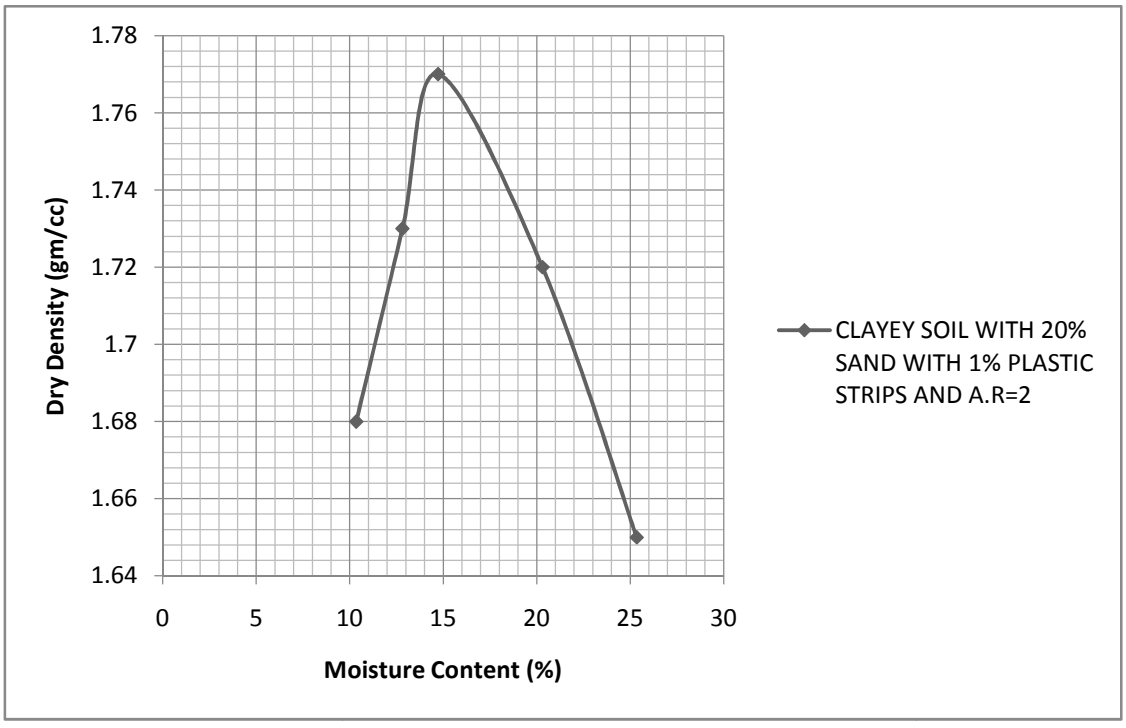

Fig. 3.104: Standard Proctor Compaction Curve

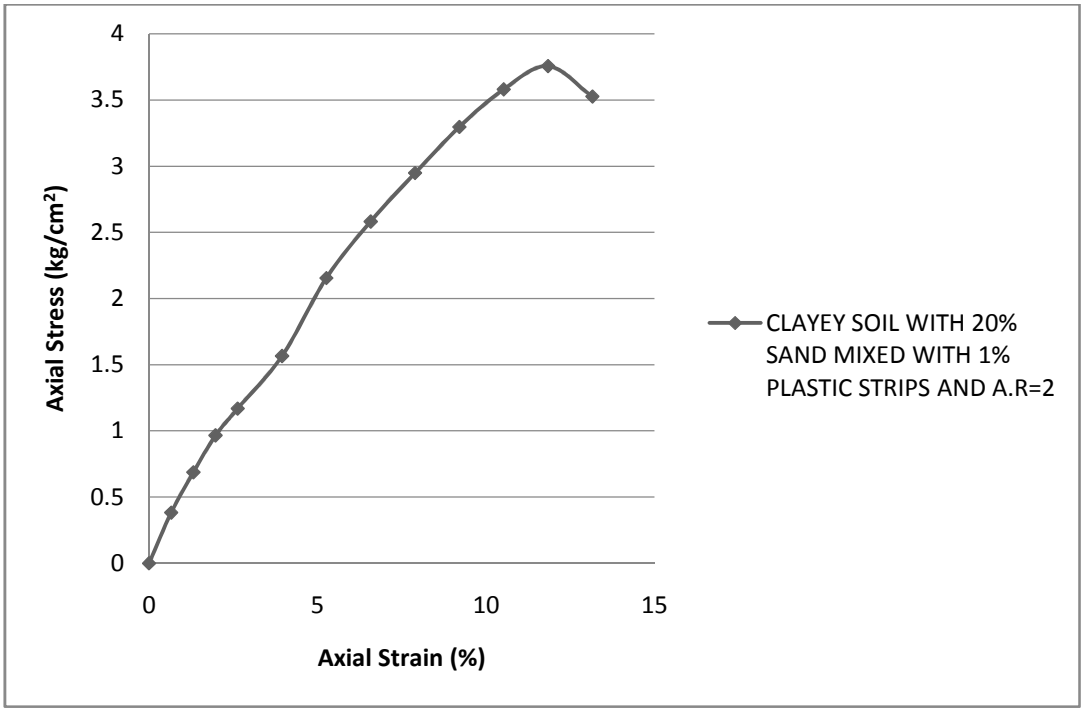

Fig. 3.105: Axial stress vs. Axial strain

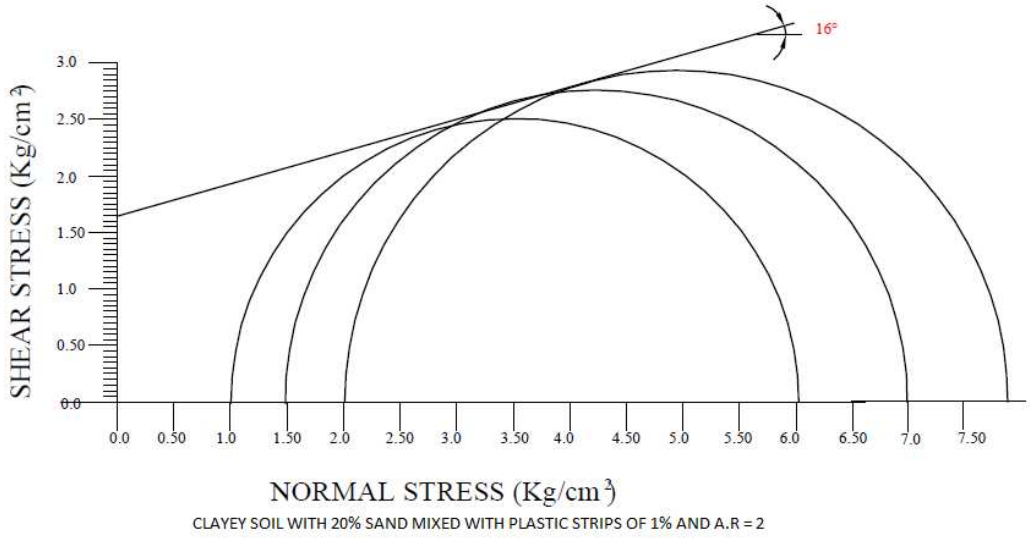

Fig. 3.106: Mohr Circle - Shear stress vs. Normal stress

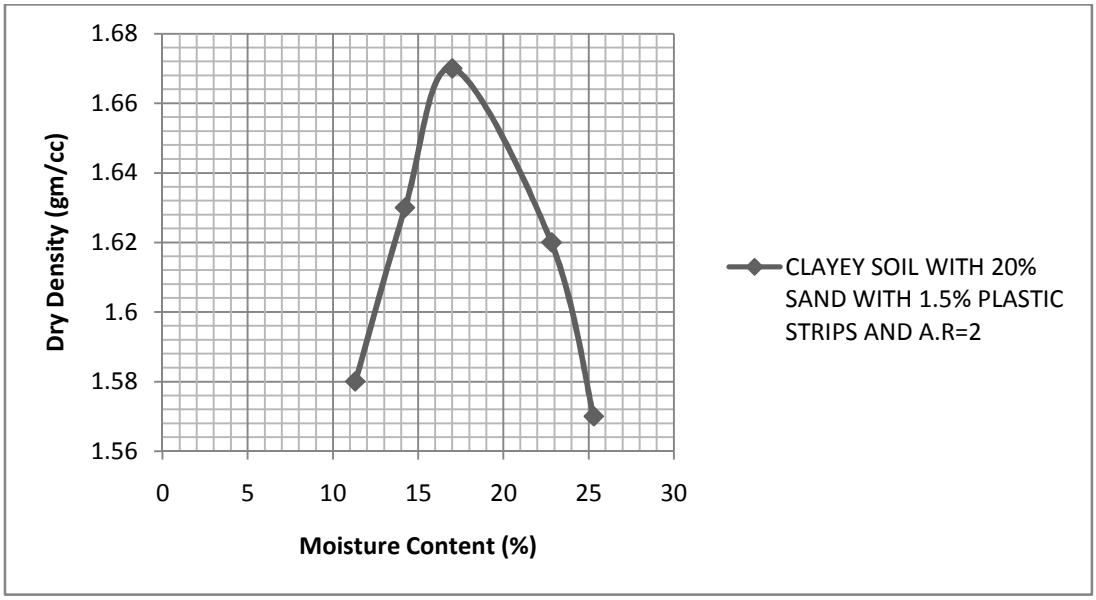

Fig. 3.107: Standard Proctor Compaction Curve

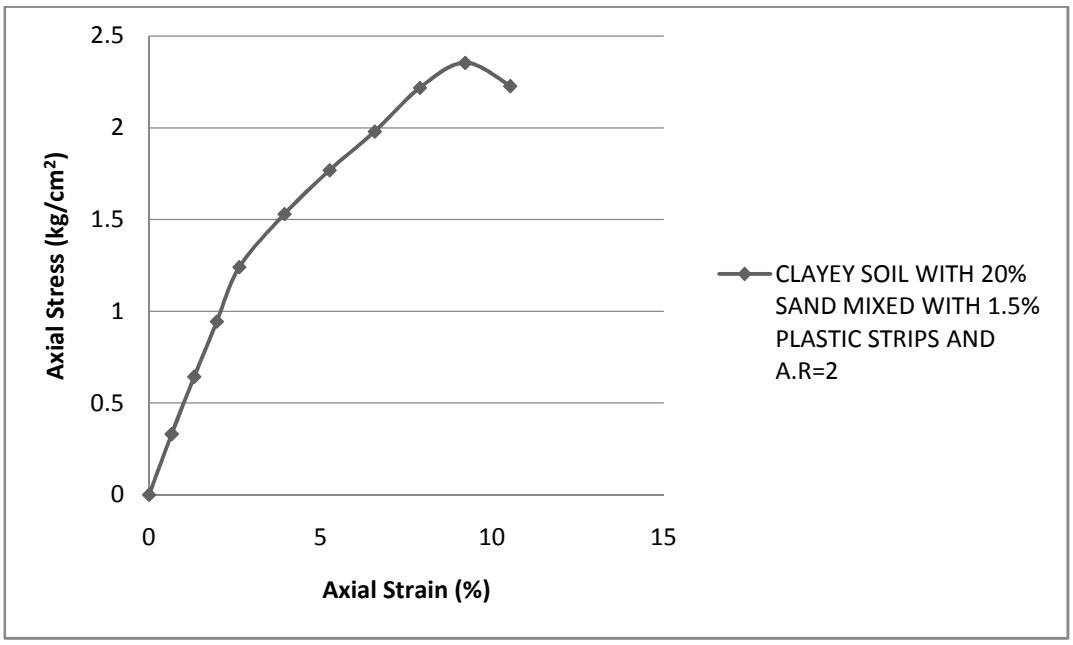

Fig. 3.108: Axial stress vs. Axial strain

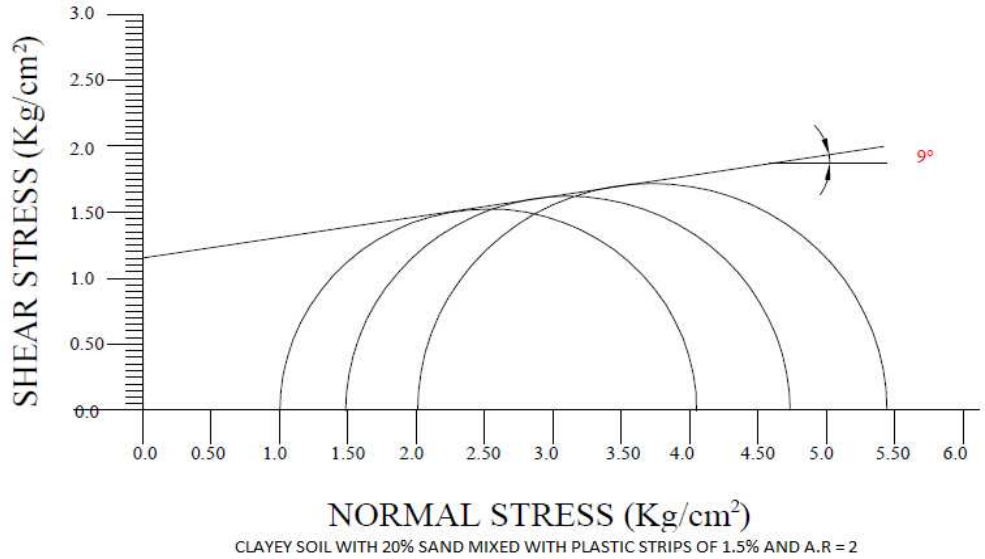

Fig. 3.109: Mohr Circle - Shear stress vs. Normal stress

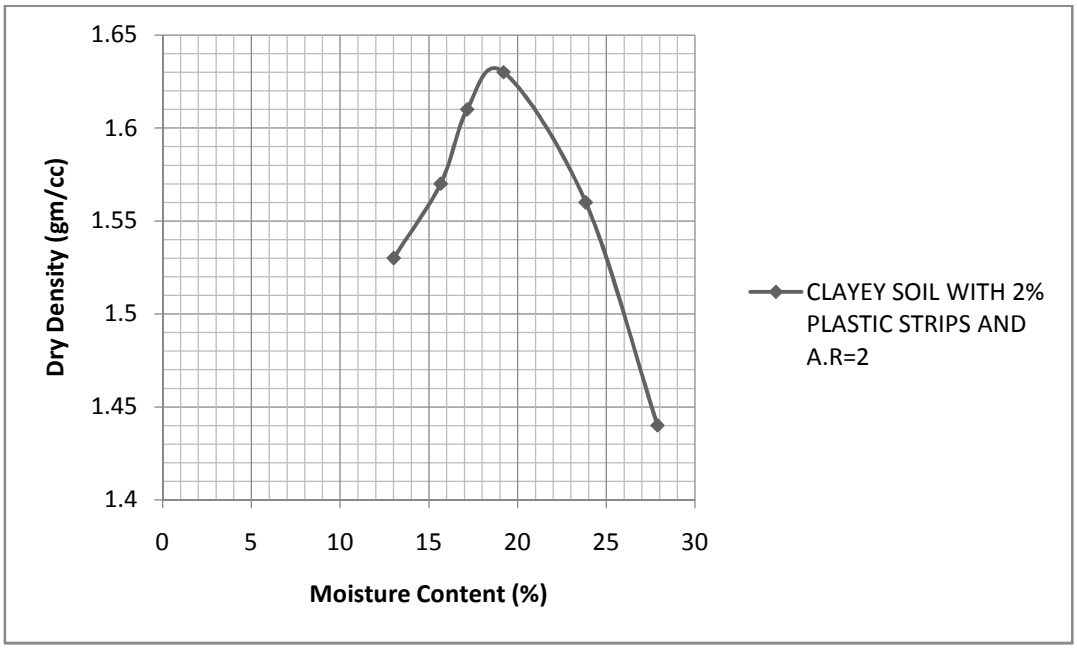

Fig. 3.110: Standard Proctor Compaction Curve

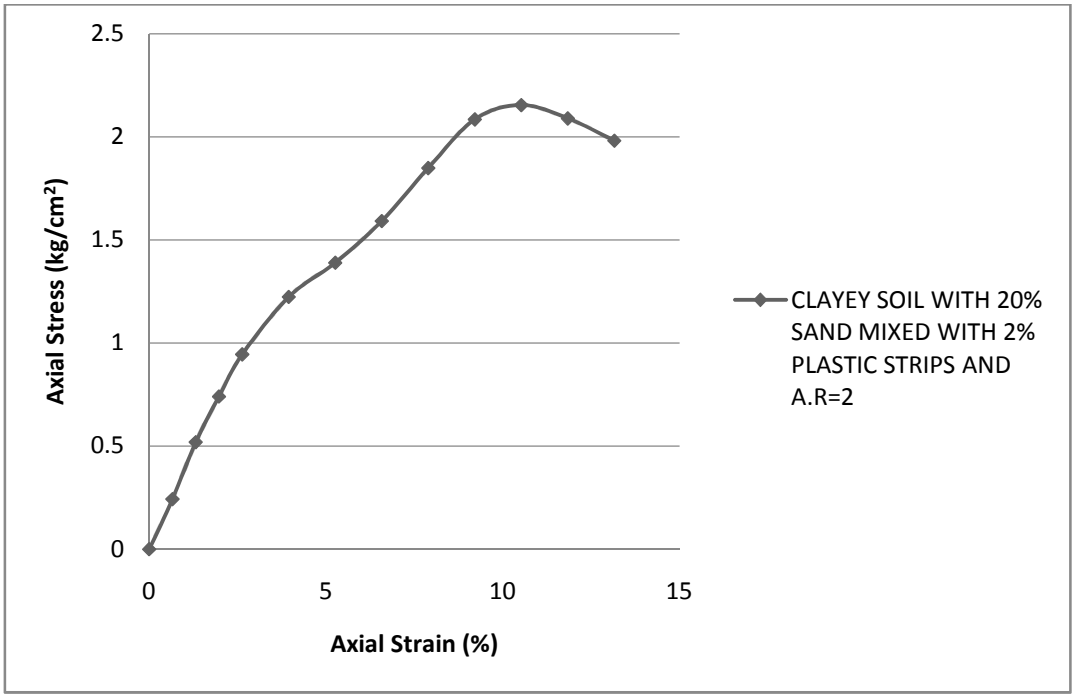

Fig. 3.111: Axial stress vs. Axial strain

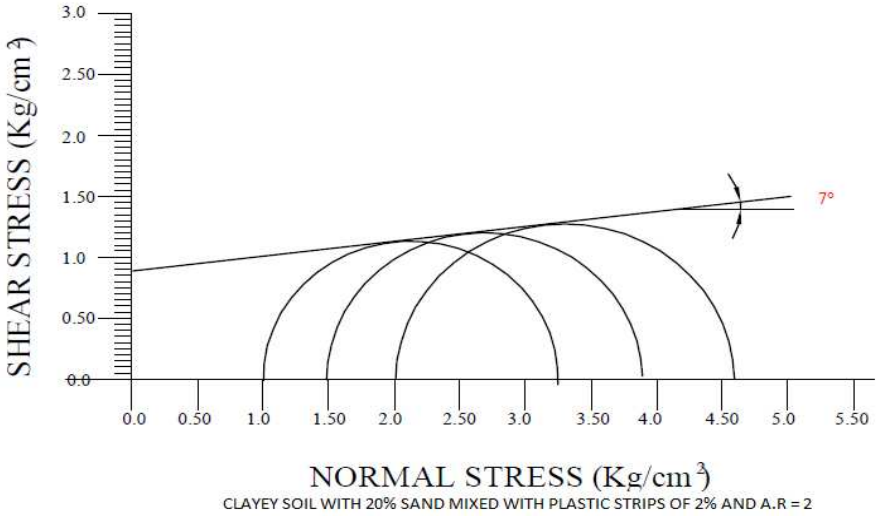

Fig. 3.112: Mohr Circle - Shear stress vs. Normal stress

3.6.12 Test Result of S3+AR3

In this section the results of tests on different types of soil have been presented to find various properties of these soil types. Standard Proctor Compaction curves, axial stress-strain curves as obtained from UU triaxial tests and Mohr circles of stress for determining shear strength

parameters for the mix for strip content of 0.5%, 1.0%, 1.5% and 2.0% have been shown in Figs. 3.113 to 3.115, 3.116 to 3.118, 3.119 to 3.121 and 3.122 to 3.124 respectively.

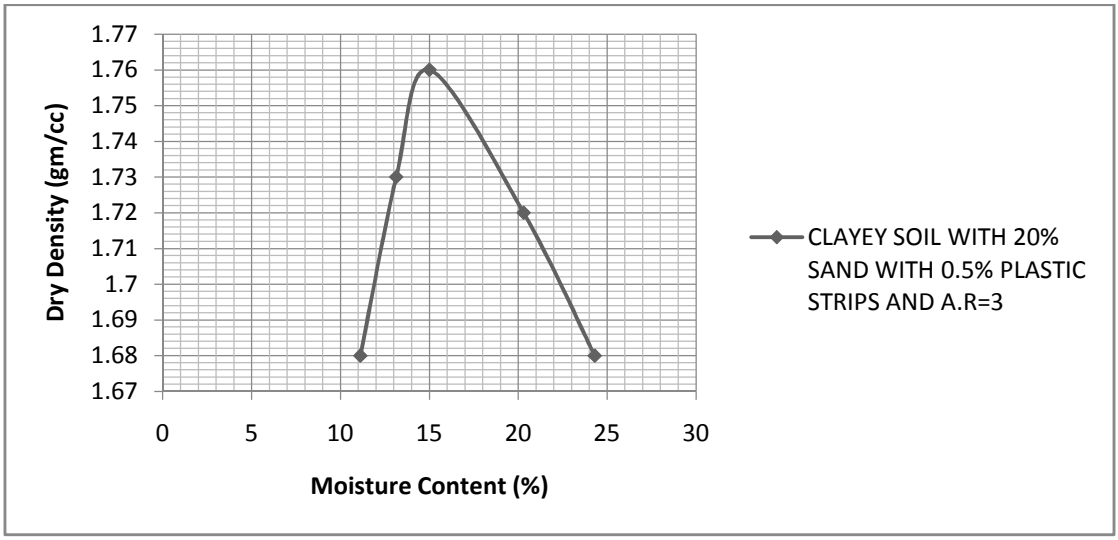

Fig. 3.113: Standard Proctor Compaction Curve

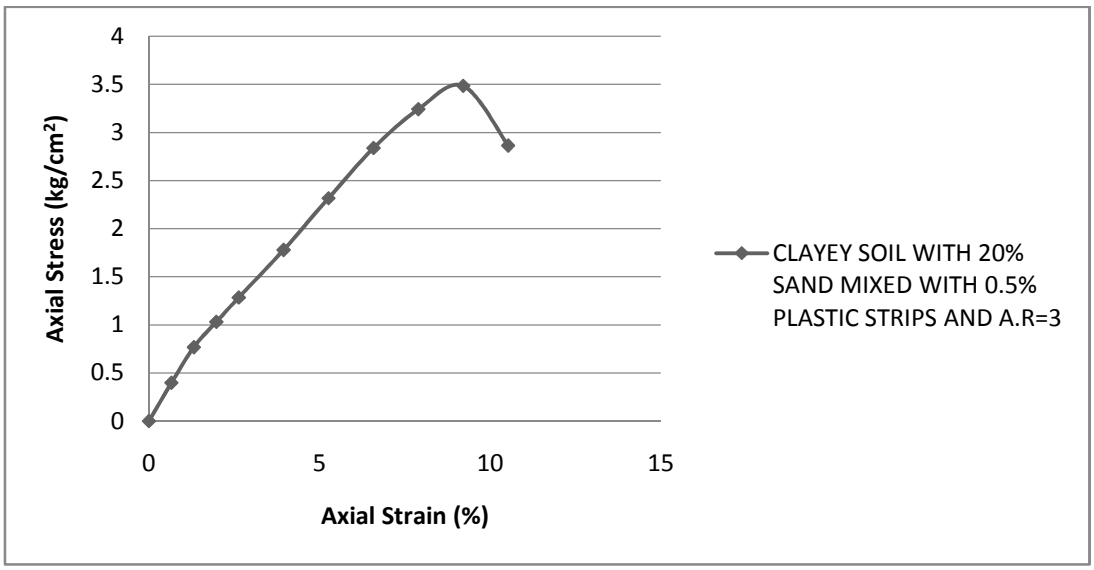

Fig. 3.114: Axial stress vs. Axial strain

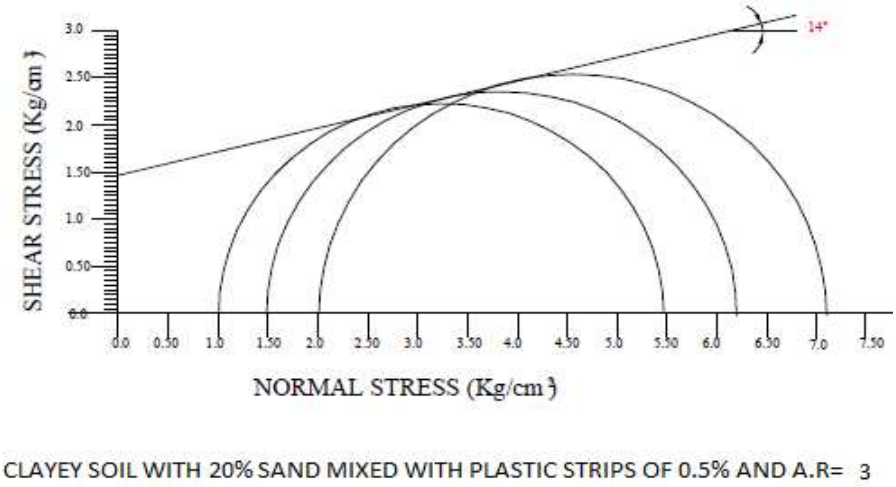

Fig. 3.115: Mohr Circle - Shear stress vs. Normal stress

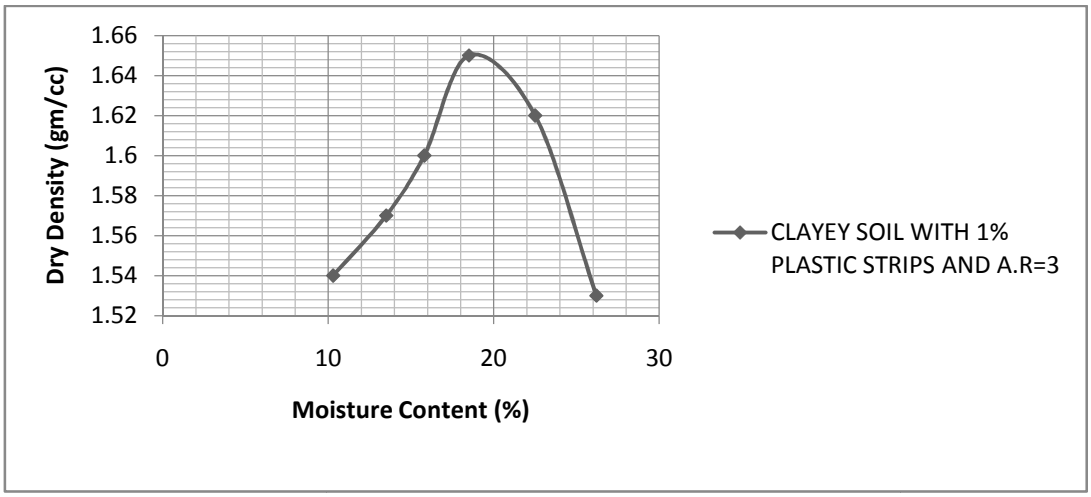

Fig. 3.116: Standard Proctor Compaction Curve

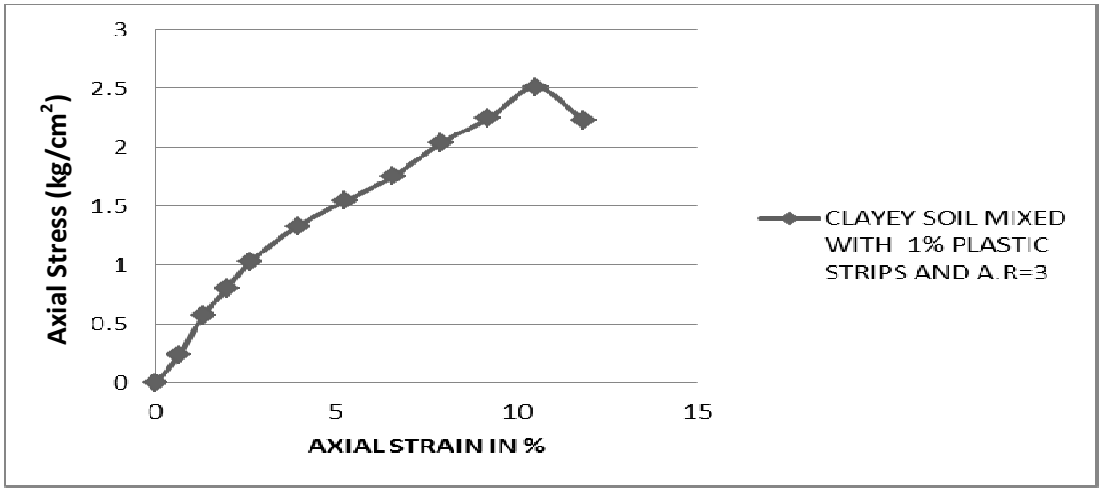

Fig. 3.117: Axial stress vs. Axial strain

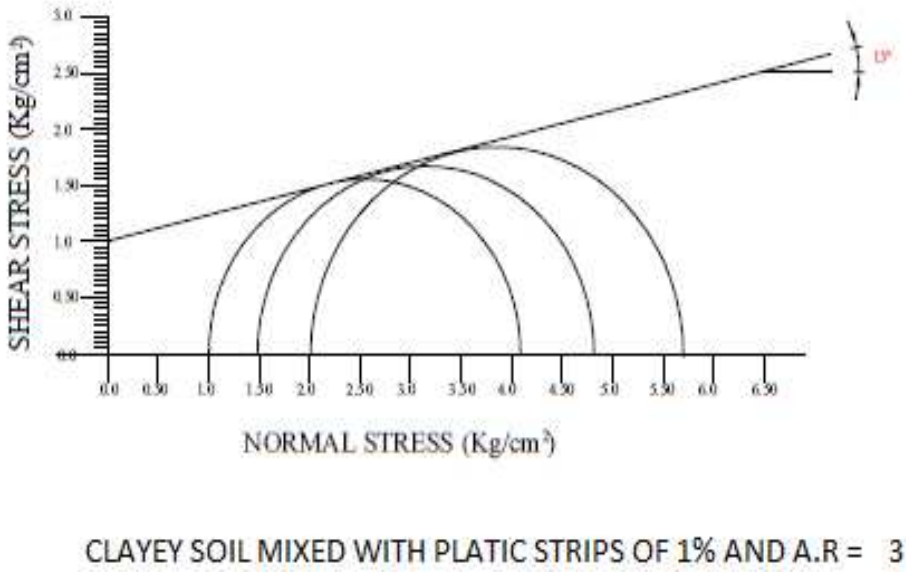

Fig. 3.118: Mohr Circle - Shear stress vs. Normal stress

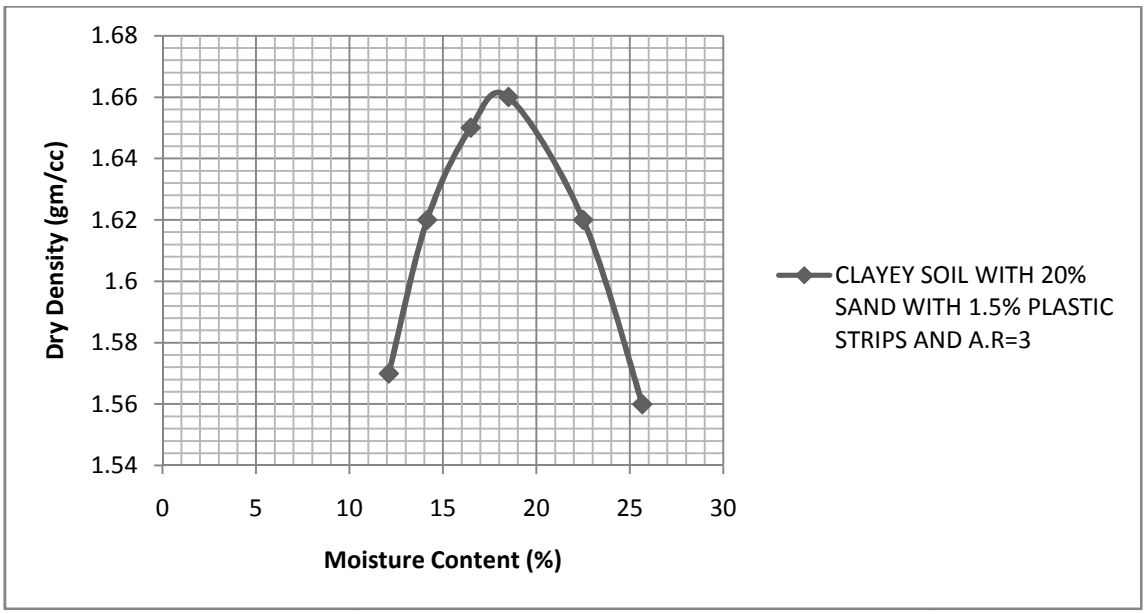

Fig. 3.119: Standard Proctor Compaction Curve

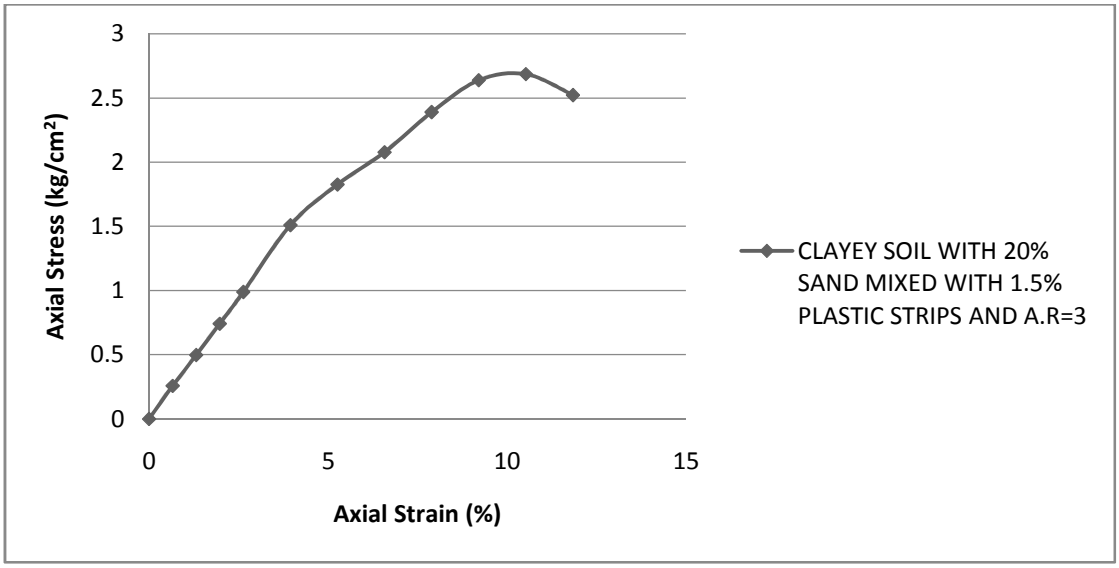

Fig. 3.120: Axial stress vs. Axial strain

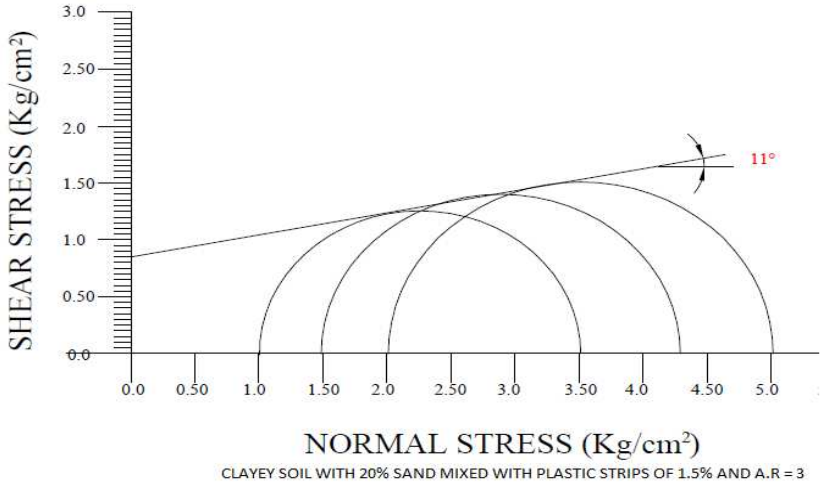

Fig. 3.121: Mohr Circle - Shear stress vs. Normal stress

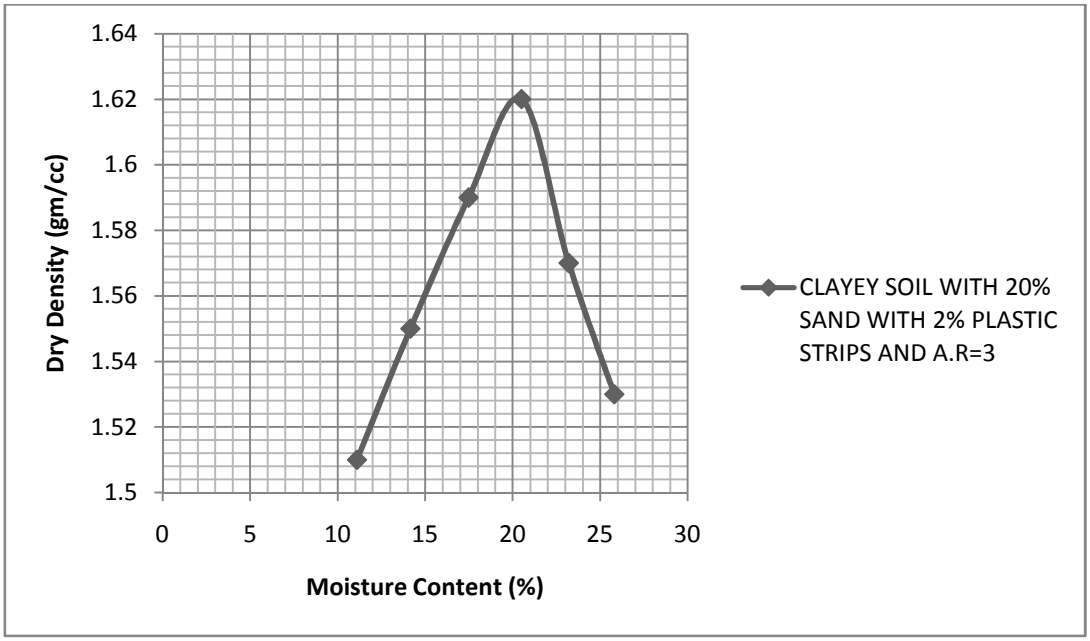

Fig. 3.122: Standard Proctor Compaction Curve

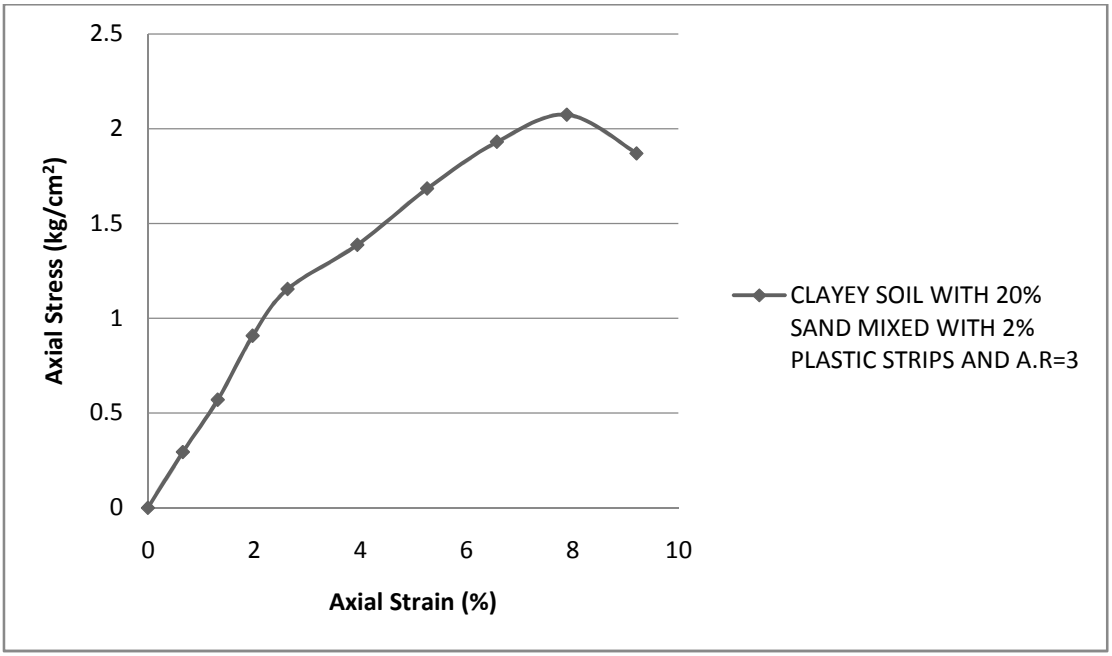

Fig. 3.123: Axial stress vs. Axial strain

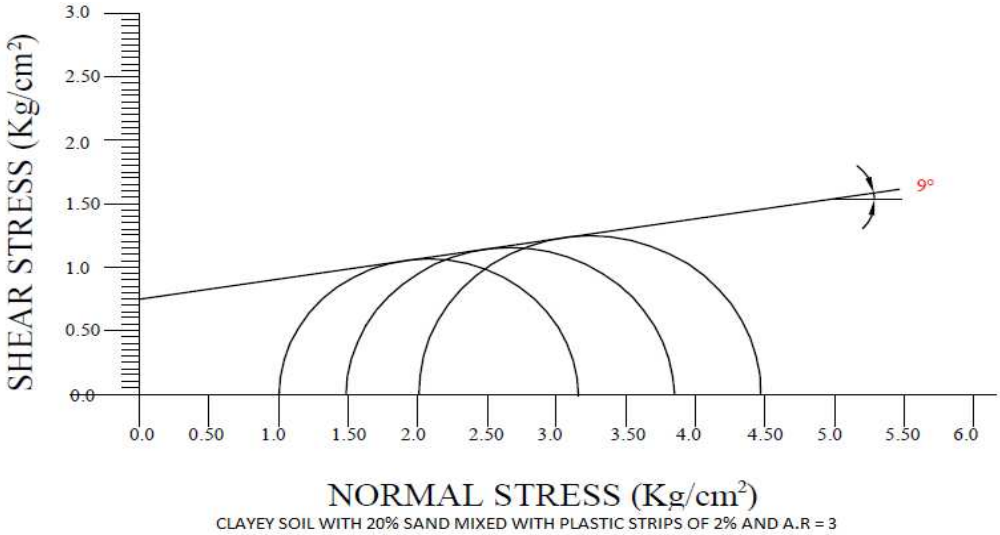

Fig. 3.124: Mohr Circle - Shear stress vs. Normal stress

Based on all these figures an attempt has been made to obtain the properties of Soil-PET bottle strips mixes prepared with 3 types of soil (S1, S2 and S3) and PET bottle strips with 3 aspect ratios (1, 2 and 3) and of 4 strip contents (0.5%,1.0%, 1.5% and 2.0%). The characterization and strength properties of different types of mixes have been presented in Table 3.8.

Table 3.8: Property of Soil-PET Bottle Strips Mix

Sl. No.	Type of soil	Dimension with percentage	Optimum water content (%)	MDD (g/ cm^3)	UCS (q_u) (kg/cm^2)	C_u (kg/cm^2)	Cohesion (c) (kg/cm^2)	Angle of internal friction ϕ
1	S1	5 mm × 5 mm (0.5%)	17.8	1.68	2.5	1.25	1.05	9^o
2	S1	5 mm × 5 mm (1.0%)	17.48	1.7	2.79	1.39	1.2	11^o
3	S1	5 mm × 5 mm (1.5%)	18	1.67	2.45	1.22	1	8^o
4	S1	5 mm × 5 mm (2.0%)	18.44	1.65	2.15	1.07	0.9	6^o
5	S1	5 mm × 10 mm (0.5%)	17.6	1.7	2.60	1.30	1.15	9^o
6	S1	5 mm × 10 mm (1.0%)	17.4	1.71	3.0	1.50	1.35	12^o
7	S1	5 mm × 10 mm (1.50%)	18.15	1.66	2.38	1.19	1.0	8^o

8	S1	5 mm × 10 mm (2.0%)	19.2	1.64	2.10	1.05	0.9	6^o
9	S1	5 mm × 15 mm (0.5%)	18.15	1.67	2.66	1.33	1.1	10^o
10	S1	5 mm × 15 mm (1.0%)	18.50	1.65	2.50	1.25	1.0	13^o
11	S1	5 mm × 15 mm (1.50%)	19.40	1.62	1.88	0.94	0.6	9^o
12	S1	5 mm × 15 mm (2.0%)	19.80	1.58	1.65	0.82	0.5	7^o
13	S2	5 mm × 5 mm (0.5%)	16.90	1.70	3.08	1.54	1.3	11^o
14	S2	5 mm × 5 mm (1.0%)	15.85	1.72	3.45	1.72	1.45	13^o
15	S2	5 mm × 5 mm (1.5%)	17.50	1.67	2.68	1.34	1.18	9^o
16	S2	5 mm × 5 mm (2.0%)	19.60	1.65	2.25	1.12	0.98	7^o
17	S2	5 mm × 10 mm (0.5%)	16.50	1.71	2.98	1.49	1.3	12^o
18	S2	5 mm × 10 mm (1.0%)	15.53	1.74	3.55	1.77	1.48	13^o
19	S2	5 mm × 10 mm (1.50%)	18.50	1.64	2.15	1.07	0.95	7^o
20	S2	5 mm × 10 mm (2.0%)	19.20	1.61	1.85	0.92	0.76	6^o
21	S2	5 mm × 15 mm (0.5%)	17.00	1.71	3.32	1.66	1.45	12^o
22	S2	5 mm × 15 mm (1.0%)	18.24	1.68	2.96	1.48	1.25	14^o
23	S2	5 mm × 15 mm (1.5%)	19.50	1.63	2.15	1.07	0.8	9^o
24	S2	5 mm × 15 mm (2.0%)	20.20	1.60	1.77	0.88	0.65	7^o
25	S3	5 mm × 5 mm (0.5%)	15.20	1.75	3.16	1.58	1.35	13^o
26	S3	5 mm × 5 mm (1.0%)	14.85	1.76	3.65	1.82	1.55	15^o
27	S3	5 mm × 5 mm (1.5%)	16.50	1.68	2.78	1.39	1.2	11^o
28	S3	5 mm × 5 mm (2.0%)	19.60	1.65	2.53	1.26	1.0	8^o

29	S3	5 mm × 10 mm (0.5%)	15.10	1.75	3.28	1.64	1.4	14^o
30	S3	5 mm × 10 mm (1.0%)	14.73	1.77	3.75	1.87	1.5	16^o
31	S3	5 mm × 10 mm (1.5%)	17.00	1.67	2.65	1.33	1.15	9^o
32	S3	5 mm × 10 mm (2.0%)	19.65	1.63	2.15	1.07	0.88	7^o
33	S3	5 mm × 15 mm (0.5%)	15.00	1.76	3.48	1.74	1.48	14^o
34	S3	5 mm × 15 mm (1.0%)	16.84	1.71	3.28	1.64	1.33	17^o
35	S3	5 mm × 15 mm (1.50%)	18.50	1.66	2.38	1.15	0.95	11^o
36	S3	5 mm × 15 mm (2.0%)	20.50	1.62	2.07	1.03	0.75	9^o

3.7 A Brief Discussion on Material Properties

It is observed that OMC decreases and MDD increases with increase of percentage of sand. Sand can retain less moisture and the density of the sand is quite higher than that of clay. Angle of internal friction (ϕ) increases with increase of percentage of plastic strips but up to 1% of plastic strips. It is obvious since qualitatively increase of shear strength occurs with increase of density of a soil. Shear strength (c) and angle of internal friction (ϕ) increases with increase of percentage of sand. Since the density of the sand is quite higher than that of clay and sand helps to increase the angle of shearing resistance of the soil. OMC decreases and MDD increases with increase of percentage of plastic strips up to 1% and it is also noticed that beyond 1% of plastic strips the OMC increases and MDD decreases because plastic fibers have no water absorption capacity and also addition of plastic fiber increases the MDD. After addition of more than 1% plastic fiber there is increase of void ratio due to separation of soil grains caused by plastic fibers. After addition of 1% of plastic strips, angle of internal friction decreases for aspect ratio 1, 2 and 3. There is an increase in MDD, UCS, modulus of elasticity and shear strength with addition of plastic strips up to 1% beyond which these properties do not show any improvement of soil in respect of strength. Further this occurs up to aspect ratio of 3. The values of co-efficient of consolidation have been obtained from time-settlement data (not presented). The c_v values have also been furnished in tables. The m_v values are obtained for getting settlement of footings used for numerical study in chapter 5. The c_v values give an idea about the time required for settlement of a footing for

occurrence of a particular degree of consolidation. The values for each soil type S1, S2 and S3 obey with reinforcement with different aspect ratios and optimum strip content of 1% have presented in the following sections.

3.8 Influence of strip content on properties of Soil-PET bottle strip mixes

In an attempt to find variation of plastic strip contents on properties of the mixes it is found necessary at this stage to find the optimum content of PET bottle strips at which the strength properties yield maximum value for each type of soil - S1, S2 and S3.

Therefore the variation of unconfined compressive strength test and also the Shear Strength parameters have been studied with variation of percent of plastic strips in the following sections.

3.8.1 Variation of UCS with % of Plastic Strips

Variation of UCS with % of plastic strips for three types of soil has been presented in Fig.3.125 (a) to (c) for soil S1, S2 and S3 respectively. It is observed that UCS increases with increase of percentage of plastic strips but up to 1% and it is also noticed that after 1% of plastic strips the UCS decreases for aspect ratio of 1 and 2. In case of aspect ratio 3, there is a reduction of UCS. Optimum value comes at aspect ratio 2. It may also be found in Table 3.6 that up to aspect ratio 2 MDD increases for addition of 1% plastic fibre and beyond this aspect ratio and percentage of strip MDD decreases. The same trend is observed in case of UCS also due to the fact that increase of MDD causes increase of shear strength and thereby increase of UCS and the vice versa. Beyond AR of 2 and after addition of 1% plastic fibre UCS decreases for the same reason.

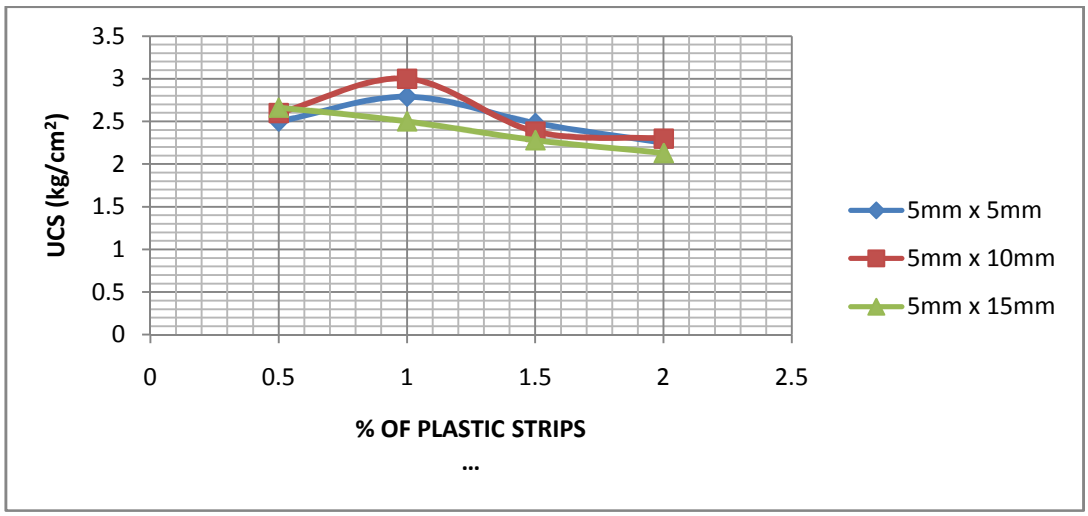

Fig. 3.125(a): UCS vs. Percentage of plastic strips – Soil S1

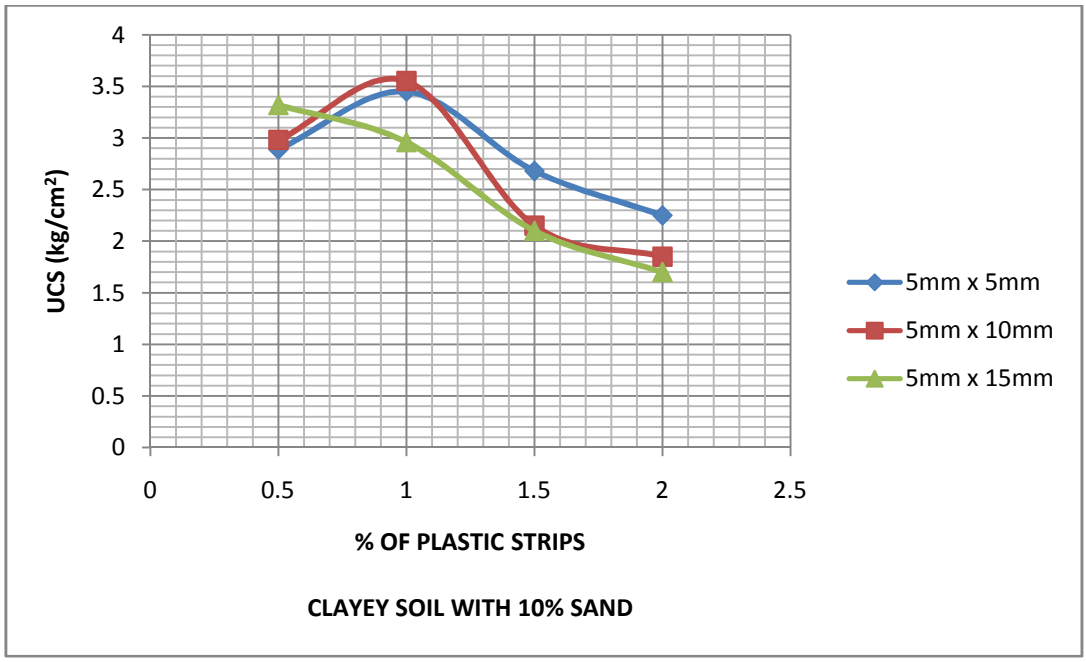

Fig. 3.125(b): UCS vs. Percentage of plastic strips - Soil S2

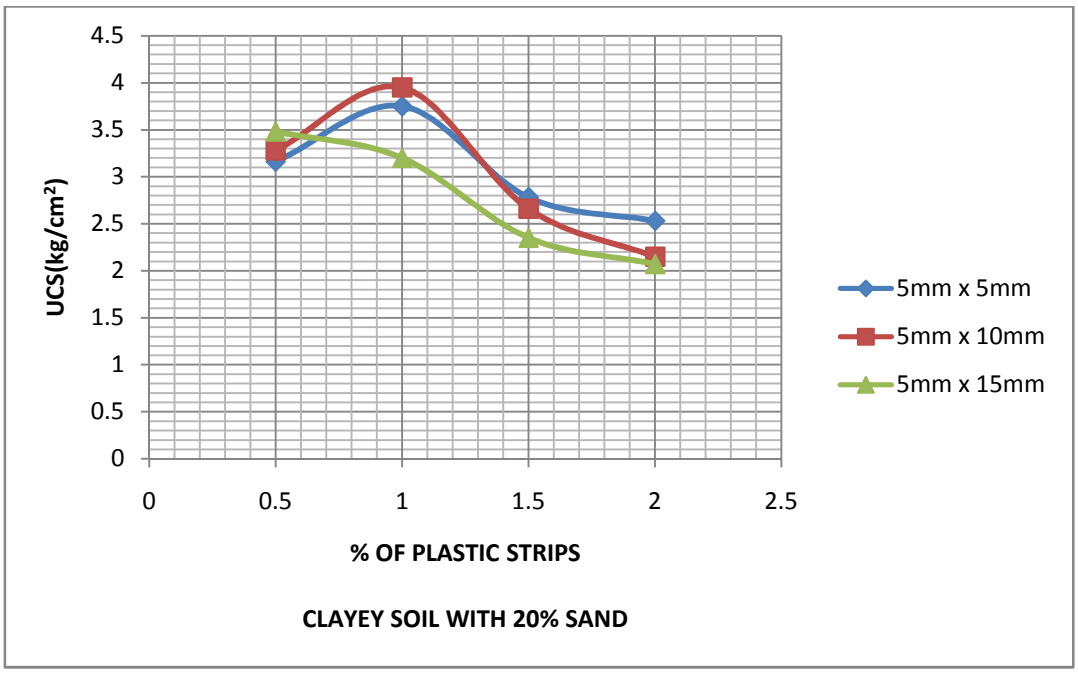

Fig. 3.125(c): UCS vs. Percentage of plastic strips - Soil S3

3.8.2 Variation of Shear Strength Parameters with % of Plastic Strips

Both the shear strength parameters C and ϕ have been considered to study the alteration of shear strength of soil due to addition of PET bottle strips.

Variation of C with % of plastic strips has been presented in Fig. 3.126(a) to (c) for soil S1, S2 and S3 respectively. Similarly variation of ϕ with % of plastic strips has been shown in Fig. 3.126(d) to (f) for soil S1, S2 and S3 respectively. It is observed that shear strength (c) increases with increase of percentage of plastic strips but up to 1%. But beyond addition of 1% of plastic fibre, c decreases for aspect ratio 1 and 2. For aspect ratio 3, there is reduction in value of c. Angle of internal friction (ϕ) increases with increase of percentage of plastic strips but up to 1% of plastic strips. After addition of 1% of plastic strips, angle of internal friction decreases for aspect ratio 1, 2 and 3. Optimum value occurs at aspect ratio of 2 for shear strength. At aspect ratio of 3, ϕ increases up to 1% of plastic strip but since there is an appreciable reduction in c, effectively the shear strength is reducing. Hence optimum value occurs at aspect ratio 2.

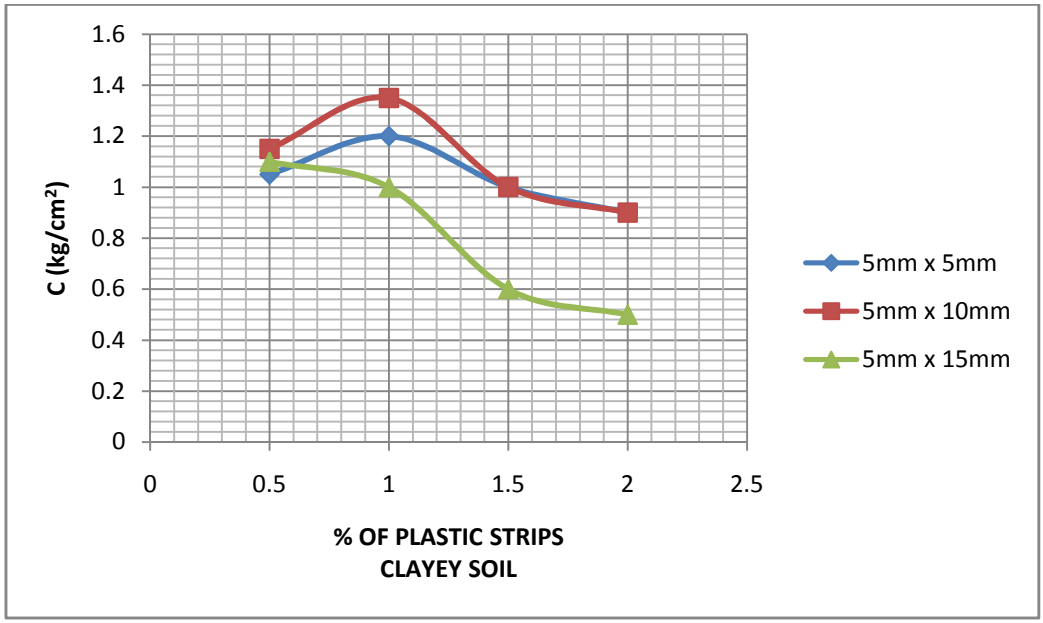

Fig. 3.126(a): C vs. Percentage of plastic strips

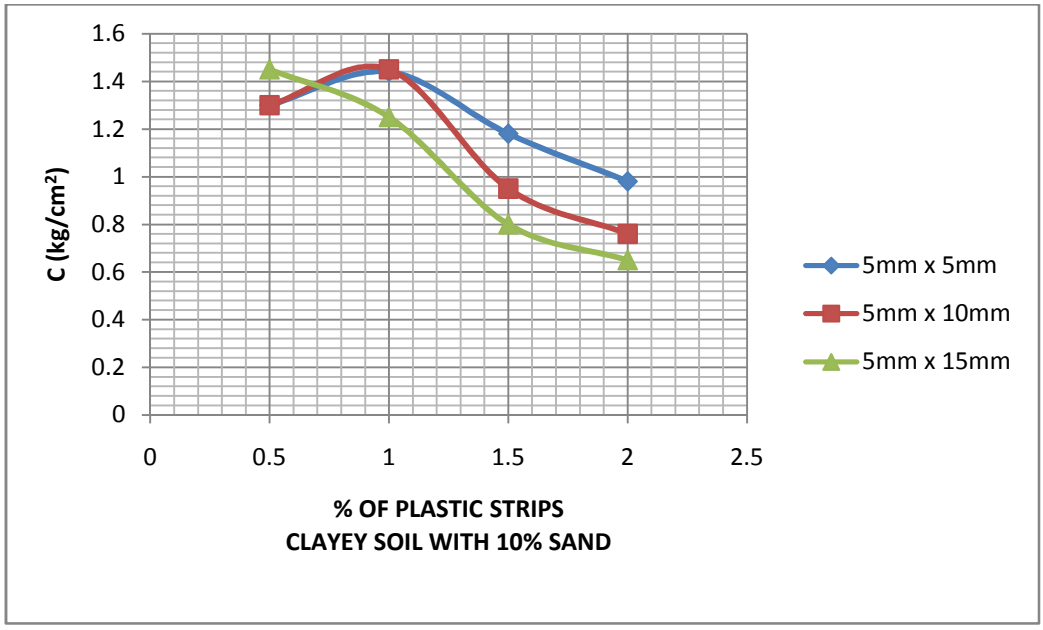

Fig. 3.126(b): C vs. Percentage of plastic strips

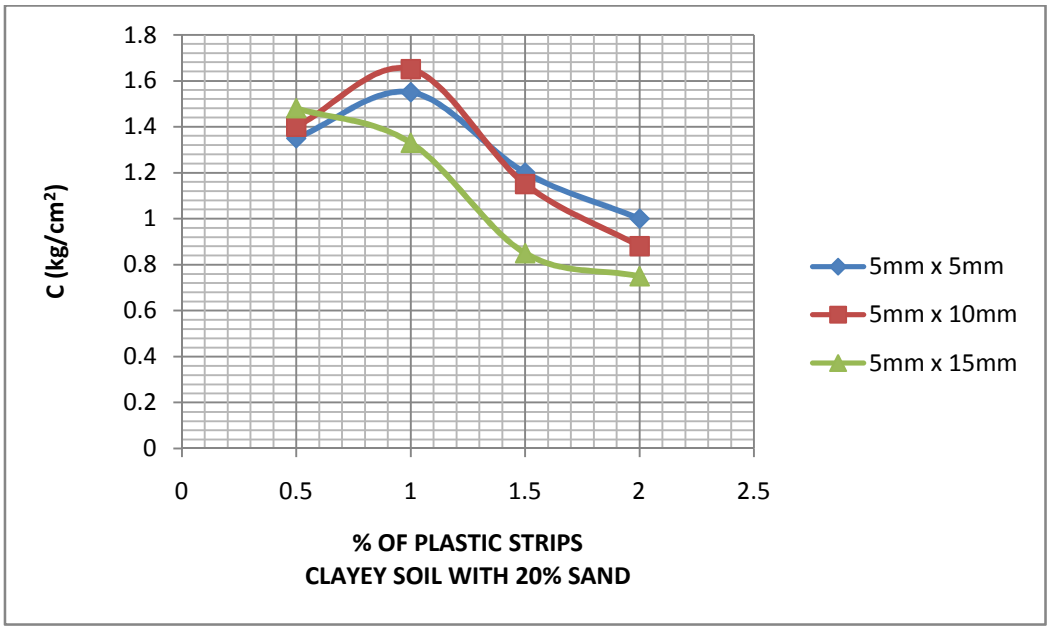

Fig. 3.126(c): C vs. Percentage of plastic strips

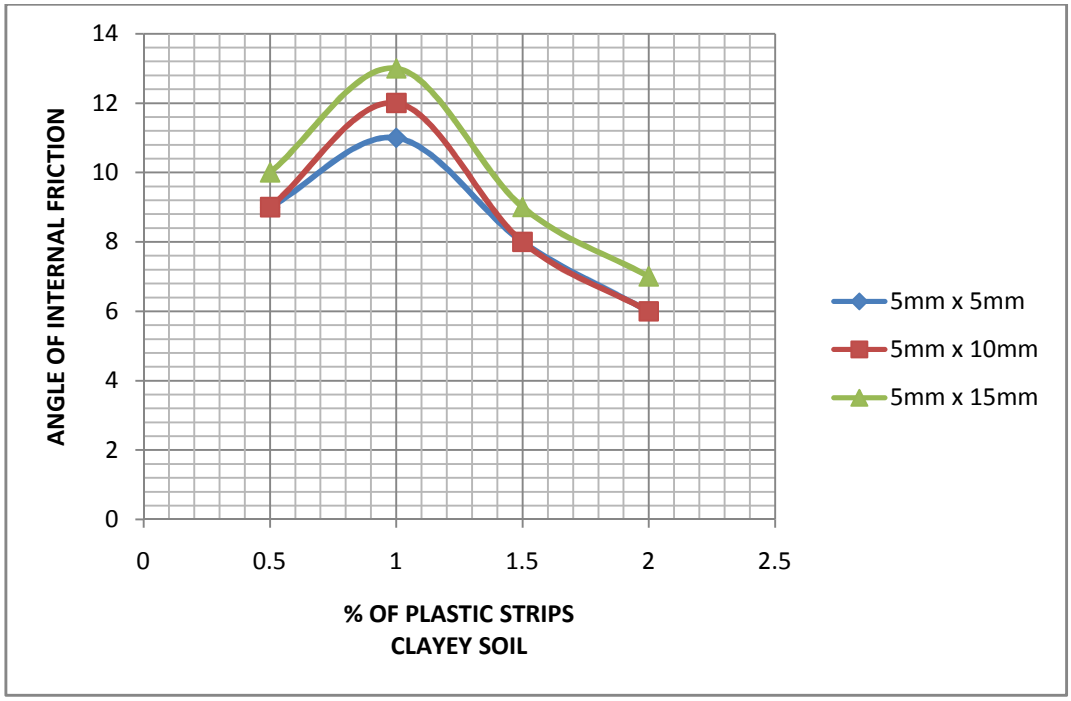

Fig. 3.126(d): Angle of internal friction vs. Percentage of plastic strips

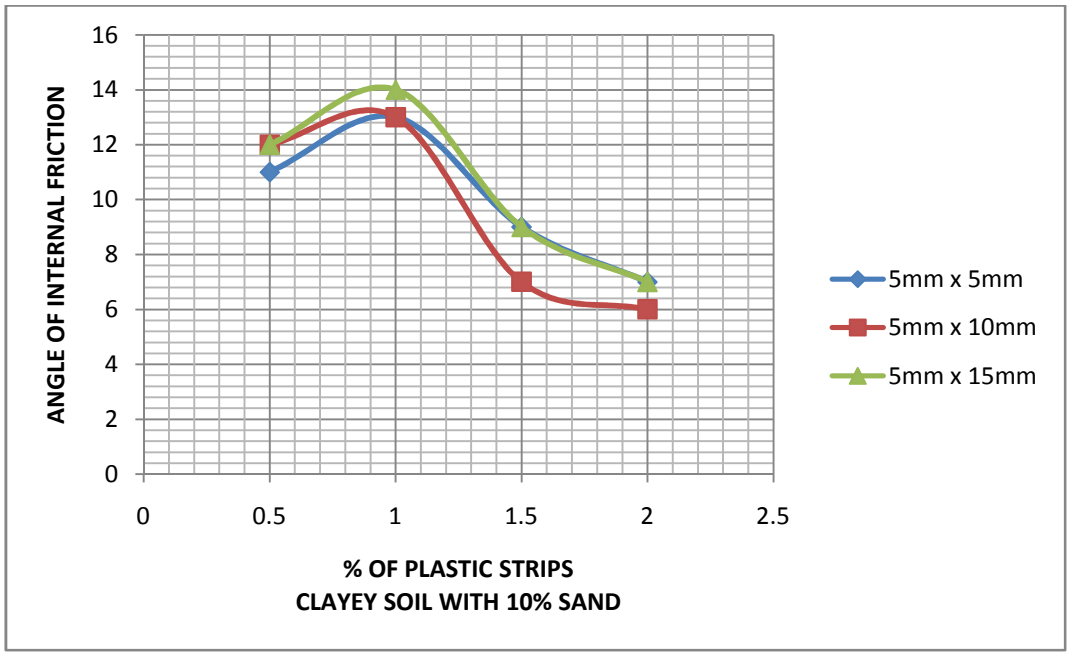

Fig. 3.126(e): Angle of internal friction vs. Percentage of plastic strips

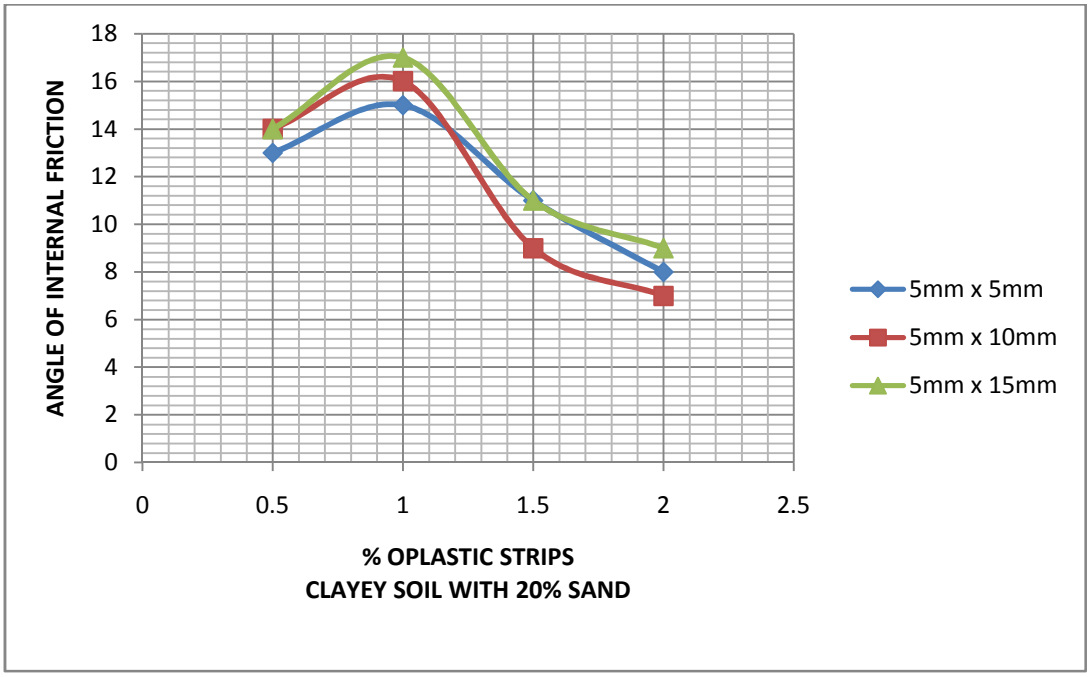

Fig. 3.126(f): Angle of internal friction vs. Percentage of plastic strips

3.8.3 Optimum Value of Aspect Ratio and Percent of Plastic Strips

Considering all the results of soil-PET bottle strip (reinforced) mixes, it appears that there is an increase in MDD, UCS, and shear strength parameters with addition of plastic strips up to 1% beyond which these properties do not show any improvement of soil in respect of strength. Further this occurs for all aspect ratios. Based on this optimum values attempts have been made to carry out consolidation tests on selected samples of reinforced soil so that the data may help in determination of allowable bearing capacity of model footings. Since this optimum percent of plastic strips occurs for all the three aspect ratios has been chosen for further part of investigation.

3.9. Consolidation Test with 1% of Optimum Reinforcement

The presence of plastic strips in soil plays a vital role in increasing the rate of consolidation of soil. To investigate the effect of plastic strip on co-efficient of volume change and co-efficient of consolidation further investigation has been carried out with optimum 1% of reinforcement.

3.9.1 Test Programme for Consolidation Test

The test programme for consolidation test of optimum plastic strip content of 1% is presented in Table 3.9.

Table 3.9: Test programme for consolidation tests

TESTS	Soil type	Plastic %	Aspect Ratio	No. of tests
Consolidation tests	S1 S2 S3	0	--	3
	S1+AR1 S1+AR2 S1+AR3	1	1	3
	S2+AR1 S2+AR2 S2+AR3	1	2	3
	S3+AR1 S3+AR2 S3+AR3	1	3	3
Total No of Tests:				12

3.9.2 Presentation of Results of Consolidation Test

In this section, the results of consolidation test on original clayey soil and soil-PET bottle strip (reinforcement) mixes have been presented. An attempt has also been made to obtain co-efficient of volume change (m_v) at different pressure ranges of surcharge. The m_v-values have been presented in tabular form in Tables 3.10 to 3.12.

Table 3.10: Coefficient of volume change for S1 soil type

Type of Soil	S1	S1 + AR 1	S1 + AR 2	S1 + AR 3
Applied Pressure (kN/m^2)	Coefficient of volume change (m^2/kN)			
0 - 12.5	0.000168421	0.000126316	0.000084211	0.000126316
12.5 – 25	0.000675105	0.000548234	0.000505796	0.000548234
25 – 50	0.000553191	0.000488323	0.000424178	0.000467091
50 – 100	0.00038835	0.000343901	0.000289389	0.000386681
100 – 200	0.000258526	0.000229634	0.000190321	0.000240964
200 – 400	0.000214568	0.000165081	0.000141353	0.000176768
400 – 800	0.000143068	0.000101273	0.000105533	0.000110529

Table 3.11: Coefficient of volume change for S2 soil type

Type of Soil	S2	S2 + AR1	S2 + AR2	S2 + AR3
Applied Pressure (kN/m^2)	Coefficient of volume change (m^2/kN)			
0 - 12.5	0.000168421	0.000126316	0.000084211	0.000210526
12.5 – 25	0.000632911	0.000506062	0.000379347	0.000548813
25 – 50	0.000489102	0.000403183	0.000359979	0.000467588
50 – 100	0.000322928	0.000267953	0.000245726	0.000311828
100 – 200	0.000246171	0.000184682	0.000173067	0.00021846
200 – 400	0.000151430	0.000116215	0.000107320	0.000178671
400 – 800	0.000096877	0.000070822	0.000067492	0.000092646

Table 3.12: Coefficient of volume change for S3 soil type

Type of Soil	S3	S3 + AR1	S3 + AR2	S3 + AR3
Applied Pressure (kN/m^2)	Coefficient of volume change (m^2/kN)			
0 - 12.5	0.000168421	0.000126316	0.000084211	0.000084211
12.5 - 25	0.000506329	0.000421719	0.000337197	0.000379347
25 - 50	0.000467091	0.000402756	0.000338624	0.000423504
50 - 100	0.000343716	0.000267666	0.000256137	0.000310326
100 - 200	0.000218579	0.000184482	0.000172973	0.000201087
200 - 400	0.000145251	0.000099502	0.000077008	0.000119246
400 - 800	0.000080552	0.000073322	0.000071229	0.000078125

3.9.3 Variation of Coefficient of Volume Change with Aspect Ratio.

As co-efficient of volume change indicates the amount of settlement that a soil will undergo, this property has been studied to understand the change in soil behaviour due to addition of plastic strips of PET bottles. The consolidation tests were carried out with optimum 1% of reinforcement.

The m_v value for the different pressures ranging from 12.5 to 800 kN/m^2 has been taken into consideration. It was found that the value of m_v was lesser for reinforced soil as compared to that of unreinforced one and the minimum value was obtained at an aspect ratio of 2 for almost entire pressure ranges in all three types of soil for 1% of reinforcement as shown in the figure 3.127(a) to 3.127(c) below.

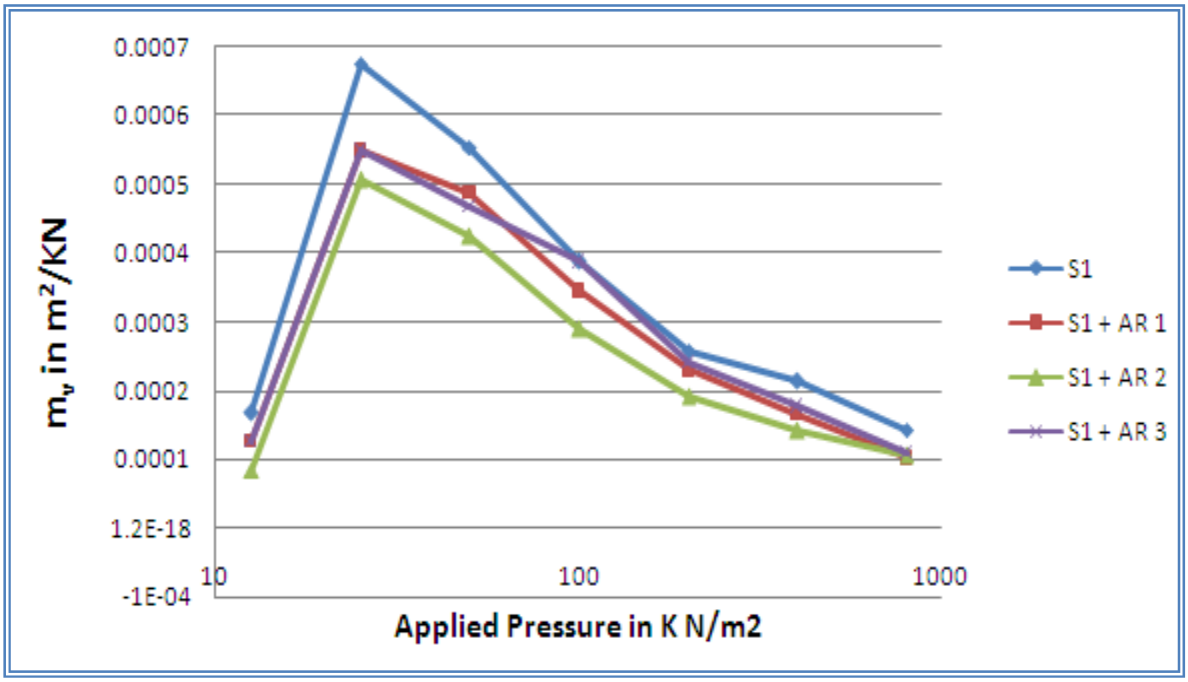

Fig. 3.127(a): Variation of m_v for different AR on Soil type S1 (Clay Only)

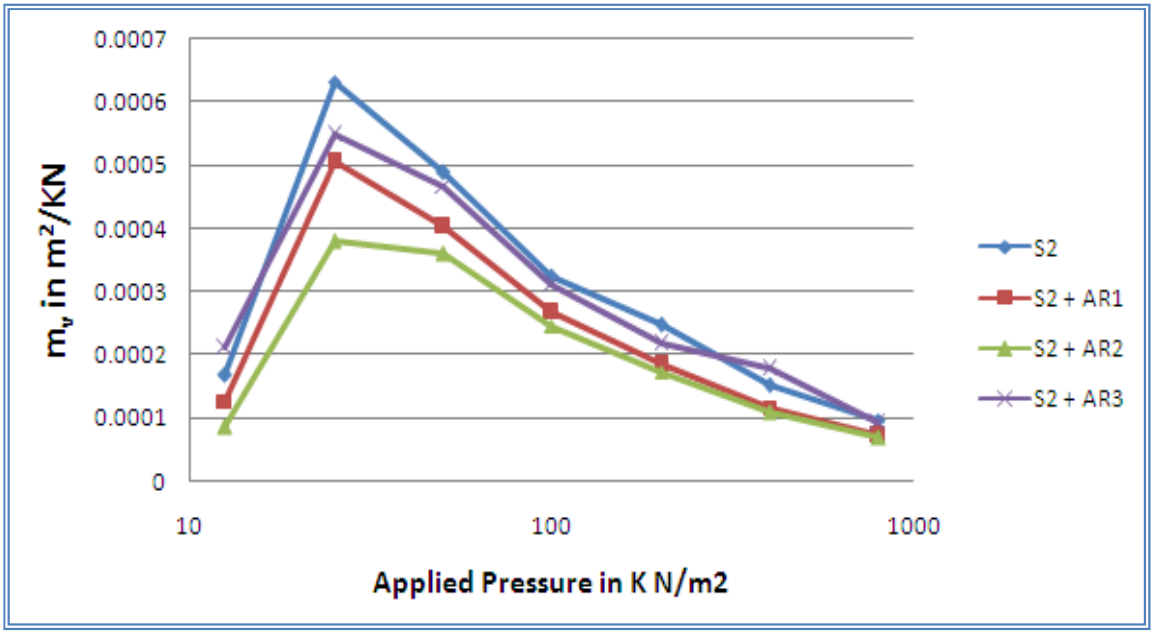

Fig. 3.127(b): Variation of m_v for different AR on Soil type S2 (90% Clay + 10% Sand)

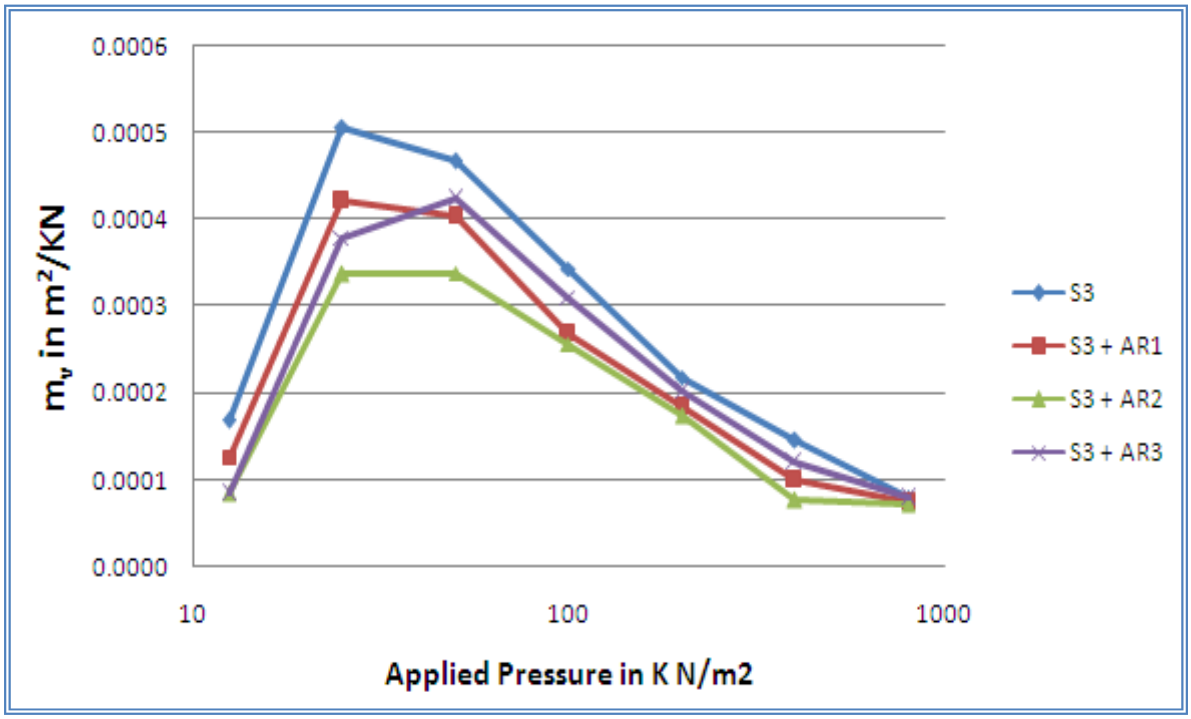

Fig. 3.127(c): Variation of m_v for different AR on Soil type S3 (80% Clay + 20% Sand)

As seen above, the reduction in coefficient of volume change is maximum for aspect ratio of 2. The decrease in coefficient of volume change for different pressure ranges and soil types for aspect ratio 2 with respect to corresponding unreinforced soil are summarized in Table 3.13.

Table 3.13: Decrement of coefficient of volume change of aspect ratio of 2

Type of Soil	S1	S1 + AR2	%	S2	S2 + AR2	%	S3	S3 + AR2	%
Applied Pressure (kN/m^2)	m_v (m^2/kN) X 10^{-3}	m_v (m^2/kN) X 10^{-3}	decrement	m_v (m^2/kN) X 10^{-3}	m_v (m^2/kN) X 10^{-3}	decrement	m_v (m^2/kN) X 10^{-3}	m_v (m^2/kN) X 10^{-3}	decrement
0 - 12.5	0.1684	0.0842	-50.00	0.1684	0.0842	-50.00	0.1684	0.0842	-50.00
12.5 - 25	0.6751	0.5058	-25.08	0.6329	0.3793	-40.06	0.5063	0.3372	-33.40
25 - 50	0.5532	0.4242	-23.32	0.4891	0.3600	-26.40	0.4671	0.3386	-27.50
50 - 100	0.3883	0.2894	-25.48	0.3229	0.2457	-23.91	0.3437	0.2561	-25.48
100 - 200	0.2585	0.1903	-26.38	0.2462	0.1731	-29.70	0.2186	0.1730	-20.86
200 - 400	0.2146	0.1414	-34.12	0.1514	0.1073	-29.13	0.1453	0.0770	-46.98
400 - 800	0.1431	0.1055	-26.24	0.0969	0.0675	-30.33	0.0806	0.0712	-11.57

Firstly it can be seen that there is reduction in m_v values for S2 soil type with respect to S1 due to presence of sand. The reduction can further be seen in S3 soil type due to more sand percentage. From the Table 3.13 it appears that the decrement in values of coefficient of volume change due to addition of Plastic strips for all pressure ranges has average values of 30.09%, 32.79% and 30.83% for S1, S2 and S3 soil type respectively. From above it is clear that presence of plastic strips in soil plays an important role in reduction of compressibility of soil.

As found above the optimum fibre content becomes 1% and optimum aspect ratio is 2 for all types of soil used in this study. This may be due to the fact that when the strip content and aspect ratio increases beyond the optimum, the effect of compactness of soil becomes less, that is, strip portion of the mix becomes too much, which results in decrease in dry density and the corresponding shear strength. Based on this, model footing tests as well as numerical study have been carried out for studying the application of soil-PET bottle strip mixes in case of bearing capacity of footings.

Chapter 4

MODEL FOOTING TEST

4.0 General

Based on the study of materials it has been found that optimum percentage of PET bottle strip reinforcements becomes 1% for all values of aspect ratios, 1, 2 and 3. Therefore to study the improvement of bearing capacity with use of reinforced soil an attempt has been made to carry out model footing tests in the laboratory. The test results have also been presented at the end. The tests have been done on soil type S1 with and without reinforcements. All the three aspect ratios (1, 2 and 3) have been considered for the reinforced soil. The tests have been carried out on square footings of sizes 5 cm and 10 cm. Equipment, program and procedure of tests have been depicted in this chapter.

4.1 Test Program, Equipment and Test Procedure

4.1.1 Test Program

The test program for eight numbers of model footing tests has been presented in Table 4.1.

Table 4.1: Test programme for model footing tests

Footing Size	Soil type	PET bottle strips (%)	Aspect Ratio	No. of tests
5 cm and 10 cm (Square footing)	S1	0	--	2
		1	1,2 and 3	6
Total No of Tests:				8

4.1.2 Equipment

A typical setup for model footing tests is shown in the Figs. 4.1A and B. The equipment required to fabricate the test setup are discussed in this section.

4.1.2.1 Test Tank

In the present study, tank with one side movable was used so that the size can be adjusted according to the size of the model footing in case of a particular test. The steel tank was fabricated with steel plates held at the corners by steel angles. The width in the present study was taken 6 times the width of the footing while the depth was made 4 times the width of

footing. With these considerations one 600 mm x 600 mm x 600 mm steel tank was fabricated. There were two wooden partitions which could be placed within slots so that the tank could be divided into two halves in both the directions of tank size. Thus one-fourth of the tank was used for tests with footing of 5 cm size (Fig. 4.1A) and the whole tank was used for 10 cm size footing (Fig. 4.1B). The depth of test tank considered for 5 cm size and 10 cm size footings were 200 mm and 400 mm respectively. Beyond this depth appropriate spacers were placed to use the tank for model footing tests.

Fig. 4.1A: Set-up for 5 cm model footing tests

Fig. 4.1B: Set-up for 10 cm model footing tests

4.1.2.2 Loading Frame

Reaction frames were used for loading model footing placed on the surface of soil in tank as shown in schematic diagram of the set up shown in Fig. 4.2. The frame has been fabricated with two steel columns fitted to bottom of tank. A horizontal sliding steel joist have been fitted above them but restrained to displace in the vertical direction by means of two adjustment bolts. This has been done to shift the loading position for tests with footings of 5 cm and 10 cm sizes.

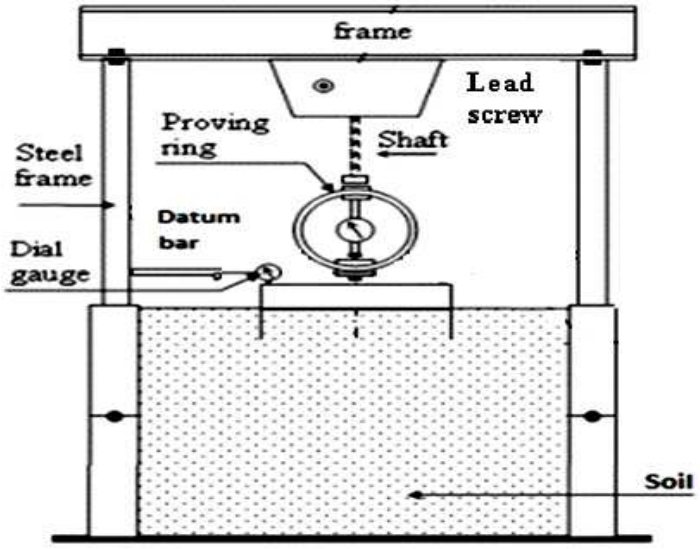

Fig.4.2: Schematic Arrangement for model footing test

4.1.2.3 Proving Ring

The proving ring is a device used to measure force. It consists of an elastic ring of known diameter with a measuring device located in the centre of the ring. The proving ring consists of two main elements, the ring itself and the dial in the middle**.** The dial gives indication of the force being applied on to the ring. The proving rings of 5 ton and 10 ton capacities were used for loading the footings in cases of 5 cm x 5 cm and 10 cm x 10 cm footings respectively**.**

4.1.2.4 Dial Gauges

Two dial gauges of least count 0.01 mm have been used to measure the settlement of the model footing. The settlement at the centre of the footing was recorded as average of the two dial gauge readings.

4.1.2.5 Model Footings

Model Footings were made up of 5 mm thick steel plates. They were made sufficiently stiff such that they do not get subjected to distress during loading. Square footings of sizes 5 cm and 10 cm were used for tests.

4.3 Test Procedure

4.3.1 Preparation of Foundation Bed

The foundation bed was prepared by compaction of the unreinforced or reinforced soil in appropriate number of layers with proper compactive effort, as required for a particular testing. The compaction was done in layers and the energy was so applied that energy per unit volume remained same as for corresponding the standard Proctor test. In order to maintain uniformity in sample preparation, it was ensured that samples taken from different depths after each test, reported more or less uniform water content and unconfined compressive strength with variation of +/-2%.

4.3.2 Application of Load

Load was applied on the model footing by means of a screw jack gradually in increments and each load increment was recorded with the help of a proving ring as shown in Fig 4.2. Each increment was kept sustained till the settlement reading became more or less constant. The next incremental load was then applied. The test was continued till failure indicated by rapid change of settlement with no application of load or by reduction in proving ring dial reading.

4.3.3 Recording of Settlement

The displacement (settlement) of the model footing was measured using dial gauges located on either side of the centre line of the footing and the settlement at the centre was obtained as average of the two dial gauge readings.

Load - settlement curve for each model footing test was plotted with load on x-axis and observed settlement on y-axis on arithmetic scale.

The load settlement curves for all the tests have been plotted and shown in Figs.4.3 to 4.10.

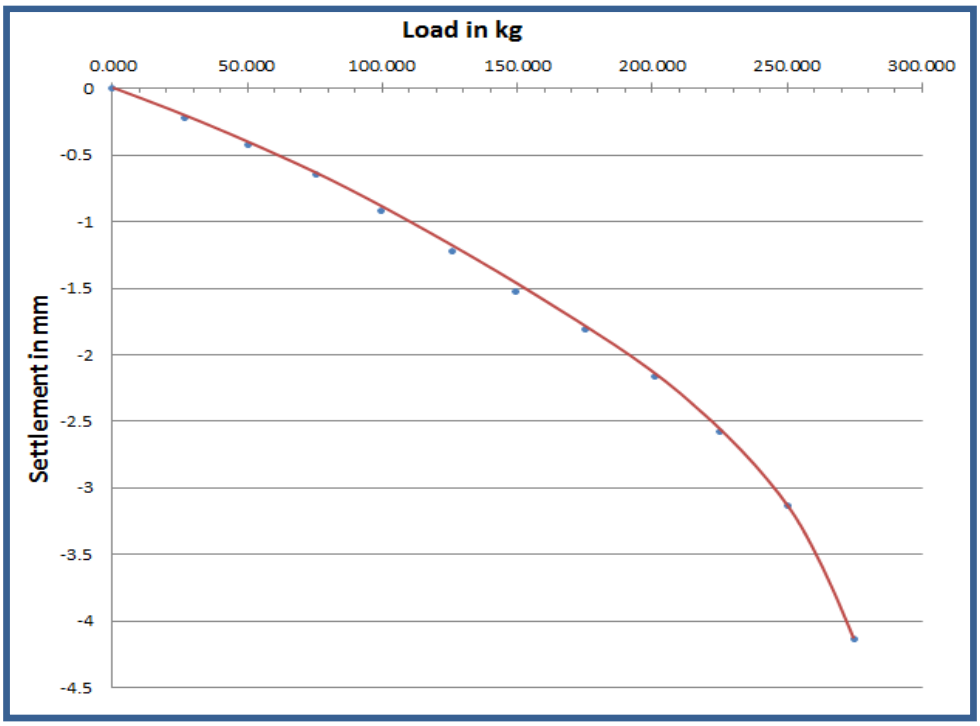

Fig.4.3: Load Settlement curve for 5 cm footing on S1 soil type

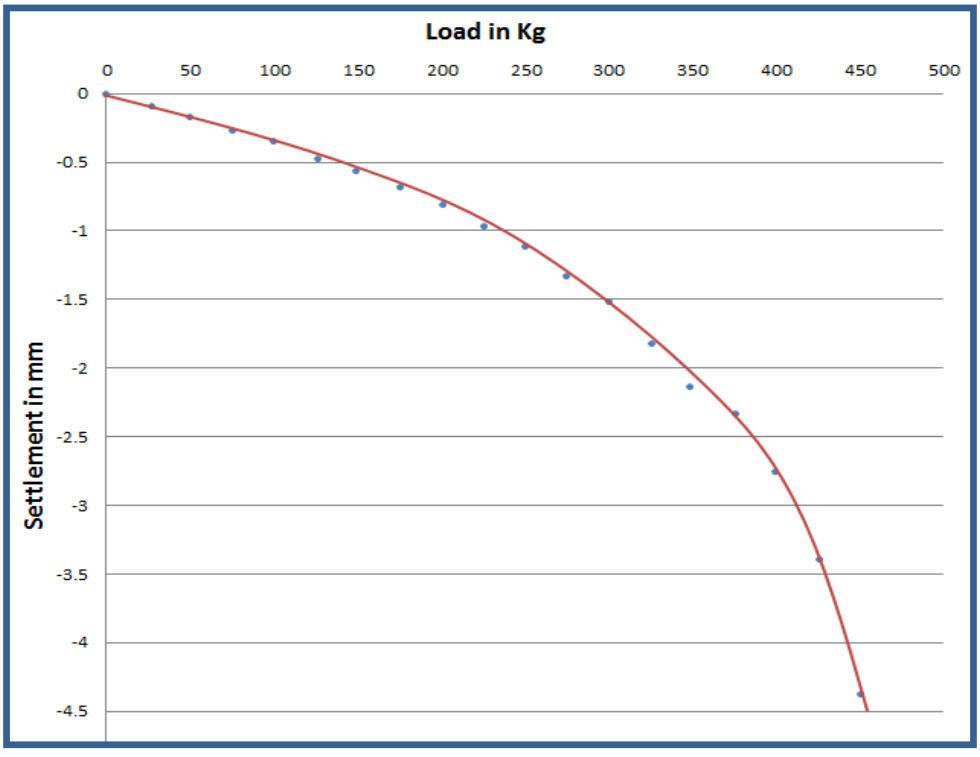

Fig. 4.4: Load Settlement curve for 5 cm footing on (S1 + AR1)

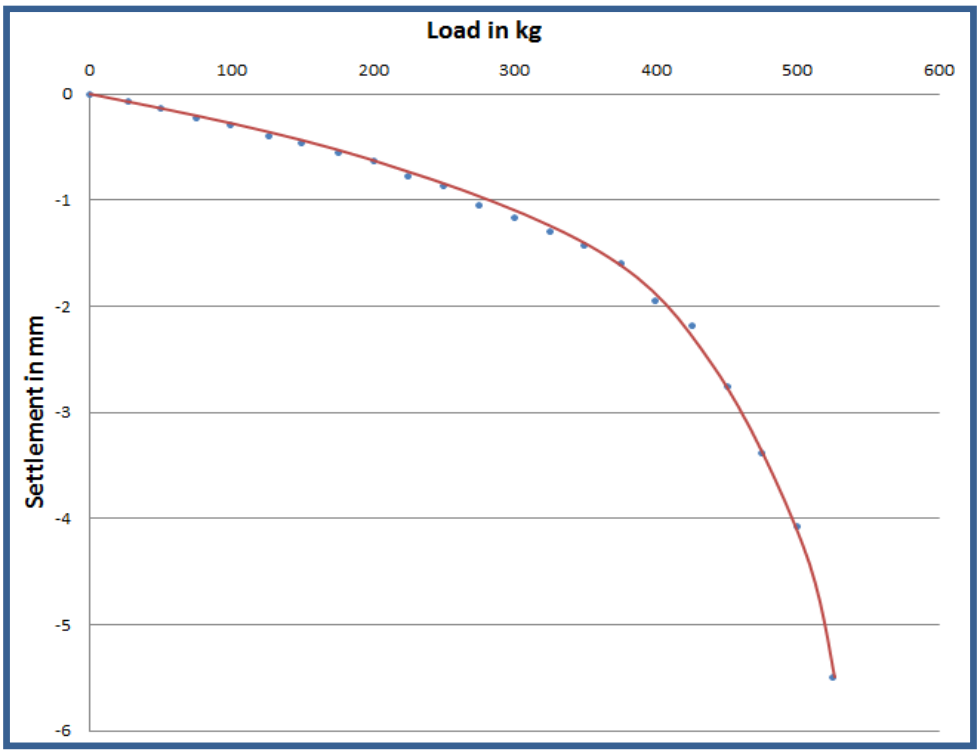

Fig.4.5: Load Settlement curve for 5 cm footing on (S1 + AR2)

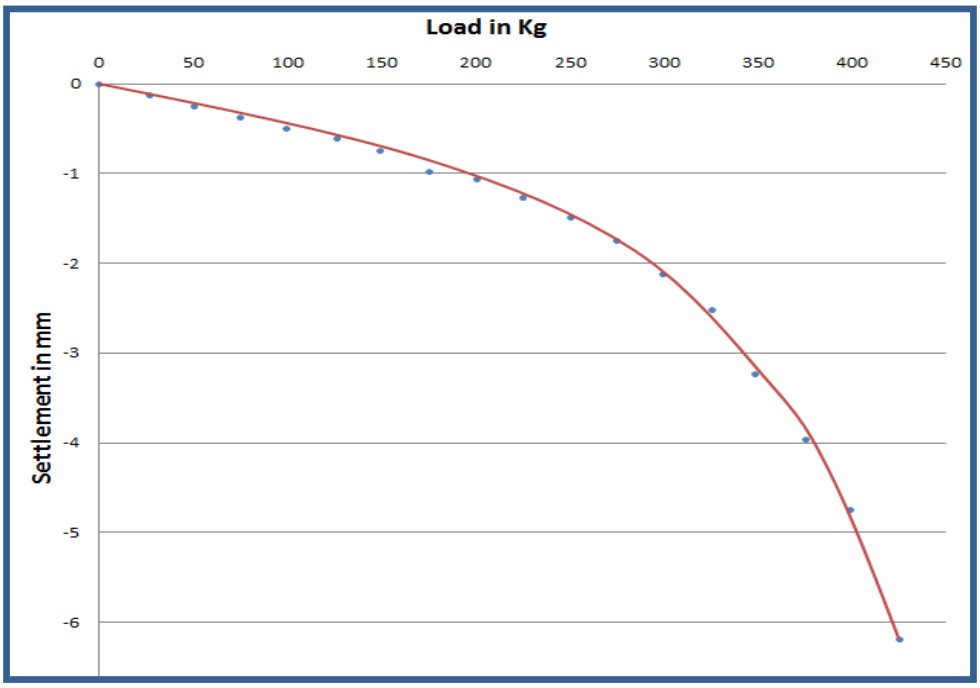

Fig.4.6: Load Settlement curve for 5 cm footing on (S1 + AR3)

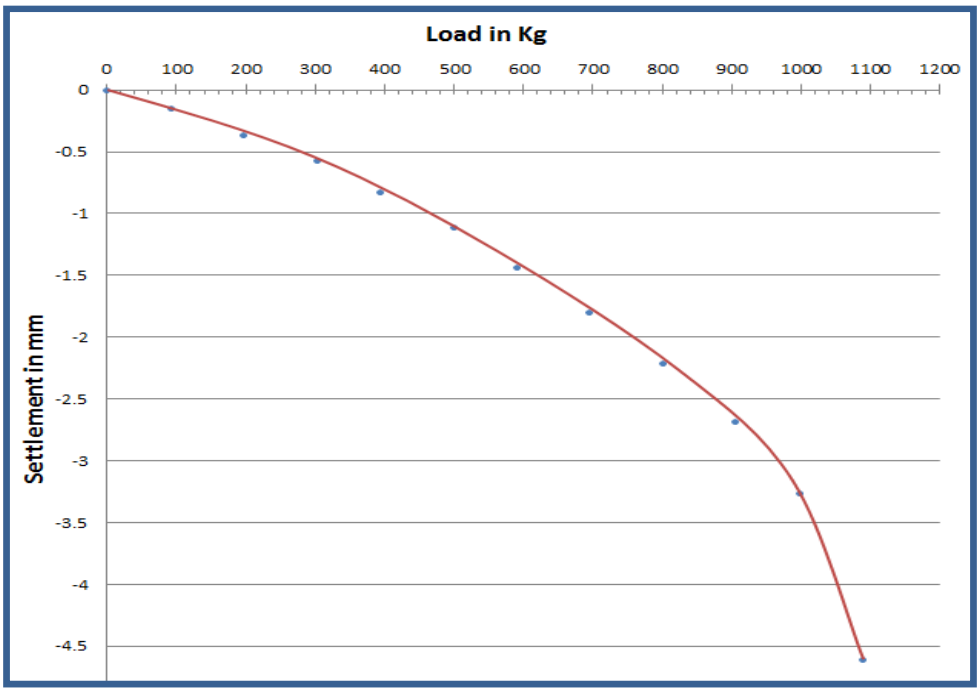

Fig.4.7: Load Settlement curve for 10 cm footing on S1

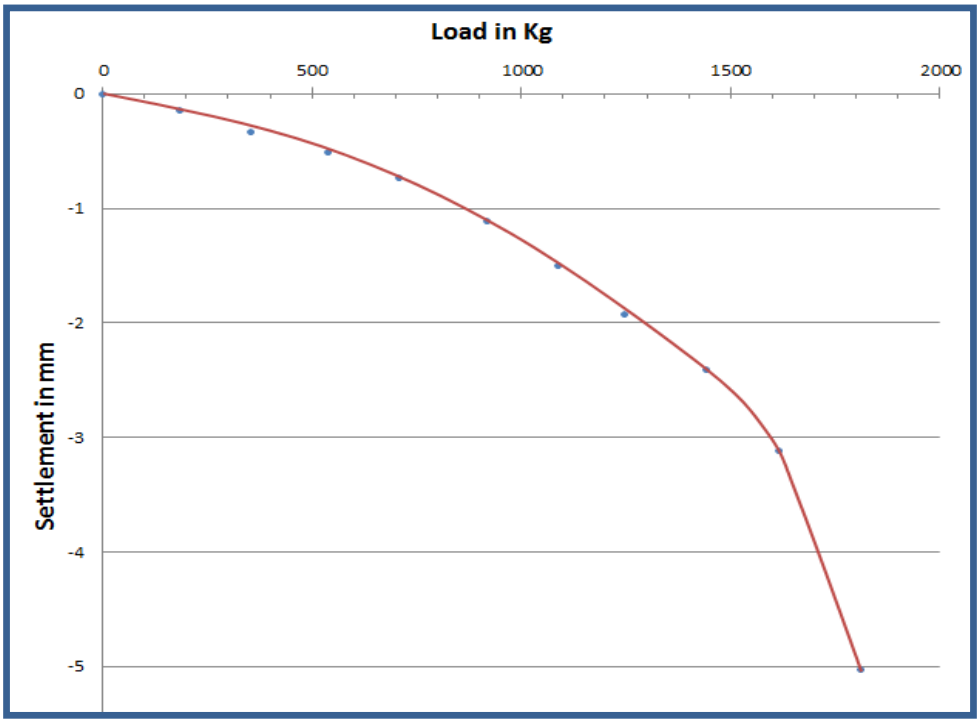

Fig.4.8: Load Settlement curve for 10 cm footing on (S1 + AR1)

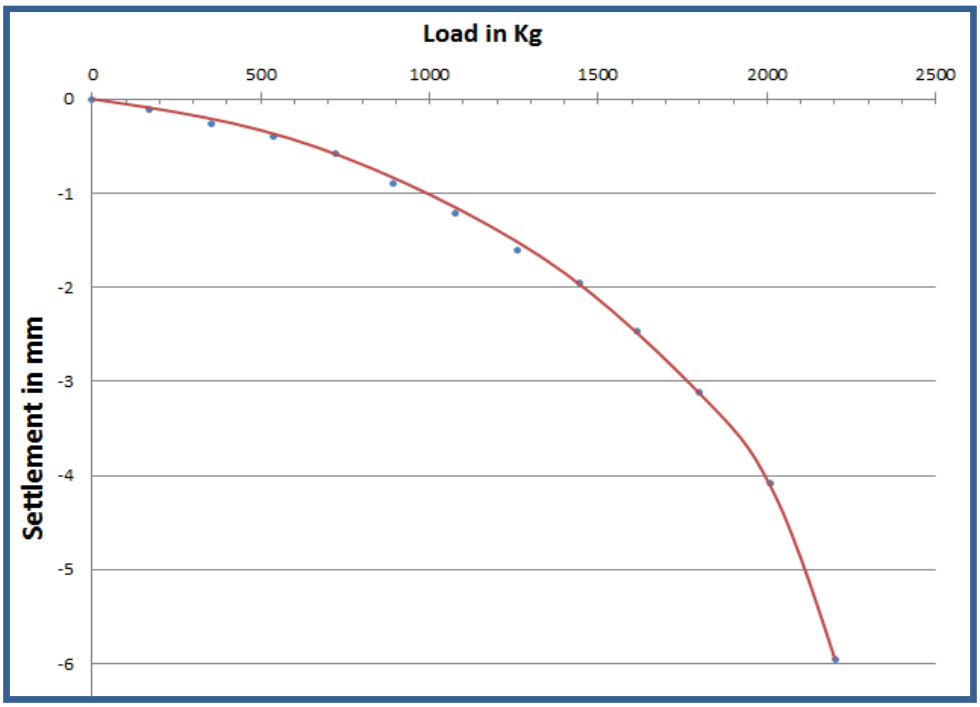

Fig.4.9: Load Settlement curve for 10 cm footing on (S1 + AR2)

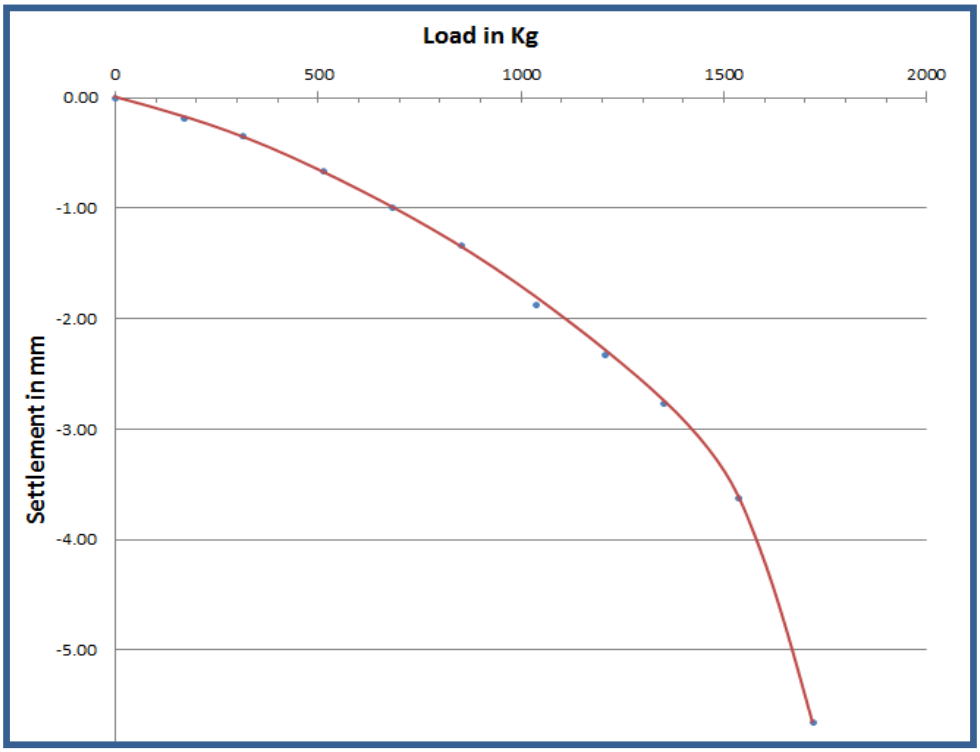

Fig4.10: Load Settlement curve for 10 cm footing on (S1 + AR3)

Chapter 5

NUMERICAL INVESTIGATION

5.0 General

In this chapter an attempt has been made to carry out numerical analysis of the model tests by finite element method using PLAXIS 3D FOUNADATION software. Material nonlinearity has been considered to model the clay using Mohr –Coulomb failure theory and elasto-plastic behaviour of clay.

5.1 Finite Element Method

It is an approximate numerical solution technique in which continuous system is discretized into many small and simple pieces called finite elements. For each element it is necessary to make an assumption as to how the primary variables, such as displacement, are distributed in terms of geometrical position. Then a set of simultaneous equations are developed for describing the constitutive or other behavior of each element in terms of discrete nodal point values of the primary variable. Each of these elements is then combined using proper compatibility relations between them and global set of simultaneous equations is obtained. Then the applications of load and boundary conditions are imposed to the global set of simultaneous equations. These equations are solved simultaneously or implicitly in a personal computer. Solutions of these equations provide the approximate results or prediction of behavior of the physical system that has been modeled. A short overview of the finite element is provided below.

At first body to be analyzed is discretized into finite elements which can be one dimensional, two dimensional or three dimensional depending on the body to be discretized and the need of the user. Within an element the displacement field *u* is obtained from the discrete nodal values in a vector *v* using interpolation functions assembled in matrix *N:*

$$u = N\nu \tag{5.1}$$

The interpolation functions in matrix *N* are often denoted as shape functions. The shape function depends entirely on the type of the element considered and its geometry. The relation between strain and displacement field vector can be formulated as:

$$\varepsilon = Lu \tag{5.2}$$

This equation expresses the six strain components, assembled in vector ε, as the spatial derivatives of the three displacement components, assembled in vector *u*, using the differential operator *L*. Substitution of Eq. (5.1) in the relation (5.2) gives:

$$\varepsilon = LN\nu = B\nu \tag{5.3}$$

In this relation *B* is the strain displacement matrix, which contains information of geometry of the element. The stress vector is then estimated from the strain vector by multiplying with constitutive matrix as:

$$s = D^e B\nu \tag{5.4}$$

Finite elements obtained by discretization of a continuum are formulated in general and systematic way. The stiffness matrix and load vectors of an element can be formulated by Rayleigh-Ritz or variational principle and Galerkin weighted residual methods. Consequently the body is reduced into a basic matrix equation form as:

$$[F] = [K][\nu] \tag{5.5}$$

$$F = f_b + f_s + f_I \tag{5.6}$$

where, $\boldsymbol{f_b}$ is the body force, $\boldsymbol{f_s}$ is the surface traction force vector and $\boldsymbol{f_I}$ concentrated or internal force vector. The matrix K defines the stiffness of the element and its basic form can be expressed as:-

$$K = \int B^T D^e B dV \tag{5.7}$$

The stiffness matrix is evaluated using any suitable numerical integration scheme. Once the element stiffness matrices are formulated they are assembled into global stiffness matrix to generate a set of simultaneous equations of all degree of freedom. For 3D analysis the dimension of the global stiffness matrix is **3n×3n**, n being number of nodes of the model. In mathematical form, the global simultaneous equations are written as:

$$F^g = K^g \nu^g \tag{5.8}$$

where, K^g = is the global stiffness matrix,

ν^g = is the global displacement vector $\{ u_1\ v_1 \ldots u_n\ v_n \}^T$

F^g= is the global force vector $\{ F_{1x} \; F_{1y} \ldots F_{nx} F_{ny} \}^T$

Once the global displacement vector is evaluated nodal displacement vector is extracted separately. Then with the help of equations (5.3) and (5.4) we can calculate the strain and stress respectively.

5.1.1 Finite Element Formulation

In the present investigation, the soil has been discretized using three dimensional 8 nodded isoparametric elements. For the 8 nodded isoparametric element, each node of the element has three degrees of freedom, displacements u, v & w in the three orthogonal directions x, y and z as shown in Fig. 5.1.

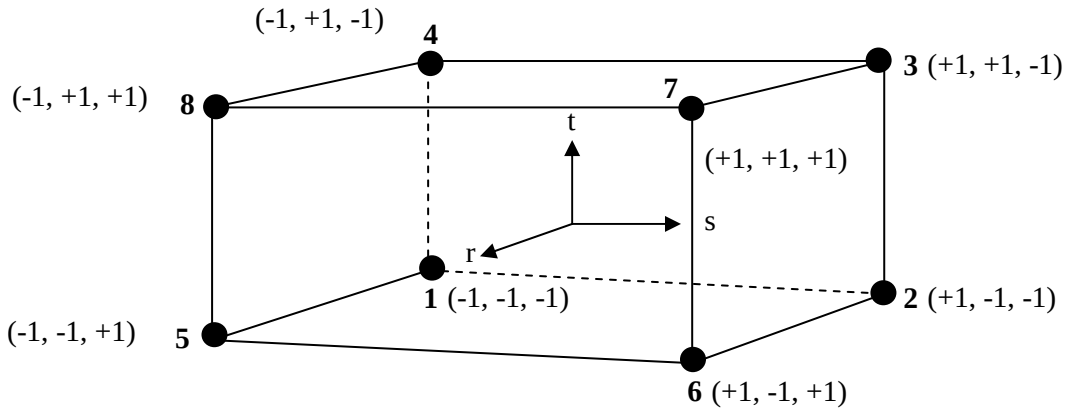

Fig. 5.1 Geometry and co-ordinates of 8 noded element

The generalized displacement vector {u} at a point within an element is related to nodal displacement vector {q} by shape function matrix [N] as,

$$\{u\} = \begin{Bmatrix} u \\ v \\ w \end{Bmatrix} = [N]\{q\} \tag{5.9}$$

where {u} = displacement vector at the point within an element,

$$\{q\}^T = \{u_1, v_1, w_1, u_2, v_2, w_2 \ldots\ldots\ldots\ldots, u_8, v_8, w_8\} \tag{5.10}$$

$$\text{and } [N] = \begin{bmatrix} N_1 & 0 & 0 & N_2 & 0 & 0 & \ldots\ldots & N_8 & 0 & 0 \\ 0 & N_1 & 0 & 0 & N_2 & 0 & \ldots\ldots & 0 & N_8 & 0 \\ 0 & 0 & N_1 & 0 & 0 & N_2 & & 0 & 0 & N_8 \end{bmatrix} \tag{5.11}$$

For isoparametric formulation, the element geometry is defined in terms of the same set of shape functions and the nodal co-ordinates and is given by

$$\{R\} = \begin{Bmatrix} X \\ Y \\ Z \end{Bmatrix} = [N]\ \{R_n\} \qquad (5.12)$$

where {R} = array for co-ordinates of the same point within the element,

[N] = shape function matrix, and

$\{R_n\}^T = \{X_1\ Y_1\ Z_1\ \ldots\ldots\ldots\ldots\ X_8\ Y_8\ Z_8\}$ = array for nodal co-ordinates

The shape functions of 8 nodded isoparametric element in local co-ordinates (s, r, t) as shown in Fig. (5.1) are taken as

$$N_1 = 1/8\ [(1-s)\ (1-t)\ (1-r)] \qquad 5.13\ (a)$$

$$N_2 = 1/8\ [(1+s)\ (1-t)\ (1-r)] \qquad 5.13\ (b)$$

$$N_8 = 1/8\ [(1-s)\ (1+t)\ (1+r)] \qquad 5.13\ (c)$$

The nodal displacements are

$$u = \sum_{i=1}^{8} N_i\ u_i \qquad 5.14\ (a)$$

$$v = \sum_{i=1}^{8} N_i\ v_i \qquad 5.14\ (b)$$

$$w = \sum_{i=1}^{8} N_i\ w_i \qquad 5.14\ (c)$$

The strain vector, {ε} is expressed in terms of the nodal displacements as given below:

$$\{\varepsilon\} = \begin{Bmatrix} \varepsilon_x \\ \varepsilon_y \\ \varepsilon_z \\ \gamma_{xy} \\ \gamma_{yz} \\ \gamma_{xz} \end{Bmatrix} = \begin{Bmatrix} \frac{\partial u}{\partial x} \\ \frac{\partial v}{\partial y} \\ \frac{\partial w}{\partial z} \\ \frac{\partial u}{\partial y} + \frac{\partial v}{\partial x} \\ \frac{\partial v}{\partial z} + \frac{\partial w}{\partial y} \\ \frac{\partial w}{\partial x} + \frac{\partial u}{\partial z} \end{Bmatrix} = [B]\ \{q\} \qquad (5.15)$$

where $\{\varepsilon\}$ = strain vector,

[B] = strain displacement transformation matrix consisting of derivatives of shape function i.e.

$$[B] = [B_1]\,[B_2]\,\ldots\ldots\ldots\,[B_8]$$

and
$$[B_i] = \begin{bmatrix} \frac{\partial N_i}{\partial x} & 0 & 0 \\ 0 & \frac{\partial N_i}{\partial y} & 0 \\ 0 & 0 & \frac{\partial N_i}{\partial z} \\ \frac{\partial N_i}{\partial y} & \frac{\partial N_i}{\partial x} & 0 \\ 0 & \frac{\partial N_i}{\partial z} & \frac{\partial N_i}{\partial y} \\ \frac{\partial N_i}{\partial z} & 0 & \frac{\partial N_i}{\partial x} \end{bmatrix} \qquad (5.16)$$

The stress-strain relationship for elastic material is expressed as,

$$\{\sigma\} = [D_e]\,\{\varepsilon\} \qquad (5.17)$$

where,

$$\{\sigma\} = \begin{Bmatrix} \sigma_x \\ \sigma_y \\ \sigma_z \\ \tau_{xy} \\ \tau_{yx} \\ \tau_{zx} \end{Bmatrix} \qquad (5.18)$$

and $[D_e]$ = elasticity matrix

$$= \frac{E(1-\upsilon)}{(1+\upsilon)(1-2\upsilon)} \begin{bmatrix} 1 & \frac{\upsilon}{1-\upsilon} & \frac{\upsilon}{1-\upsilon} & 0 & 0 & 0 \\ & 1 & \frac{1}{1-\upsilon} & 0 & 0 & 0 \\ & & 1 & 0 & 0 & 0 \\ & & & \frac{1-2\upsilon}{2(1-\upsilon)} & 0 & 0 \\ & & & & \frac{1-2\upsilon}{2(1-\upsilon)} & 0 \\ & & & & & \frac{1-2\upsilon}{2(1-\upsilon)} \end{bmatrix} \qquad (5.19)$$

where E = modulus of elasticity, υ being the Poisson's ratio

The shape functions used for describing the geometry of the element and displacement variation are expressed in terms of local co-ordinates (s, t, r) and it is required to determine

the derivatives of the functions with respect to global coordinates (x, y, z). From chain rule of differentiation the relationship between two co-ordinate systems is given below:

$$\begin{Bmatrix} \frac{\partial N_i}{\partial x} \\ \frac{\partial N_i}{\partial y} \\ \frac{\partial N_i}{\partial z} \end{Bmatrix} = J^{-1} \begin{Bmatrix} \frac{\partial N_i}{\partial s} \\ \frac{\partial N_i}{\partial r} \\ \frac{\partial N_i}{\partial t} \end{Bmatrix} \tag{5.20}$$

$$\text{where } [J] = \text{Jacobian Matrix} = \begin{bmatrix} \frac{\partial x}{\partial s} & \frac{\partial y}{\partial s} & \frac{\partial z}{\partial s} \\ \frac{\partial x}{\partial r} & \frac{\partial y}{\partial r} & \frac{\partial z}{\partial r} \\ \frac{\partial x}{\partial t} & \frac{\partial y}{\partial t} & \frac{\partial z}{\partial t} \end{bmatrix} \tag{5.21}$$

and $[J]^{-1}$ is the inverse of Jacobian Matrix

The variational function for the displacement method is given by the potential energy Π_p of the system and it can be expressed as:

$$\Pi_p = \int_v dv(u,v,w)dv - \int_v (\bar{x}u + \bar{y}v + \bar{z}w)dv$$

$$\Pi_p = \int_v dv(u, v, w)\, dv - \int_v (\bar{x}\,u + \bar{y}\,v + \bar{z}\,w)\, dv \tag{5.22}$$

where, dv (u, v, w) = strain energy per unit volume

$\bar{x}, \bar{y}, \bar{z}$ = components of body forces

v = volume of element

For a linearly elastic isotropic material behaviour,

$$dv = \tfrac{1}{2} \{\varepsilon\}^T \{\sigma\}\, dv \tag{5.23}$$

$$\therefore \Pi_p = \int_v \tfrac{1}{2} \{\varepsilon\}^T [D_e] \{\varepsilon\}\, dv - \int_v \{u\}^T \{F\}\, dv \tag{5.24}$$

$$= \int_v \tfrac{1}{2} \{q\}^T [B]^T [D_e] [B] \{q\}\, dv - \int_v \{q\}^T [N]^T \{F\}\, dv \tag{5.25}$$

where $\{F\} = \{ \bar{x}, \bar{y}, \bar{z} \}^T$

Now for static equilibrium of a system, condition of minimum potential energy is to apply for which

$$\frac{\partial(\Pi_p)}{\partial\{q\}} = 0 \qquad (5.26)$$

$$\text{Now } \frac{\partial(\Pi_p)}{\partial\{q\}} = \int_v [B]^T [D_e] [B] \{q\}\, dv - \int_v [N]^T \{F\}\, dv = 0 \qquad (5.27)$$

$$\text{or } \int_v [B]^T [D_e] [B] \{q\}\, dv = \int_v [N]^T \{F\}\, dv \qquad (5.28)$$

The above equation may be represented by

$$[K] \{q\} = \{Q\}$$

$$\text{Where, } [K] = \int_v [B]^T [D_e] [B]\, dv \qquad [5.29\ (a)]$$

= stiffness matrix

$$\text{And, } \{Q\} = \int_v [N]^T \{F\}\, dv \qquad [5.29\ (b)]$$

= Equivalent nodal vector

In global relationship the stiffness matrix [K] for the entire system is given by

$$[K] \{\delta\} = \{F_s\} \qquad (5.30)$$

where, [K] = global stiffness matrix

$\{\delta\}$ = global nodal displacement

$\{F_s\}$ = global nodal force vector

The global stiffness matrix has been obtained by adding appropriately for the individual contributions from elements which are common to a node.

5.1.2 Material Nonlinearity

At higher stress level, the stress-strain characteristic of clay becomes nonlinear. Therefore, clay has been idealised as an elastic-perfectly plastic material satisfying Mohr-Coulomb yield criterion. Mohr-Coulomb model requires a total of five parameters, which are generally familiar to most geotechnical engineers and which can be obtained from basic tests on clay samples. These parameters with their standard units are listed below.

E = Young's modulus (kN/m^2); υ = Poisson's ratio; ψ = Dilatancy angle; c = cohesion;

ϕ = Friction angle.

It is quite generally postulated as an experimental fact that yielding can occur only if stress σ satisfies the general yield criterion:

$$F(\sigma, K_h) = 0 \tag{5.31}$$

Where, K_h = hardening parameter and F is the yield function.

For isotropic cases the yield surface is conveniently expressed in terms of the three stress invariants, i.e.,

$$\sigma_m = \text{Pure hydrostatic stress} = J_1/3 = (\sigma_x+\sigma_y+\sigma_z)/3 \tag{5.32}$$

However, in this formulation $\sigma_z = 0$, under plane strain condition

$$\sigma = (J_2)^{1/2} = [1/2(S_x^2+S_y^2+S_z^2) + \tau^2_{xy}+\tau^2_{yz}+\tau^2_{zx}]^{1/2} \tag{5.33}$$

A potential surface is defined by $Q = Q(\sigma, K_h)$ which defines the plastic strain increment $d\varepsilon p$ as

$$d\varepsilon p = \lambda \delta Q/\delta\sigma \tag{5.34}$$

where, $$\lambda = \{\delta F/\delta\sigma\}^T[De]\{d\varepsilon\}/\{\delta F/\delta\sigma\}^T[De]\{\delta Q/\delta\sigma\}+A \tag{5.35}$$

The particular case of Q = F is known as associated plasticity, otherwise the plasticity follows non associated flow rule. The elasto plastic matrix $[D_{ep}]$ is derived as

$$[D_{ep}] = [D_e]-[D_e]\{\delta Q/\delta\sigma\}\{\delta F/\delta\sigma\}^T[D_e]x\,[A+\{\delta F/\delta\sigma\}^T[D_e]\{\delta Q/\delta\sigma]^{-1} \tag{5.36}$$

For ideal plasticity with no hardening, A becomes equal to zero. The stress increment vector $\{\Delta\sigma\}$ is related to strain increment vector $\{\Delta\varepsilon\}$ as

$$\{\Delta\sigma\} = [D_{ep}]\{\Delta\varepsilon\} \tag{5.37}$$

5.2 Modelling by PLAXIS 3D

PLAXIS 3D is a finite element package intended for three-dimensional analysis of deformation and stability in geotechnical engineering. It is equipped with features to deal with various aspects of complex geotechnical structures and construction processes using robust and theoretically sound computational procedures. With PLAXIS 3D, complex geometry of soil and structures can be defined in two different modes. These modes are specifically defined for Soil or Structural modelling. Independent solid models can automatically be intersected and meshed. The staged constructions mode enables a realistic simulation of construction and excavation processes by activating and deactivating soil volume clusters and structural objects, application of loads, changing of water tables, etc. The

output consists of a full suite of visualization tools to check details of the complex inner structure of a full 3D underground soil-structure model. PLAXIS 3D is a user friendly 3D geotechnical program offering flexible and interoperable geometry, realistic simulation of construction stages, a robust and reliable calculation kernel, and comprehensive and detailed post-processing, making it a complete solution for geotechnical design and analysis.

Numerical analysis was carried out by PLAXIS 3D Foundation geotechnical finite element package which is specifically preferred for advanced analysis for piles and pile-raft foundations. In the following paragraphs a short review of this program is given.

PLAXIS 3D Foundation program consists of four basic components, namely Input, Calculation, Output and Curves. In the Input program the boundary conditions, problem geometry with appropriate material properties are defined. The problem geometry is the representation of a real three-dimensional problem and it is defined by work-planes and boreholes. The model includes an idealized soil profile, structural objects, construction stages and loading. The model should be large enough so that the boundaries do not influence the results. Boreholes are points in the geometry model that define the idealized soil layers and the groundwater table at that point. Multiple boreholes are used to define the variable soil profile of the project. During 3D mesh generation soil layers are interpolated between the boreholes so that the boundaries between the soil layers coincide with the boundaries of the elements. Work planes are horizontal planes with different y-coordinates that show the top view of the model geometry. They were used to draw, activate and deactivate the structural elements and loads. Each work-plane holds the same geometry lines but vertical distance between them may vary. Within work-planes, points, lines and clusters are used to describe a 2D geometry mode

After creating the 2D geometry model in a work-plane, 2D was automatically generated based on the composition of the clusters and lines in 2D geometry model. However, the 3D finite element mesh was the extension of 2D mesh into the third dimension and it was generated after generating 2D mesh. The 2D mesh generation in the program is fully automatic while 3D mesh generation is semi automatic. Mesh dimensions should be appropriately defined, to prevent the effects of boundary conditions. The 2D mesh was constructed before proceeding to the 3D mesh extension. The mesh element size can be adjusted by using a general mesh size varying from very coarse to very fine and also by using line, cluster and point refinements. Very fines meshes was avoided in order to reduce the number of elements, thus to reduce the memory consumption and calculation time. The

program does not allow entering a new structural element or a new soil cluster after the mesh is generated. If a new element or cluster is added to the geometry model, the mesh generation has to be repeated with the new input. 3D finite element mesh is composed of elements, nodes and stress points. During a finite element analysis, displacement values are calculated at the nodes and a specific node can be selected before calculation steps in order to generate the load displacement curves. On the contrary, stresses and strains are calculated at individual stress points (Gaussian integration points) rather than at the nodes. However, stress and strain values at stress points are extrapolated to the nodes for the output purposes. At the bottom of the 3D finite element mesh, total fixities were used that restrain the movements in both horizontal and vertical directions. For upper part, 3D finite element mesh had no fixities. Besides, for right and left sides, roller supports were used in order to restrain only the horizontal movements and vertical displacements were left free.

After defining the model geometry and 3D mesh generation, initial stresses are applied by using either K_0-procedure or gravity loading. The calculation procedure can be performed automatically or manually. The initial stresses in the soil are affected by the weight of the soil and history of the soil formation. Stress state is characterized by vertical and horizontal stresses. Initial vertical stress depends on the weight of the soil and pore pressures; whereas initial horizontal stresses are related to the vertical stresses by the coefficient of lateral earth pressure at rest. This relation is provided by the K_0-procedure in this study.

In this analysis the effect of ground water table is not taken into account. If it would have been taken into account then the initial stress would have been calculated by effective stress consideration as this is not so here is would be done by the total stress consideration only.

$$\sigma_h = K_o \, \sigma_v \tag{5.38}$$

where $$K_o = (1- \sin\phi) \tag{5.39}$$

The construction stages are defined by activating or deactivating the structural elements or soil clusters in the work-planes and a simulation of the construction process can be achieved. A construction period can also be specified for each construction stage but the soil material model should be selected as “MOHR COLUMB MODEL”.

The mechanical behavior of soils may be modeled at various degrees of accuracy. Hooke's law of linear, isotropic elasticity, for example, may be thought of as the simplest available stress-strain relationship. As it involves only two input parameters, i.e. Young's modulus, *E*, and Poisson's ratio, ν, it is generally too crude to capture essential features of soil and rock

behavior. For modeling massive structural elements and bedrock layers, however, linear elasticity tends to be appropriate. The most important calculation type in PLAXIS 3D Foundation is the staged construction. In every calculation step, the material properties, geometry of the model, loading condition and the ground water level can be redefined. During the calculations in each construction step, a multiplier that controls the staged construction process (ΣM stage) is increased from zero to the ultimate level that is generally 1.0. The constructions that are not completed fully can be modeled by using this feature.

5.3 Numerical Analysis

An attempt has been made to carry out numerical analysis of the model tests by finite element method using PLAXIS 3D FOUNADATION software. A total of 78 cases have been carried out. The properties of soil as used in the numerical study have been given in **Table 5.1.**

Table 5.1: Values of various parameters for numerical analysis

Sl. No.	Soil type	Percentage of Reinforcement	Aspect Ratio	Footing Width	Optimum Moisture Content	Maximum Dry Density	Cohesion	Angle of friction
		P_r (%)	AR	B (cm)	OMC (%)	MDD (gm/cc)	c (kg/cm^2)	ϕ (degree)
1	S1	0	0	5	19	1.65	0.9	7
2				10	19	1.65	0.9	7
3	S1	0.5	1	5	17.8	1.68	1.05	9
4				10	17.8	1.68	1.05	9
5	S1	1		5	17.48	1.7	1.2	11
6				10	17.48	1.7	1.2	11
7	S1	1.5		5	18	1.67	1	8
8				10	18	1.67	1	8
9	S1	2		5	18.44	1.65	0.9	6
10				10	18.44	1.65	0.9	6

Table 5.1: Values of various parameters for numerical analysis... contd.

Sl. No.	Soil type	Percentage of Reinforcement	Aspect Ratio	Footing Width	Optimum Moisture Content	Maximum Dry Density	Cohesion	Angle of friction
		P_r (%)	AR	B (cm)	OMC (%)	MDD (gm/cc)	c (kg/cm^2)	ϕ (degree)
11	S1	0.5	2	5	17.6	1.7	1.15	9
12				10	17.6	1.7	1.15	9
13	S1	1		5	17.4	1.71	1.35	12
14				10	17.4	1.71	1.35	12
15	S1	1.5		5	18.15	1.66	1	8
16				10	18.15	1.66	1	8
17	S1	2		5	19.2	1.64	0.9	6
18				10	19.2	1.64	0.9	6
19	S1	0.5	3	5	18.15	1.67	1.1	10
20				10	18.15	1.67	1.1	10
21	S1	1		5	18.5	1.65	1	13
22				10	18.5	1.65	1	13
23	S1	1.5		5	19.4	1.62	0.6	9
24				10	19.4	1.62	0.6	9
25	S1	2		5	19.8	1.58	0.5	7
26				10	19.8	1.58	0.5	7
27	S2	0	0	5	18	1.72	1.1	10
28				10	18	1.72	1.1	10
29	S2	0.5	1	5	16.9	1.7	1.3	11
30				10	16.9	1.7	1.3	11
31	S2	1		5	15.85	1.72	1.48	13
32				10	15.85	1.72	1.45	13
33	S2	1.5		5	17.5	1.67	1.18	9
34				10	17.5	1.67	1.18	9
35	S2	2		5	19.6	1.65	0.98	7
36				10	19.6	1.65	0.98	7
37	S2	0.5	2	5	16.5	1.71	1.3	12
38				10	16.5	1.71	1.3	12
39	S2	1		5	15.53	1.74	1.45	13
40				10	15.53	1.74	1.48	13
41	S2	1.5		5	18.5	1.64	0.95	7
42				10	18.5	1.64	0.95	7
43	S2	2		5	19.2	1.61	0.76	6
44				10	19.2	1.61	0.76	6

Table 5.1: Values of various parameters for numerical analysis... contd.

Sl. No.	Soil type	Percentage of Reinforcement	Aspect Ratio	Footing Width	Optimum Moisture Content	Maximum Dry Density	Cohesion	Angle of friction
		P_r (%)	AR	B (cm)	OMC (%)	MDD (gm/cc)	c (kg/cm^2)	ϕ (degree)
45	S2	0.5	3	5	17	1.71	1.45	12
46				10	17	1.71	1.45	12
47	S2	1		5	18.24	1.68	1.25	14
48				10	18.24	1.68	1.25	14
49	S2	1.5		5	19.5	1.63	0.8	9
50				10	19.5	1.63	0.8	9
51	S2	2		5	20.2	1.6	0.65	7
52				10	20.2	1.6	0.65	7
53	S3	0	0	5	15.4	1.8	1.2	12
54				10	15.4	1.8	1.2	12
55	S3	0.5	1	5	15.2	1.75	1.35	13
56				10	15.2	1.75	1.35	13
57	S3	1		5	14.85	1.76	1.55	15
58				10	14.85	1.76	1.55	15
59	S3	1.5		5	16.5	1.68	1.2	11
60				10	16.5	1.68	1.2	11
61	S3	2		5	19.6	1.65	1	8
62				10	19.6	1.65	1	8
63	S3	0.5	2	5	15.1	1.75	1.4	14
64				10	15.1	1.75	1.4	14
65	S3	1		5	14.73	1.77	1.5	16
66				10	14.73	1.77	1.5	16
67	S3	1.5		5	17	1.67	1.15	9
68				10	17	1.67	1.15	9
69	S3	2		5	19.65	1.63	0.88	7
70				10	19.65	1.63	0.88	7
71	S3	0.5	3	5	15	1.76	1.48	14
72				10	15	1.76	1.48	14
73	S3	1		5	16.84	1.71	1.33	17
74				10	16.84	1.71	1.33	17
75	S3	1.5		5	18.50	1.66	0.95	11
76				10	18.50	1.66	0.95	11
77	S3	2		5	20.5	1.62	0.75	9
78				10	20.5	1.62	0.75	9

5.4 Presentation of Numerical Results

The load-settlement curve for each case has been presented in Figs. 5.2 to 5.27 from the output of PLAXIS 3D FOUNDATION software.

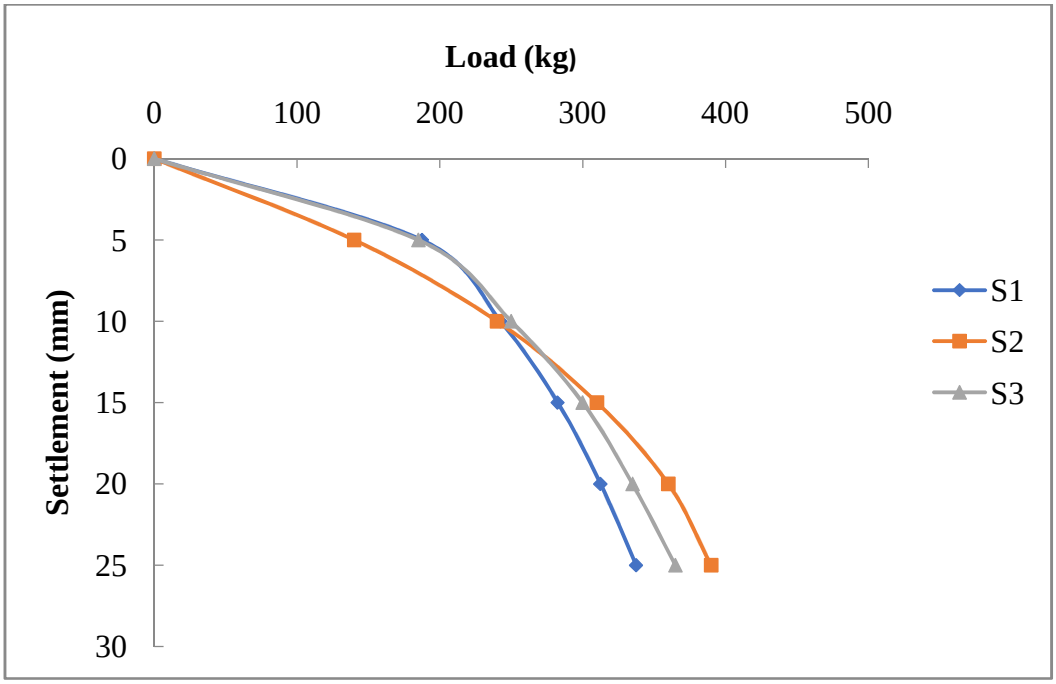

Fig. 5.2: Load - settlement curve for 5 cm × 5 cm footing on unreinforced soil

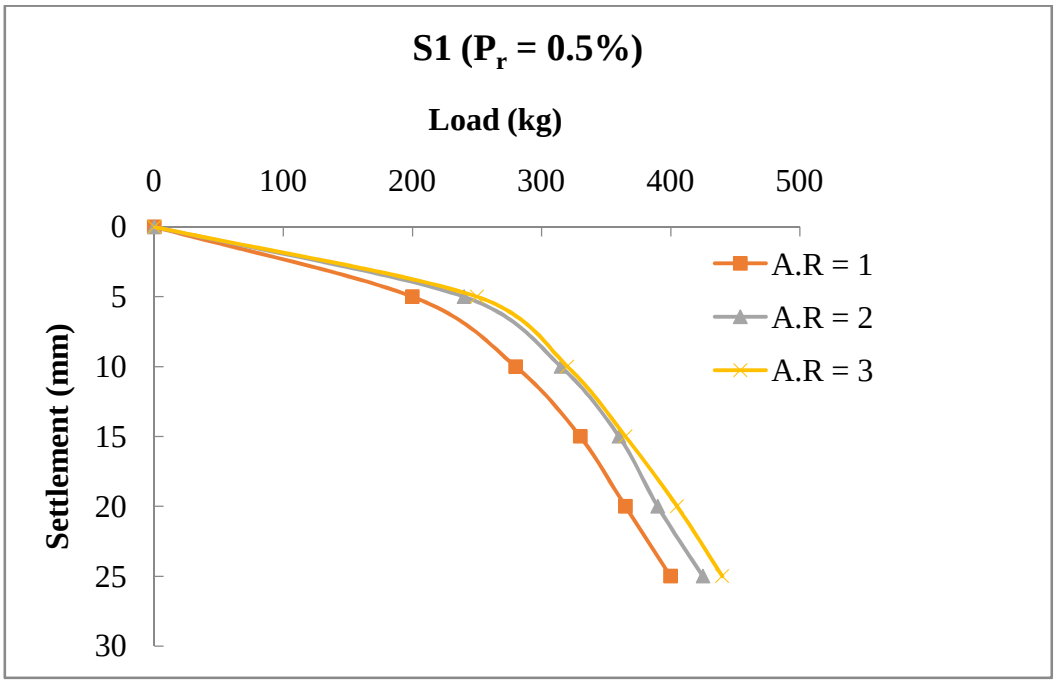

Fig. 5.3: Load - settlement curve for 5 cm × 5 cm footing on S1 (P_r = 0.5%)

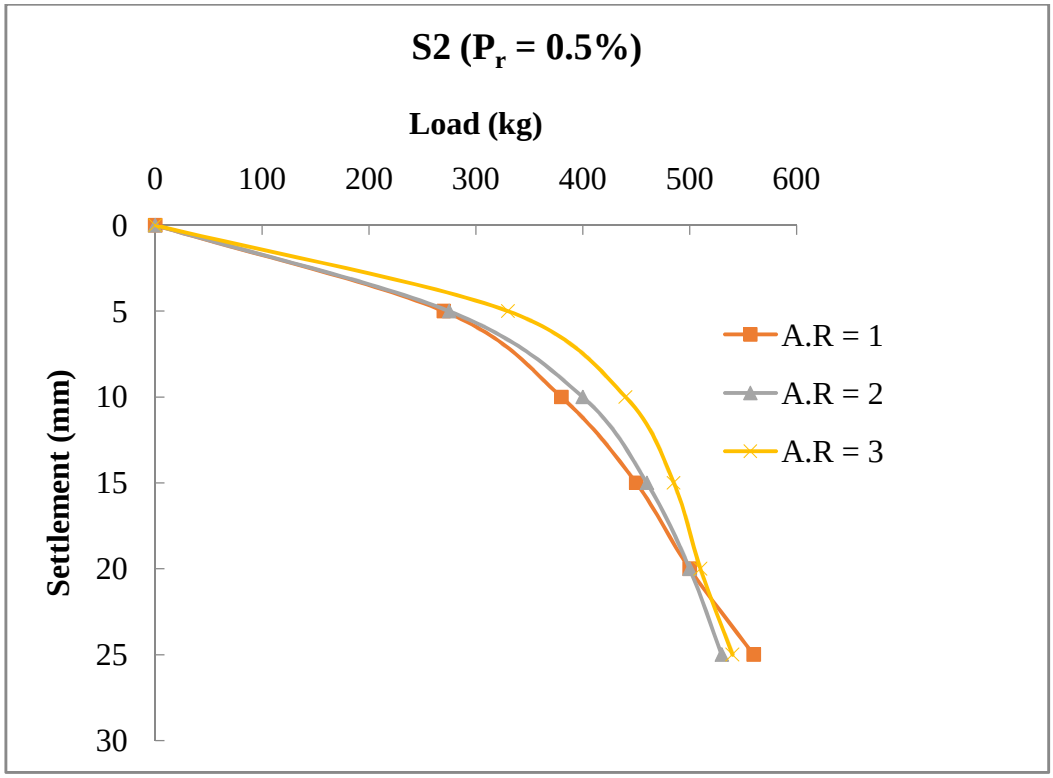

Fig. 5.4: Load - settlement curve for 5 cm × 5 cm footing on S2 (P_r = 0.5%)

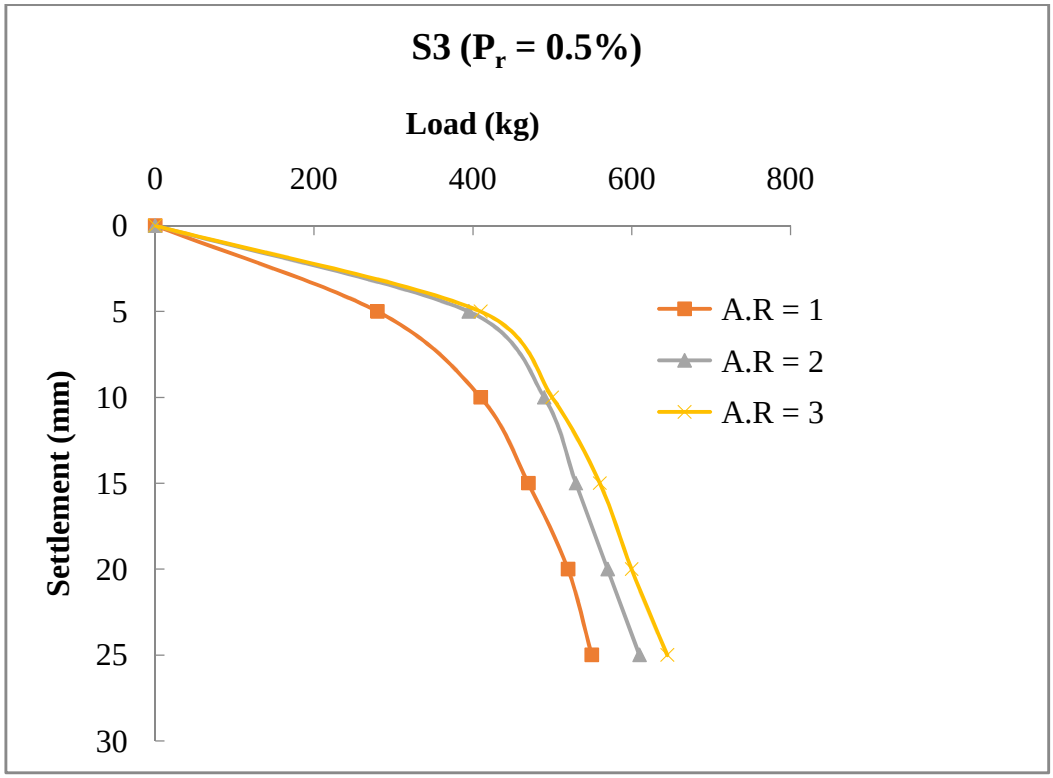

Fig. 5.5: Load - settlement curve for 5 cm × 5 cm footing on S3 (P_r = 0.5%)

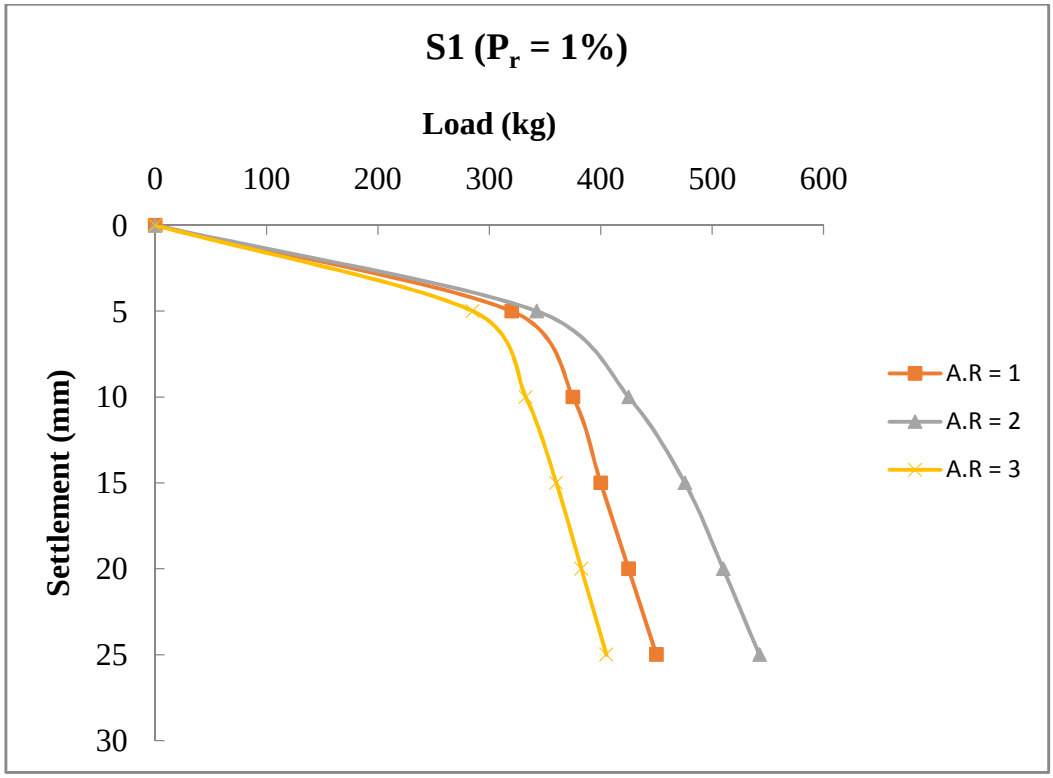

Fig. 5.6: Load - settlement curve for 5 cm × 5 cm footing on S1 (P_r = 1%)

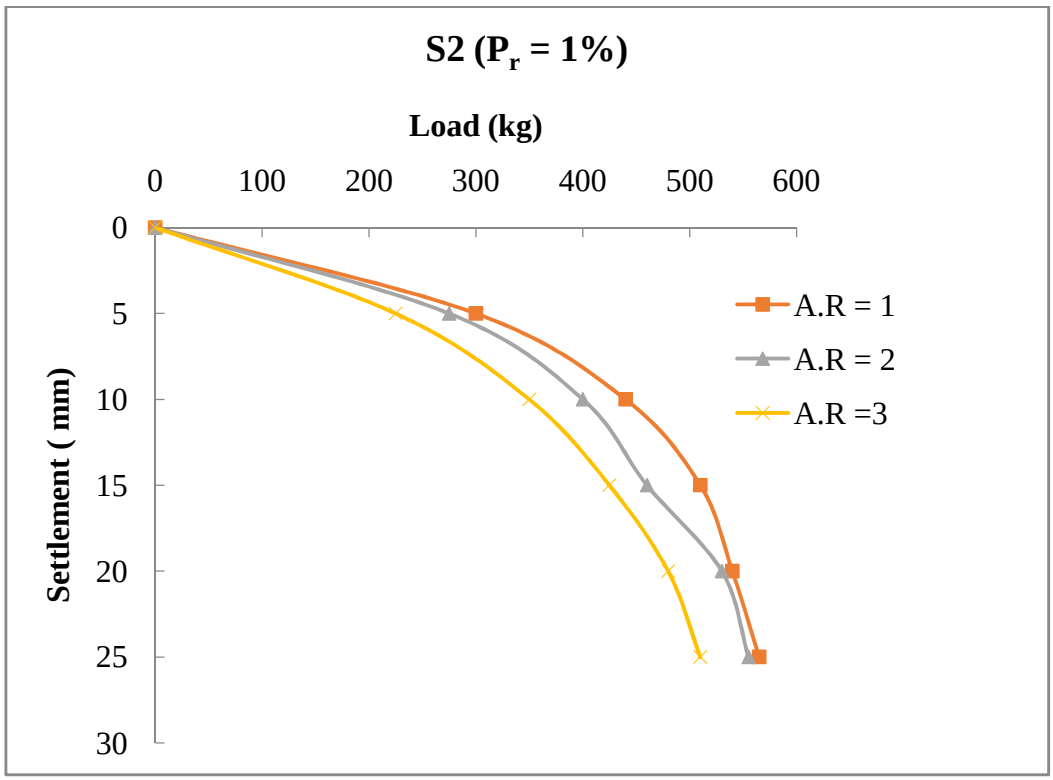

Fig. 5.7: Load - settlement curve for 5 cm × 5 cm footing on S2 (P_r = 1%)

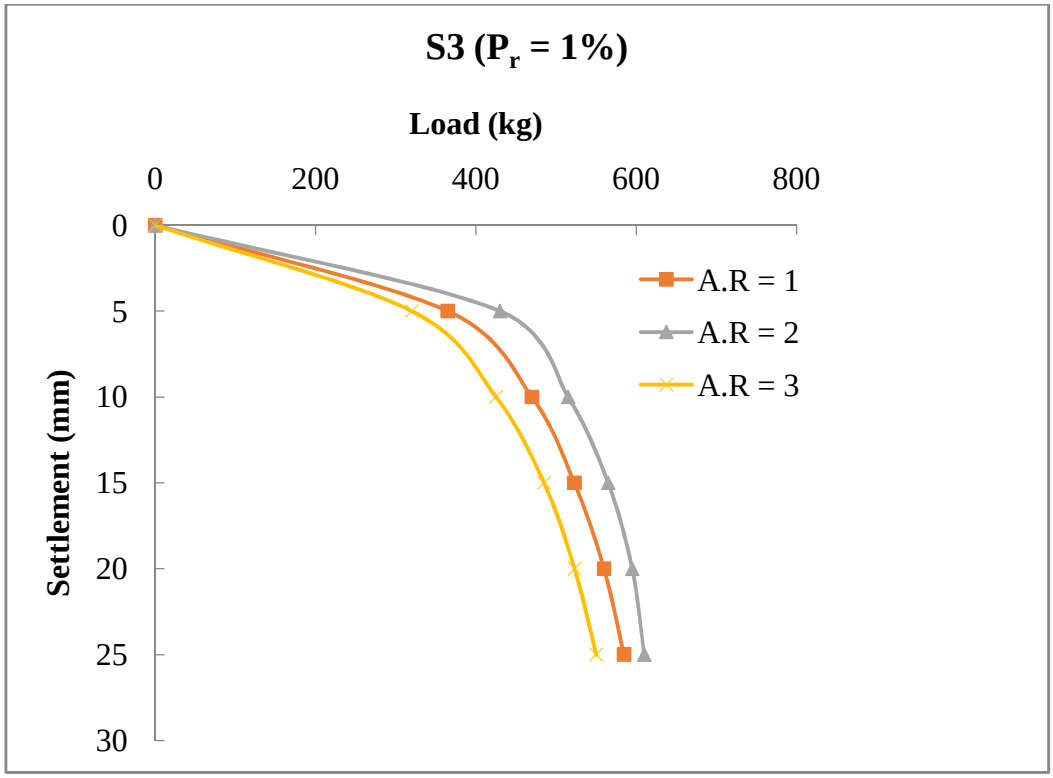

Fig. 5.8: Load - settlement curve for 5 cm × 5 cm footing on S3 (P_r = 1%)

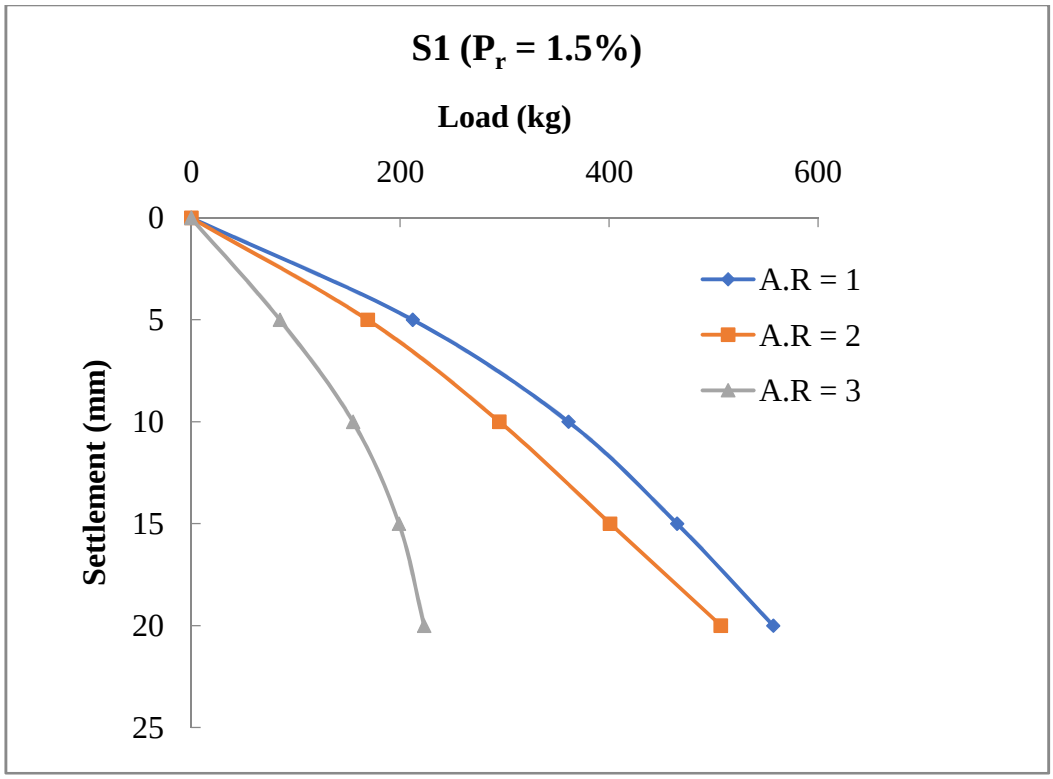

Fig. 5.9: Load - settlement curve for 5 cm × 5 cm footing on S1 (P_r = 1.5%)

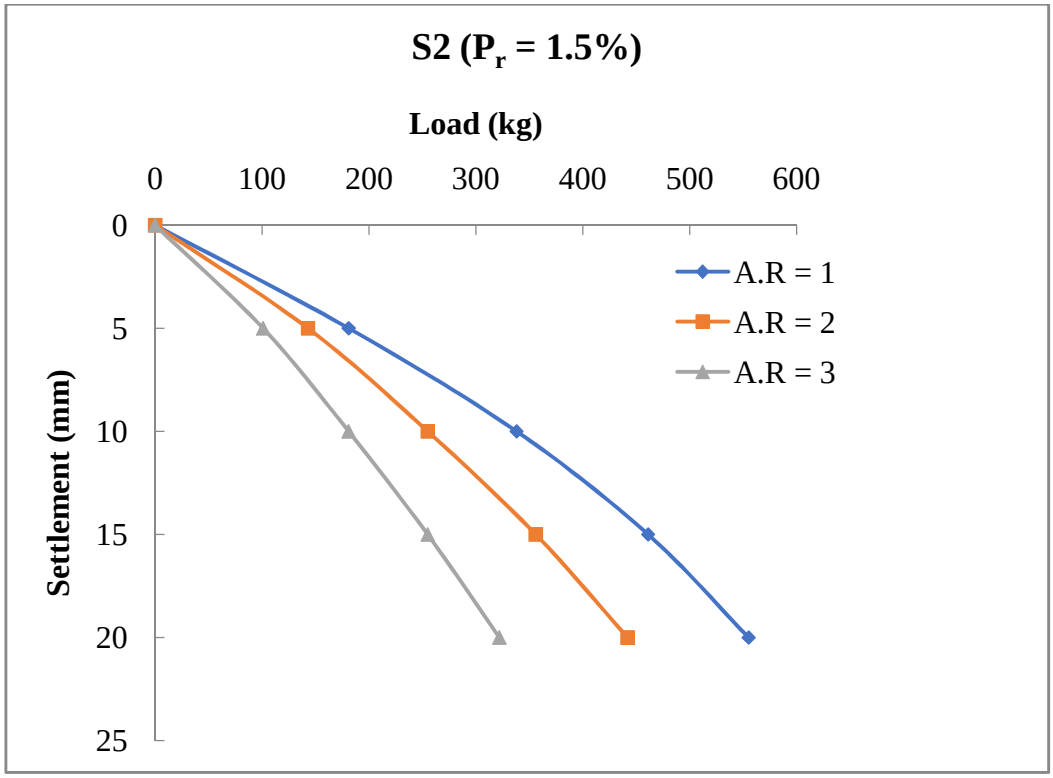

Fig. 5.10: Load - settlement curve for 5 cm × 5 cm footing on S2 (P_r = 1.5%)

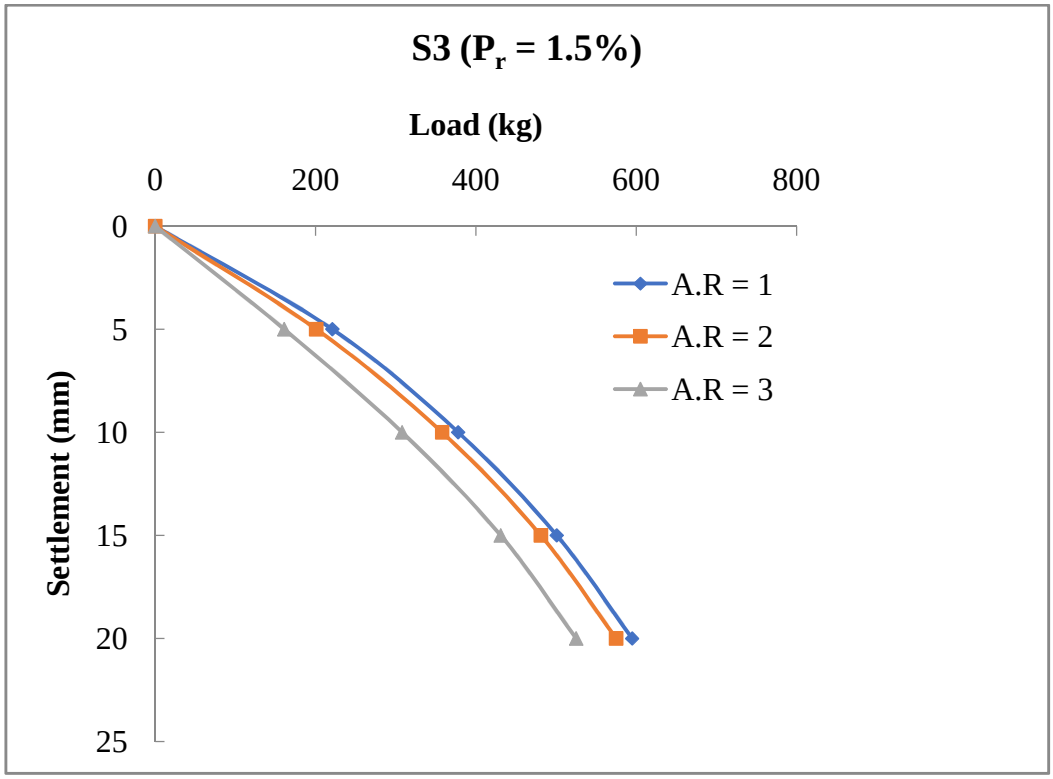

Fig. 5.11: Load - settlement curve for 5 cm × 5 cm footing on S3 (P_r = 1.5%)

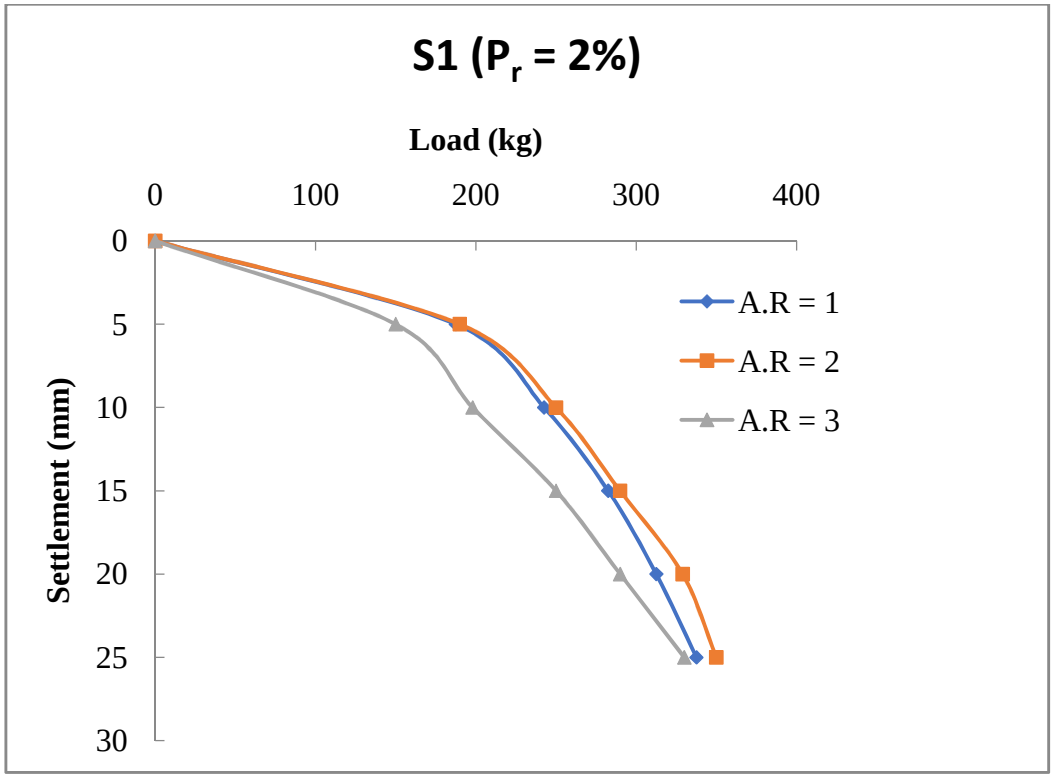

Fig. 5.12: Load - settlement curve for 5 cm × 5 cm footing on S1 (P_r = 2%)

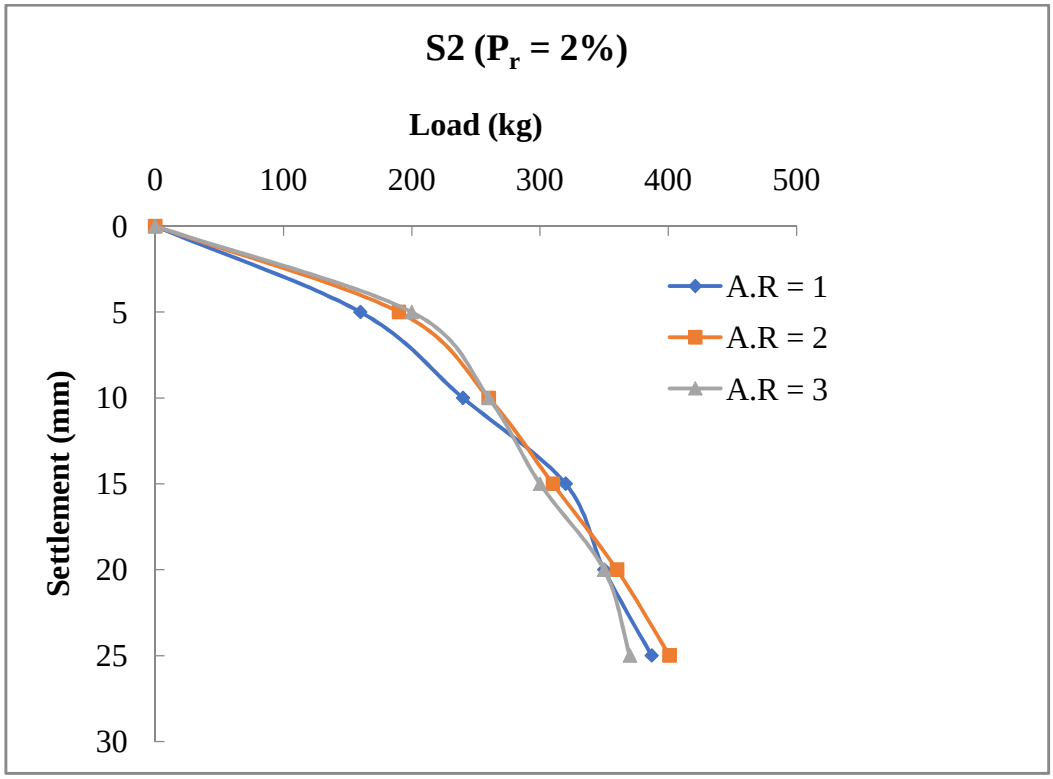

Fig. 5.13: Load - settlement curve for 5 cm × 5 cm footing on S2 (P_r = 2%)

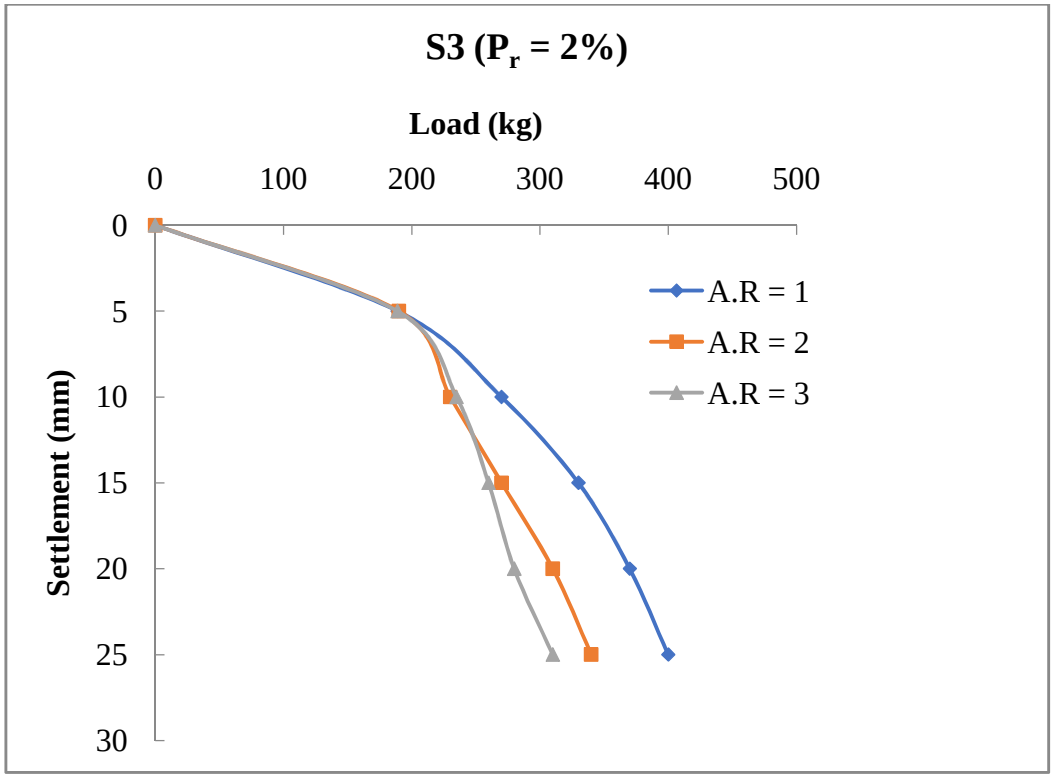

Fig. 5.14: Load - settlement curve for 5 cm × 5 cm footing on S3 (P_r = 2%)

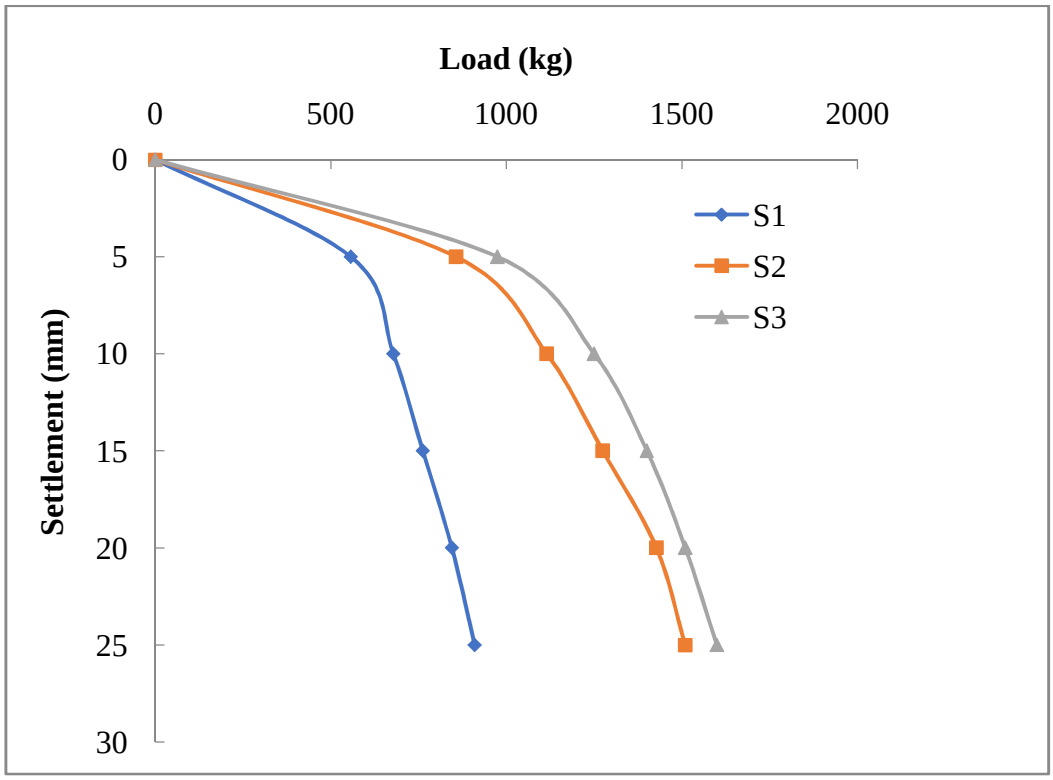

Fig. 5.15: Load - settlement curve for 10 cm × 10 cm footing on unreinforced soil

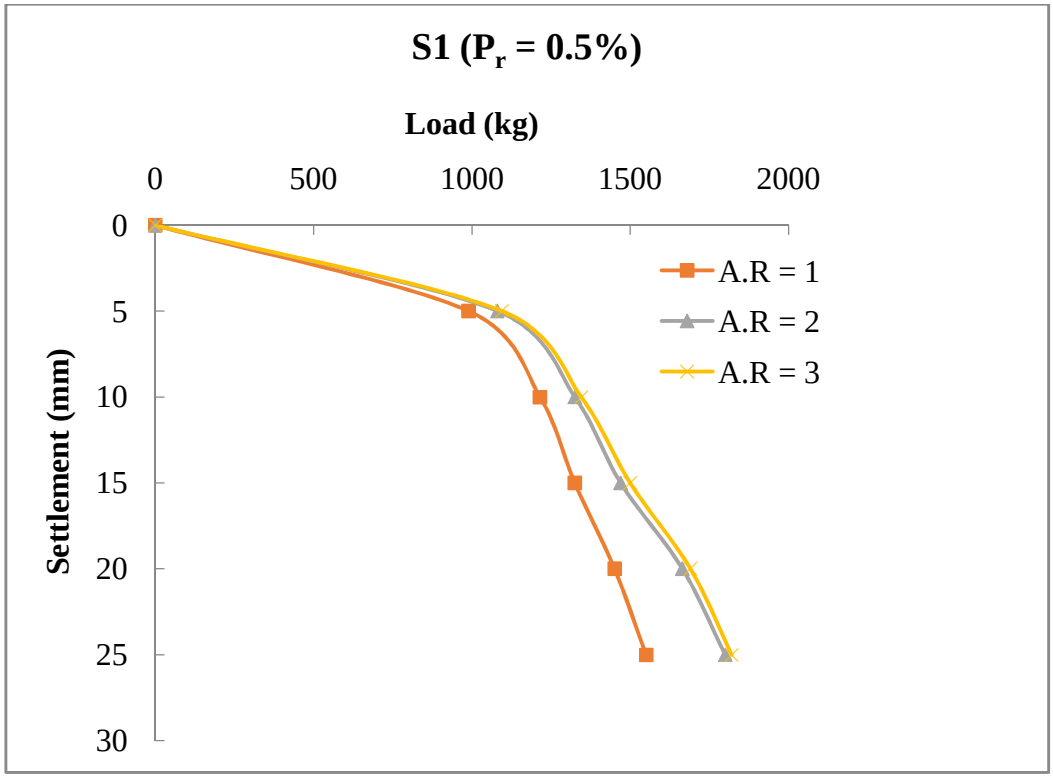

Fig. 5.16: Load - settlement curve for 10 cm × 10 cm footing on S1 (P_r = 0.5%)

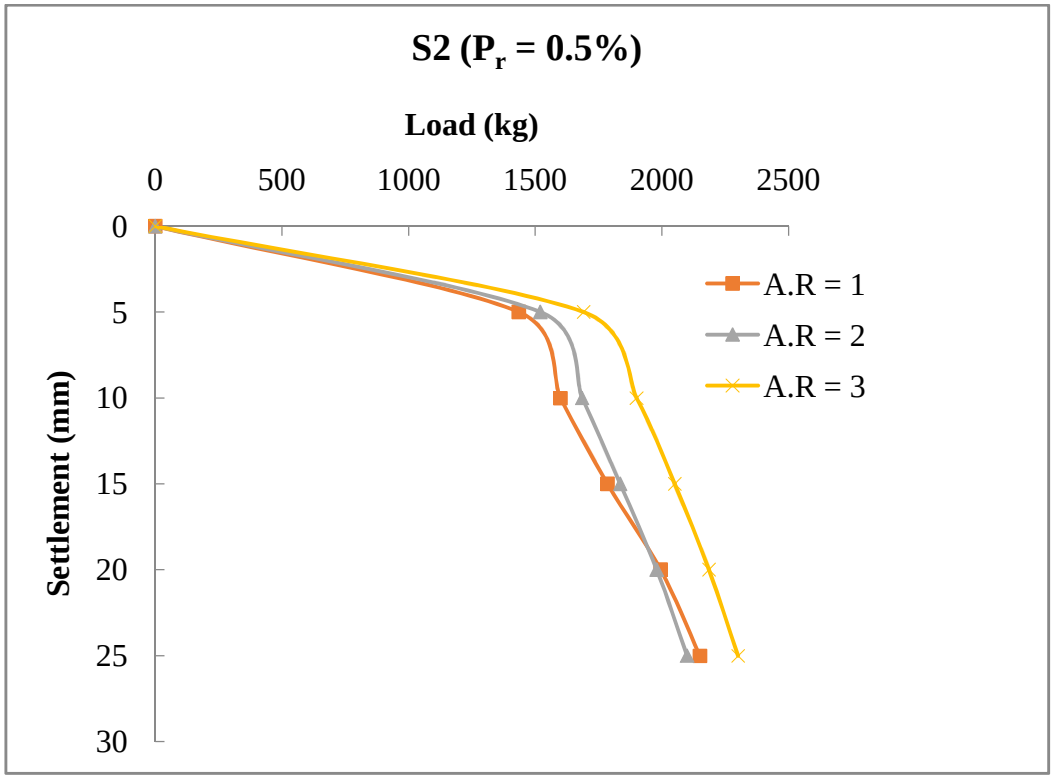

Fig. 5.17: Load - settlement curve for 10 cm × 10 cm footing on S2 (P_r = 0.5%)

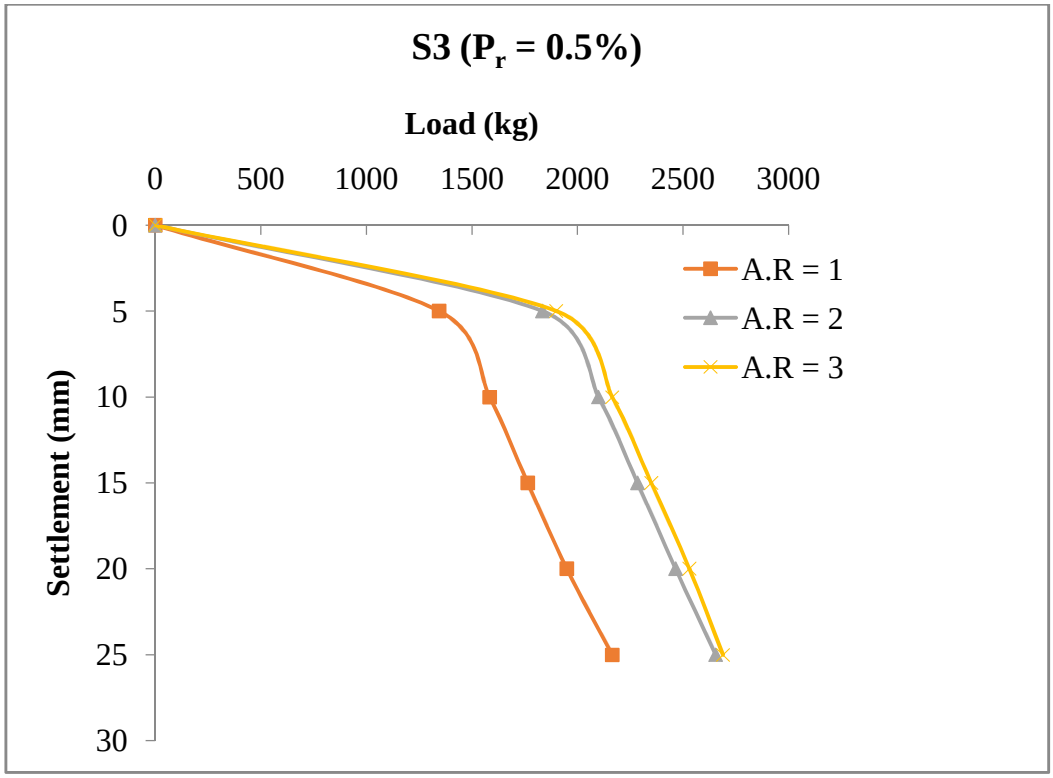

Fig. 5.18: Load - settlement curve for 10 cm × 10 cm footing on S3 (P_r = 0.5%)

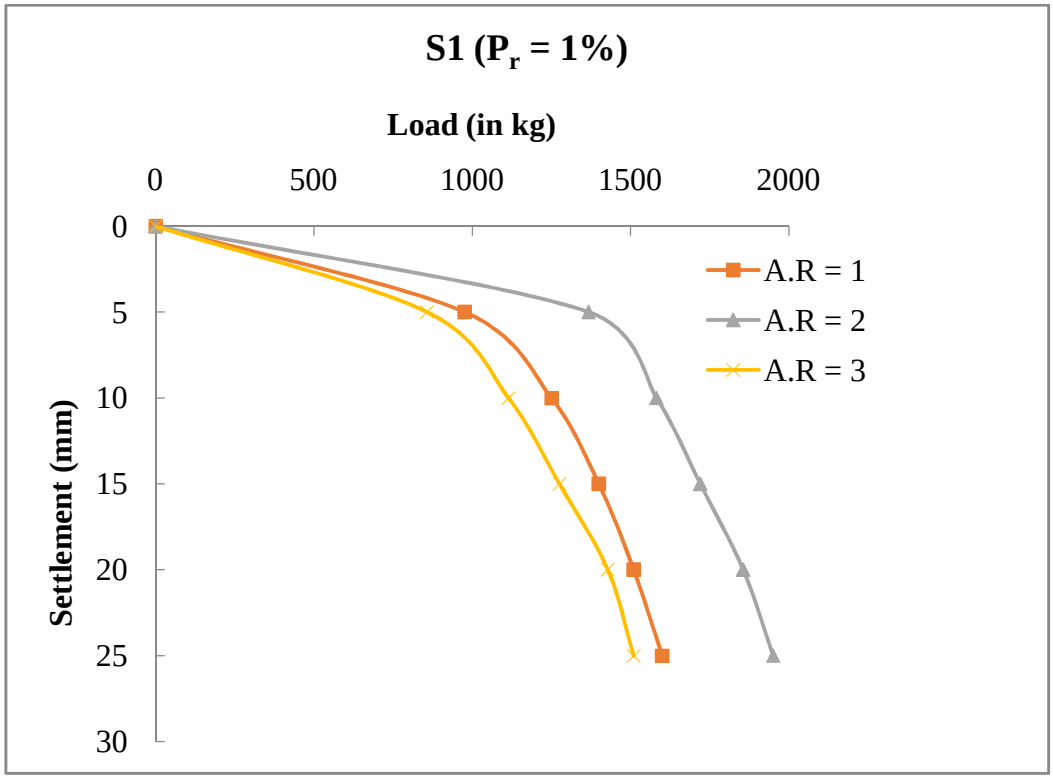

Fig. 5.19: Load - settlement curve for 10 cm × 10 cm footing on S1 (P_r = 1%)

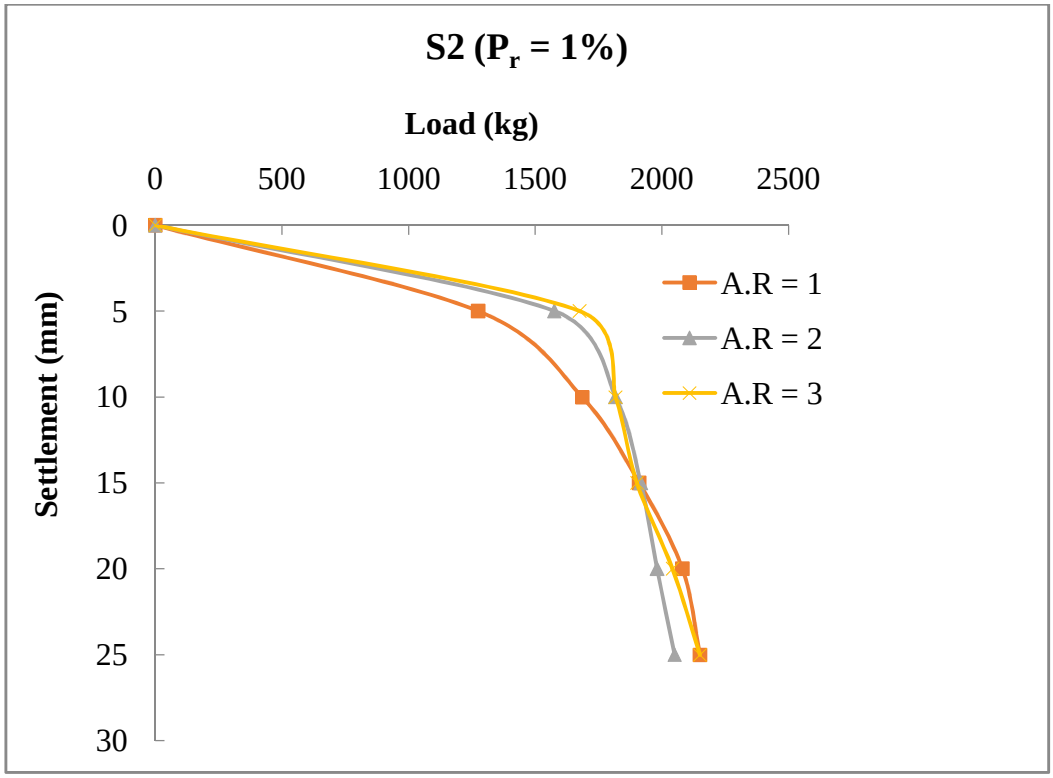

Fig. 5.20: Load - settlement curve for 10 cm × 10 cm footing on S2 (P_r = 1%)

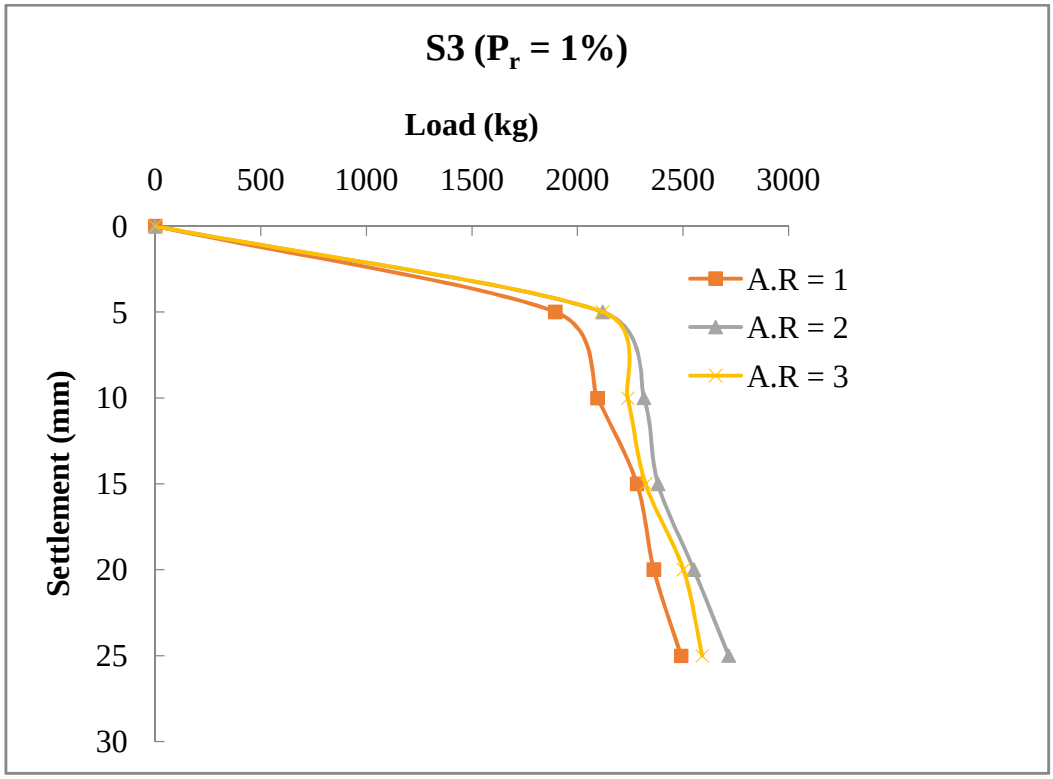

Fig. 5.21: Load - settlement curve for 10 cm × 10 cm footing on S3 (P_r = 1%)

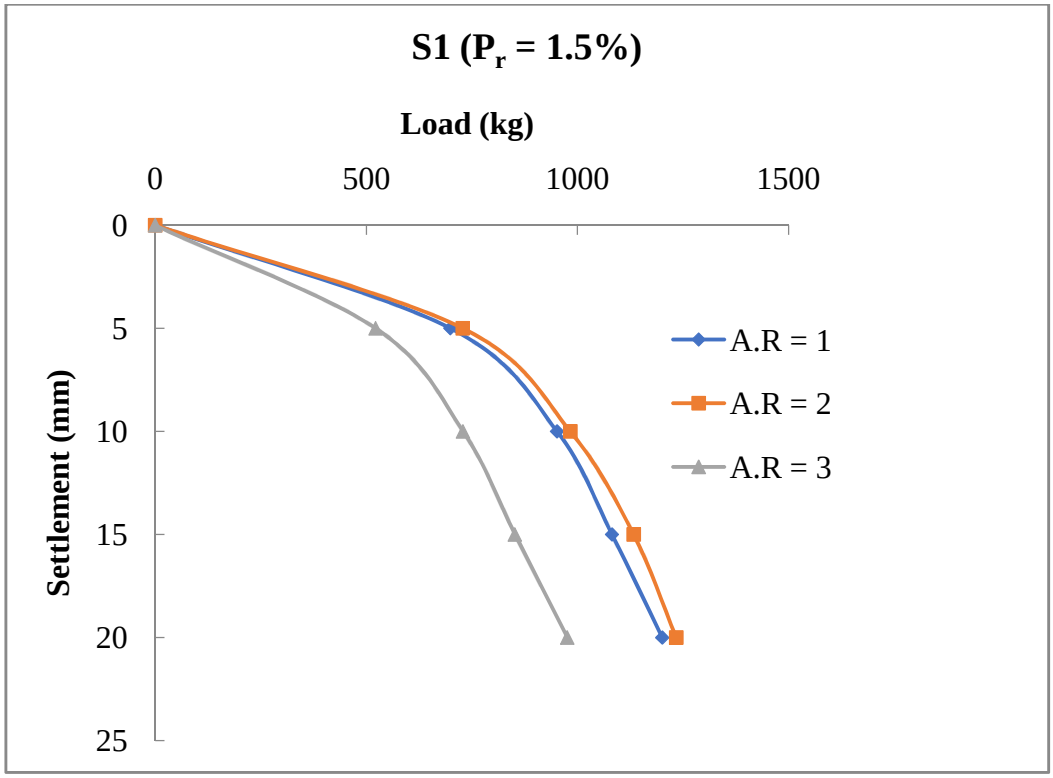

Fig. 5.22: Load - settlement curve for 10 cm × 10 cm footing on S1 (P_r = 1.5%)

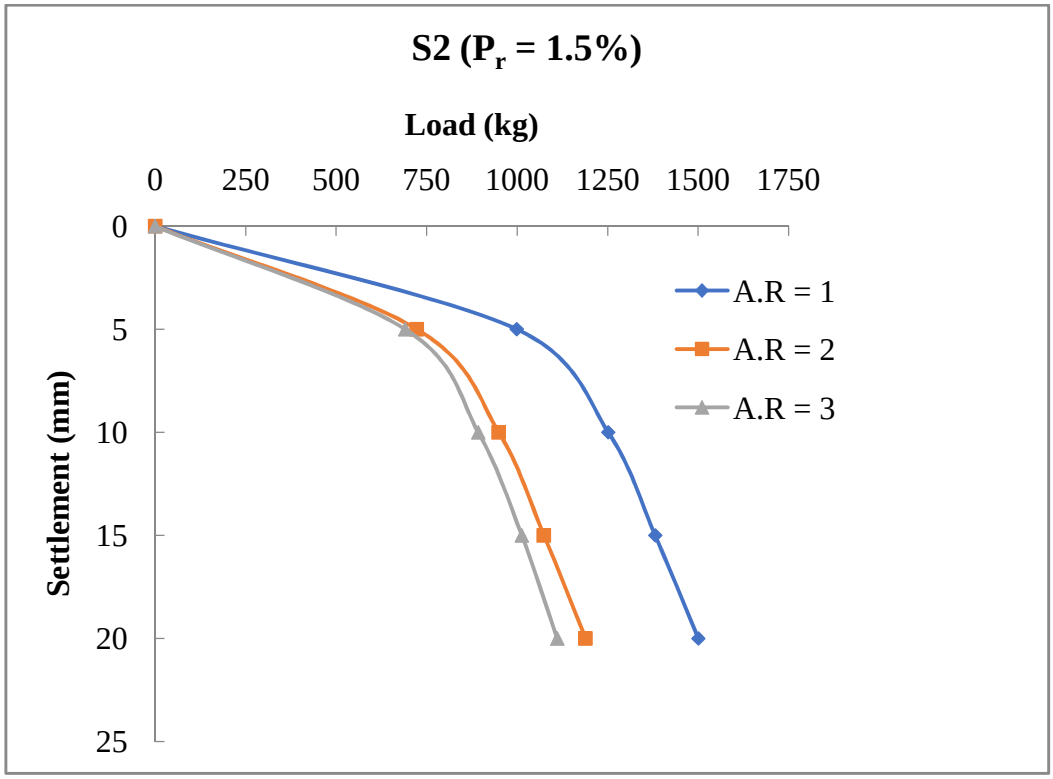

Fig. 5.23: Load - settlement curve for 10 cm × 10 cm footing on S2 (P_r = 1.5%)

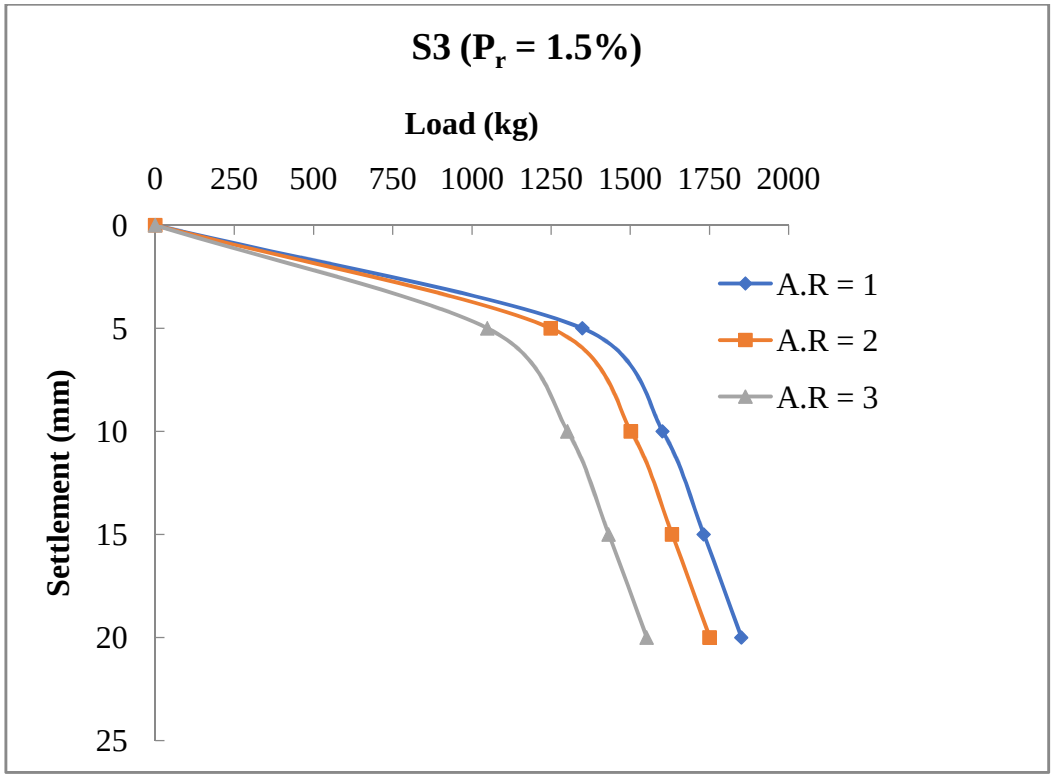

Fig. 5.24: Load - settlement curve for 10 cm × 10 cm footing on S3 (P_r = 1.5%)

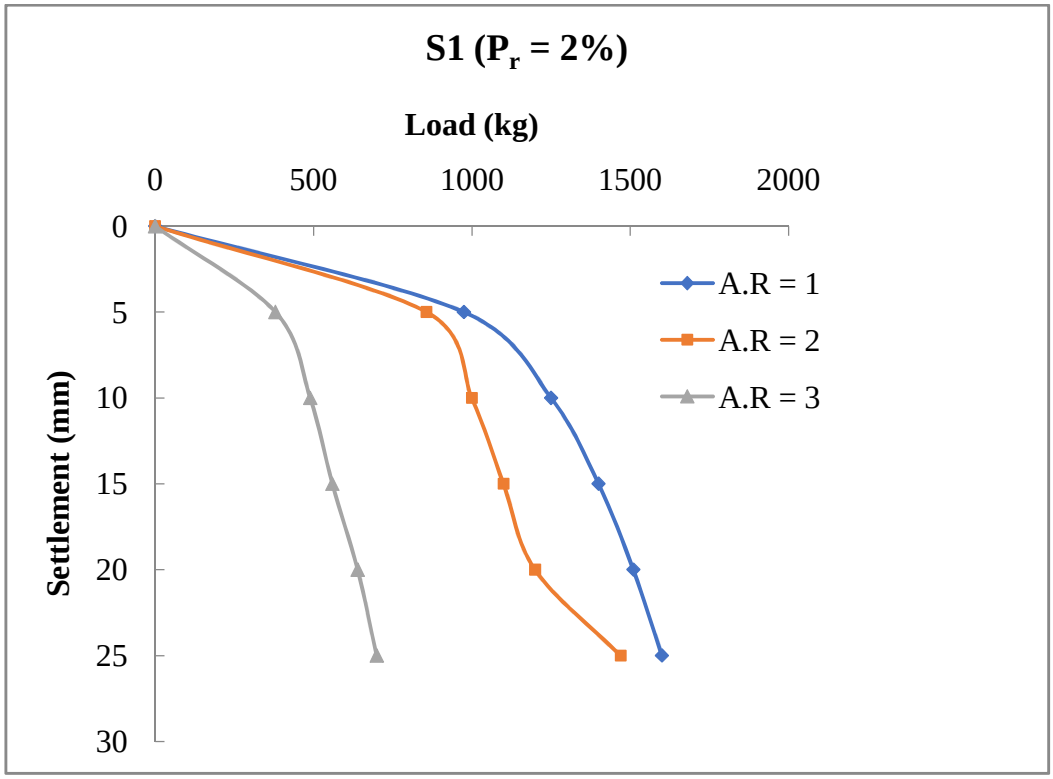

Fig. 5.25: Load - settlement curve for 10 cm × 10 cm footing on S1 (P_r = 2%)

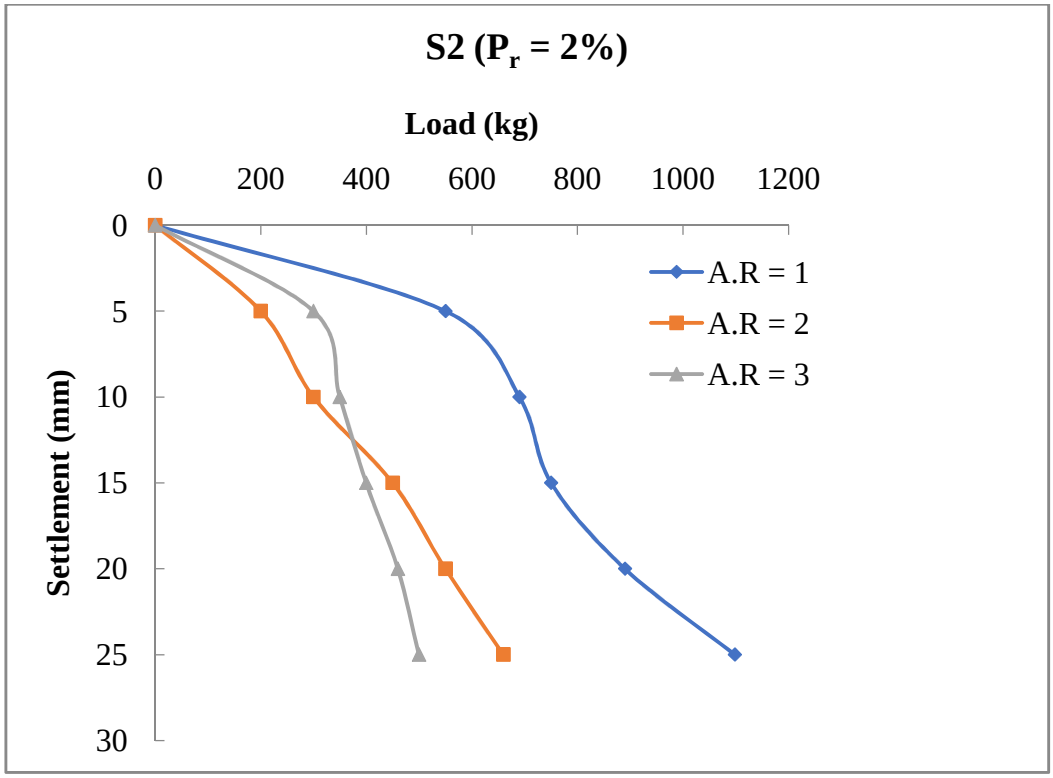

Fig. 5.26: Load - settlement curve for 10 cm × 10 cm footing on S2 (P_r = 2%)

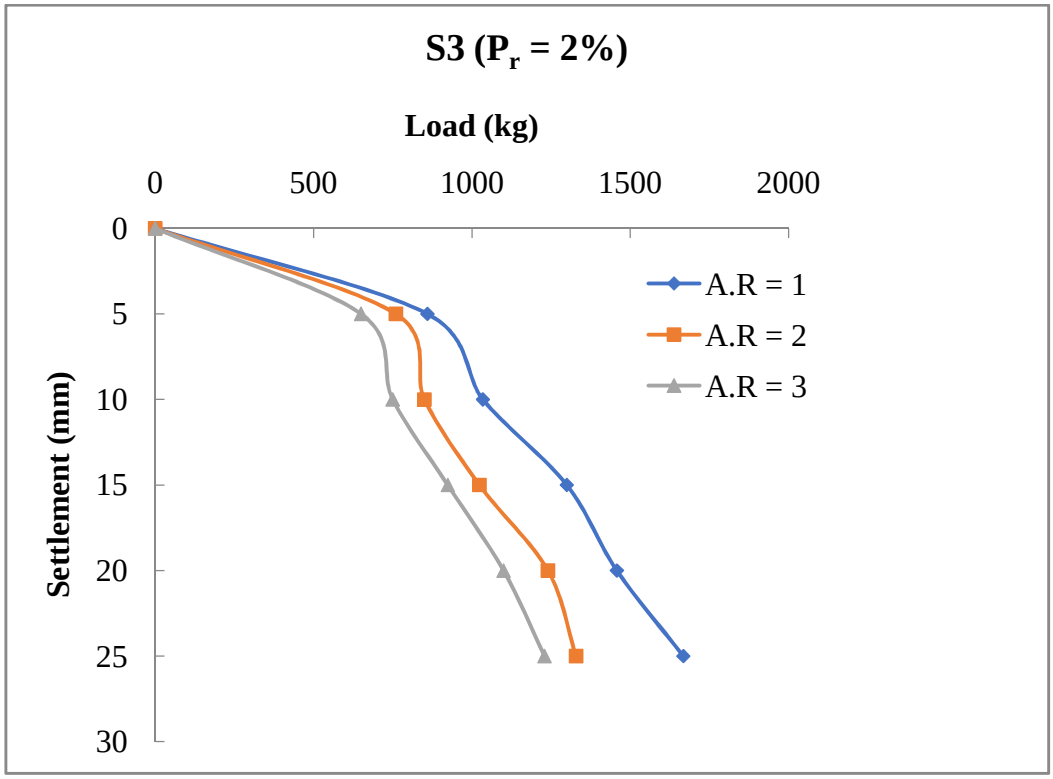

Fig. 5.27: Load - settlement curve for 10 cm × 10 cm footing on S3 (P_r = 2%)

Chapter 6

DISCUSSION ON RESULTS OF EXPERIMENTAL AND NUMERICAL STUDIES

6.0 General

Based on the results obtained from experimental investigation and numerical analysis an attempt has been made in this chapter to study the effect of PET bottle strip reinforcements on ultimate bearing capacity of footings.

6.1 Load - Settlement Curves

Load - settlement curves for footings of sizes 5 cm x 5 cm and 10 cm x 10 cm as obtained from experiments and output of PLAXIS 3D software have been presented earlier in Chapter 4 (Figs. 4.3 to 4.10) and Chapter 5 (Figs. 5.2 to 5.27) respectively. It is observed that experimentally and numerically obtained curves follow continuously curvilinear trend and hence the ultimate loads have been obtained from these curves by double tangent method. From the curves, it can be seen that for both sizes of the footings, ultimate load carried by soil reinforced with PET bottle strips is maximum for strip content of 1% and aspect ratio 2, compared to that of all other mixes, both for experimental and numerical cases. Table 6.1 presents the experimental and numerical values of ultimate bearing capacities for square footings of sizes 5 cm and 10 cm. The values were 442 kg and 1740 kg for 5 cm and 10 cm square footings respectively as obtained for 1% strip content and aspect ratio 2 from experiments. On the other hand 395 kg and 1605 kg were the respective values for 5 cm and 10 cm square footings as obtained from numerical analysis. Although values for aspect ratio 1 and 3 were lower than the corresponding value for aspect ratio 2, they were higher compared to the corresponding values for respective unreinforced soil type. It can also be seen that the initial nature of load-settlement curves obtained from experimental and numerical data agree within reasonable range of variation. Further, it can be observed that the experimental values obtained are higher than that of corresponding numerical value. On an average they vary by 12.72% and 9.29% for 5 cm and 10 cm footing size respectively.

Table 6.1 Ultimate Load from Experimental and Numerical Analysis (for 1% strip content)

Sl. No	Size of Footing	Aspect Ratio	Ultimate Load (kg)		% variation of experimental from numerical results
			Experimental	Numerical	(%)
1	5 cm	0	225	205	9.76
2		1	379	332	14.16
3		2	442	395	11.90
4		3	351	305	15.08
5	10 cm	0	930	840	10.71
6		1	1460	1370	6.57
7		2	1740	1610	8.07
8		3	1420	1270	11.81

PLAXIS 3D has been used as a tool for determining ultimate bearing capacities for all soil types, mixes and two footing sizes of 5 cm and 10 cm because for 8 experimental cases the values of ultimate bearing capacity matches with that of corresponding numerical cases. Thus for total 78 numerical cases considered for the numerical study, as mentioned in Chapter 5, the ultimate bearing capacities obtained from load settlement curves presented in Chapter 5 are furnished in Table 6.2.

Table 6.2: Ultimate bearing capacities obtained from numerical analysis

Sl. No.	Soil type	Percentage of reinforcement	Aspect ratio	Footing width	Ultimate bearing capacity
		P_r (%)	AR	B (cm)	q (kg/cm^2)
1	S1	0	0	5	8.273
2	S1	0	0	10	8.275
3	S1	0.5	1	5	10.652
4	S1	0.5	1	10	10.702
5	S1	1	1	5	13.518
6	S1	1	1	10	13.584
7	S1	1.5	1	5	9.695
8	S1	1.5	1	10	9.708
9	S1	2	1	5	7.913
10	S1	2	1	10	7.875

Sl. No.	Soil type	Percentage of reinforcement	Aspect ratio	Footing width	Ultimate bearing capacity
		P_r (%)	AR	B (cm)	q (kg/cm^2)
11	S1	0.5	2	5	11.643
12	S1	0.5	2	10	11.655
13	S1	1	2	5	16.064
14	S1	1	2	10	16.194
15	S1	1.5	2	5	9.744
16	S1	1.5	2	10	9.637
17	S1	2	2	5	7.816
18	S1	2	2	10	7.875
19	S1	0.5	3	5	11.784
20	S1	0.5	3	10	11.744
21	S1	1	3	5	12.597
22	S1	1	3	10	12.565
23	S1	1.5	3	5	6.087
24	S1	1.5	3	10	6.085
25	S1	2	3	5	4.587
26	S1	2	3	10	4.586
27	S2	0	0	5	11.74
28	S2	0	0	10	11.745
29	S2	0.5	1	5	14.628
30	S2	0.5	1	10	14.678
31	S2	1	1	5	18.565
32	S2	1	1	10	18.134
33	S2	1.5	1	5	11.996
34	S2	1.5	1	10	11.975
35	S2	2	1	5	9.053
36	S2	2	1	10	9.083
37	S2	0.5	2	5	15.507
38	S2	0.5	2	10	15.508
39	S2	1	2	5	18.263
40	S2	1	2	10	18.615
41	S2	1.5	2	5	8.707
42	S2	1.5	2	10	8.694
43	S2	2	2	5	6.618
44	S2	2	2	10	6.691
45	S2	0.5	3	5	17.288
46	S2	0.5	3	10	17.288

Sl. No.	Soil type	Percentage of reinforcement	Aspect ratio	Footing width	Ultimate bearing capacity
		P_r (%)	AR	B (cm)	q (kg/cm^2)
47	S2	1	3	5	16.581
48	S2	1	3	10	16.656
49	S2	1.5	3	5	8.115
50	S2	1.5	3	10	8.119
51	S2	2	3	5	5.952
52	S2	2	3	10	5.965
53	S3	0	0	5	14.267
54	S3	0	0	10	14.257
55	S3	0.5	1	5	17.021
56	S3	0.5	1	10	17.011
57	S3	1	1	5	21.843
58	S3	1	1	10	21.771
59	S3	1.5	1	5	13.558
60	S3	1.5	1	10	13.522
61	S3	2	1	5	9.725
62	S3	2	1	10	9.742
63	S3	0.5	2	5	18.639
64	S3	0.5	2	10	18.578
65	S3	1	2	5	22.242
66	S3	1	2	10	22.261
67	S3	1.5	2	5	11.665
68	S3	1.5	2	10	11.656
69	S3	2	2	5	8.13
70	S3	2	2	10	8.124
71	S3	0.5	3	5	19.631
72	S3	0.5	3	10	19.659
73	S3	1	3	5	20.95
74	S3	1	3	10	20.964
75	S3	1.5	3	5	10.822
76	S3	1.5	3	10	10.696
77	S3	2	3	5	7.716
78	S3	2	3	10	7.642

6.2 Effect of ultimate bearing capacity on aspect ratio and fibre content

In order to study the effect of PET bottle strip reinforcement on ultimate bearing capacity, ultimate bearing capacity vs. aspect ratio graphs have been plotted for different strip contents as shown in Figs. 6.1, 6.2 and 6.3 for three different soil types S1, S2 and S3 respectively.

6.2.1 Aspect Ratio

The effect of aspect ratio on ultimate bearing capacity of the footings was studied by varying the strip content in the soil mix. Tests were carried out for unreinforced soil and reinforced soil with PET bottle strips having aspect ratios of 1, 2 and 3. The results suggested an increase in bearing capacity with increase in aspect ratio up to the value of 2. Thereafter, the bearing capacities were found to decrease. The results of tests conducted on footing sizes of 5 cm and 10 cm were in accordance with the above stated trend. Thus, the maximum bearing capacities of the soils S1, S2 and S3 were recorded for aspect ratio of 2 corresponding to 10 cm footing size.

6.2.2 Fibre Content

The bearing capacity of soil calculated for both cases i.e. for widths of square footings 5 cm and 10 cm was found to increase initially with the increase in fibre content. The tests were conducted for fibre contents of 0.5%, 1%, 1.5% and 2% with the optimum value being achieved corresponding to 1% fibre content. For fibre content greater than 1% the bearing capacities were found to decrease subsequently. This variation was same for all three types of soils S1, S2 and S3. The ultimate bearing capacities for soil types S1, S2 and S3 for aspect ratio of 2 and fibre content of 1% were found to be 16.064 kg/cm^2, 18.263 kg/cm^2 and 22.242 kg/cm^2 for width corresponding to 5 cm and 16.194 kg/cm^2, 18.134 kg/cm^2 and 22.261 kg/cm^2 for width corresponding to 10 cm respectively.

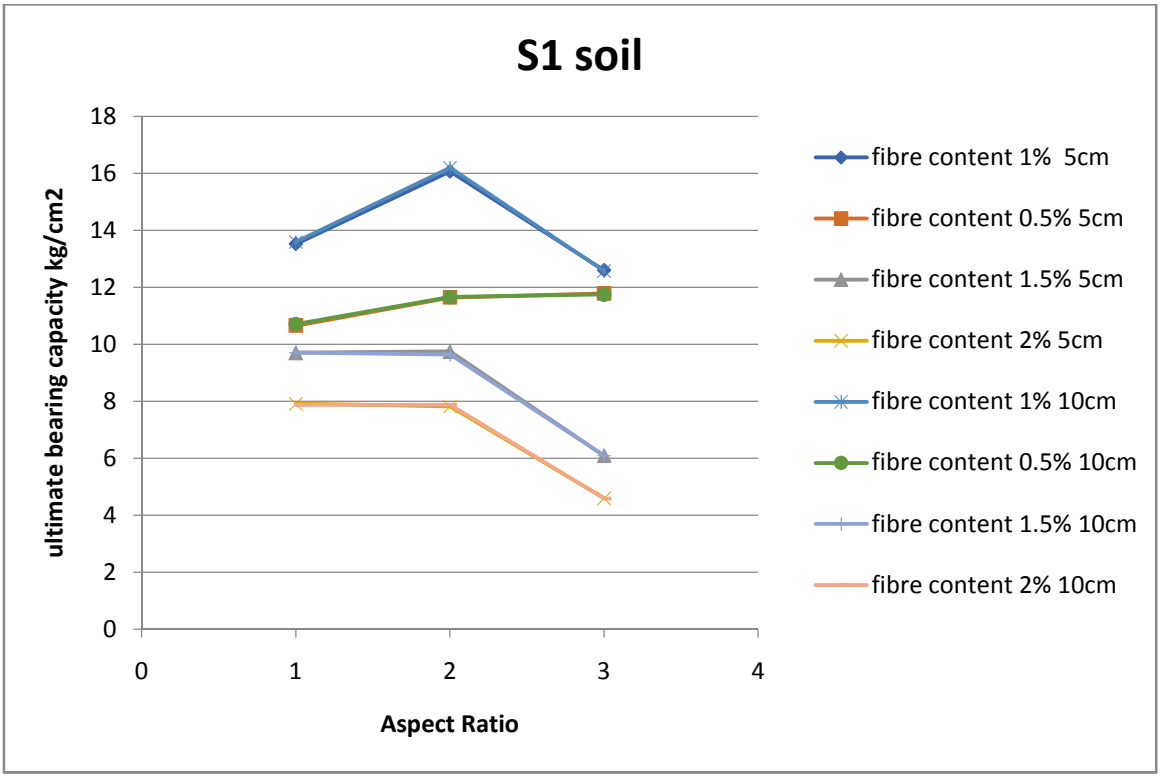

Fig. 6.1: Variation of bearing capacity with aspect ratio for various fibre content for soil S1

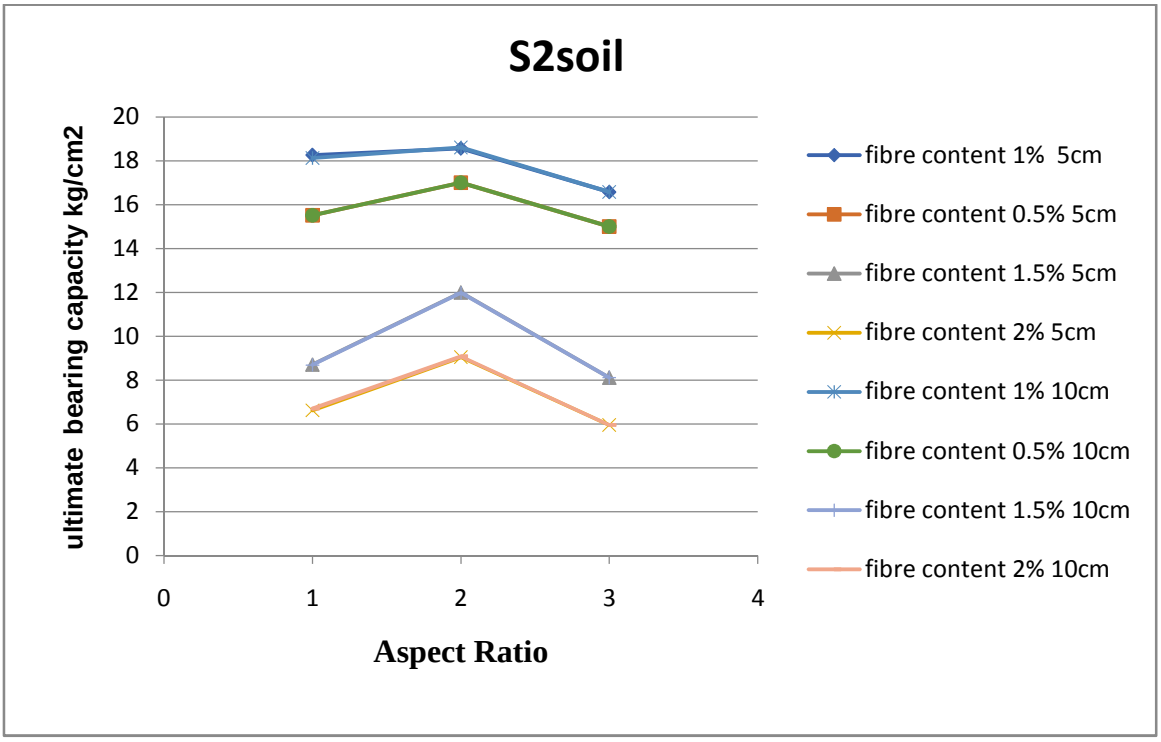

Fig. 6.2: Variation of bearing capacity with aspect ratio for various fibre content for soil S2

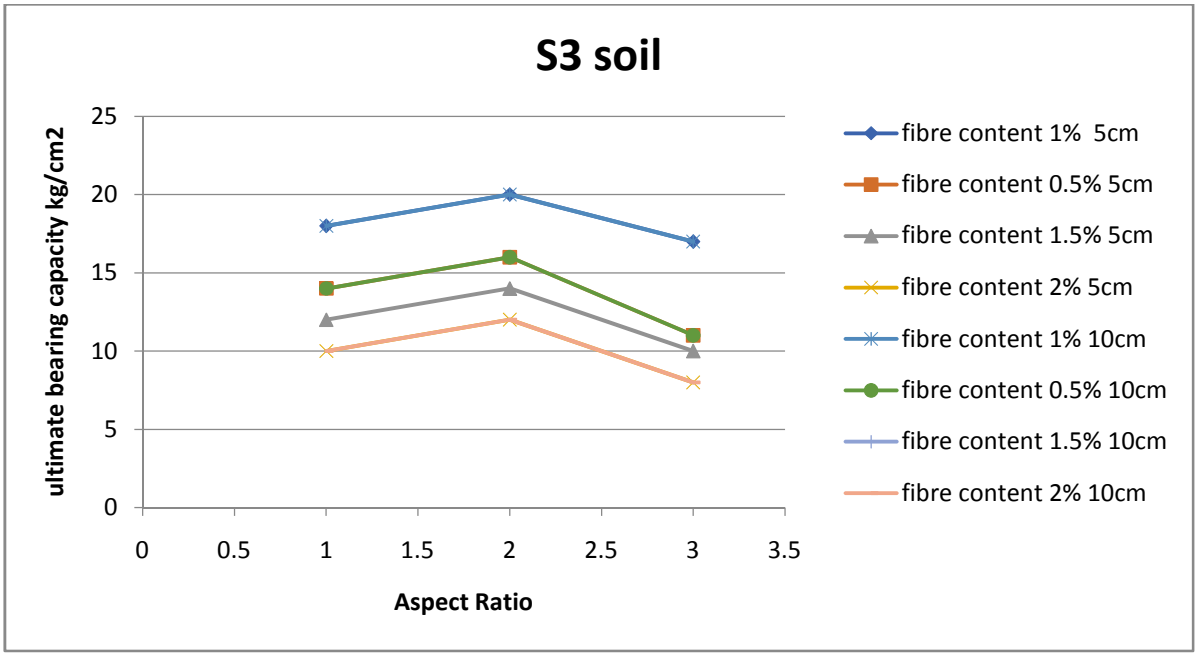

Fig. 6.3: Variation of bearing capacity with aspect ratio for various fibre content for soil S3

6.3 Comparison of Ultimate Bearing Capacity from Small Scale Model Footing Tests with That from PLAXIS 3D Analysis, Terzaghi's Analysis and IS Code Method (IS 6403-1984)

Ultimate loads as per Terzaghi and IS code method were estimated using the values of parameters obtained from the material testing of different soils and mixes. A comparison of ultimate loads from various analyses were made to understand the resemblance of results of model footing tests, numerical analysis and Terzaghi's and IS Code methods as shown in Figs. 6.4a and 6.4b for footing sizes of 5 cm and 10 cm respectively. From the graphs, it can be seen that the ultimate bearing capacity increases with the inclusion of PET bottle strips and this increase has been found to be maximum at aspect ratio of 2, beyond which a decrease in ultimate bearing capacity can been seen. The experimental and numerical results have shown similar pattern as also found in case of classical theories. It has been found that for both footing sizes, the values obtained from the footing tests lie just below the results of Terzaghi's analysis and above those of IS code method and PLAXIS 3D numerical analysis. The variation of experimental result with respect to Terzaghi's analysis, IS code method and PLAXIS 3D numerical analysis was found to be -6.64%, +9.09% and +11.01% on an average respectively. The results of PLAXIS 3D analysis were found in close proximity with those of IS code method with a variation of only +1.70%. Thus it is seen that the results of IS code

method and Numerical analysis lie within admissible limits. This is probably due to the fact that IS code method is more rational than Terzaghi's method and both the methods consider plastic failure. However, the experimental results overestimate the numerical value reasonably.

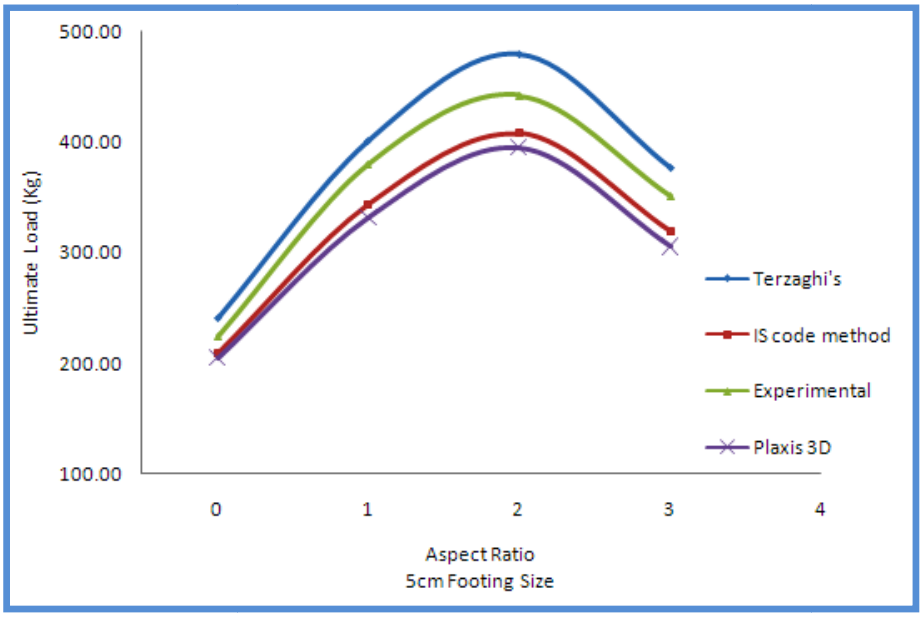

Fig. 6.4a: Variation of Ultimate loads with aspect ratio for various analyses

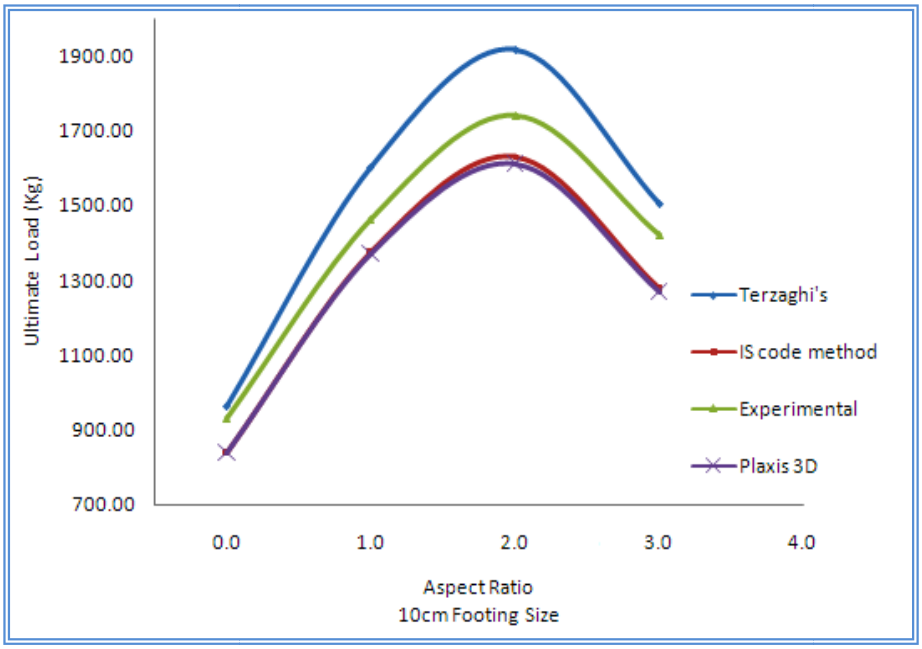

Fig. 6.4b: Variation of Ultimate load with aspect ratio for various analyses

6.4 Statistical Modelling

From the results found from numerical analysis, an attempt has been made to obtain a statistical model by performing regression analysis so that bearing capacity (q) can be predicted in terms of optimum moisture content (OMC), maximum dry density (MDD), percentage of reinforcement (P_r), aspect ratio (AR), cohesion (c), angle of friction (ϕ) and footing width (B). The ultimate bearing capacities for various soil mixes and footing sizes were obtained from numerical analysis using PLAXIS 3D software. The values of different parameters for the statistical modelling are given in the Table 6.3.

Table 6.3 Values of various parameters for regression analysis

Sl. No.	Soil type	Percentage of reinforcement	Aspect ratio	Footing width	Optimum moisture content	Maximum dry density	Cohesion	Angle of friction	Ultimate bearing capacity
		P_r (%)	AR	B (cm)	OMC (%)	MDD (gm/cc)	c (kg/cm^2)	ϕ (degree)	q (kg/cm^2)
1	S1	0	0	5	19	1.65	0.9	7	8.273
2				10	19	1.65	0.9	7	8.275
3	S1	0.5	1	5	17.8	1.68	1.05	9	10.652
4				10	17.8	1.68	1.05	9	10.702
5	S1	1		5	17.48	1.7	1.2	11	13.518
6				10	17.48	1.7	1.2	11	13.584
7	S1	1.5		5	18	1.67	1	8	9.695
8				10	18	1.67	1	8	9.708
9	S1	2		5	18.44	1.65	0.9	6	7.913
10				10	18.44	1.65	0.9	6	7.875
11	S1	0.5	2	5	17.6	1.7	1.15	9	11.643
12				10	17.6	1.7	1.15	9	11.655
13	S1	1		5	17.4	1.71	1.35	12	16.064
14				10	17.4	1.71	1.35	12	16.194
15	S1	1.5		5	18.15	1.66	1	8	9.744
16				10	18.15	1.66	1	8	9.637
17	S1	2		5	19.2	1.64	0.9	6	7.816
18				10	19.2	1.64	0.9	6	7.875

Sl. No.	Soil type	Percentage of reinforcement	Aspect ratio	Footing width	Optimum moisture content	Maximum dry density	Cohesion	Angle of friction	Ultimate bearing capacity
		P_r (%)	AR	B (cm)	OMC (%)	MDD (gm/cc)	c (kg/cm^2)	ϕ (degree)	q (kg/cm^2)
19	S1	0.5	3	5	18.15	1.67	1.1	10	11.784
20				10	18.15	1.67	1.1	10	11.744
21	S1	1		5	18.5	1.65	1	13	12.597
22				10	18.5	1.65	1	13	12.565
23	S1	1.5		5	19.4	1.62	0.6	9	6.087
24				10	19.4	1.62	0.6	9	6.085
25	S1	2		5	19.8	1.58	0.5	7	4.587
26				10	19.8	1.58	0.5	7	4.586
27	S2	0	0	5	18	1.72	1.1	10	11.740
28				10	18	1.72	1.1	10	11.745
29	S2	0.5	1	5	16.9	1.7	1.3	11	14.628
30				10	16.9	1.7	1.3	11	14.678
31	S2	1		5	15.85	1.72	1.48	13	18.565
32				10	15.85	1.72	1.48	13	18.134
33	S2	1.5		5	17.5	1.67	1.18	9	11.996
34				10	17.5	1.67	1.18	9	11.975
35	S2	2		5	19.6	1.65	0.98	7	9.053
36				10	19.6	1.65	0.98	7	9.083
37	S2	0.5	2	5	16.5	1.71	1.3	12	15.507
38				10	16.5	1.71	1.3	12	15.508
39	S2	1		5	15.53	1.74	1.45	13	18.263
40				10	15.53	1.74	1.45	13	18.615
41	S2	1.5		5	18.5	1.64	0.95	7	8.707
42				10	18.5	1.64	0.95	7	8.694
43	S2	2		5	19.2	1.61	0.76	6	6.618
44				10	19.2	1.61	0.76	6	6.691
45	S2	0.5	3	5	17	1.71	1.45	12	17.288
46				10	17	1.71	1.45	12	17.288
47	S2	1		5	18.24	1.68	1.25	14	16.581
48				10	18.24	1.68	1.25	14	16.656
49	S2	1.5		5	19.5	1.63	0.8	9	8.115
50				10	19.5	1.63	0.8	9	8.119
51	S2	2		5	20.2	1.6	0.65	7	5.952
52				10	20.2	1.6	0.65	7	5.965

Sl. No.	Soil type	Percentage of reinforcement	Aspect ratio	Footing width	Optimum moisture content	Maximum dry density	Cohesion	Angle of friction	Ultimate bearing capacity
		P_r (%)	AR	B (cm)	OMC (%)	MDD (gm/cc)	c (kg/cm^2)	ϕ (degree)	q (kg/cm^2)
53	S3	0	0	5	15.4	1.8	1.2	12	14.267
54				10	15.4	1.8	1.2	12	14.257
55	S3	0.5	1	5	15.2	1.75	1.35	13	17.021
56				10	15.2	1.75	1.35	13	17.011
57	S3	1		5	14.85	1.76	1.55	15	21.843
58				10	14.85	1.76	1.55	15	21.771
59	S3	1.5		5	16.5	1.68	1.2	11	13.558
60				10	16.5	1.68	1.2	11	13.522
61	S3	2		5	19.6	1.65	1	8	9.725
62				10	19.6	1.65	1	8	9.742
63	S3	0.5	2	5	15.1	1.75	1.4	14	18.639
64				10	15.1	1.75	1.4	14	18.578
65	S3	1		5	14.73	1.77	1.5	16	22.242
66				10	14.73	1.77	1.5	16	22.261
67	S3	1.5		5	17	1.67	1.15	9	11.665
68				10	17	1.67	1.15	9	11.656
69	S3	2		5	19.65	1.63	0.88	7	8.130
70				10	19.65	1.63	0.88	7	8.124
71	S3	0.5	3	5	15	1.76	1.48	14	19.631
72				10	15	1.76	1.48	14	19.659
73	S3	1		5	16.84	1.71	1.33	17	20.950
74				10	16.84	1.71	1.33	17	20.964
75	S3	1.5		5	18.50	1.66	0.95	11	10.822
76				10	18.50	1.66	0.95	11	10.696
77	S3	2		5	20.5	1.62	0.75	9	7.716
78				10	20.5	1.62	0.75	9	7.642

The 78 sets of data have been used for regression analysis as illustrated in the following section.

6.4.1 Regression Analysis

Multiple linear regression has been done using Microsoft Excel, with ultimate bearing capacity (q) as response and optimum moisture content (OMC), maximum dry density (MDD), percentage of reinforcement (P_r), aspect ratio (AR), cohesion (c), angle of friction (ϕ) and footing width (B) as predictors. From the values of parameters furnished in Table 6.3,

the values from serial nos. 1 to 52 have been used to obtain the required equation 6.1 with R^2 value of 0.9948.

$$q = 8.0721 + 0.2371*(P_r) - 0.0161*(AR) + 0.0019*(B) - 0.1273*(OMC) - 7.4888*(MDD) + 11.2183*(c) + 0.6343*(\phi) \quad \text{..... (6.1)}$$

The testing of the above equation has been done with the help of the values of serial nos. 53 to 78 given in Table 6.3 and variations of result as obtained are given in Table 6.4 below. It can be seen that the variation of results obtained from the above equation and numerical analysis are well within 9.519%.

Table 6.4: Validation of the regression equation

Sl. No.	Soil type	P_r (%)	AR	B (cm)	OMC (%)	MDD (gm/cc)	c (kg/cm^2)	ϕ (degree)	q (from PLAXIS analysis) (kg/cm^2)	q (from Regression analysis) (kg/cm^2)	Percentage variation in results (%)
53	S3	0	0	5	15.4	1.8	1.2	12	14.267	13.715	3.870
54	S3	0	0	10	15.4	1.8	1.2	12	14.257	13.724	3.736
55	S3	0.5	1	5	15.2	1.75	1.35	13	17.021	16.534	2.859
56	S3	0.5	1	10	15.2	1.75	1.35	13	17.011	16.544	2.746
57	S3	1	1	5	14.85	1.76	1.55	15	21.843	20.135	7.820
58	S3	1	1	10	14.85	1.76	1.55	15	21.771	20.144	7.472
59	S3	1.5	1	5	16.5	1.68	1.2	11	13.558	14.179	-4.579
60	S3	1.5	1	10	16.5	1.68	1.2	11	13.522	14.188	-4.927
61	S3	2	1	5	19.6	1.65	1	8	9.725	9.981	-2.630
62	S3	2	1	10	19.6	1.65	1	8	9.742	9.990	-2.549
63	S3	0.5	2	5	15.1	1.75	1.4	14	18.639	17.726	4.898
64	S3	0.5	2	10	15.1	1.75	1.4	14	18.578	17.736	4.534
65	S3	1	2	5	14.73	1.77	1.5	16	22.242	20.132	9.485
66	S3	1	2	10	14.73	1.77	1.5	16	22.261	20.142	9.519
67	S3	1.5	2	5	17	1.67	1.15	9	11.665	12.344	-5.824
68	S3	1.5	2	10	17	1.67	1.15	9	11.656	12.354	-5.987
69	S3	2	2	5	19.65	1.63	0.88	7	8.130	8.128	0.029
70	S3	2	2	10	19.65	1.63	0.88	7	8.124	8.137	-0.161
71	S3	0.5	3	5	15	1.76	1.48	14	19.631	18.545	5.530
72	S3	0.5	3	10	15	1.76	1.48	14	19.659	18.555	5.617
73	S3	1	3	5	16.84	1.71	1.33	17	20.950	19.024	9.192
74	S3	1	3	10	16.84	1.71	1.33	17	20.964	19.034	9.207
75	S3	1.5	3	5	18.5	1.66	0.95	11	10.822	11.237	-3.836
76	S3	1.5	3	10	18.5	1.66	0.95	11	10.696	11.247	-5.148
77	S3	2	3	5	20.5	1.62	0.75	9	7.716	7.888	-2.235
78	S3	2	3	10	20.5	1.62	0.75	9	7.642	7.898	-3.349

Further, the ultimate bearing capacity values obtained from experimental analysis and corresponding values obtained from Eq. 6.1 predicted by regression analysis, a graph have been presented in Table 6.5.

Table 6.5: Ultimate bearing capacity from Experimental investigation and Regression analysis (for 1% strip content)

Sl. No	Size of Footing	Aspect Ratio	Ultimate Bearing Capacity (kg/cm^2)		% variation of regression analysis results from experimental values
			Experimental	Regression	(%)
1	5 cm	0	9.00	7.84	12.86
2		1	15.16	13.79	9.07
3		2	17.68	16.02	9.38
4		3	14.04	13.02	7.24
5	10 cm	0	9.30	7.85	15.57
6		1	14.60	13.80	5.51
7		2	17.40	16.03	7.87
8		3	14.20	13.03	8.22

It appears from the table that with respect to the experimental values the predicted values deviate from 7.24% to 12.86% and from 8.22% to 15.57% for square footings of sizes 5 cm and 10 cm respectively. This may be considered to be quite reasonable in respect of prediction of ultimate bearing capacities of footings resting on PET bottle strips reinforced soil.

6.5 Improvement Factor

In the present study an improvement factor may be defined as the ratio of ultimate bearing capacity of footing on reinforced soil to that on unreinforced soil. For this purpose, an attempt has been made to find this improvement factors for different cases as presented in Table 6.6.

Table 6.6: Improvement Factors

Sl. No.	Soil type	Percentage of Reinforcement	Aspect Ratio	Footing Width	Ultimate Bearing capacity	Improvement Factors
		P_r (%)	AR	B (cm)	q (kg/cm^2)	
1	S1	0	0	5	8.273	1
2	S1	0.5	1	5	10.652	1.29
3	S1	1	1	5	13.518	1.63
4	S1	1.5	1	5	9.695	1.17
5	S1	2	1	5	7.913	0.96
6	S1	0.5	2	5	11.643	1.41
7	S1	1	2	5	16.064	1.94
8	S1	1.5	2	5	9.744	1.18
9	S1	2	2	5	7.816	0.94
10	S1	0.5	3	5	11.784	1.42
11	S1	1	3	5	12.597	1.52
12	S1	1.5	3	5	6.087	0.74
13	S1	2	3	5	4.587	0.55
14	S1	0	0	10	8.275	1.00
15	S1	0.5	1	10	10.702	1.29
16	S1	1	1	10	13.584	1.64
17	S1	1.5	1	10	9.708	1.17
18	S1	2	1	10	7.875	0.95
19	S1	0.5	2	10	11.655	1.41
20	S1	1	2	10	16.194	1.96
21	S1	1.5	2	10	9.637	1.16
22	S1	2	2	10	7.875	0.95
23	S1	0.5	3	10	11.744	1.42
24	S1	1	3	10	12.565	1.52
25	S1	1.5	3	10	6.085	0.74
26	S1	2	3	10	4.586	0.55
27	S2	0	0	5	11.74	1.00
28	S2	0.5	1	5	14.628	1.25
29	S2	1	1	5	18.565	1.58
30	S2	1.5	1	5	11.996	1.02
31	S2	2	1	5	9.053	0.77
32	S2	0.5	2	5	15.507	1.32
33	S2	1	2	5	18.263	1.56
34	S2	1.5	2	5	8.707	0.74
35	S2	2	2	5	6.618	0.56
36	S2	0.5	3	5	17.288	1.47
37	S2	1	3	5	16.581	1.41
38	S2	1.5	3	5	8.115	0.69

39	S2	2	3	5	5.952	0.51
40	S2	0	0	10	11.745	1.00
41	S2	0.5	1	10	14.678	1.25
42	S2	1	1	10	18.134	1.54
43	S2	1.5	1	10	11.975	1.02
44	S2	2	1	10	9.083	0.77
45	S2	0.5	2	10	15.508	1.32
46	S2	1	2	10	18.615	1.58
47	S2	1.5	2	10	8.694	0.74
48	S2	2	2	10	6.691	0.57
49	S2	0.5	3	10	17.288	1.47
50	S2	1	3	10	16.656	1.42
51	S2	1.5	3	10	8.119	0.69
52	S2	2	3	10	5.965	0.51
53	S3	0	0	5	14.267	1.00
54	S3	0.5	1	5	17.021	1.19
55	S3	1	1	5	21.843	1.53
56	S3	1.5	1	5	13.558	0.95
57	S3	2	1	5	9.725	0.68
58	S3	0.5	2	5	18.639	1.31
59	S3	1	2	5	22.242	1.56
60	S3	1.5	2	5	11.665	0.82
61	S3	2	2	5	8.13	0.57
62	S3	0.5	3	5	19.631	1.38
63	S3	1	3	5	20.95	1.47
64	S3	1.5	3	5	10.822	0.76
65	S3	2	3	5	7.716	0.54
66	S3	0	0	10	14.257	1.00
67	S3	0.5	1	10	17.011	1.19
68	S3	1	1	10	21.771	1.53
69	S3	1.5	1	10	13.522	0.95
70	S3	2	1	10	9.742	0.68
71	S3	0.5	2	10	18.578	1.30
72	S3	1	2	10	22.261	1.56
73	S3	1.5	2	10	11.656	0.82
74	S3	2	2	10	8.124	0.57
75	S3	0.5	3	10	19.659	1.38
76	S3	1	3	10	20.964	1.47
77	S3	1.5	3	10	10.696	0.75
78	S3	2	3	10	7.642	0.54

From the table it is observed that the improvement factor increases initially with PET bottle strip content and aspect ratio of strip. Also, it has been observed from the literature review

that **Chandrasekhar et al. (1998), Basudhar et al. (2007), Sharma et al. (2009), Madhavilatha and Somwanshi (2009), Al-Saidi (2009), Kumar and Kaur (2012)** found that use of reinforcements results in increase in bearing capacity of footing placed on reinforced soil compared to that for unreinforced soil. The optimum values are obtained for 1% strip content and aspect ratio of 2; beyond these values this factor reduces appreciably and even it reaches to values of less than 1 in some cases. The optimum improvement factor for S1, S2 and S3 soil with 1% fibre content and aspect ratio 2 are 1.94, 1.56 and 1.56 respectively for 5 cm wide square footing. In case of 10 cm wide square footing those values are 1.96, 1.58 and 1.54 for S1, S2 and S3 type of soil. The improvement factor, in case of S2 and S3 soils, are less compared to that of S1 soil. This is probably due to the fact that they contain 10% and 20% sand by weight respectively. This reflects that the decrease of plasticity index imparted by increase of sand content causes less improvement meaning thereby PET bottle strip reinforcement is more effective in case of cohesive soil with more plasticity.

Chapter 7

SUMMARY AND CONCLUSIONS

7.1 Summary

Scarcity of land with appreciable bearing capacity for construction of structures is increasing day by day with progress of civilization and industrialization. At the same time there are many waste materials deposited due to human activities all over the world. Such a waste is PET bottle used and thrown away by people as waste. Recycling of this may reduce environmental hazard as well as help in construction on weak ground. It further appears that there is scope of study on behaviour of clay mixed with randomly distributed plastic fibre obtained from waste PET bottles lies in recycling of plastic waste to reduce environmental hazard. Mixing of waste plastic strips with soil may therefore be done to increase the strength and stability of soil.

With this in view the present study has been carried out with a locally available clayey soil. This has been mixed with 10% and 20% sand to make two more types of amended soils. Thus three types of soils have been obtained as follows:

a) Original soil S1,
b) S2 (Soil+10% sand) and
c) S3 (soil+20% sand).

Further PET bottles have been procured and they have been cut into pieces of 5mm width with aspect ratio of 1, 2 and 3. For each aspect ratio four strip contents, 0.5%, 1%, 1.5% and 2% have been mixed with each type of soil.

So, there are 3 soil types and for each soil type there are 3 (soil types) x 3 (aspect ratio) x4 (fibre content) = 3 soils + 3 x 3 x 4 (=36) mixes. Different tests, such as, grain size analysis and Atterberg's limits have been done for characterization. Unconfined compressive strength and UU triaxial tests have been done to obtain strength of these three types of soil and 36 mixes at optimum moisture content obtained earlier with the help of standard Proctor test. In

case of tests with PET bottle strip reinforcements, 1% PET bottle strips and aspect ratio of 2 have been found to be optimum.

Further model footing tests have been done to study the effect of PET bottle strips admixture on bearing capacity of footings. Model footing tests have been done with selective number of mixes for optimum percent of PET bottle strips for soil type S1 only. A total 8 number of model footing tests have been done on square footings of 5 cm and 10 cm sizes.

An attempt has also been made to carry out numerical analysis of the model tests by finite element method using PLAXIS 3D FOUNADATION software. Material nonlinearity has been considered to model the soils and mixes using Mohr –Coulomb failure theory and elasto- plastic behaviour. Soil has been idealized as an elastic-perfectly plastic material satisfying Mohr-Coulomb yield criterion.

Subsequently statistical modelling has been done to obtain an expression for bearing capacity of footings resting on the reinforced soil in terms of maximum dry density, optimum moisture content, shear strength parameters, aspect ratio and percentage of PET bottle strip reinforcements.

7.2 Conclusions

The following conclusions may be drawn from the present study in respect of material properties as well as model footing tests and numerical study.

A. On material properties

- Maximum dry density of PET bottle strip (fibre) – soil mix increases with increase in PET bottle strip (fibre) content, but it occurs up to its addition of 1% when other parameters do not alter. Optimum value occurs at aspect ratio 2.
- Optimum moisture content of fiber soil mix decreases with increase in fiber content but it occurs up to its addition of 1% when other parameters do not change. Optimum value has been achieved at aspect ratio 2.
- UCS and shear strength parameters of fiber soil mix increases with increase in fiber content but it occurs up to its addition of 1% when other parameters do not alter. Optimum value comes at aspect ratio 2.

B. From model footing test and numerical analysis

- For 5 cm x 5 cm and 10 cm x 10 cm sizes of footing, trend of load settlement curves appears to be similar for both experimental and numerical studies
- For 5 cm x 5 cm and 10 cm x 10 cm sizes of footing, ultimate load carried by soil reinforced with PET strips of aspect ratio 2 is maximum compared to that of all other mixes.
- The ultimate bearing capacities obtained from experiment and numerical analysis agreed with reasonable variation. The variation in ultimate bearing capacities between experimental and numerical values was from 6.5% to 15%.
- Ultimate bearing capacity values obtained by IS code method and PLAXIS 3D software are very close and however, the experimental values overestimate them.
- Ultimate bearing capacity values predicted by regression analysis deviate from that obtained in the experimental investigation by 7.24 % to 12.86 % and 8.22 % to 15.57 % for square footings of sizes 5 cm and 10 cm respectively. This may be considered to be quite reasonable in respect of prediction of ultimate bearing capacities of footings resting on PET bottle strips reinforced soil.
- The optimum improvement factor for S1, S2 and S3 soil with 1% fibre content and aspect ratio 2 are 1.94, 1.56 and 1.56 respectively for 5 cm wide square footing. In case of 10 cm wide square footing those values are 1.96, 1.58 and 1.54 for S1, S2 and S3 type of soil. Less improvement is obtained with PET bottle strip reinforcements in case of S2 and S3 type of soil containing sand.
- Improvement with PET bottle strip reinforcements is more effective in case of cohesive soil with more plasticity.
- From the results of regression analysis following equation has been obtained with R^2 = 0.9948

$$q = 8.0721 + 0.2371*(P_r) - 0.0161*(AR) + 0.0019*(B) - 0.1273*(OMC) - 7.4888*(MDD) + 11.2183*(c) + 0.6343*(\varphi)$$

7.3 Limitations of the Present Study

The limitations of the present study are as follows:

a) Higher footing sizes and more cases of foundation soil mixes have not been considered.
b) The effect of overburden pressure has not been considered as the footing rests on the soil surface. So, bearing capacity in this case cannot be normalized with overburden pressure or surcharge, which is a normal practice..
c) Settlement considerations have not been included in the present study.

7.4 Scope of Further Research

It is recommended to carry out further research in this relevant field as follows:

a) To study application of PET bottle strips in case of weak subgrade and embankment under seismic and non seismic condition with laboratory models.

b) Field study with ground improvement by PET bottle strips in case of weak subgrade, highway embankment and bearing capacity of footings.

c) Numerical studies of the above mentioned cases under seismic and non seismic conditions.

d) Impact of PET bottle strips on environment may be studied by leachate analysis for examining its eco-friendliness in connection with its use in ground improvement as geo-environmental study.

REFERENCES

1. Ahmadi, H. and Masoud, H.B. (2012) Experimental and analytical investigations on bearing capacity of strip footing in reinforced sand backfills and flexible retaining wall, Acta Geotechnica. 7(4):357-373.
2. Alawaji, H. (2001) Settlement and bearing capacity of geogrid-reinforced sand over collapsible soil, Geotextiles and Geomembranes. 19(2):75-88.
3. Al-saidi, A. (2009) Evaluation the behaviour of reinforced loose sand under inclined loading". Journal of Kerbala University. 7(3):98-108.
4. ASTM D638 - 14 Standard Test Method for Tensile Properties of Plastics.
5. ASTM D792-13 Standard Test Methods for Density and Specific Gravity (Relative Density) of Plastics by Displacement.
6. Babu, G L S and Chouksey, Sandeep. (2010) Stress-strain response of plastic waste mixed soil, Waste management. 31(3):481-488.
7. Basudhar, P.K., Saha, S. and Deb, K. (2007) Circular footings resting on geotextile-reinforced sand bed, Geotextiles and Geomembranes. 25(6):377-384.
8. Belal, A. M. and George, K. P. (2000) Finite element analysis of reinforced soil retaining walls subjected to seismic loading, 12th WCEE, paper no. 0842.
9. Boushehrian, J.H., Hataf, N. (2003) Experimental and numerical investigation of the bearing capacity of model circular and ring footings on reinforced sand, Geotextiles and Geomembranes. 23(2):144-173.
10. Casagrande, M. D. T., Coop, M. R. and Consoli, N. C. (2006) The behaviour of a fiber-reinforced bentonite at large shear displacements, Journal of Geotechnical and Geoenvironmental Engineering, ASCE. 132(11):1505-1508.
11. Casagrande, M. D.T. (2005) Behaviour of fiber-reinforced soils under large shear strains, Ph.D. thesis, Federal University of Rio Grande do Sul, Porto Alegre, Brazil (in Portuguese).
12. Chandrashekar arya et al (2013) A study on CBR behavior of waste plastic (pet) on stabilized red mud and fly ash, Int. J. Struct. & Civil Engg. Res.
13. Chandra, S., Viladkar, M. and Prashant, P. N. (2008) Mechanistic approach for fiber-reinforced flexible pavements. Journal of Transportation Engineering, ASCE, 134(1):15-23.
14. Choudhary, A.K., Jha, J.N. and Gill, K.S. (2010) A study on CBR behaviour of waste plastic strip reinforced soil, Emirates Journal for Engineering Research, 15(1):51-57.

15. Choudhary, A.K., Jha, J.N. and Gill, K.S. (2010) Laboratory investigation of bearing capacity behaviour of strip footing on reinforced fly ash slope, Geotextiles and Geomembranes. 28(4): 393-402.
16. Consoli, N.C., Casagrande, M.D.T. and Coop, M.R. (2005) Effect of fiber reinforcement on the isotropic compression behaviour of sand, Journal of Geotechnical and Geoenvironmental Engineering, ASCE. 131(11):1434-1436.
17. Consoli, N.C., Montardo, J.P., Prietto, P.D.M. and Pasa, G.S., (2002) Engineering behaviour of a sand reinforced with plastic waste, Journal of Geotechnical and Geoenvironmental Engineering, ASCE. 128(6):462-472.
18. Dash, S.K., Krishnaswamy, N.R. and Rajagopal, K. (2001a) Bearing capacity of strip footings supported on geocell-reinforced sand, Geotextiles and Geomembranes. 19(4):235-256.
19. Dash, S.K., Krishnaswamy, N.R., Rajagopal, K., (2001b) Strip footing on geocell reinforced sand beds with additional planar reinforcement, Geotextiles and Geomembranes. 19(8):529-538.
20. Dutta, R.K. and Rao, G.V. (2007) Regression models for predicting the behaviour of sand reinforced with waste plastic, Turkish J. Eng. Env. Sci. 31:119-126.
21. Fatani, M. N., Bauer, G. E. & A1-Joulani, N. (1991) Reinforcing soil with aligned and randomly oriented metallic fibres, Geotechnical Testing Journal, ASTM. 14(1), 78-87.
22. Gosavi, M. and Patil, Kailas. (2004) Improvement of properties of black cotton soil subgrade through synthetic reinforcement, Journal of the Institution of Engineers (India): Civil Engineering Division. 84.
23. Gray, D.H. and Al-Refeai, T. (1986), Behaviour of fabric-versus fiber-reinforced sand, Journal of Geotechnical Engineering, ASCE. 112(8):804-820.
24. Gray, D.H. and Maher, M.H. (1989) Admixture stabilization of sands with random fibers, Proceedings of the Twelfth International Conference on Soil Mechanics and Foundation Engineering, Balkema, Vol. 2, Rio de Janeiro, Brazil, pp.1363-1366.
25. Gray, D.H. and Ohashi, H., (1983) Mechanics of fiber reinforcement in sand, Journal of Geotechnical Engineering, ASCE. 108(3):335-353.
26. Haider Mohammed Mekkiyah (2013), Improvement of soil by using polymer fiber materials underneath square footing, Journal of Engineering. 19.
27. IS 2720 (Part XI): (1993) Method of tests for soils - Determination of the shear strength parameters of a specimen tested in unconsolidated undrained triaxial compression without the measurement of pore water pressure.

28. IS: 2720 (Part IV): (1980) Method of tests for soils - Grain size analysis
29. IS: 2720 (Part V): (1980) Method of tests for soils - Determination of liquid and plastic limits
30. IS: 2720 (Part VII): (1980) Method of tests for soils - Determination of water content-dry density relation using light compaction.
31. IS: 2720 (Part X): (1991) Method of tests for soils - Determination of unconfined compressive strength.
32. IS: 2720 (Part XV): Method of tests for soils – Determination of consolidation properties.
33. Jie Gu. (2011) Computational modelling of geogrid reinforced soil foundation and geogrid reinforced base in flexible pavement, LSU Doctoral Dissertations. 1920.
34. Kellezi, L and Stromann, H. (2003) FEM analysis of jack-up spud can penetration for multi-layered critical soil conditions. BGA International Conference on Foundations, Innovations, Observations, Design and Practice.
35. Kumar, A. and Kaur, A (2012) Model tests of square footing resting on fiber reinforced sand bed, Geosynthetics International. 19(5):385-392.
36. Kumar, S and Tabor, E. (2003) Strength characteristics of silty clay reinforced with randomly oriented nylon fibers. Electronic Journal of Geotechnical Engineering. http://www.ejge.com/2003/Ppr0310/Ppr0310.htm
37. Lindh, E. and Eriksson, (1991) Sand Reinforcement with plastic fibres, A field experiment, performance of reinforced soil structures, McGown, A., Yeo, K., and Andrawes, K. Z., Editors, Thomas Telford, Proceeding of International Reinforced soil conference soil held in Glasgow, Scotland. 471-473.
38. Madhavilatha Gali and Somwanshi Amit. (2009) Effect of reinforcement form on the bearing capacity of square footings on sand, Geotextiles and Geomembranes. 27(6):409-422.
39. Mahali, K.P. and Sinha, A.K. (2015) Utilization of stonedust with plastic waste for improving the subgrade in highway pavement construction, International Journal of Research in Engineering and Technology. 4(6):29-35.
40. Maher, M. H. and Ho, Y. C. (1994) Mechanical properties of kaolinite/fiber soil composite", Journal of Geotechnical Engineering, ASCE. 120(8):1381-1393.
41. Maheshwari, B.K., Singh, H.P. and Saran, S. (2012) Effects of reinforcement on the liquefaction resistance of Solani sand, Journal of Geotechnical and Geoenvironmental Engineering, ASCE. 138(7) :831-840.

42. Mandal J.N. and Manjunath V.R. (1995) Bearing capacity of strip footing resting on reinforced sand subgrades, Construction and Building Materials. 9(1):35-38.
43. McGown, A., Andrawes, K.Z. and Al-Hasani, M.M. (1978) Effect of inclusion properties on the behavior of sand, Geotechnique. 28(3):327-346.
44. Michalowski, R.L. and Zhao, A (1996) Failure of fiber reinforced granular soils, Journal of Geotechnical Engineering, ASCE, 122(3):226-234.
45. Mohamed, M. H. A. (2010) Two dimensional experimental study for the behaviour of surface footings on unreinforced and reinforced sand beds overlying soft pockets, Geotextiles and Geomembranes, 28 (6):589-596.
46. Naeini, S.A. and Sadjadi, S.M. (2008) Effect of Waste Polymer Materials on Shear Strength of Unsaturated Clays, EJGE Journal. 13(k):(1-12).
47. Nataraj, M.S. and McManis, K. L. (1997) Strength and deformation properties of soils reinforced with fibrillated fibers, Geosynthetics International. 4(1):65-79.
48. Phanikumar, B. R., Rao, A.S. and Suresh, K. (2008) Field behaviour of granular pile-anchors in expansive soils, Ground Improvement. 161(4):199-206.
49. Ranjan, G., Vasan, R. M., and Charan, H. D. (1994) Behaviour of plastic fibre-reinforced sand, Geotextiles and Geomembranes, 13(8):555–565.
50. Ranjan, Gopal, Singh, Bhupal and Charan, H. D. (1999) Experimental study of soft clay reinforced with sand fiber core, Indian Geotechnical Journal. 29(4):281-291.
51. Setty, K.R.N.S. and Rao, S.V.G. (1987), “Characteristics of fiber reinforced lateritic soil". Proc. Indian Geotechnical Conference, Bangalore. 329-333.
52. Sharma, R., Chen, Q., Abu-Farsakh, M. and Yoon, S. (2009) Analytical modelling of geogrid reinforced soil foundation, Geotextiles and Geomembranes. 27(1):63-72
53. Vinod, P., Ajitha, B. and Sreehari, S. (2009) Behaviour of a square model footing on loose sand reinforced with braided coir rope, Geotextiles and Geomembranes. 27(6):464-474.
54. Waldron, L. J., (1997) Shear Resistance of Root-Permeated Homogeneous and Stratified Soil, Soil Science Society of America Proceedings. 41: 843-849.
55. Wasti, Y. and Butun, M.D. (1996) Behaviour of model footings on sand reinforced with discrete inclusions, Geotextiles and Geomembranes. 14(10):575-584.
56. Yamamoto, K. and Otani, J. (2002) Bearing capacity and failure mechanism of reinforced foundations based on rigid-plastic finite element formulation, Geotextiles and Geomembranes. 20(6):367-393.